2006

Bench Scale Analysis Of Experimental Fouling-resistent Low Pressure Reverse Osmosis Membranes Using High Organic Surface Water And Synthetic Colloidal Water

Matthew Doan
University of Central Florida

BENCH SCALE ANALYSIS OF EXPERIMENTAL FOULING-RESISTENT LOW PRESSURE RO MEMBRANES USING HIGH ORGANIC SURFACE WATER AND SYNTHETIC COLLOIDAL WATER

by

MATTHEW A. DOAN, P.E.
B.S. University of Central Florida, 1999

A thesis submitted in partial fulfillment of the requirements
for the degree of Master of Science
in the Department of Civil and Environmental Engineering
in the College of Engineering and Computer Science
at the University of Central Florida
Orlando, Florida

Fall Term
2006

ABSTRACT

The utilization of membrane treatment for the production of potable water has become more prevalent in today's industry. As drinking water regulations become more stringent this trend is expected to continue. Widespread use is also a result of membrane treatment being the best available treatment in many cases. While membrane treatment is a proven technology that can produce a consistently superior product to conventional treatment methods, membrane fouling and concentrate disposal are issues that drive up the cost of membrane treatment and can effectively eliminate it from consideration as a treatment alternative.

This research focused on membrane fouling. A series of filtration experiments were conducted on various membranes to investigate the physical and chemical factors that influence fouling. The effects of both organic and colloidal fouling were explored by conducting research on various commercial membranes and experimental membranes by Saehan Industries, Inc. (Saehan). Saehan's membranes were in various stages of development in their process of creating a more fouling resistant membrane (FRM). Various hydrodynamic and chemical conditions were used to characterize the evolution of the Saehan commercial products to the experimental FRMs.

The developmental stage of the membrane tested included analysis of the various trade secret coating techniques termed single, double, and special. A proprietary post-treatment process was also utilized in combination with each of the coating techniques.

The developmental membranes were also compared to commercially available FRMs. The existing FRMs showed better fouling resistance than Saehan's commercially available products in high organic surficial groundwater testing. Synthetic colloidal water testing demonstrated the superior performance of the FRMs, but was not acute enough to differentiate the fouling performance within the group of FRMs or Saehan products. Average roughness decreased slightly as coating technique progressed from single to double to special. Post-treatment increased roughness in single coated membranes and reduced the roughness in double and special coated membranes. The relative charge differences in the developmental membranes were exhibited among non post-treated membranes. Post-treatment membranes did not demonstrate relative surface charge differences consistent with the manufacturer. Initial mass transfer coefficient, determined by clean water testing, increased as coating moved from single to double to special. Clean water testing showed increased initial mass transfer coefficient for membranes with post-treatment. Single coated membranes showed the best salt rejection capability among non post-treated membranes. Post-treatment increased selectivity for all membrane coating techniques. The coating effect on fouling potential had an inverse relationship between single coated versus double and special coated membranes. The post-treatment increased fouling resistance for the single coated membranes, but decreased fouling resistance of double and special coated membranes. The SN7 membranes showed the best performance of the developmental membranes.

This work is dedicated to my family and friends who supported me throughout this long and winding road. Thank you Allen, Barbara, Greg, Jen, Ewald, Florence, Michelle and especially Christine.

ACKNOWLEDGMENTS

I would like to thank my advisors Dr. Seungkwan (SK) Hong and Dr. Andrew Randall for their support and patience. I would also like to thank Dr. Debra Reinhart and Dr. James Taylor for taking time from their schedules to sit on my committee. I appreciate the opportunity to learn from all of them through this experience and from the direction they provided in the laboratory and the classroom. I would also like to express my gratitude to Dr. Taylor for taking additional time to help me complete my graduate work.

Thank you to everyone who helped throughout the process: Colin Hobbs (membrane flat sheet filtration unit and acquisition of raw water), Anjani Patel (AFM), Sonia Holmquist (EKA QA/QC), and Dr. Norris (TOC).

TABLE OF CONTENTS

LIST OF FIGURES

LIST OF TABLES

LIST OF ACRONYMS/ABBREVIATIONS

AFM	Atomic Force Microscopy
DBPs	Disinfection By-products
EDCs	Endocrine Disrupting Chemicals
EKA	Electrokinetic Analyzer
EPOCs	Emerging Pollutants of Concern
gpm	Gallons per Minute
gsfd	Gallons per Square Foot per Day
HAAs	Hormonally Active Agents
MF	Microfiltration
MTC	Mass Transfer Coefficient
NDF	Net Driving Force
NF	Nanofiltration
OWCs	Organic Wastewater Contaminants
PCPs	Personal Care Products
PhACs	Pharmaceutically Active Compounds
psi	Pounds per Square Inch
RO	Reverse Osmosis
TDS	Total Dissolved Solids
UF	Ultrafiltration

CHAPTER 1: INTRODUCTION

As drinking water standards become more stringent and the availability of pristine source waters decline, the use of membrane technology will increase to meet the demand for proper treatment. The 1996 Safe Drinking Water Act (SDWA) amendments brought this situation to the forefront by calling for new regulations concerning the levels of chemical and biological toxins in the drinking water supply. These regulations will require significant improvements in existing water treatment processes and in some cases may exceed the limitations of these processes or prove them to be cost prohibitive. Utilities will be forced to pass costs on to the consumer or invest in technology that is more cost-effective while meeting the increasingly strict standards. Membrane technology can meet this need in many cases and should see a dramatic rise in presence in the drinking water industry.

All technologies, however, have their limitations, and membrane treatment processes are limited by membrane fouling. Fouling is the deterioration of membrane performance due to the characteristics of the source water. Foulants include a wide variety of substances, but the major causes of membrane fouling are scaling, biological growth, organic matter and particulates. These foulants ultimately shorten the life of the membrane life and cause increased operation and maintenance costs.

The effects of organic and colloidal fouling were explored by conducting research on various commercial membranes and experimental membranes by Saehan Industries, Inc. (Saehan), Kongduk-Dong, Mapo-Ku Seoul, Korea. Saehan's membranes were in various

stages of development in their process of creating a more fouling resistant membrane. Various hydrodynamic and chemical conditions were used to characterize the evolution of the Saehan commercial products to the experimental fouling resistant membranes. This fundamental and practical study tested the performance of the membranes under actual drinking water conditions.

CHAPTER 2: PROJECT SCOPE AND OBJECTIVES

The factors influencing membrane fouling can be classified as follows: membrane characteristics, operational conditions, biological growth conditions, foulant properties, hydrodynamic conditions, and feed chemistry. This objective of this study was to address each area, specifically, the research studied the relative change in Saehan's membrane characteristics and how they performed relative to each other as the foulant properties, hydrodynamic conditions, and feed water chemistry are carefully altered. The general goal of this research was to systematically investigate the existing Saehan products and guide the research and development efforts in the creation of a more fouling resistant membrane. The specific objectives were:

- To investigate the effect of surface properties on colloidal fouling by conducting a series of membrane filtration experiments.
- To investigate the effect of surface properties on organic matter fouling by conducting a series of membrane filtration experiments.
- To compare Saehan's existing prototype membrane products to commercial fouling resistant membranes available in the United States.
- To demonstrate the performance of the prototype fouling resistant membranes by conducting a series of colloidal and organic fouling experiments at actual drinking water treatment conditions.
- To provide recommendations on the relative property changes between the Saehan prototype fouling resistant membranes used in testing.

CHAPTER 3: LITERATURE REVIEW

3.1 Overview of Membrane Processes

Membrane processes produce high quality product water and have the ability to meet new and pending stringent regulatory requirements. Membrane treatment is the best available technology for several contaminants. Some advantages of membrane processes include the ability to remove particulate matter with less chemicals/coagulants, the reduction in the number of plant operators, the ability to automate the plant treatment process, a smaller footprint, and greater versatility in planned plant expansions and capacities. Disadvantages include cost considerations, membrane fouling and concentrate disposal. Costs for membrane treatment are decreasing due to technology innovation and membrane plants can be very cost effective for small facilities. Membrane fouling and concentrate disposal continue to be significant challenges. Concentrate disposal has become more difficult with increased regulation and limited disposal options.

Ultrafiltration (UF) and microfiltration (MF) are size exclusion membranes that can control particles, turbidity, and some pathogens. These processes are used to target removal of larger particles than diffusion controlled membranes and are commonly used as pretreatment processes. Nanofiltration (NF) and reverse osmosis (RO) are diffusion controlled membrane processes that can remove total dissolved solids (TDS), chlorides, hardness, and disinfection byproducts (DBP) precursors. Electro-dialysis reversal (EDR)

is a charge controlled membrane process that can control TDS, chlorides, hardness, and other charged constituents (Duranceau and Henthorne 2004).

3.2 Membrane Fouling Mechanisms

Membrane fouling is widely accepted as one of the most critical problems limiting widespread proliferation of membrane treatment in water and wastewater treatment applications. Membrane fouling is the gradual decline in membrane performance due to accumulation of substances (foulants) within the membrane pores or onto the membrane surface. Loss of production and increased energy costs are directly related to fouling. Membrane system degradation can be mitigated by utilizing pretreatment to control foulants and by optimizing the treatment process.

Determination of optimum operating factors includes recovery, flux, operating pressures/vacuums, backwash cycle frequency, utilization of chemically enhanced backwash (CEB), and cleaning frequency. These factors are critical to reducing the impact of fouling on membrane processes. While adding pretreatment and optimizing the treatment process can slow fouling and increase time between cleanings, membrane fouling can not be prevented. Addition of pretreatment processes also increases the cost of membrane treatment (Duranceau and Henthorne 2004; Kinslow and Hudkins 2004).

3.2.1 Scaling

When the solubility of a sparingly soluble salt is exceeded the resulting precipitation is mineral scaling (Nemeth 1997). Calcium carbonate and sulfate salts are examples of sparingly soluble salts which were initially and remain the driving force of most pretreatment chemical selection for RO processes. Silica, hydrogen sulfide, iron, manganese, and aluminum are some of the other constituents to consider. Historically, acid addition for pH adjustment has been used to prevent scaling in membrane systems. Systems with the potential for calcium carbonate scale formation and scaling by other inorganic compounds typically use a combination of acid addition and scale inhibitors. The type of anti-scalant and the required dosage can be determined by calculating the solubility limit of the Limiting Salt. The Limiting Salt is found by analyzing the feed water quality and solubility products of potential limiting salts.

There have been significant advances made in the area of scale inhibitors. Many of today's proprietary pretreatment chemicals offer solutions to a variety of membrane applications. Some applications where it was previously a significant challenge to treat and others where the water was accepted as a poor quality, which resulted in increased operation and maintenance costs. A specific scale inhibitor is typically best suited for a particular source water. Factors for selection of a scale inhibitor include feed water source, water quality, recovery, water temperature, membrane material, and the presence of other contaminants such as biological containments (Kinslow and Hudkins 2004).

As membrane systems are integrated treatment processes for removal of a variety of constituents, the treatment of scaling can not be viewed in a vacuum. While membrane manufacturers typically provide a recommended pH level to prevent scaling in their system, this pH level is usually not ideal for other applications or unit processes. An example is removal of hydrogen sulfide in feed water. The presence of hydrogen sulfide in gaseous form is a secondary standard issue for odor and, as Sulfate and elemental sulfur, it can irreversibly damage reverse osmosis membranes. To combat these effects, it is common practice to operate a system where the feed water supply and membrane system itself exclude the introduction of air to protect the membranes. A post-treatment such as counter-current forced draft aeration is used to remove the gaseous fraction to reduce odors.

Christopher et al (2002) found that optimizing acid addition feed locations was a way to limit scaling while also optimizing hydrogen sulfide removal in the post–treatment two stage wet scrubber. The original plant operation included one acid addition feed point prior to cartridge filtration where the pH of the raw water feed was lowered using sulfuric acid to prevent scaling in the membranes and improve removal of gaseous hydrogen sulfide efficiency in the scrubber. Trying to accomplish both pretreatments at one injection point resulted in a pH significantly lower then what the manufacturer recommended for scaling and a high acid demand because the Floridan aquifer source water had a high alkalinity. Lowering the pH was also detrimental to removal of dissolved ions of sulfide species as the pH forced the distribution to the gaseous forms. The resulting permeate plus blend water had a high chlorine demand since the dissolved

sulfide species were not removed by the membranes. By adding a second acid feed point after the membranes the facility was able to reduce acid dosage, increase control of hydrogen sulfide, increase removal of total sulfide species, and reduce the amount of chlorine needed for disinfection. Optimizing the use of acid is important as plants move toward scale inhibitor only pretreatment of membranes.

3.2.2 Biological Growth

Biofouling is the accumulation of microorganisms at or near the surface of the membrane. It is a widespread problem in membrane treatment applications. Biofouling occurs in two processes: attachment and growth. Detecting biofilm formation in biofouling processes in the earliest stages is critical to efficient and cost effective protection of many membrane systems (Fonseca et al 2003). Aerobic surface or groundwaters typically require bio-fouling control which can be achieved by addition of NH_2Cl or other bactericidal agents (Duranceau and Henthorne 2004).

3.2.3 Organic Matter

Dissolved naturally occurring organic substances have been recognized as a cause of membrane fouling in facilities that treat natural waters. The major component of natural organic matter (NOM) in aquatic environments is typically humic substances (Letterman et al 1999). Humic substances do not have a well-defined structure and are typically low to moderate molecular weight. Hong and Elimelech (1997) found and increased flux

decline is associated with larger molecular weight (MW) species. Depending on the type of substance, dissolved organic matter fouling can change the charge properties of the membrane.

Organic fouling can occur in surface water systems with total organic carbon (TOC) greater then 3-6 mg/L. Organics are typically removed by coagulation, sedimentation, and filtration. Integrated membrane systems (IMSs) can also be used to limit organic fouling. While the reality of organic fouling is known the significance of this type of fouling compared to others is not (Duranceau and Henthorne 2004).

3.2.4 Particulates/Colloidal Fouling

Colloidal particulate fouling can be accomplished by adsorption, pore blocking, or deposition/cake formation. Adsorption is internal fouling and occurs at the surface and in pores when the diameter of the particle is less than the diameter of the membrane pore. Adsorption typically occurs in the initial stages of operation and can result in a significant drop in performance. Loss of permeate flow is irreversible except by backwash and chemical cleaning. In particulate fouling by adsorption the number of membrane pores remains constant, however, the diameter of the pore decreases. The change in pore volume due to fouling is proportional to the filtrate volume.

Pore blocking is another type of internal fouling where the diameter of the particle is equal to the diameter of the pore. In this type of fouling the diameter of the pores

remains constant but the total number of pores decreases. The change in pore volume due to fouling is proportional to the filtrate volume. Pore blocking is generally observed in commercial membranes due to the broad pore size distribution. A large drop in permeate flow can be seen in initial stages of operation because the larger pores that are blocked make up a major fraction of the pore volume available for the flow. Pore blocking may continue for extended periods of time in polydisperse suspensions (Hong 1999).

Cake layer deposition is an external fouling mechanism where the diameter of the particle is greater then the diameter of the pore. The increase in foulant deposited mass is proportional to the filtrate volume. The drop in permeate flux is due to increased resistance through the cake. The cake layer produces a sieving action at the surface of the membrane. Formation of this cake layer can improve the removal of small particles in UF and MF membranes that would otherwise pass through. Cake layer deposition can be controlled by washing the membranes and increasing crossflow velocity.

3.3 Fundamentals of Particle Fouling

Colloidal and suspended particles are a major foulant in natural source waters. Colloids are suspended particles in the size range of 0.01 to 10 μm. They are ubiquitous in most natural and wastewaters and are a principal cause of membrane fouling. The discussion of fundamental colloidal fouling to follow focuses on crossflow membrane configuration. Colloidal fouling mechanisms in a membrane system can be can be categorized as

colloidal transportation and deposition and cake layer formation and growth (Hong 1999).

The permeation flow yields an accumulation of particles at the membrane surface, which causes an increase in the particle concentration. The concentration gradient in the solution induces a diffusive flux of solute particles back into the bulk solution. This force is small compared to permeate drag, thus sieving and ultimately cake formation occurs. Concentration polarization is a precursor to cake formation. The particles reach a maximum value and then form a cake that grows until it reaches a steady state balance with the tangential forces produced by the crossflow velocity (Hong 1999).

Permeation drag is caused by friction between the solvent and retained particles. This friction results in a pressure drop. Incorporating the influence of neighboring particles on the hydrodynamic drag force can be achieved through Happel's cell model or through statistical mechanical procedures based on Stokes' equation. Happel's cell model is applied in a concentrated system where the hydrodynamic interactions are considerably modified due to the presence of neighboring particles. In a dilute system friction is represented by the classical Stokes friction factor (Hong 1999).

The classical Derjaguin-Landau-Verwey-Overbeek (DLVO) potential is commonly used to determine the colloidal interactions between particles. Electrostatic double layer force and van der Waals force are the main types of colloidal interactions (Hong 1999). Electrostatic or Coulombic interactions are between charged atoms. Electrostatic forces

occur in membrane treatment because when a body is immersed in water or other solvent the surface of the body acquires a charge that must be balanced by oppositely charge ions in solution. The van der Waals force arises from the dispersion forces between the atoms constituting the colloidal particles. The van der Waals force is a single lumped force of Debye (permanent dipole/induced dipole), Keesom (permanent dipole/permanent dipole), and London (induced dipole/induced dipole) interactions. The force is always attractive in aqueous media.

Colloidal forces, Brownian forces, and permeation drag govern the structure of the cake layer. Colloidal forces are dictated by interparticle separation, solution ionic strength and particle charge. Gravity and inertia forces affect colloidal fouling but are dictated by particle size so their impact is typically much smaller.

Colloidal fouling theory and the models developed to predict colloidal fouling are complex and influenced by many physical and chemical factors. These factors can be broadly categorized as membrane and particle properties, membrane hydrodynamics, and feed water chemistry (Hong 1999).

3.3.1 Membrane Surface Properties

Pore Size

Pore size has minimal effect on permeate flux when the pore size is less than the size of the particle. However, when the particle is smaller then the pore the permeate flux increases with decreasing pore size. The degree of fouling is highly dependant on the penetration of the particle into the membrane surface.

Roughness

Surface roughness has been shown to have a profound effect on colloidal fouling. Vrijenhoek et al (2001) conducted a study of four RO/NF membranes to characterize the factors that influence the initial colloidal fouling of the membranes. Atomic Force Microscopy (AFM), zeta potential, contact angle, pure water permeability, and observed salt rejection were used to evaluate the membranes performance. The analysis found that pure water permeability had a weakly negative correlation to fouling while salt rejection had a moderate-to-strong positive correlation. Surface roughness, represented by average roughness, had a very strong correlation with fouling compared toe the other factors. As the average roughness increased the flux decline also increased. For two membranes with the same salt rejection the less rough membrane exhibited a lower percent flux decline. Cellulose acetate and aromatic polyamide thin-film composite RO membranes were compared in a study by Elimelech et al. (1997) to demonstrate the effect of surface

morphology on colloidal fouling. The study found that the fouling rate of the thin-film composite membranes were significantly higher then the cellulose acetate membranes. The higher fouling potential was attributed to the greater surface roughness in the thin-film composite membranes.

Charge

The materials and manufacturing processes used to produce RO and NF membranes result in various surface charges. Surface charge behaves as intuition would dictate. If the repulsion forces decrease the fouling increases. Due to the immobile Stern layer it is not possible to directly measure the surface potential energy. It is possible to calculate the zeta potential by measuring the streaming potential. This is done by forcing an electrolyte solution through a channel formed by the surface to be measured using hydraulic pressure. This generates a streaming current which results in a potential difference. The measured potential difference at equilibrium conditions is the streaming potential (Elimelech and Childress 1996).

Vrijenhoek et al (2001) used 0.10 μm (±0.03μm) silica particle in an aqueous solution to characterize colloidal fouling. Zeta potential for all membranes tested was between –13 and –25 mV. These negative values at testing conditions indicate that the repulsive electrostatic double layer interactions should develop with the negatively charged silica particles and the membrane surface. A correlation to fouling behavior was not reported

and lack of a clear trend was attributed to surface roughness differences in the membranes studied.

An increase in zeta potential results in lower fouling and increase permeate flux for oppositely charged particles and membrane surfaces. Decreasing charge allows more deposition of particles on the surface due to the lower repulsive forces. A reduced charge can produces flocs of increased size that results in a less dense cake which allows better filtration.

Hydrophobicity

Some data shows no difference between hydrophilic and hydrophobic membranes. However, the consensus is that hydrophilic membranes outperform hydrophobic membranes based on the nature of the hydrophilic membrane. Hydrophilic membranes have a thin layer of H_2O surrounding the surface when immersed which makes deposition of particles difficult.

3.3.2 Membrane Hydrodynamics

Hydrodynamic forces in a simplified membrane model without a spacer can be represented as two-dimensional forces that are tangential and normal to the membrane surface. They arise from hydrodynamic interactions resulting from the relative motion of solvent with respect to colloidal particles and various thermodynamic forces resulting

from chemical potential gradients and interparticle or particle to membrane interactions. Formation of the cake layer is dominated by the interplay of permeation drag, Brownian Forces and interparticle interactions with permeation drag being the most critical.

Permeation Velocity

The force normal to the membrane surface is due to permeation flow and the corresponding permeation velocity. Permeate flux decline is directly proportional to the permeation velocity. Increasing permeate velocity increases the rate of particle deposition due to the increased permeate drag. The increased permeate drag compresses the cake layer due to the increased pressure. Faibish et al, (1998) filtered a colloidal suspension at various pressures to study the effects of initial permeation rate on permeate flux. The study found that as the transmembrane pressure increased the permeate stream flux decreases. This was attributed to the higher rate of transport of particles to the surface and greater packing density of the cake layer caused by the higher permeation velocity.

Crossflow Velocity

The tangential force arising from crossflow velocity is inertial lift. Inertial lift may be negligible for small colloids. Permeate flux decline is proportional to the cross flow velocity with permeate flux decline decreasing with increasing cross flow velocity.

The crossflow membrane filtration configuration is more popular due to the lower fouling that results from the crossflow velocity.

Turbulence

Turbulence can have an impact on flux decline. Increasing turbulence results in a reduction in the permeate flux decline. Turbulence can be induced by spacers or altering the membrane configuration.

3.3.3 Feed Water Chemistry

The possibility of tailoring the cake layer properties by tailoring the feed solution composition is an attraction option in controlling membrane fouling. The manipulation of solution properties can produce cake layers of different permeability and thickness.

pH

The impact of pH on permeate flux decline is difficult to summarize without discussing the electro kinetic properties of the particle and the membrane. In general, permeate flux decline will decline faster where both are neutrally charged.

Ionic Strength

The permeate flux decline increases with increasing ionic strength. As the ionic strength increases the electrostatic forces between particle/particle and particle/membrane decreases. High ionic strength results in larger flocs. Larger flocs form a more permeable cake layer. As ionic strength increases the electrostatic double layer forces are reduced producing a denser cake layer.

Divalent Cations / Hardness

The presence of divalent cations, or ions with a positive two charge, has an influential role on fouling. Since calcium is typically the dominant portion of hardness in natural water supplies it is usually chosen as a representative divalent cation. The presences of the calcium ion is significant as the precipitation of calcium carbonate, calcium-organic complexes, co-precipitation of organics and calcite, and adsorption of organics onto calcite can all attribute to fouling of membrane treatment systems (Her et al2000).

Particle Size

Decreasing particle size increases the fouling of the membrane and develops a thicker cake. This is due to smaller particles being less susceptible to shear induced hydrodynamic conditions and inertial migration. Increasing size results in lower resistance through the cake layer due to the larger flow channels. Increase in particle concentration increases fouling with a thicker cake that has R_H proportional to the

concentration (Hong 1999). Hong, et al. (1997) conducted an experiment utilizing 100 nm and 300 nm silica particles suspended in a 0.01 M KCl solution. The synthetic colloidal water was filtered using a tubular ceramic membrane. The study determined that permeate flux decreases as particle size decreases and attributed this finding to the higher hydraulic resistance created by the smaller particles.

3.4 Methods to Control Particle Fouling

Much research has been conducted to study factors that can be adjusted to minimize particulate/colloidal fouling. Optimization of membrane properties or conditions within a membrane treatment system can combat particulate/colloidal fouling. A reduction of the membranes surface roughness or enhancing the surface charge can reduce fouling. Depending upon the foulant, enhancement of the surface charge could have a detrimental effect by increasing the attractive forces between the particle and the membrane.

Optimization of the membrane treatment system is a common way to combat fouling. Addition of MF or UF membrane treatment prior to NF or RO membranes can remove or reduce particulates/colloids. Increasing the colloid size by addition of coagulants is popular and creates a more permeable cake layer. Coagulation in combination with MF or UF will increase the removal of colloidal particles. Addition of a stabilizer to enhance the charge of colloids can also be effective in applications with oppositely charged membranes.

Operation at a lower permeation flux or below the calculated critical flux for the feedwater can reduce fouling. Increasing the crossflow velocity and enhancing turbulence are other physical ways to reduce colloidal fouling. Optimization of the feed solution chemistry can also be beneficial. Decreasing the salt concentrations, reducing divalent cations, and optimizing pH are all ways to minimize colloidal fouling.

In theory, the options above are all viable solution to reduce the effects of colloidal fouling, however, in practice most are not feasible. Outside of laboratory conditions, most are eliminated from consideration due operational cost and complexity. The two methods commonly used to control colloidal particle fouling are particle stabilization and reduction of particle concentration. Particles are stabilized by adding a dispersing agent and the particle concentration is typically reduced by conventional coagulation sedimentation filtration (CSF) processes, MF and/or UF, and MF/UF with in-line coagulation. Optimization of the membrane treatment process design and operating conditions such as flux, backwash, recovery, membrane configuration, and chemical cleaning successfully reduce overall fouling but have not been fundamentally shown to specifically target colloidal fouling.

3.5 Membrane Monitoring Methods

As drinking water standards become more stringent and more utilities turn to membrane treatment as the solution, the quality of membrane manufacturing techniques and testing methods to quantify membrane integrity in field conditions will become more of a focus

of the industry. The development and utilization of non-invasive and on-line membrane fouling monitoring in laboratory and industrial applications may enable the effectiveness of fouling remediation and cleaning strategies to be quantified and improved in public and private utilities that operate membrane treatment processes. For years, membrane manufacturers have developed testing that can be categorized as either direct or in-direct techniques. Some states require integrity testing while in others testing is at the discretion of the utility.

In low pressure membrane applications, the most widely used testing techniques are the pressure hold (pressure decay) test for detecting minor breaches of membrane integrity and particle counting and/or turbidity monitoring to detect more pronounced membrane integrity failures and to meet regulatory requirements (Farahbakhsh et al 2003).

Membrane testing can be categorized as either direct or indirect. Direct techniques include the Bubble Point Test, Pressure Decay and Diffusive Airflow Tests, and the Vacuum Hold Test. Particle Counting, Particle Monitoring, and Turbidity Monitoring are indirect monitoring techniques.

3.6 Emerging Pollutants of Concern

A “new” group of contaminants has recently been introduced t the water and wastewater industries: Emerging Pollutants of Concern (EPOCs). Until recently researchers did not have the means, equipment, or know-how to even detect theses contaminants (Kavanaugh

2003). EPOCs is the coverall term for a group of currently unregulated chemicals that have been determined to be harmful to humans and wildlife. These chemicals consist of Disinfection By-products (DBPs), Endocrine Disrupting Chemicals (EDCs), Hormonally Active Agents (HAAs), Organic Wastewater Contaminants (OWCs), Personal Care Products (PCPs), and Pharmaceutically Active Compounds (PhACs) (Manning Hudkins and Schmidt 2003). EDCs are derived from man-made chemicals and interfere with the normal functioning of the endocrine systems of humans and wildlife. HAAs include birth control, estrogen, steroids, and other hormonal modifying medications. PCPs include chemical agents found in cosmetics, deodorants, fragrances, lotion, etc. PhACs include prescribed and non-prescribed medications (Manning Hudkins and Schmidt 2003). These pollutants find their way into water supplies as treated wastewater effluent, surface water runoff, and other natural pathways such as excretion and waste disposal. The concerns of EPOCs are ever evolving and the issue is complicated by limited environmental data. Recent studies have suggested that relatively low concentrations of EPOCs could affect human health and the sustainability of aquatic ecosystems (Schmidt and Manning Hudkins 2004).

The concern of the effect of EPOCs is even more relevant with the proliferation of indirect and direct potable reuse operations. Groundwater recharge with treated wastewater is the most common example of indirect recharge. Unplanned indirect reuse is also a reality as wastewater treatment facilities effluent disposal discharges and water treatment facilities source waters share common surface and ground waters. Kavanaugh (2003), however, reported a study by the US Army corps of Engineers where a

conventional WTP incorporating GAC following filtration produced a superior water quality utilizing a 50:50 mixture of Potomac river water and secondary effluent from a nitrification plant than the local WTPs utilizing surface water only. Later studies confirmed the results of this study however uncertainties with the performance exceeded the potential benefit of utilizing this water for potable use. The experiment did raise the question of at what point does a surface water source become unacceptable as a source for conventional treatment and would then require GAC or other more advanced technologies (Kavanaugh 2003). Bellona et al, (2003) cites high-pressure membrane treatment such as RO or NF following MF as the industry standard for indirect potable reuse.

While there is limited data on affect and amount of EPOCs in the environment, several studies have shown the effectiveness of RO for the treatment of a wide variety of EPOC categories including antibiotics, pharmaceuticals, hormones and industrial chemicals (Adams et al 2002, Kimura et al 2003, and Li et al, 2004). During bench and pilot scale studies Li et al, (2004) found that RO treatment of wastewater allowed for partial rejection of EPOCs with molecular weights below the molecular weight cut-off of the membranes. Other studies have utilized membrane bioreactor (MBR) technology utilizing MF or UF membranes for the removal of EPOCs. Bellona et al, (2003) listed zeta potential/charge, surface morphology/roughness, molecular weight cut-off, pore size/distribution, hydrophobicity/contact angle and diffusion/partition coefficient as key membrane properties to assess and predict rejection of EPOCs. Drewes, et al (2004)

conducted research on negatively charged hydrophilic compounds and found that they are removed by RO and NF membranes through electrostatic exclusion.

CHAPTER 4: MATERIALS AND EXPERIMENTAL METHODS

4.1 Membranes Tested

The research tested a total of 20 different RO membranes, including three commercially manufactured thin film composite polyamidic RO membranes. The fouling resistant membranes used for comparison to the existing Saehan products were LFC-1 (Hydranautics), X-20 (Trisep), and BW30FR (Dow-FilmTec). Initial water mass transfer coefficients (MTCs) were 0.09 to 0.15 gsfd/psi, and all three manufacturers considered the membranes to be low pressure RO. All other membranes in this report are products in various stages of development from Saehan.

4.2 Membrane Filtration Unit

Membrane filtration experiments were performed using two filtration units shown in Figure 4.1. Both units utilized Osmonics Sepa CF membrane cells. Filtration unit one used one high foulant stainless steel test cell and filtration unit two consisted of two identical, low foulant, stainless steel test cells (Sepa CF, Osmonics Inc., Minnetonka, MN) operated in parallel. All cells had channel dimensions of 14.5 cm (5.7 in) in length and 9.4 cm (3.7 in) in width, yielding an effective membrane area of 1.361×10^{-2} m^2 (21.1 in^2). The high foulant cell had a channel height of 1.72 mm (0.068 in), while the low foulant cells were 0.86 mm (0.034 in) in height. The feed solution for both units was contained in a 20 L (5 gal) HDPE Nalgene Cylindrical Tank and was mechanically

agitated by a Thernolyne Cimarec 3 magnetic stirring plate. The feed solution was pumped out of the reservoirs and pressurized by identical Hydracell pumps (Wanner Engineering), which delivered 4.2 lpm (1.1 gpm) at a maximum pressure of 3.4 Mpa (500 psi). The temperature of the feed solution was maintained at 20°C (68°F) by refrigerated recirculators (Neslab CFT-33) used in combination with stainless steel heat exchange coils. The concentrate flow (crossflow velocity) was monitored by means of a floating disk flowmeter (Blue White Industries) and could be adjusted with a by-pass valve (Swagelok). The feed pressure was controlled by a back pressure regulator (U.S. Paraplate) located immediately downstream of the test cell concentrate exit. The crossflow velocity and feed pressure could be finely controlled by careful adjustment of the by-pass valve and the back pressure regulator. The permeate flow, operation time, and cumulative volume of permeate were continuously monitored and recorded by digital flow meters (Humonics,) interfaced with PCs. Figure 4.2 shows the process flow diagram for the low foulant unit. Process flow was identical for the high foulant cell with the exception of only having one cell instead of two as shown in Figure 4.2.

4.3 Membrane Filtration Experiments

Flat sheet testing was used to characterize the membranes as well as perform initial fouling potential analysis. Membrane characterization was achieved by clean water testing, and fouling potential by various source waters.

4.3.1 Clean Water Non-fouling Experiments

Analysis of the productivity of the SN membranes was determined by a series of well-controlled non-fouling tests (detailed protocol follows). These flat sheet tests were performed on all 15 membranes according to the following procedure. Each membrane was placed in the flat sheet Sepa Cell module (Osmonics) and circulated with stabilization solution. The stabilization solution, 20 liters of 10-3 NaHCO3 held at 20oC by means of a recirculating chiller and mixed constantly with a magnetic stirrer, was consistent with that of the fouling runs. Also consistent with the fouling runs, the flux was set at 17 gsfd (6.57 mL/min). The membrane was allowed to stabilize for 125 minutes, after which the flux was verified and adjustments to the pressure were made to recover flux, if necessary. Stabilization of the membrane was continued for an additional 30 minutes and then the pressure was recorded. At this point, NaCl was added to create a 2000 ppm solution. The pressure was readjusted to recover the loss in flux due to the affect of osmotic pressure. After the flux was recovered, the saline solution was run for 30 minutes similar to all other flat sheet tests. Feed and permeate samples were then collected for analysis and were measured with a conductance meter (Model 32, YSI) to determine selectivity.

Figure 4.1 Flat Sheet Membrane Filtration Units
Top: Testing Unit 1 using One 68 mil Osmonics Cell.
Bottom: Testing Unit 2 using Two 34 mil Osmonics Cells.

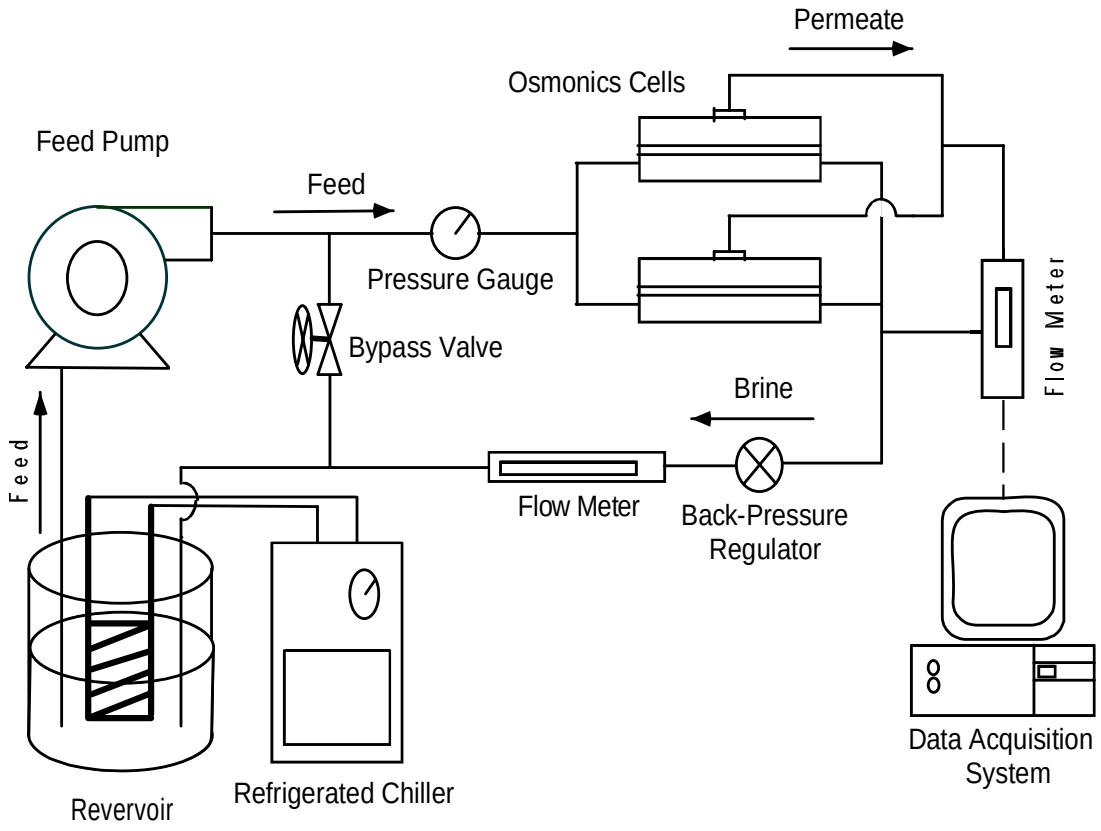

Figure 4.2 Flat Sheet Membrane Filtration Unit Configuration

Initial Cleaning Protocol

1. Disconnect permeate line from flowmeter and recycle flow
2. Verify Osmonics cell does not membrane, place empty cell in cell holder, and pressurize.
3. Fill reservoir with approximately 16 liters of tap water.
4. Add one spoon each of SLS and EDTA and mix thoroughly.
5. Clear excess fluid from the system lines.
6. Circulate solution for 45 minutes minimum.
7. Rinse system with tap water.
8. Prepare pH 10 solution using DI water and NaOH.
9. Clear excess fluid from the system lines.
10. Circulate solution for 45 minutes minimum.
11. Prepare pH 3 solution using DI water and Citric Acid.
12. Clear excess fluid from the system lines.
13. Circulate solution for 45 minutes minimum.
14. Rinse system thoroughly with DI water.

Protocol

1. Verify that O-rings in the cell body bottom fit properly in the grooves.
2. Install the feed spacer in the cell body bottom so that it lies flat and is contained within the central cavity.

3. Cut the flat sheet membrane sample so that the outer edge fits between the inner and outer O-rings. Punch holes in the sample to fit the four alignment pins.
4. Place membrane sample over the feed spacer with the active side down.
5. Wet the permeate carrier (permeate spacer) with DI water and place in the cavity on the cell body top.
6. Place the cell body top on the cell body bottom.
7. Insert cell body into the cell holder until it rests against the two stops on the cell holder.
8. Using the hydraulic hand pump provided by Osmonics, pressurize the cell holder to approximately 1000 psig.
9. Place pump inlet hose in stabilization solution. Stabilization solution is 20 liters of 10^{-3} $NaHCO_3$ held at $20^{o}C$ by means of a recirculating chiller and mixed constantly with a magnetic stirrer.
10. Place bypass and concentrate lines into a 4 liter graduated cylinder.
11. Start pump with the bypass valve completely open, the feed valve completely closed, and the concentrate valve completely open.
12. Allow the pump to stabilize and enough stabilization solution to pass through the bypass line into the graduated so that it is flushed completely of any entrapped air or fluid (2 liters).
13. Transfer the bypass line from the graduated cylinder to the stabilization solution reservoir.
14. Slowly open the feed valve until it reaches the fully open position.

15. Slowly close the bypass valve until it reaches the fully closed position.
16. Allow enough stabilization solution to pass through the tubing to flush the system.
17. Transfer the concentrate line from the graduated cylinder to the stabilization solution reservoir when 2 liters of total discharge is reached.
18. Slowly increase pressure on the membrane by closing the backpressure regulator valve until approximately 6.57 mL/min (17 gsfd) is reached on the flowmeter.
19. Adjust pressure until a consistent reading appears on the flowmeter.
20. Open flowmeter software and set the system to run for 125 minutes.
21. Record initial inlet and outlet pressures and concentrate and permeate flow rates.
22. Maintain initial pressure readings (± 2 psig) for the duration of the stabilization period.
23. After 125 minutes verify flux is 6.57 mL/min (17 gsfd), adjust pressure if necessary to recover flux.
24. Run stabilization solution for additional 30 minutes.
25. Record final inlet and outlet pressures and concentrate and permeate flow rates.
26. Add NaCl to reach 2000 ppm.
27. Verify flux is 6.57 mL/min (17 gsfd); adjust pressure if necessary to recover flux.
28. Run saline solution for additional 30 minutes.

29. Record final inlet and outlet pressures and concentrate and permeate flow rates.
30. To end run slowly open bypass valve until it reaches the completely open position.
31. Slowly close feed valve until it reaches the completely closed position.
32. Turn off pump.

Cleaning Protocol

1. Disconnect permeate line from flowmeter and recycle flow
2. Verify Osmonics cell does not membrane, place empty cell in cell holder, and pressurize.
3. Fill reservoir with DI water.
4. Rinse system thoroughly with DI water for 30 minutes.

4.3.2 Fouling Experiments

The fouling potential of each membrane was assessed through bench-scale filtration experiments. Filtration experiments consisted of three phases: cleaning, stabilization, and fouling (see detailed protocol following this section). Prior to fouling experiments, the membrane filtration units were cleaned thoroughly using (SDS/SLS), sodium hydroxide, and citric acid solutions. The membrane sections were then placed in each test cell and sealed using a hydraulic press. All filtration experiments were preceded by a

stabilization period of 18-24 hours in which the membranes were equilibrated with deionized (DI) water that contained 10^{-3} M $NaHCO_3$ (pH ≈ 7.9) at a pressure that produced the predetermined initial flux for the given run e.g. 29 lmh (17 gfd). After stabilization, the test unit was flushed with 3.8 liters (1.0 gallons) of the testing solution to remove the sodium bicarbonate solution from the system. The membranes were then evaluated for 48 hours with 16 liters (4.2 gallons) of the testing solution at an initial flux of 29 lmh (17 gfd). Variations in permeate flux were monitored and plotted against operation time in order to assess the performance of the membranes. The selectivity of each membrane was evaluated for each fouling experiment at the beginning of each fouling test. Both feed and permeate samples were collected for TDS and TOC or TDS and Turbidity analyses, whichever was appropriate for feed chemistry. The conductance of both the feed and permeate streams were measured with a conductance meter (Model 32, YSI). TOC data were obtained through the use of a TOC analyzer (Phoenix 8000 UV-Persulfate Analyzer, Dohrmann). Turbidity was determined with a HACH Ratio Turbidimeter (Model 18900).

Stabilization Protocol

1. Verify that O-rings in the cell body bottom fit properly in the grooves.
2. Install the feed spacer in the cell body bottom so that it lies flat and is contained within the central cavity.

3. Cut the flat sheet membrane sample so that the outer edge fits between the inner and outer O-rings. Punch holes in the sample to fit the four alignment pins.
4. Place membrane sample over the feed spacer with the active side down.
5. Wet the permeate carrier (permeate spacer) with DI water and place in the cavity on the cell body top.
6. Place the cell body top on the cell body bottom.
7. Insert cell body into the cell holder until it rests against the two stops on the cell holder.
8. Using the hydraulic hand pump provided by Osmonics, pressurize the cell holder to approximately 1000 psig.
9. Place pump inlet hose in stabilization solution. Stabilization solution is 16 liters of 10^{-3} $NaHCO_3$ held at $20^{o}C$ by means of a recirculating chiller and mixed constantly with a magnetic stirrer.
10. Place bypass and concentrate lines into a 2 liter graduated cylinder.
11. Start pump with the bypass valve completely open, the feed valve completely closed, and the concentrate valve completely open.
12. Allow the pump to stabilize and enough stabilization solution to pass through the bypass line into the graduated so that it is flushed completely of any entrapped air or fluid.
13. Transfer the bypass line from the graduated cylinder to the stabilization solution reservoir.
14. Slowly open the feed valve until it reaches the fully open position.

15. Slowly close the bypass valve until it reaches the fully closed position.
16. Allow enough stabilization solution to pass through the tubing to flush the system.
17. Transfer the concentrate line from the graduated cylinder to the stabilization solution reservoir when 2 liters of total discharge is reached.
18. Slowly increase pressure on the membrane by closing the backpressure regulator valve until approximately 6.57 mL/min (17 gsfd) is reached on the flowmeter.
19. Adjust pressure until a consistent reading appears on the flowmeter.
20. Open flowmeter software and set the system to run for 18 hours.
21. Record initial inlet and outlet pressures and concentrate and permeate flow rates.
22. Maintain initial pressure readings (± 2 psig) for the duration of the stabilization period.
23. After 18 hours record final inlet and outlet pressures and concentrate and permeate flow rates.
24. To end stabilization run slowly open bypass valve until it reaches the completely open position.
25. Slowly close feed valve until it reaches the completely closed position.
26. Turn off pump.

Fouling Protocol

1. Prepare 20 L of the fouling solution within 2 hours of the end of stabilization.
2. Using the hydraulic hand pump provided by Osmonics, pressurize the cell holder to approximately 1000 psig.
3. Place pump inlet hose in fouling solution.
4. Place bypass and concentrate lines into a 2 liter graduated cylinder.
5. Start pump with the bypass valve completely open, the feed valve completely closed, and the concentrate valve completely open.
6. Allow the pump to stabilize and enough fouling solution to pass through the bypass line into the graduated so that it is flushed completely of any entrapped air or fluid.
7. Transfer the bypass line from the graduated cylinder to the fouling solution reservoir.
8. Slowly open the feed valve until it reaches the fully open position.
9. Slowly close the bypass valve until it reaches the fully closed position.
10. Allow enough fouling solution to pass through the tubing to flush the system.
11. Transfer the concentrate line from the graduated cylinder to the fouling solution reservoir when 2 liters of total discharge is reached.
12. Slowly increase pressure on the membrane by closing the backpressure regulator valve until approximately 6.57 mL/min (17 gsfd) is reached on the flowmeter.
13. Adjust pressure until a consistent reading appears on the flowmeter.

14. Open flowmeter software and set the system to run for 48 hours.
15. Record initial inlet and outlet pressures and concentrate and permeate flow rates.
16. Maintain initial pressure readings (± 2 psig) for the duration of the fouling period.
17. After thirty minutes passes collect permeate and raw water samples.
18. Measure conductance and turbidity.
19. After 48 hours record final inlet and outlet pressures and concentrate and permeate flow rates.
20. To end fouling run slowly open bypass valve until it reaches the completely open position.
21. Slowly close feed valve until it reaches the completely closed position.
22. Turn off pump.
23. Release pressure on cell and carefully remove membrane.

Cleaning Protocol

1. Disconnect permeate line from flowmeter and recycle flow
2. Verify Osmonics cell does not membrane, place empty cell in cell holder, and pressurize.
3. Fill reservoir with approximately 16 liters of tap water.
4. Add one spoon each of SLS and EDTA and mix thoroughly.
5. Clear excess fluid from the system lines.

6. Circulate solution for 45 minutes minimum.
7. Rinse system with tap water.
8. Prepare pH 10 solution using DI water and NaOH.
9. Clear excess fluid from the system lines.
10. Circulate solution for 45 minutes minimum.
11. Prepare pH 3 solution using DI water and Citric Acid.
12. Clear excess fluid from the system lines.
13. Circulate solution for 45 minutes minimum.
14. Rinse system thoroughly with DI water.

4.4 Source Water Analysis

After each source water was obtained, the basic parameters of water quality were conducted immediately after returning to the laboratory. All analysis was conducted according to the 19th edition of Standard Methods for the Examination of Water and Wastewater. Hardness was determined by the EDTA titrametric method, while alkalinity was performed using the titration method outline in Section 2-25. TDS was obtained through conductance measurement with a YSI Model 32 Conductance Meter. TOC data were gathered through the use of a Phoenix 8000 UV-Persulfate TOC Analyzer (Dohrmann). A HACH Ratio Turbidimeter (Model 18900) was used to determine turbidity.

4.5 Membrane Surface Characterization

The rate and extent of colloidal fouling in RO/NF processes are greatly influenced by membrane properties, particularly surface charge and roughness. In order to correlate fouling potential to membrane surface characteristics, all membranes were carefully characterized prior to fouling experiments. The surface roughness was characterized by Atomic Force Microscopy (AFM) and Scanning Electron Microscopy (SEM). The surface charge was measured by Streaming Potential Analyzer (SPA).

4.5.1 Surface Charge

The zeta potential of the membrane surface was determined using a streaming potential analyzer (BI-EKA, Brookhaven Instruments Co.). All measurements were performed at room temperature (approximately 22°C) with a background electrolyte solution of 10^{-2} NaCl. To avoid ionic interference, the acid and base legs (based on the initial pH) were titrated with separate membrane samples in order to generate a zeta potential curve from pH 3 to 11 (see detailed protocol following this section). Two separate tests were performed for each membrane, and trend lines were developed using the best-fit logarithmic model for both tests.

Protocol for Zeta Potential

Note: The following protocol is written in terms of a single titration direction (acid or base). Therefore, this procedure must be carried out twice in order to develop a complete pH-ZP curve from pH 3 to pH 11.

1. Prepare the following solutions:
    a. Membrane soak solution: 1000 mL of 0.01 M NaCl
    b. Electrolyte solution S1: 1000 mL of 0.01 M NaCl
    c. Electrolyte solution S2: 1000 mL of 0.01 M NaCl
    d. Electrode soak solution: 250 mL of 0.001 M NaCl
    e. Acid titrant T1: 100 mL of 0.1 M HCl
    f. Base titrant T2: 100 mL of 0.1 M NaOH
    g. Dilute pH buffer solutions at pH's of 4, 7, and 10 (100 mL)

2. 24 hours prior to measurement session, prepare samples as follows:
    a. For each sample, cut two (2) membrane specimens in 127 mm x 50 mm rectangles (Cut membranes with active side down on parafilm).
    b. Use Exacto knife and templates provided (see page 22 of EKA Manual) to cut channel openings and locator pin holes in samples.
    c. Rinse thoroughly with DI water.
    d. Place in soak solution for 24 hours.

3. Rinse cell and all spacers, sample and parafilm gaskets (obtained from cutting the sample) thoroughly with DI water.
4. Assemble rectangular measurement cell:
    a. Starting with top half of cell (the half with locator pins), install PTFE sealing foil (the foil with inlet and outlet but without longitudinal slit).
    b. Install parafilm gasket (the sample with inlet and outlet).
    c. Install first membrane specimen (the specimen with inlet and outlet).
    d. Install two (2) PTFE channel spacers (the ones with longitudinal slit).
    e. Install second membrane specimen (the specimen with locator pin holes only).
    f. Install parafilm gasket (the one with locator pin holes only).
    g. Install lower PTFE sealing foil.
    h. Install lower half of cell.
    i. Tighten clamps.

5. Turn on computer and EKA analyzer (version 4.24); start EKS program in DOS (do not run DOS through windows).
    a. Type EKS at prompt.
    b. Choose sample test.
    c. Type in appropriate headings.
    d. Choose Monitor (F2).

6. Install cell onto EKA analyzer by slipping cell gently onto stainless steel holder.
    a. Remove electrodes from soak solution and insert into cell all the way into each channel. Be careful not to damage electrode tips. Note: with multiple runs it is advantageous to leave electrodes in the cell while changing the sample. This prevents damage to tips and reduces downtime.
        1. Short circuit the electrodes by connecting them to each other with one wire.
        2. Loosen clamps and rest them gently on the electrodes.
        3. Change the sample using procedure above.
    b. Attach hoses to cell by pressing downward until they snap into place.

7. Rinse 2 times with no recirculation with DI water. Use 15/20 rinse (15 seconds for each bypass direction and 20 seconds for each cell direction). When rinsing the cell with flow from right to left (<), gently pull cell outward away from EKA analyzer and twist 30^{o} counter-clockwise to remove entrapped air. When the flow is from left to right (>), gently pull cell outward away from EKA analyzer and twist 30^{o} clockwise.

8. Calibrate pH probe at two points and check with a third depending upon what pH range is being tested (monitor pH between runs and repeat calibration when necessary).
    a. Calibrate with pH 4 and 7 and check with 10 for the acid half of pH-ZP curve.
    b. Calibrate with pH 7 and 10 and check with 4 for the base half of pH-ZP curve.

9. Calibrate external conductivity probe using one shot standard (for multiple runs **be sure to check conductivity calibration often** and repeat when drift occurs). Lack of accurate conductivity calibration is the major cause of non-reproducible data.

10. Rinse with S1 using a 15/20 rinse and no recirculation while stirring with a magnetic stirrer.

11. Rinse with S2 using a 30/30 rinse while recirculating with 5 repeats. Ensure that all entrapped air is removed from the cell by repeating the procedure for removing air as outlined in step 7 above.

12. Take measurement using 300 mbar, reversing flow, 8-step program (see instruction manual for loading).

13. Assuming measurement program is loaded:
    a. Go to Single Test by escaping from Monitor mode.
    b. Press F1 (Start).
    c. When measurement is complete, save data and return to Monitor mode (do not correct for surface conductance). Measurement recorded is for "natural" pH.

14. Adjust pH in the direction that the pH probe was calibrated (either acid or base).

15. Rinse with circulation for 10 minutes using 30/30 rinse with 5 repeats. Note: pH adjustment will be required until the pH stabilizes. Also, it is necessary to increase rinse time for pH 7 to 20-30 minutes to be sure the solution has stabilized.

16. Repeat steps 11-14 for a range of pHs to develop either the acid or base half of the pH-ZP curve (Be sure to proceed from natural pH to either acid or base. Do not develop the entire pH-ZP curve with one set of membrane samples.).

17. After reaching pH 3 or 10, titrate back to natural pH.

18. If developing a complete pH-ZP curve:
    a. Disassemble cell and rinse all components thoroughly with DI water.
    b. Reassemble the cell with two new specimens of the same sample.
    c. Repeat steps 6 through 16 except recalibrate the pH probe and titrate in the opposite direction.

19. When shutting down the EKA:
    a. Rinse two (2) times with DI water using 15/20 rinse and no recirculation.
    b. Remove electrodes, place tips in protective plastic sleeves, and place in soak solution.
    c. Remove tubes from cell and lift cell off of EKA.
    d. Disassemble cell and rinse all components thoroughly with DI water.
    e. Rinse pH probe with DI water and place in saturated KCl solution.

f. Drain internal tubing of EKA to deter biological growth.

g. Turn off EKA and computer.

h. Clean all glassware and equipment.

4.5.2 Surface Roughness

The roughness of a membrane surface is dependent on not only the size and shape of the "peaks" or surface projections, but also on their frequency and distribution. The surface roughness of each membrane was characterized by Atomic Force Microscopy (AFM) and verified by Scanning Electron Microscopy (SEM). The Digital Instruments (DI) NanoScope™ was selected to analyze the surface roughness for all membrane samples. In order to minimize sample damage and maximize resolution, the DI AFM was operated in Tapping Mode. This mode operated by scanning a tip attached to the end of an oscillating cantilever across the surface of the sample, which resulted in the "tapping" of the tip on the surface of the sample. The vertical position of the scanner at each (x, y) data point was stored by the computer, which formed a topographic image of the sample surface. In addition, the computer analyzed these data which made it possible to determine a host of parameters, including average roughness and 3-dimensional surface area. In order to ensure representative data, a total of ten scans were performed for each membrane, each on a separate membrane section. These data were then tabulated and the best five were determined and then averaged and analyzed to evaluate membrane surface roughness. Furthermore, SEM photographs (JOEL 6400F Scanning Electron Microscope) were taken to validate the results obtained through the DI AFM.

In order to ensure representative data, a total of three scans were performed for each membrane, each on a separate membrane section. These data were then tabulated, averaged, and analyzed to evaluate the effects of surface roughness on the rate and extent of membrane fouling. Furthermore, SEM photographs were taken on a JOEL 6400F scanning electron microscope to validate the results obtained through the DI AFM. The results of AFM and SEM scans are presented in Appendix A in Figures A.1 to A.5 and Tables A.1 to A.5. The SEM pictures exhibited a very good visual agreement with AFM scans for all of the membranes tested.

4.6 Membrane Performance Analysis

Membrane productivity performance was developed by determining the water mass transfer coefficient (MTC), flux decline ratio (FDR), and rejection (R). The MTC of the membrane system was determined by relating the adjusted water flux and the NDF as shown in Equation 1:

$$K_w = F_w / NDF \qquad (1)$$

Where K_w is the water mass transfer coefficient, F_w is the water flux, and NDF is the net driving force across the membrane. The water flux of the system was determined by dividing permeate flow rate by total available membrane surface area which was the area of Sepa Cell flat inside the O-ring. The net driving force is the amount of energy supplied to produce permeate water and was defined as the pressure applied by the back pressure

regulator across the membrane. The flux decline ratio was determined according to the following equation:

$$FDR = Flux_F / Flux_0 \qquad (2)$$

Where FDR is the flux decline ratio, $Flux_F$ is the average flux of the last five data points which encompass the last 144 minutes of the 48-hour experiment, and $Flux_0$ is the initial flux. Rejection calculations for TDS, TOC, and turbidity were developed similarly, according to equation 3:

$$R = C_p / C_f \qquad (3)$$

Here R is the overall rejection, C_p is the concentration of the constituent in the permeate, and C_f is the concentration of the feed solution.

CHAPTER 5: RESULTS AND DISCUSSION

The analysis of Saehan's membranes was split into two major areas of study: 1) a comparison of Saehan's commercial products to commercial (USA) FRMs and 2) evaluation of Saehan experimental membranes. The membranes were first characterized by surface roughness and surface charge and then their relative performances were measured using flat sheet testing for different feed waters. Performance parameters were defined in the Methods Chapter and were flux decline, MTC, % TOC, % TDS and % turbidity rejection.

Table 5.1 shows the membranes analyzed and the parameters determined during the testing. Membranes tested included two (2) Saehan commercial membranes, three (3) non-Saehan commercial fouling resistant membranes (FRMs) available in the United States, seven (7) Saehan experimental membranes, and 8 Saehan experimental membranes with post-treatment. The commercial Saehan membranes performance was compared to existing FRMs with groundwater and synthetic colloidal water. The experimental Saehan membranes with and without post-treatment was analyzed with clean water and surface water experiments.

Table 5.1 Membranes Analyzed, Characteristics Measured, and Feed Water Condition

	Characteristics		Clean Water				
Membranes	Roughness	Charge	J/Jo	MTC	% TDS Rejection	% TOC Rejection	% Turbidity Rejection
3 Commercial	x	x					
7 Saehan Experimental	x	x		X	x		
8 Saehan Experimental with Post-Treatment	x	x		X	x		
2 Saehan Commercial	x	x					
	Characteristics		Groundwater				
Membranes	Roughness	Charge	J/Jo	MTC	% TDS Rejection	% TOC Rejection	% Turbidity Rejection
3 Commercial	x	x	x	X	x	x	
7 Saehan Experimental	x	x					
8 Saehan Experimental with Post-Treatment	x	x					
2 Saehan Commercial	x	x	x	X	x	x	
	Characteristics		Surface Water				
Membranes	Roughness	Charge	J/Jo	MTC	% TDS Rejection	% TOC Rejection	% Turbidity Rejection
3 Commercial	x	x					
7 Saehan Experimental	x	x	x	X	x	x	
8 Saehan Experimental with Post-Treatment	x	x	x	X	x	x	
2 Saehan Commercial	x	x					
	Characteristics		Colloidal Water				
Membranes	Roughness	Charge	J/Jo	MTC	% TDS Rejection	% TOC Rejection	% Turbidity Rejection
3 Commercial	x	x	x	X	x		x
7 Saehan Experimental	x	x					
8 Saehan Experimental with Post-Treatment	x	x					
2 Saehan Commercial	x	x	x	X	x		x

5.1 Evaluation of Existing Non-Saehan FRM's and Saehan Commercial Membranes

This section details the performance of Saehan's membrane products at various physical (hydrodynamic) and chemical operating conditions in comparison with commercial non-Saehan FRMs available in the United States. The investigation outlined in this section illustrates the operation of Saehan's commercial membranes under actual and simulated drinking water treatment conditions. Two source waters, a groundwater from a surficial aquifer in southern Florida and a synthetic colloidal water (Chapter 3) were used to show these effects. This research provides fundamental and practical information which is essential for developing Saehan's FRM. In addition, the results will also systematically investigate the effect of membrane surface properties on particulate and organic matter fouling in RO and/or NF membrane filtration.

5.1.1 Natural Groundwater Fouling

In order to evaluate fouling potentials, a high organic groundwater from the City of Plantation in southern Florida was obtained and characterized. Currently, the City of Plantation utilizes two membrane water softening treatment facilities, the 12.0 MGD Central Water Treatment Plant and the 6.0 MGD East Water Treatment Plant. Experimental source water used in the current research was obtained from the Central Water Treatment Plant. The Central Water Treatment Plant source water comes from the Biscayne Aquifer. This surficial aquifer is tapped by eight wells, each 140 feet deep,

which can provide a total feed flow rate of 16 MGD. These wells provide the Central Plant with a very consistent quality of source water.

5.1.1.1 Source Water Quality

The groundwater samples were taken from one of eight wells that supply the Central Water Plant with water from the surficial Biscayne Aquifer. Samples were collected from the City of Plantation's Central Water Plant on July 28, 1999 for testing purposes. These samples were immediately analyzed to determine water quality parameters. The average values of the measured parameters followed relatively closely to the values reported by the Plantation City water utilities (Table 5.2), with few exceptions.

Table 5.2 Source Water Quality of Groundwater (Hobbs 2000)

	Plantation (Central), FL	
	Wet Season	Dry Season
Parameter	Average	Average
PH	7.1	7.2
TDS (mg/L)	349	349
Hardness (mg/L as $CaCO_3$)	307	306
Alkalinity (mg/L as $CaCO_3$)	275	277
Iron (mg/L)	1.4	1.5
Turbidity (NTU)	N/A	N/A
TOC (mg/L)	22	22
Silt Density Index	0.70-0.95	0.70-0.95
Temperature (^oF)	77	77

The measured pH value of the samples averaged to be 7.87, which was slightly higher than the reported value of 7.1-7.2. The total dissolved solids also measured higher, 427

mg/L, than the reported value of 349 mg/L. Total organic carbon measured less than the value reported by the utility at 17.5 mg/L. Hardness and alkalinity values of 333 mg/L as $CaCO_3$ and 281 mg/L as $CaCO_3$, respectively, agreed very well with the reported values of 307 mg/L as $CaCO_3$ and 276 mg/L as $CaCO_3$. However, the silt density index (SDI_{15}) obtained through the testing of these samples, 6.1, is significantly higher than the values of 0.70-0.95 the utility reports and above the accepted normal range for treatable waters (< 3.0). It is likely that this unusual reading is the result of precipitation due to oxygen being introduced to the groundwater. Lastly, the modified fouling index (MFI) and turbidity measurements yielded values of 7.68 s/L^2 and 3.4 NTU, respectively.

5.1.1.2 Groundwater Fouling Test Results

The fouling behavior of Saehan's products (Saehan A and Saehan B) and the non-Saehan commercial FRMs (LFC1, X-20, and BW30FR) were first studied using this organic rich groundwater utilized by the membrane softening plant of City of Plantation, Florida. A series of bench-scale, flat sheet, fouling experiments were performed by following the experimental protocol summarized in Chapter 4. Tables 5.3 and 5.4 show the results of the fouling experiments for the groundwater and colloidal water, respectively. Statistical analysis performed on this data is summarized in Table 5.5.

Table 5.3 Results of Flat Sheet Testing Commercial Saehan Membranes and FRMs with Groundwater

Commercial Membrane	Ground Water - Plantation						
	Roughness (nm)	Charge (mV)	J/Jo	MTC* (gsfd/psi)	% TDS Rejection	% TOC Rejection	Pressure
LFC1	52	-5.41	100	0.112	98.7	98	134
X20	33.4	-15.18	92.6	0.084	97.2	97.9	174
BW30FR	56.7	-6.19	95.6	0.096	98.1	98.1	154
Saehan A	60.8	-7.02	92	0.087	98.2	98.3	173
Saehan B	60.2	-6.78	92.5	0.094	98.6	98.3	161

* Measured after 18 to 20 hrs of Stabilization run as described in Chapter 3.

Table 5.4 Results of Flat Sheet Testing Commercial Saehan Membranes and FRMs with Synthetic Colloidal Water

Commercial Membrane	Colloidal Water						
	Roughness (nm)	Charge (mV)	J/Jo	MTC* (gsfd/psi)	% TDS Rejection	% Turb	Pressure
LFC1	52	-5.44	99.5	0.107	98.9	99.6	160
X20	33.4	-15.20	98.4	0.093	99	99.8	184
BW30FR	56.7	-6.21	98.8	0.107	99.3	99.9	159
Saehan A	60.8	-7.05	97.1	0.100	98.9	99.9	172
Saehan B	60.2	-6.79	97.9	0.108	99.4	99.6	158

* Measured after 18 to 20 hrs of Stabilization run as described in Chapter 3.

Table 5.5 Statistical Analysis of Commercial Saehan Membranes and FRMs

Membrane Group	Feed Water	y-variable	Coefficients			P-value		
			Intercept	Roughness	Charge	Intercept	Roughness	Charge
Commercial	Ground Water - Plantation	J/J_0	140.1	-0.580	1.853	**9.358E-05**	**0.0010**	**0.0008**
		MTC	0.220	-0.002	0.006	**0.0132**	**0.048**	**0.029**
		% TDS Rej	99.6	-0.005	0.150	**0.0005**	~~0.89~~	0.23
		% TOC Rej	96.3	0.028	-0.045	**9.605E-06**	**0.020**	0.058
	Synthetic Colloidal Water	J/J_0	110.8	-0.168	0.450	**0.0006**	**0.044**	**0.049**
		MTC	0.125	0.000	0.002	**0.0468**	~~0.76~~	0.24
		% TDS Rej	98.1	0.016	-0.028	**0.0005**	~~0.65~~	~~0.77~~

[1] **Bold** = significant with 95% interval, normal font = significant with 75% interval, and ~~strikethrough~~ = not significant

The results of the regression shown in Table 5.5 were as follows:

1. For Groundwater testing of the Commercial Membranes

    a. J/Jo decreases as negative surface charge and roughness increase

    b. MTC decreases as negative surface charge and roughness increase

    c. % TDS rejection is independent of surface charge and roughness

    d. % TOC rejection increases as negative surface charge and roughness increase

2. For Colloidal water testing of the Commercial Membranes

    a. J/Jo decreases as negative surface charge and roughness increase as did groundwater testing

    b. MTC was independent of roughness and decreased as surface charge increased

    c. % TDS rejection is independent of surface charge and roughness as was observed in groundwater testing

The following summarizes the findings for the analysis performed for comparison of Saehan's existing membrane products with commercial non-Saehan FRMs available in the United States:

1. Membranes with less negative surface charge or roughness will foul less and have higher MTCs.

2. TDS rejection is independent of surface charge or roughness for both groundwater and synthetic colloidal water.

3. The effects of surface roughness and charge on % TOC rejection were opposite to flux decline and the MTC, which is rational and indicates the mass transfer of water and TOC is similar with respect to surface roughness and charge, and somewhat indicates the majority of TOC removal is controlled by size exclusion.

Figures B.1 to B.21 (in Appendix B) show the permeate flux versus operation time for the membranes tested. The permeate flux shown in these figures is the average permeate

flux for two side-by-side fouling tests. Inspection of these figures reveals the rate or extent of fouling for each individual membrane over the time of operation. For purpose of comparison, it is important to note permeate flux decline is presented as flux decline ratio, which is defined as MTC_{final} / $MTC_{initial}$. The three commercial fouling resistant membranes, LFC-1, X-20, and BW-30FR, yielded flux decline ratios of 100%, 92.6 %, and 95.6%, respectively during 48 hrs of testing period, while both Saehan membranes A and B yielded ratios of 92.0% and 92.5%. Flux decline ratio is presented in Figure 5.1, which illustrates the superior performance of the FRMs.

- The data clearly show that the LFC-1 membrane is by far the most fouling resistant membrane of the five membranes tested based on fouling potential defined as the flux decline ratio. The calculated flux decline ratio of 100% indicates that there was no evidence of fouling over this period of time. All FRMs performed better than the Saehan membranes; although Saehan A and B are not "fouling resistant," they did perform similarly to the low end of the FRMs results. This was clearly evident when comparing to X-20. Figure A.2.2 shows the rapid flux deterioration exhibited at the early stage of the filtration experiment.

The superior performance of commercially available FRMs was evident from this series of testing, and statistical analysis demonstrated the effect of reduced surface roughness and more neutrally charged surfaces. Table 5.5 shows that surface roughness and surface charge are statistically significant to J/J_0 and MTC at the 95% confidence interval.

Surface roughness has a negative coefficient so the higher the roughness the lower the J/J_0. Surface charge had a positive coefficient so a more negative charge resulted in a lower J/J_0. X-20, however, did not perform as well as the other FRMs, and had fouling potentials much closer to those of Saehan's commercial products. The explanation seems to be in the large disparity of surface charge, which was nearly triple the magnitude of both the other FRMs and Saehan membranes. This more negative surface proved detrimental to X-20's performance, with this specific water, by actually pulling foulants to the membrane surface and increasing fouling potential. An additional argument could be made on the basis of surface roughness. Differentiating between average roughness and surface area difference when assessing the roughness of a membrane surface is an important concept (Hobbs 2000). Surface roughness results can have a wide variance depending on the frequency and distribution of surface projections. For example, the LFC-1 membrane had an average roughness of 52.0 ± 67.4 nm however, due to low peak counts (average of 146), LFC-1 exhibited a small surface area difference, which was measured at 16.9%. The X-20 membrane, in contrast, had almost six times as many peaks (average of 859) as LFC1, but these peaks were about half the size, averaging 33.4 ± 41.6 nm. Due to this high peak frequency, the surface area difference of X-20 membrane (32.7%) was nearly twice as large as that of the LFC-1 membrane. While an increase in peak count does not significantly affect the average roughness, it can dramatically increase the surface area difference (Hobbs 2000), as is the case with X-20. X-20's greater flux decline than LFC1 can be attributed to this larger surface area difference, which increases the surface area available for adsorption of organic foulants. Roughness was analyzed as average roughness for the comparison of Saehan products to

FRMs. Linear regression analysis of the membranes found that membranes with less roughness had less fouling potential. The results of surface roughness analysis can be found in Appendix A.

The study of the Plantation source water by Hobbs (2000) was conducted on additional RO and NF membranes indicated that membrane fouling became more severe with increasing surface roughness, as measured by the surface area difference, which accounts both magnitude and frequency of surface peaks. In their study, Membrane surface charge, however, was loosely related to permeate flux decline, compared to surface roughness. No clear correlation was established between hydrophobicity and flux decline ratio, primarily due to the narrow range of membrane hydrophobicity studied.

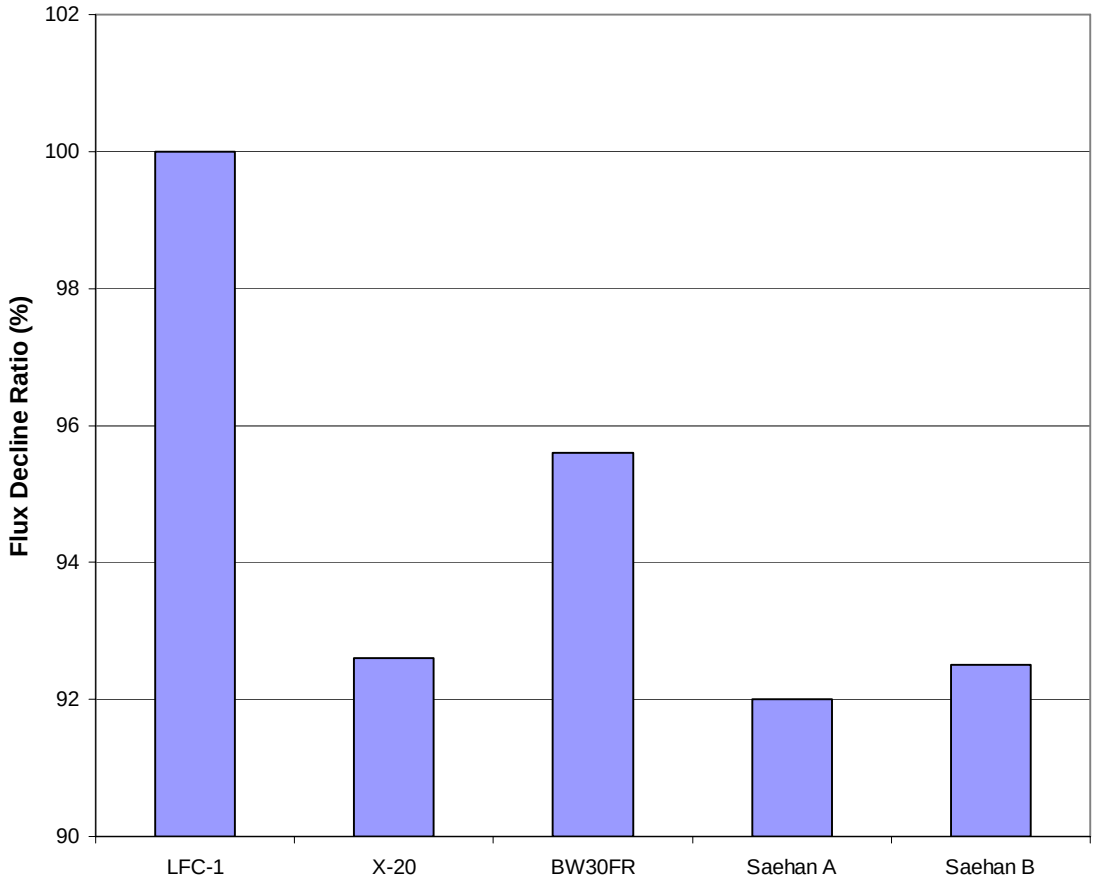

Figure 5.1 Flux Decline Ratio for FRMs and Saehan Products with Groundwater.

5.1.1.3 Rejection Capability

The selectivity of the FRMs and Saehan membranes was evaluated using the groundwater. At the beginning of each fouling test (30 minutes after the initial record), both feed and permeate samples were collected for TDS and TOC analysis. The feed and permeate TDS were obtained through conductance measurement with a YSI Model 32 Conductance Meter. Similarly, TOC data were gathered through the use of a Phoenix 8000 UV-Persulfate TOC Analyzer (Dohrmann). Table 5.3 shows both the TDS and TOC rejection data for each of the selected membranes. LFC-1 was the top performing FRM with salt rejection averaging 98.7% and TOC rejection averaging 98.0%. BW30FR also rejected TDS and TOC well at an average of 98.0% and 98.1%, respectively. Both Saehan membranes A and B performed very well with TDS rejection of 98.2% and 98.6% and TOC rejection of 98.3% and 98.3%, respectively. The membrane with the overall worst rejection capability was the X-20 with a TDS rejection of 97.2% and a TOC rejection of 97.9%. Statistical analysis of the relative performance is summarized in Table 5.5. Surface roughness was statistically significant to TOC rejection at the 95^{th} percentile while surface charge was not statistically significant. Surface roughness had a positive coefficient, so the more rough membranes had better TOC rejection.

Surface roughness was not statistically significant to TDS rejection, however, surface charge was significant at the 75^{th} percentile. Consistent with J/J_0 and MTC, the surface charge coefficient was positive indicating a more negatively charged surface would lower the TDS rejection. Analysis of the entire TDS data set, however, results in rejections

lower than all of the manufacturer's specifications. This may be a result of the wide disparity between NaCl concentration for the manufacturer's (1500-2000 ppm) and the experimental fouling (427 ppm) testing conditions. Investigation of this possible discrepancy can be found in Section 5.2.2. The Saehan membranes performance with regard to TDS and TOC rejection followed the trend of performance from Table 5.3. The Saehan membranes had results similar to the FRMs and outperformed X-20.

The effects of surface roughness and charge on % TOC rejection were opposite to flux decline and the MTC, which is rational and indicates the mass transfer of water and TOC is similar with respect to surface roughness and charge, and somewhat indicates the majority of TOC removal is controlled by size exclusion.

5.1.2 Synthetic Colloidal Water

Fouling potentials were also evaluated by testing the fouling behavior of the membranes using a synthetic water. The water consisted of a solution containing 10^{-3} M $NaHCO_3$, 7×10^{-3} M NaCl (400 ppm), and 0.001% MP-1040 silica particles (Nissan Chemical Industries, LTD). The performance of existing Saehan membranes was evaluated using this solution and compared to the FRMs.

5.1.2.1 Source Water Quality

A detailed analysis of constituents present in synthetic source waters is presented in this section. This source water contained MP-1040 colloidal Silica particles from Nissan Chemical Industries, Ltd. The characteristics of MP-1040 listed in the manufacturer's Certificate of Analysis are reproduced in Table 5.6.

Table 5.6 Characteristics of MP-1040 Colloidal Silica

Specific Gravity (at 20°C)	1.301 [-]
Concentration SiO_2	40.7 [wt%]
Na_2O	510 [ppm]
pH	9.1 [pH]
Viscosity (at 25°C)	2.6 [cp/mPa-sec]
Particle Diameter	0.10 [μm]

Concentration of MP-1040 particle stock suspension was determined to be 43.4 weight percent of stock solution by the gravimetric analysis, which compares favorably to the manufacturer's value of 40.7 percent (as SiO_2). The difference can be attributed to the trace amount of Na_2O (<0.8%) known to be present in the composition of the particles, as well as, some minor experimental/measurement error. Density of MP-1040 particles was determined to be 2.11 [g/cc] which compares well with other reported values. Density (equivalent to specific gravity) of MP-1040 stock solution was determined to be 1.29 [g/cc], which is very close to the manufacturer's reported value of 1.301.

The size of colloidal silica used in the screening studies was determined by Photon Correlation Spectroscopy (PCS) of quasi-elastically scattered light (Zeta PLUS,

Brookhaven Instruments Corp.). This technique correlates the fluctuations about the average, scattered, laser light intensity, which is used to calculate the translational diffusion coefficient. The particle diameter is then calculated by the Stokes-Einstein diffusivity relation. The average diameter of MP-1040 colloidal Silica was determined to be approximately 138 nm by this technique as shown in Figure 5.2 (a). The particle size measured is larger than the value reported by the manufacturer, probably due to the presence of doublets. This observation was also confirmed by SEM image presented in Figure 5.2 (b).

Particle Zeta Potential behavior of MP-1040 particles was determined by measurement of Electrophoretic Mobility by Phase Analysis Light Scattering (PALS) and subsequent calculation of Zeta Potential (Zeta PALS, Brookhaven Instruments Corp.) internally by PALS software. PALS is an extension of laser Electrophoretic Light Scattering (ELS), but is more sensitive than conventional ELS (capable of measuring velocities up to 1000 times smaller than ELS). Figure 5.3 shows the Zeta Potential behavior of MP-1040 at 10^{-2} M-NaCl and various pH conditions. The isoelectric point of these colloids was determined to be approximately 2, consistent with previous electrokinetic studies involving silica colloids. As pH increased, the silica colloids became more negatively charged.

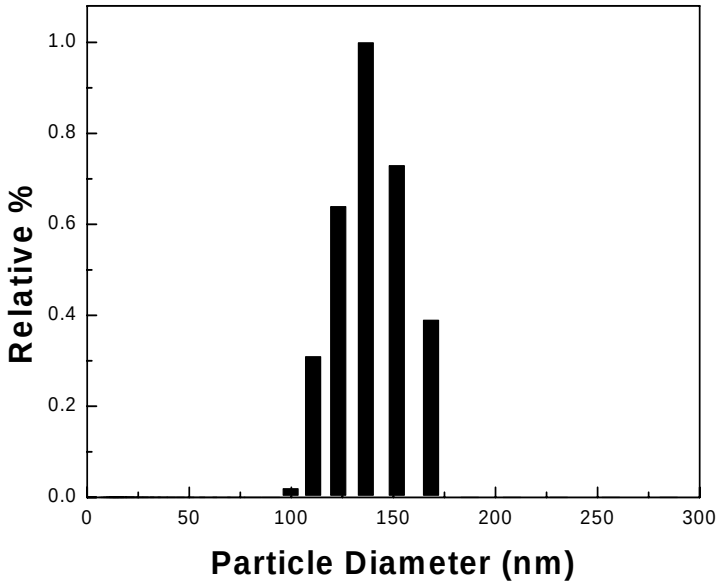

(a)

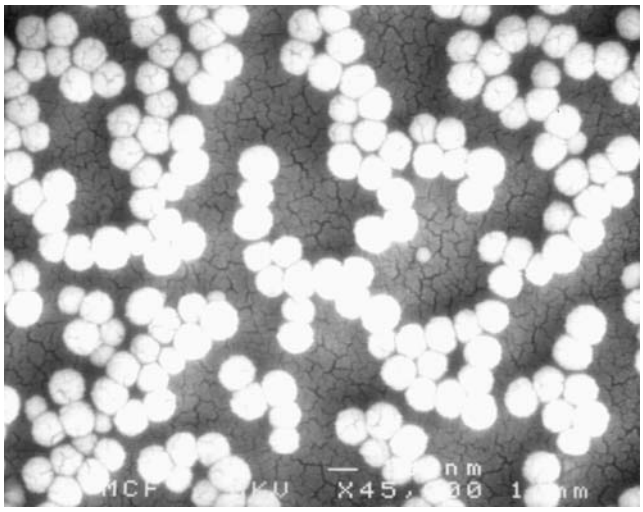

(b)

Figure 5.2 Size of Colloidal Silica (MP-1040)
(a) - PCS analysis
(b) - SEM analysis.

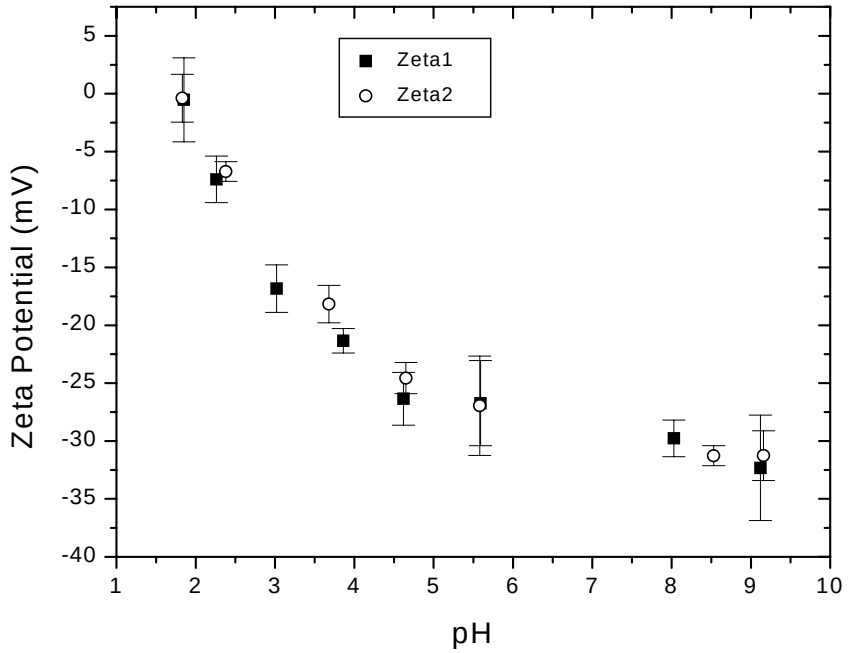

Figure 5.3 Zeta Potential Behavior of MP-1040 Colloidal Silica

5.1.2.2 Synthetic Water Fouling Test Results

Synthetic water was used to further determine the fouling Behavior of the commercial FRMs and Saehan membranes. The permeate flux versus operation time for the five membranes tested is shown in Figures A.2.6-A.2.10. All data sets appear to have data consistent with the intrinsic variation of flat sheet testing. Table 5.4 provides flux decline ratio, initial flux, and initial pressure data for each membrane tested. The flux decline ratio defines the extent of flux change for the 48-hour testing period. The three commercial fouling resistant membranes, LFC-1, X-20, and BW30FR, demonstrated flux decline ratios of 99.5%, 98.4%, and 98.8%, respectively. Saehan A had a flux decline

ratio of 97.1%, while Saehan B had a ratio of 97.9%. Statistical analysis of the membranes performance can be found in Table 5.5. Surface roughness and surface charge were significant for J/J_0 in the 95^{th} percentile and had negative and positive coefficients, respectively. Thus a rougher and more negatively charged membrane will have a lower J/J_0. Surface roughness was not statistically significant for MTC or TDS performance. Surface charge was not statistically significant for TDS removal, but was significant in the 75^{th} percentile for MTC. Since the coefficient was positive a more negatively charged membrane had a lower MTC.

In agreement with the groundwater and surface water testing, the FRMs outperformed both Saehan membranes in fouling potential as measured by J/J_0. This indicates that the 0.01 μm silica colloidal particles were deposited and accumulated much less on the surface of the commercial FRMs. This observation suggests that small colloidal particles were more easily captured by the rougher surface of Saehan membranes. However, as Figure 5.4 depicts, the relative difference between the membranes was not as significant as it was in the natural groundwater testing (Figure 5.1).

It is important to note that no claims or trends on the relative performance between the FRMs or the Saehan membranes are being enumerated as a result of this set of testing. The evaluation is reserved to the general performance of the FRMs to Saehan A and B, which concurred with the previous source waters. The basis for this limitation in the overall assessment of the membranes is the testing conditions themselves. Synthetic water experiments were conducted at 17 gsfd, but unlike the natural water tests they also

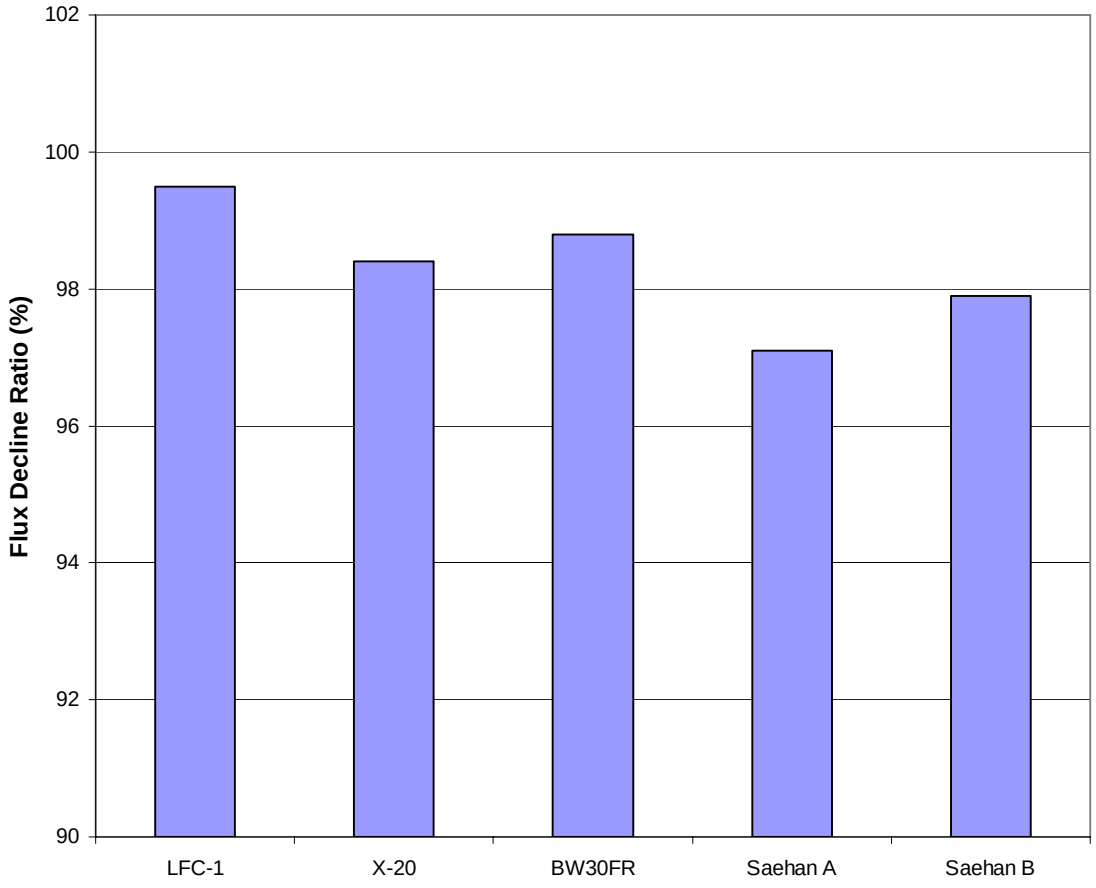

Figure 5.4 Flux Decline Ratio for FRMs and Saehan Products with Synthetic Colloidal Water.

included feed spacers. Spacers were not included in fouling experiments because the turbulence created by the spacers significantly decreased the fouling potential measured in the 48-hr experiments. Turbulence in the cross flow could account for reduced fouling potential. Quantification of the various RO and NF membrane performance can be found in the recent study by Hobbs 2000. In this work, colloidal fouling is conducted with the same silica particles, but at a much higher flux (30 gsfd) and without the presence of feed spacers. It was concluded that colloidal fouling was directly related to the surface roughness. The more rough the surface the more probable that particles would accumulate in the "valleys" of the surface, and therefore the potential for "valley clogging" would be greatly increased. This type of fouling does not occur on smoother surfaces, thus the flux decline due to this type of colloidal fouling would be less severe for less rough membranes.

5.1.2.3 Rejection Capability

The selectivity of the FRMs and Saehan membranes was evaluated using the synthetic water. Feed and permeate samples were collected for TDS and Turbidity analysis consistent with that of Section 5.1.1.3. The feed and permeate TDS were obtained through conductance measurement with a YSI Model 32 Conductance Meter. Turbidity data were gathered through the use of a HACH Ratio Turbidimeter (Model 18900). TDS and Turbidity rejection data for each of the selected membranes appears is Table 5.4. The lowest rejection for either parameter was 98.9%, indicating the excellent selectivity for all membranes. This superb performance resulted in an inability to develop a clear

trend from either parameter. Statistical analysis shown in Table 5.5 found that TDS rejection was independent of surface charge and roughness.

5.2 Evaluation of Saehan's Developmental Fouling Resistant Membranes

With assessment of Saehan's commercial membranes compared to existing FRMs complete, this section will focus on the characteristics and performance of Saehan's systematic development of their version of a fouling resistant membrane. The Saehan membrane progression can be separated into three coating techniques: **(1) single, (2) double, and (3) special**.

Coating techniques are patent pending and considered trade secrets, but the intent was to improve the fouling potential of the existing Saehan products by varying surface properties such as the charge and hydrophilicity. In addition to surface chemistry alterations, both stages subjected the Saehan commercial product to a **post-treatment** process with the purpose of increasing the mass transfer coefficient and TDS rejection. The parameters of most interest in the progression of Saehan's new membranes are the coating technique and post-treatment effects.

In order to study these effects, the series of new membranes were first evaluated according to the differences in membrane properties, and then each membrane was subjected to both clean water and fouling flat sheet testing. Tables 5.7 and 5.8 show the results of the clean water testing. Tables 5.9 and 5.10 show the results of the fouling

experiments for the surface water. Statistical analysis performed on this data is summarized in Table 5.11.

Table 5.7 Results of Flat Sheet Testing Saehan Experimental Membranes with Clean Water

Saehan-Experimental Membrane		Clean Water				
		Roughness (nm)	Charge (mV)	MTC (gsfd/psi)	% TDS Rejection	Initial MTC no salt (gsfd/psi)
SN2	Single Coat Negative	99.3	-3.48	0.0719	98.2	0.0794
SN3	Single Coat Neutral	97.7	-3.38	0.0667	98.9	0.0769
SN4	Double Coat Neutral	107.6	-3.07	0.0765	96.6	0.0858
SN5	Double Coat Positive	101.6	-1.27	0.0717	96.2	0.085
SN6	Special Coat Negative	90.4	-2.99	0.072	97.6	0.0813
SN7	Special Coat Neutral	99.3	-2.62	0.0769	95.8	0.0848
SN8	Special Coat Positive	83.2	-1.64	0.0853	95.8	0.093

Table 5.8 Results of Flat Sheet Testing Saehan Experimental Membranes with Post Treatment with Clean Water

Saehan-Experimental Membrane with Post Treatment		Clean Water				
		Roughness (nm)	Charge (mV)	MTC (gsfd/psi)	% TDS Rejection	Initial MTC no salt (gsfd/psi)
SN1CP	Commercial	58.5	-2.08	0.1108	94.9	0.1347
SN2P	Single Coat Negative	103.8	-2.93	0.0794	99.1	0.0897
SN3P	Single Coat Neutral	111.5	-3.28	0.0788	99.2	0.0884
SN4P	Double Coat Neutral	103.9	-3.79	0.0811	98.4	0.0925
SN5P	Double Coat Positive	77.8	-2.53	0.0816	98.5	0.0944
SN6P	Special Coat Negative	77.8	-4.31	0.0938	99.4	0.1105
SN7P	Special Coat Neutral	89	-4.86	0.1077	99.1	0.124
SN8P	Special Coat Positive	81.9	-5.03	0.1077	98.3	0.1375

Table 5.9 Results of Flat Sheet Testing Saehan Experimental Membranes with Cocoa Surface Water

Saehan-Experimental Membrane		Surface Water - Cocoa					
		Roughness (nm)	Charge (mV)	J/Jo	MTC (gsfd/psi)	% TDS Rejection	% TOC Rejection
SN2	Single Coat Negative	99.3	-3.06	96	0.0562	96.5	99.4
SN3	Single Coat Neutral	97.7	-2.99	92.7	0.0632	96.4	98.8
SN4	Double Coat Neutral	107.6	-2.66	99.8	0.0637	98	99.4
SN5	Double Coat Positive	101.6	-0.82	99.2	0.0704	96.5	99.4
SN6	Special Coat Negative	90.4	-2.63	99.3	0.0702	98	99.4
SN7	Special Coat Neutral	99.3	-2.15	100	0.0748	96.9	99.4
SN8	Special Coat Positive	83.2	-1.26	98.3	0.0797	97.6	99.4

Table 5.10 Results of Flat Sheet Testing Saehan Experimental Membranes with Post Treatment with Cocoa Surface Water

Saehan-Experimental Membrane with Post Treatment		Surface Water - Cocoa					
		Roughness (nm)	Charge (mV)	J/Jo	MTC (gsfd/psi)	% TDS Rejection	% TOC Rejection
SN1CP	Commercial	58.5	-1.75	96.3	0.1033	97.4	99.4
SN2P	Single Coat Negative	103.8	-2.64	99.5	0.0741	97.6	98.8
SN3P	Single Coat Neutral	111.5	-2.94	98.7	0.0719	97.3	99.4
SN4P	Double Coat Neutral	103.9	-3.42	96.1	0.084	97.2	99.4
SN5P	Double Coat Positive	77.8	-2.24	95.5	0.0911	97.8	99.4
SN6P	Special Coat Negative	77.8	-3.87	95.5	0.1009	96	99.4
SN7P	Special Coat Neutral	89	-4.38	98.8	0.1137	96.8	99.4
SN8P	Special Coat Positive	81.9	-4.53	96.2	0.1142	97.4	99.4

Table 5.11 Statistical Analysis of Saehan Experimental Membranes

Membrane Group	Feed Water	y-variable	Coefficients			P-value		
			Intercept	Roughness	Charge	Intercept	Roughness	Charge
Experimental	Clean Water	MTC	0.107	0.000	0.003	**0.0214**	~~0.45~~	~~0.41~~
		% TDS Rej	96.0	-0.020	-1.131	**3.963E-05**	~~0.72~~	0.08
	Surface Water - Cocoa	J/J_0	94.8	0.069	1.609	**0.0025**	~~0.67~~	~~0.31~~
		MTC	0.123	-0.0004	0.005	**0.0101**	0.20	0.10
		% TDS Rej	99.3	-0.025	-0.081	**2.016E-05**	~~0.62~~	~~0.85~~
		% TOC Rej	99.4	0.0020	0.106	**1.649E-07**	~~0.89~~	~~0.44~~
Experimental with Post-treatment	Clean Water	MTC	0.126	-0.00064	-0.007	**0.0010**	**0.019**	**0.088**
		% TDS Rej	91.9	0.050	-0.568	**1.475E-07**	**0.078**	0.18
	Surface Water - Cocoa	J/J_0	92.4	0.059	0.165	**9.092E-07**	0.14	~~0.79~~
		MTC	0.127	-0.00079	-0.011	**9.358E-05**	**0.0010**	**0.0008**
		% TDS Rej	97.6	0.0075	0.331	**3.874E-09**	~~0.56~~	0.17
		% TOC Rej	99.6	-0.0052	-0.070	**3.942E-11**	~~0.33~~	~~0.45~~

[1] **Bold** = significant with 95% interval, normal font = significant with 75% interval, and ~~strikethrough~~ = not significant

The results of the regression shown in Table 5.11 were as follows:

1. For Testing of Saehan's Experimental Membranes
    a. With Clean Water
        i. MTC was independent of surface charge and roughness
        ii. % TDS rejection increased with negative surface charge and was independent of roughness
    b. With Surface Water
        i. Flux decline was independent of surface charge and roughness
        ii. MTC decreased with negative surface charge and roughness over time
        iii. % TDS rejection is independent of surface charge and roughness
        iv. % TOC rejection is independent of surface charge and roughness
2. For Testing of Saehan's Experimental Membranes with post treatment
    a. With Clean Water
        i. MTC increased with negative surface charge and decreased with increasing surface roughness
        ii. % TDS rejection increased with negative surface charge and with surface roughness
    b. With Surface Water
        i. Flux decline was independent of surface charge and increased with roughness
        ii. MTC increased with negative surface charge and decreased with roughness
        iii. % TDS rejection is independent of roughness and decreased with negative surface charge
        iv. % TOC rejection is independent of surface charge and roughness

The following summarizes the findings for the analysis performed on Saehan's experimental membrane products:

1. The productivity (MTC decline) and solute mass transfer (TDS and TOC) of Saehan's Experimental Membranes was generally independent of surface roughness and charge.

2. The productivity (MTC decline) and flux decline Saehan's Experimental Membranes with Post Treatment was generally dependent on surface roughness and charge; whereas, the solute mass transfer (TDS and TOC) of Saehan's Experimental Membranes without Post Treatment was generally independent of surface roughness and charge.

    a. Productivity increased with negative surface charge and decreased with roughness in both clean and surface water
    b. TDS rejection increased with negative surface charge in both clean and surface water

3. The effects of surface charge on % TDS rejection were opposite to its effect on MTC, which is rational and indicates the mass transfer of water and TDS is similar with respect to charge.

All examination in this section was conducted on the most recent shipment of Saehan's membranes, which included an existing commercial product (SN1CP, which was similar to the Saehan A and B membranes in the previous section), the new generation without post-treatment (SN2-SN8), and the new generation with post-treatment (SN2P-SN8P). Samples of the membrane were taken from 3-inch diameter by 12-inch long spiral wound elements. The investigation will provide information to the selection or further development of Saehan's FRM.

5.2.1 Membrane Properties

Before evaluation of the fouling potential of the Saehan Experimental or Saehan New (SN) membranes was initiated, the membranes surface properties were characterized by Atomic Force Microscopy (AFM) for surface roughness, and streaming potential analysis (EKA) for surface charge. These surface properties will be essential for analysis and correlation of fouling potentials.

5.2.1.1 Surface Roughness

Atomic Force Microscopy (AFM) was used to characterize the surface roughness of each membrane. Roughness has been shown to be an extremely important factor, with all other factors held constant, in the fouling potential of membranes in the presence of colloidal and organic foulants. Relevant figures can be found in Appendix A. The Digital Instruments (DI) NanoScope™ was selected to analyze the surface roughness for all membrane samples. Roughness analysis was conducted in two stages as SN membranes became available. SN2 through SN5, all without post-treatment, were the first group of membranes examined. In this group the data were tabulated and the best five of seven scans were determined, averaged, and analyzed to evaluate membrane surface roughness. The second stage included SN1CP, SN6-SN8, and SN2P-SN8P. This group of membranes included additional scans as the data was based on the best eight of ten scans. The average surface roughness for all membranes along with general coating information can be found in Tables 5.7 - 5.10.

SN1CP had an average roughness that agreed within 2.5 nm of the values reported for Saehan A and B, (60.8 nm and 60.2 nm respectively). Contrary to prior discussions with Saehan, the surface properties of the Saehan commercial product were not held constant while surface roughness was adjusted with little change to surface functional groups that can also directly affect the fouling potential of a membrane. Instead, it was these surface properties that were adjusted with an attempt to minimize roughness in the process. Therefore, it was not appropriate to compare the roughness of SN1CP to the rest of the developmental membranes, as other factors unknown to the researchers have been adjusted and not yet fully characterized for a proper discussion of the ramifications of these changes.

As noted, the key characteristics of interest in the SN products are the coating and post-treatment effects. Figures D.1 and D.2 illustrate the effect of coating on average surface roughness for SN membranes without and with post-treatment, respectively. Most of the membranes without post-treatment had surface roughness near 100 nm, but there was a trend of reduced roughness as coating moved from single to double to the special technique. This tendency agrees with the progression of membrane research and development from single coated membranes to the double and special coated membranes. Post-treatment did not change the trend as the single coated membranes were more rough than the double and special coated membranes.

Post-treatment effect for individual coating types are displayed in Figures D.3-D.5. Membranes SN2 and SN3, single coating, showed increased roughness with the addition of post-treatment to the new technology. Increases ranged from approximately 5-10 nm. However in contrast, the overall roughness was lowered with post-treatment in both the double and special coating cases, with roughness reduction generally around 10 nm. The more rough the surface the more probable that particles will accumulate on the surface, therefore the fouling potential will be greatly increased. The trend of reduced roughness from single to double and special coating techniques increases the likelihood that the double and special coated membranes will outperform the single coated membranes in colloidal and organic fouling applications.

5.2.1.2 Surface Charge

Ionizable functional groups located on the surface of the membrane give the surface its charge. Due to the immobile Stern layer the direct measurement of the surface potential energy is not possible, however, the zeta potential at the plane of shear can be quantified through the measurement of the streaming potential. A streaming potential analyzer (BI-EKA, Brookhaven Instruments Co.) was used to determine the zeta potential of the membrane surface. Each membrane was subjected to two separate tests performed in two separate legs (acid and base), to avoid ionic interferences, and trend lines were developed using the best-fit logarithmic model for both tests. Figures C.1-B.1.20 contain the results for each test and display the logarithmic model used to determine the zeta potential at pH 7.9. Consistent to previous testing, all figures clearly demonstrate that the zeta potential

of each membrane becomes more negative as the value of pH increases. Zeta potential measurements generally agree with the trends of the streaming potential data supplied by Saehan, but the magnitude of the zeta potential is lower. Tables 5.7 – 5-11 contain the zeta potential for each membrane at the feed water pH. Due to most membranes samples similarity and some conflicting results, the charge associated with the membrane coating was assumed to be associated with solution chemistry during membrane manufacturing rather then intent to vary the surface charge in a specific range.

Figures D.6 and D.7 demonstrate the effect of Saehan's coating processes on surface charge. Membranes without the post-treatment process tended to have less negative zeta potentials as coating moved from single to double to special. The exact opposite trend was true for membranes with post-treatment. The sole exception to both trends was the SN5 and SN5P double coated membranes which exhibited the least negative potential of all ten developmental membranes. While clear trends were demonstrated in testing, the difference between the membranes with the highest and lowest absolute charge was small. This minor difference should not be significant enough to affect the fouling potential. The effect of post-treatment on each coating type is shown in Figures D.8 through D.10. Single coated membranes showed a reduction in the negativity of the surface, while double and special coated membranes demonstrated an increase in the magnitude of the charge. The similarity of the properties of the double and special coated membranes with respect to post-treatment effects, and their reverse relationship to the properties of the single coated membranes was the same as with the surface roughness trends. This discovery will allow comparison of the performance of single coating (phase

1) versus double and special coating (phase 2), as well as evaluation of all three membrane coating techniques separately.

The membrane surface charge characteristics supplied by Saehan were validated through streaming potential analysis. Membranes charge characteristics can be seen in Tables 5.7 – 5-11. The Membranes without post-treatment exhibited the expected results. SN2 was more negative than SN3, SN5 was more positive than SN4, and the magnitude of negative zeta potential decreased from SN6 to SN7 to SN8. Although the membranes agreed with Saehan's description, it should be noted that while clear trends were demonstrated in testing, the difference between the membranes with the highest and lowest absolute charge was small. Membranes with post-treatment did not display the relative surface charges outlined by Saehan. The answer behind these unexpected results is currently unknown, but since both the surface chemistry of the membranes resulting from the different coating techniques and the post-treatment process have not been made available to the investigators, definitive arguments for this finding can not be made at this time.

5.2.2 Clean Water Testing

In order to carefully analyze the productivity of the SN membranes, a series of well-controlled non-fouling tests were conducted systematically. These flat sheet tests were performed on all 15 membranes according to the following procedure. Each membrane was placed in the flat sheet Sepa Cell module (Osmonics) and circulated with stabilization solution. The stabilization solution, 20 liters of 10^{-3} $NaHCO_3$ held at $20^{o}C$

by means of a recirculating chiller and mixed constantly with a magnetic stirrer, was consistent with that of the fouling runs. Also consistent with the fouling runs, the flux was set at 17 gsfd (6.57 mL/min). The membrane was allowed to stabilize for 125 minutes, after which the flux was verified and adjustments to the pressure were made to recover flux, if necessary. Stabilization of the membrane was continued for an additional 30 minutes and then the pressure was recorded. At this point, NaCl was added to create a 2000 ppm solution. The pressure was readjusted to recover the loss in flux due to the affect of osmotic pressure. After the flux was recovered, the saline solution was run for 30 minutes similar to all other flat sheet tests. Feed and permeate samples were then collected for analysis.

5.2.2.1 Initial Mass Transfer Coefficient Evaluation

The water mass transfer coefficient (MTC) has been a common parameter for the characterization of the productivity of a membrane. The initial MTCs shown in Tables 5.7 and 5.8 reflect the performance of the Saehan developmental products. Statistical analysis of the results found for testing of Saehan's Experimental Membranes MTC was independent of surface charge and roughness. For testing of Saehan's Experimental Membranes with post treatment MTC increased with negative surface charge and decreased with increasing surface roughness.

Most coated membranes had initial MTC values lower than the commercial product, but SN8P was the exception, having an MTC slightly higher than SN1CP. SN1CP exhibited

a loss of 17.7% of its initial MTC, while the single, double, and special coated membranes had averages losses of 11.3%, 13.1%, and 13.2%, respectively. This again shows the correlation between the double and special coated membranes as more similar when compared to the properties of the single coated membranes. With only two exceptions, SN3 and SN5, the post-treated membranes showed a larger decline then those membranes without post-treatment. The effect was most dramatic in the SN7 and SN8 membranes.

Figure D.12 displays the effect of coating on initial MTC for the membranes without post-treatment, both with and without salt addition. Performance of one coating technique to another is not clearly distinguishable, but a trend of increasing initial MTC can be seen from single to double to special coated membranes. The post-treated membranes in Figure D.16 show an even more distinct trend of increasing initial MTC from single to double to special coating. According to the manufacturer, the intent of double/special membranes was to correct for the loss of MTC encountered while correcting the fouling potential of single coating membranes compared to the commercial product. Additionally, the special coating technique membranes exhibited a large increase compared to both the single and double coating, with average percent increases as a group of approximately 16% and 21% with and without salt addition, respectively. This figure shows the first set of data where one coating technique distinguishes itself from the others.

Figures D.18-D.20 show the post-treatment effect pertaining to initial MTC for each coating. All coating techniques showed increased initial MTC with post-treatment. The effect was not, however, as dramatic in the single and double coated membranes as it was in the special coated membranes where MTC increased anywhere from 21% to 30%. The effect of post-treatment on initial MTC was not specified by Saehan, but it was clear that the increased MTC in the special coated membranes was significant.

5.2.2.2 Total Dissolved Solids Rejection

The selectivity of the SN membranes was conducted to further evaluate the performance of the membranes under non-fouling conditions. Feed and permeate TDS were obtained through conductance measurement with a YSI Model 32 Conductance Meter. TDS rejection data are shown in Tables 5.7 and 5.8. Every SN membrane showed higher TDS rejection than the existing commercial membrane, Saehan A and B. The results of a linear regression run on the data are summarized in Table 5-11. The statistical analysis found for testing of Saehan's Experimental Membranes % TDS rejection increased with negative surface charge and was independent of roughness. For testing of Saehan's Experimental Membranes with post treatment % TDS rejection increased with negative surface charge and with surface roughness.

The highest rejecting membranes without post-treatment were the single coated membranes, SN2 and SN3, rejecting over 98% of the salt. Figure D.21 shows that these specimens out-performed the double and single coated membranes, whose rejection

hovered around 96%. There was no individual coating type that stood out with the best rejection capacity in the post-treated membranes (Figure D.22) however overall rejection capability was improved. The double coated membranes did have the lowest rejection as a group, but all rejections were above 98%. Saehan did not specify coating effect, however, it was obvious the single coated membranes without post-treatment out performed the others, while no trend was evident in the post-treated membranes.
The post-treatment effect is illustrated in Figures 5.22-5.24. All post-treated membranes showed higher rejection than non post-treated membranes. The double and special coated membranes showed the most improvement, but had more need for improvement as the single coated membranes had better rejection values to start. This gap in performance was successfully overcome, as double and special coated post-treated membranes had rejections between 98.3% and 99.4%, while the single coated membranes performance was only increased from the non post-treated rejection averaging 98.5% to an average of 99.1% when post-treatment was applied to the membranes. Post-treatment seemed to increase the rejection capability of the membranes.

5.2.3 Fouling Water Testing

Fouling potentials of the membranes were investigated by utilizing a surface water from the Cocoa Water Treatment Plant reservoir. This water is currently used as drinking source water for consumers in the central Florida area. Historical water quality data available from the plant was limited, however, the water was analyzed prior to fouling experiments consistent to the other source waters tested. Water samples were collected

from the Cocoa WTP January 1, 2001. Samples were grab samples taken from the reservoir surface. The water was tested at the University of Central Florida for general water quality parameters, which are summarized in Table 5.12. The water obtained from Cocoa had low TDS, hardness, and alkalinity, but the TOC value was very high, 17.2 ppm.

Table 5.12 Source Water Quality of Cocoa Raw Water

Parameter	Average Values Reported by Municipality	Measured Values
pH	7.2	7.4
TDS (mg/L)	62	49
Hardness (mg/L)	N/A	36
Alkalinity (mg/L)	N/A	20.3
Turbidity (NTU)*	2.9	1.80
TOC (mg/L)*	N/A	17.2
Temperature (^{o}C)	N/A	20.0

*Measurements reported on Cocoa Raw Water after passing it through 5 μm filter.

5.2.3.1 Fouling Potential

In order to characterize the fouling behavior of the developmental membranes, flat sheet testing was conducted using Cocoa raw water. The permeate flux versus operation time curves for all fifteen membranes are available in Appendix B. As in the previous fouling potential testing, flux decline ratio was the parameter chosen for comparison and critical records (beginning point and end five points) not characteristic of the data set were removed and are not reflected in the values assigned in Table 5.9 and Table 5.10. A

linear regression was run on the data with results found in Table 5.11. For testing of Saehan's Experimental Membranes:

- Flux decline was independent of surface charge and roughness
- MTC decreased with negative surface charge and roughness over time

For testing of Saehan's Experimental Membranes with post treatment:

- Flux decline was independent of surface charge and increased with roughness
- MTC increased with negative surface charge and decreased with roughness

Operating pressure, initial MTC, and flux decline ratio reflect the average of multiple tests, when applicable. Verification up to this point focused mainly on the special coated membranes with post-treatment. The table shows a dramatic rise in the pressure required for single coated membranes when compared to the commercial product. However, as coating technique progressed from single to double to special, the initial pressure requirements decreased and eventually reached a level equivalent to or better than SN1CP. Both SN7P and SN8P had initial MTCs higher than the commercial product. These results are comparable to the findings in the clean water testing, where SN8P performed better than the commercial product and SN7P had an initial MTC nearly identical to that of SN1CP.

The effect of coating on flux decline ratio appears in Figures D.26 and D.27 for membranes without and with post-treatment, respectively. Membranes without post-treatment showed much better fouling potentials with double and special coating than with single coating. SN4 and SN7, both neutrally charged membranes, stand out with 99.8% and 100.0% flux decline ratios (SN7 showed no fouling therefore the FDR was set at 100%), but the performance of double and special coated membranes was good as a whole. Figure 5.26, however, displays the reverse trend. When membranes are post-treated, single coating provided better fouling resistance. SN7P was the observable exception. Testing for this membrane was repeated with nearly identical results, and as mentioned all data in this report reflects the average of multiple runs when verification was conducted. In order to additionally verify the results of SN7P, SN6P and SN8P were also repeated and showed no significant changes. Additional flat sheet testing would be beneficial in validating all results (QA/QC), as well as, improving possible correlations of membrane surface properties including roughness, surface charge, initial MTC, and salt rejection. Correlations, at this point, are not clear, and are poor for some properties. Looking at these preliminary fouling potentials, while coating technique had contrasting effect depending upon whether the post-treatment was applied to the membrane, the SN7 membrane with or without post-treatment showed the most consistent performance. Any concrete recommendations at this point would be premature, however, SN7 does have some highly desirable surface properties, namely, a less rough (than most single and double coated membranes) and more neutral surface. Both attributes, especially a neutral surface, seem to be the direction manufacturers in the United States are moving.

Nonetheless, pilot scale testing is required to more clearly determine the fouling potential of the new membranes.

The post-treatment effect on each coating technique was closely examined in Figures D.28 through D.30. Single coated membranes showed 3.5-6% improvement in fouling potential with post-treatment. Double and special coated membranes had similar results with lost performance with post-treatment in both cases. SN4 and SN5 (double) lost about 3.5% of their fouling potentials, while SN6-8 (special) had declines between approximately 1 and 3.5%. SN7 was on the low side of flux decline ratio loss for the special coated membranes.

5.2.3.2 Total Organic Carbon Rejection Capability

The fouling resistance of the developmental Saehan membranes was also evaluated according to the selectivity of the membranes. A linear regression was run on the data with results found in Table 5.11.

For testing of Saehan's Experimental Membranes:

- % TDS rejection is independent of surface charge and roughness
- % TOC rejection is independent of surface charge and roughness

For testing of Saehan's Experimental Membranes with post treatment:

- % TDS rejection is independent of roughness and decreased with negative surface charge
- % TOC rejection is independent of surface charge and roughness

The major foulant in the Cocoa raw water was organic matter, therefore TOC rejection was the parameter of choice. All Saehan membranes had extremely low TOC levels in the permeate streams resulting in high rejections of 99.4% or 98.8%. These excellent rejections show almost complete rejection. In some cases, the analyzer measured TOC values close to zero, which were reported as <0.1 ppm. Also, according to QA/QC protocol the measurements for the permeate based on the capabilities of the equipment and standards used could not be reported beyond one tenth. Therefore most membranes had TOC values of 0.1 ppm or <0.1 ppm. In either case, TOC was reported as 0.1 ppm for rejection calculation (Tables 5.9 and 5.10), which explains the number of membranes with identical rejections. Due to the capabilities and background noise associated with the Phoenix 8000 UV-Persulfate TOC Analyzer (Dohrmann) machine, a run containing at least five replicates per membrane and standards every 0.05 ppm from 0 to 0.5 ppm would be required to attempt to distinguish between the membranes with confidence.

CHAPTER 6: CONCLUSIONS AND RECOMMENDATIONS

In summary, this project was conducted to investigate the existing Saehan products and guide the research and development efforts in the creation of a fouling resistant membrane that can compete in the U.S. market. Performance was determined as the changes in Saehan's membrane characteristics were monitored, and the foulant properties, hydrodynamic conditions, and feed water chemistry were carefully altered. Membranes tested included two (2) Saehan commercial membranes, three (3) non-Saehan commercial fouling resistant membranes (FRMs) available in the United States, seven (7) Saehan experimental membranes, and 8 Saehan experimental membranes with post-treatment. The commercial Saehan membranes performance was compared to existing FRMs with groundwater and synthetic colloidal water. The experimental Saehan membranes with and without post-treatment was analyzed with clean water and surface water experiments.

Section 6.1 lists the conclusions developed from comparison of Saehan's products to commercially available FRMs. Section 6.2 lists the conclusions pertaining to testing Saehan's developmental membranes. Sections 6.3 details some of the recommendations made in response to results up to this point of the project.

6.1 FRMs versus Saehan Commercial Product Conclusions

6.1.1 Groundwater testing of the Commercial Membranes found:

a. J/Jo decreases as negative surface charge and roughness increase
b. MTC decreases as negative surface charge and roughness increase
c. % TDS rejection is independent of surface charge and roughness
d. % TOC rejection increases as negative surface charge and roughness increase

6.1.2 Colloidal water testing of the Commercial Membranes found:

a. J/Jo decreases as negative surface charge and roughness increase as did groundwater testing
b. MTC was independent of roughness and decreased as surface charge increased
c. % TDS rejection is independent of surface charge and roughness as was observed in groundwater testing

6.1.3 Membranes with less negative surface charge or roughness will foul less and have higher MTCs.

6.1.4 TDS rejection is independent of surface charge or roughness for both groundwater and synthetic colloidal water.

6.1.5 The effects of surface roughness and charge on % TOC rejection were opposite to flux decline and the MTC, which is rational and indicates the mass transfer of water and TOC is similar with respect to surface roughness and charge, and somewhat indicates the majority of TOC removal is controlled by size exclusion.

6.1.6 The existing FRMs showed better fouling resistance than Saehan's commercially available products in surficial groundwater testing and in synthetic colloidal water

testing. The three commercial fouling resistant membranes, LFC-1, X-20, and BW-30FR, yielded flux decline ratios of 100%, 92.6 %, and 95.6%, respectively during 48 hrs of testing period, while Saehan membranes A and B yielded ratios of 92.0% and 92.5% during groundwater testing. Synthetic colloidal water testing yielded flux decline ratios of 99.5%, 98.4%, and 98.8% for LFC-1, X-20, and BW30FR, respectively. Saehan A had a flux decline ratio of 97.1% and Saehan B had a ratio of 97.9%.

6.2 Saehan Developmental Membranes Conclusions

The Saehan membrane progression can be separated into three coating techniques: **(1) single, (2) double, and (3) special**. Coating techniques are patent pending and considered trade secrets, but the intent was to improve the fouling potential of the existing Saehan products by varying surface properties such as the charge and hydrophilicity. In addition to surface chemistry alterations, the Saehan commercial products were subjected to a **post-treatment** process with the purpose of increasing the mass transfer coefficient and TDS rejection. The parameters of most interest in the progression of Saehan's new membranes are the coating technique and post-treatment effects.

6.2.1 For Testing of Saehan's Experimental Membranes with Clean Water

a. MTC was independent of surface charge and roughness
b. % TDS rejection increased with negative surface charge and was independent of roughness

6.2.2 For Testing of Saehan's Experimental Membranes with Surface Water

a. Flux decline was independent of surface charge and roughness
b. MTC decreased with negative surface charge and roughness
c. % TDS rejection is independent of surface charge and roughness
d. % TOC rejection is independent of surface charge and roughness

6.2.2 For Testing of Saehan's Experimental Membranes with post treatment with Clean Water

a. MTC increased with negative surface charge and decreased with increasing surface roughness
b. % TDS rejection increased with negative surface charge and with surface roughness

6.2.3 For Testing of Saehan's Experimental Membranes with post treatment with Surface Water

a. Flux decline was independent of surface charge and increased with roughness
b. MTC increased with negative surface charge and decreased with roughness
c. % TDS rejection is independent of roughness and decreased with negative surface charge
d. % TOC rejection is independent of surface charge and roughness

6.2.4 The productivity (MTC decline) and solute mass transfer (TDS and TOC) of Saehan's Experimental Membranes was generally independent of surface roughness and charge.

6.2.5 The productivity (MTC decline) and flux decline Saehan's Experimental Membranes with Post Treatment was generally dependent on surface roughness and charge; whereas, the solute mass transfer (TDS and TOC) of Saehan's Experimental Membranes without Post Treatment was generally independent of surface roughness and charge.

a. Productivity increased with negative surface charge and decreased with roughness in both clean and surface water
b. TDS rejection increased with negative surface charge in both clean and surface water

6.2.6 The effects of surface charge on % TDS rejection were opposite to its effect on MTC, which is rational and indicates the mass transfer of water and TDS is similar with respect to charge.

6.2.7 Average roughness decreased slightly as coating technique progressed from single to double to special.

Saehan’s development from single/double coating to special coating demonstrated a reduction of average surface roughness, which may prove to be beneficial to performance.

6.2.8 Post-treatment increased roughness in single coated membranes and reduced the roughness in double and special coated membranes.

Membranes without post-treatment had surface roughness with little variation, ranging from 83.2 to 107.6 nm, while membranes subjected to the process had roughness ranging

from as low as 77.8 nm up to 111.5 nm. Single coated membranes showed increased roughness ranging from 5-10 nm with the addition of post-treatment to the new technology. In contrast, the overall roughness was lowered with post-treatment in both the double and special coating cases, with a roughness reduction generally around 10 nm.

6.2.9 The relative charge differences in the developmental membranes as noted by Saehan were exhibited among non post-treated membranes.

The membrane surface charge characteristics were validated through streaming potential analysis. SN2 was more negative than SN3, SN5 was more positive than SN4, and the magnitude of negative zeta potential decreased from SN6 to SN7 to SN8, as expected. It is important to note that while clear trends were demonstrated in testing, the difference between the membranes with the highest and lowest absolute charge was small.

6.2.10 Membranes with post-treatment did not demonstrate relative surface charge differences consistent with the manufacturer.

The membranes subjected to post-treatment did not display the relative surface charges outlined by Saehan and/or evident in non post-treated membranes. The reason for the unexpected zeta potentials was unknown at the time of study. Since both the surface chemistry of the membranes resulting from the different coating techniques and the post-treatment process have not been specified to the investigators, explicit arguments for this finding can not be elucidated.

6.2.11 Initial mass transfer coefficient, determined by clean water testing, increased as coating moved from single to double to special.

Both post-treated and non post-treated membranes demonstrated the trend of increased MTC, however, the trend was more distinct for post-treated membranes. Performance of one coating technique to another is not clearly distinguishable, but a trend of increasing initial MTC can be seen in the progression from single coated to double and special coated membranes. Within the post-treated group, the special coating technique membranes exhibited a large increase compared to both the single and double coating, with average percent increases as a group of approximately 16% and 21% with and without salt addition, respectively.

6.2.12 Clean water testing showed increased initial mass transfer coefficient for membranes with post-treatment.

All coating techniques showed increased initial MTC with post-treatment. The effect was not, however, as dramatic in the single and double coated membranes as it was in the special coated membranes where MTC increased anywhere from 21% to 30%.

6.2.13 Single coated membranes showed the best salt rejection capability among non post-treated membranes.

The highest rejecting membranes without post-treatment were the single coated membranes, SN2 and SN3, rejecting over 98% of the salt. These specimens outperformed the double and single coated membranes, whose rejections hovered around 96%. This finding may be attributed to tighter membrane structure of single coated membranes, which was evidenced by low initial MTC values.

6.2.14 Post-treatment increased selectivity for all membrane coating techniques.

All post-treated membranes showed higher rejection than non post-treated membranes. Although, the double coated membranes had the lowest magnitude of rejection, no individual coating type stood out with the best rejection capacity with all rejections above 98%. The double and special coated membranes showed the most improvement, but had more need for improvement as the single coated membranes had better rejection values to start. The gap in performance was successfully overcome, as double and special coated post-treated membranes had rejections between 98.3% and 99.4%, while the single coated membranes performance was only increased from the non post-treated rejection averaging 98.5% to an average of 99.1% when post-treatment was applied to the membranes. Clearly, post-treatment was critical in the rejection capability of the membranes.

6.2.15 The post-treatment increased fouling resistance for the single coated membranes, but decreased fouling resistance of double and special coated membranes.

Single coated membranes SN2 and SN3 had flux decline ratios of 96.0% and 92.7%, respectively, but showed 3.5-6% improvement in fouling resistance with post-treatment. Double and special coated membranes, on the other hand, lost performance with post-treatment. More specifically, flux decline ratios were 99.8%, 99.2%, 99.3%, 100%, and 98.3% for SN4, SN5, SN6, SN7, and SN8. The fouling potential increased with post-treatment as flux decline ratios slipped to 96.1%, 95.5%, 95.5%, 98.8%, and 96.2%, respectively.

6.2.16 The coating effect on fouling potential had an inverse relationship between single coated versus double and special coated membranes.

During filtration of high organic surface water (TOC ≈17 mg/L), membranes without post-treatment showed much better fouling potentials with double and special coating than with single coating. SN4 and SN7 stand out with very small fouling potentials. When membranes are post-treated, single coating provided better fouling resistance, with an exception of SN7P which presented comparable fouling resistance.

6.2.17 The SN7 membranes showed the best performance of the developmental membranes.

Looking at the preliminary testing results, SN7 and SN7P outperformed the rest of the new Saehan membranes. While coating technique had contrasting effect depending upon whether the post-treatment was applied to the membrane, the SN7 membrane with or without post-treatment showed consistent performance. The high initial MTC, high selectivity, low fouling potential and desirable surface properties (i.e. less rough and neutral surface) make SN7 membranes a prime candidate for selection as Saehan's new commercial product.

6.3 Recommendations

6.3.1 Additional fouling experiments need to be performed to confirm the results obtained from preliminary testing.

While select experiments have already been repeated, due to unavoidable delays and limitations in the time available to test the new Saehan membranes, fouling potential data collected are greatly limited. As many experiments as possible were conducted within the project schedule, however, each flat sheet test required four to five days including cleaning time, resulting in limited experimental trials. In order to obtain statistically reliable and more conclusive results, a more thorough set of experimental verification is desired with different source waters and under various operating conditions.

6.3.2 Pilot scale verification is necessary.

Flat sheet testing is appropriate for initial fouling potential studies, but pilot scale testing is required to more effectively describe the performance of membranes. Any recommendations without pilot scale testing data in addition to bench scale analysis would be premature.

6.3.3 Source water analysis requires more comprehensive study, including careful characterization of the organic and particle content of the natural waters.

General water quality parameters were obtained and verified, however, a more specific study is desirable to more thoroughly describe the fouling potential of the waters and the possible relationship to membrane characteristics.

6.3.4 More controlled experiments are required to clearly distinguish both the effects of organic and colloidal foulants on the membranes, as well as, to develop possible relationships based on surface properties.

A series of experiments with clearly defined solution chemistry, such as the silica particle experiments contained in this report, would be beneficial to more clearly explain the changes made by Saehan. Natural water testing is important for comparing fouling

potential, but is more difficult to manipulate and characterize than synthetic solutions. This manipulation of chemistry is necessary to elucidate the trends already developed.

6.3.5 Membrane properties including hydrophobicity and functional groups need to be further characterized and verified through various analytical techniques.

While trends of parameters such as zeta potential and surface roughness are similar to other studies, including Saehan's internal testing, the magnitude of results varies significantly. As the magnitude of results can be intrinsic to specific equipment, especially streaming potential analyzers, a series of round robin testing is recommended to verify the absolute numbers involved. Also critical to proper analysis and selection of a Saehan FRM is a clear understanding of the fundamental effects of coating and post-treatment on the membrane properties. When patents are secured, a clear picture of the processes involved and more thorough study of surface properties using various sophisticated analytical techniques, specifically changes to functional groups, would greatly increase the level of understanding on correlation between fouling potential and membrane surface chemistry.

APPENDIX A

SURFACE ROUGHNESS FIGURES

Figure A.1: 3-Dimensional AFM Image of LFC-1

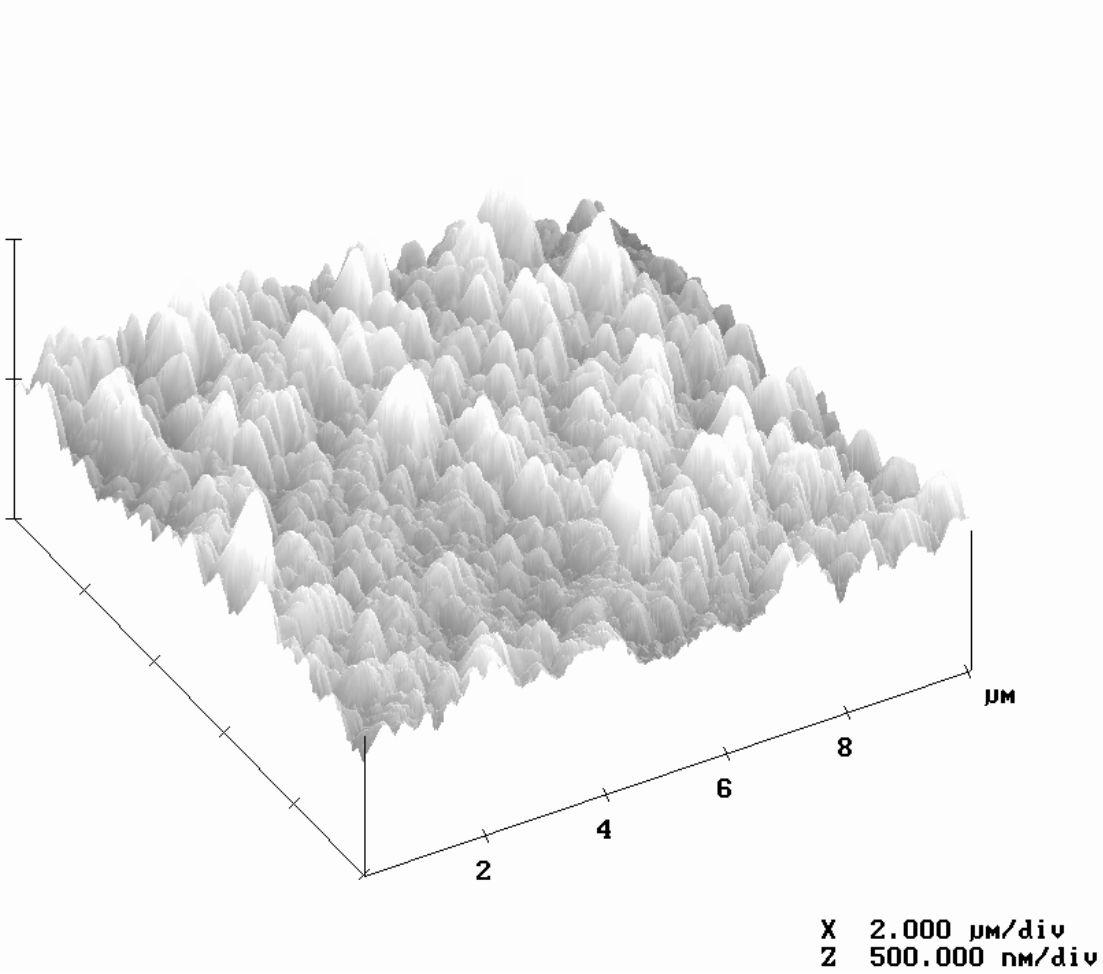

Table A.1: AFM Results for LFC-1

Parameter	Scan 1	Scan 2	Scan 3	Average
Z Range (nm)	555.01	578	589.23	574.08
Mean (nm)	0.154	0.150	0.138	0.147
RMS (nm)	66.384	72.713	63.039	67.379
R_a	50.856	57.062	48.138	52.019
Surface Area (μm^2)	114.47	119.74	116.37	116.86
Projected Surface Area (μm^2)	100.00	100.00	100.00	100.00
Surface Area Difference (%)	14.47	19.74	16.37	16.86
Peak Threshold (nm)	66.384	72.713	63.039	67.379
Peak Count	125	140	174	146

Figure A.2: 3-Dimensional AFM Image of X-20

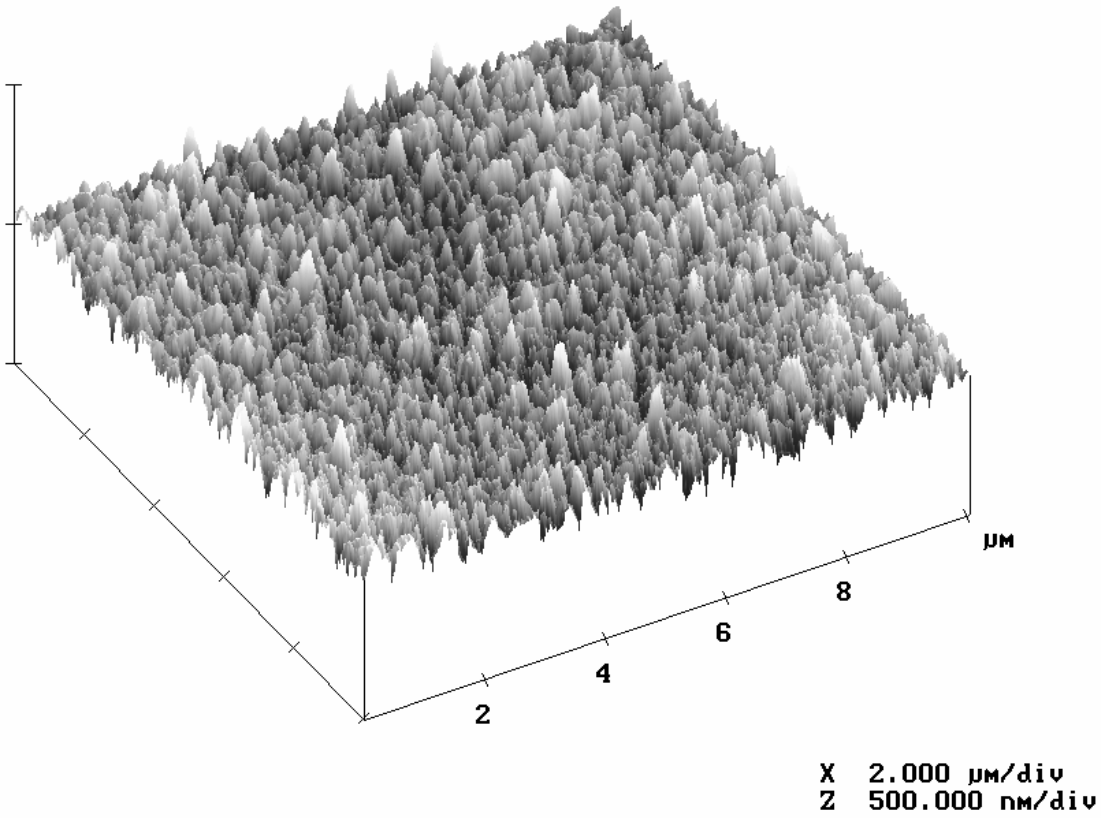

Table A.2: AFM Results for X-20

Parameter	Scan 1	Scan 2	Scan 3	Average
Z Range (nm)	396.09	389.35	333.58	373.01
Mean (nm)	0.056	0.036	0.056	0.0493
RMS (nm)	40.570	44.380	39.982	41.644
R_a	32.273	35.660	32.130	33.354
Surface Area (μm^2)	125.56	138.70	133.77	132.68
Projected Surface Area (μm^2)	100.00	100.00	100.00	100.00
Surface Area Difference (%)	25.56	38.70	33.77	32.68
Peak Threshold (nm)	40.570	44.380	39.982	41.644
Peak Count	735	887	956	859

Figure A.3: 3-Dimensional AFM Image of BW-30FR

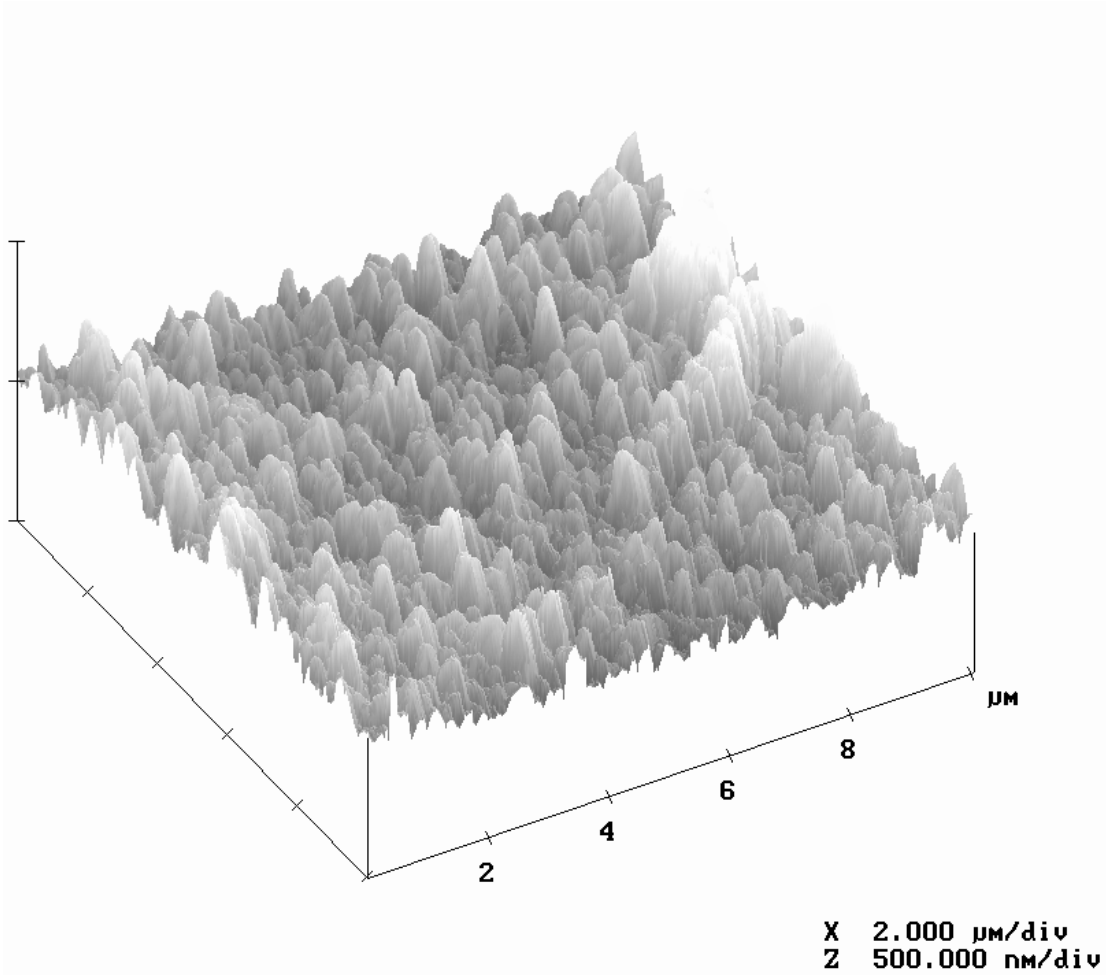

Table A.3: AFM Results for BW-30FR

Parameter	Scan 1	Scan 2	Scan 3	Average
Z Range (nm)	686.34	528.17	639.34	617.95
Mean (nm)	0.166	0.182	0.075	0.141
RMS (nm)	77.212	65.205	77.240	73.219
R_a	59.107	51.073	59.896	56.692
Surface Area (μm^2)	125.96	125.88	125.55	125.80
Projected Surface Area (μm^2)	100.00	100.00	100.00	100.00
Surface Area Difference (%)	25.96	25.88	25.55	25.80
Peak Threshold (nm)	77.212	65.205	77.240	73.219
Peak Count	166	208	173	182

Figure A.4: 3-Dimensional AFM Image of Saehan A

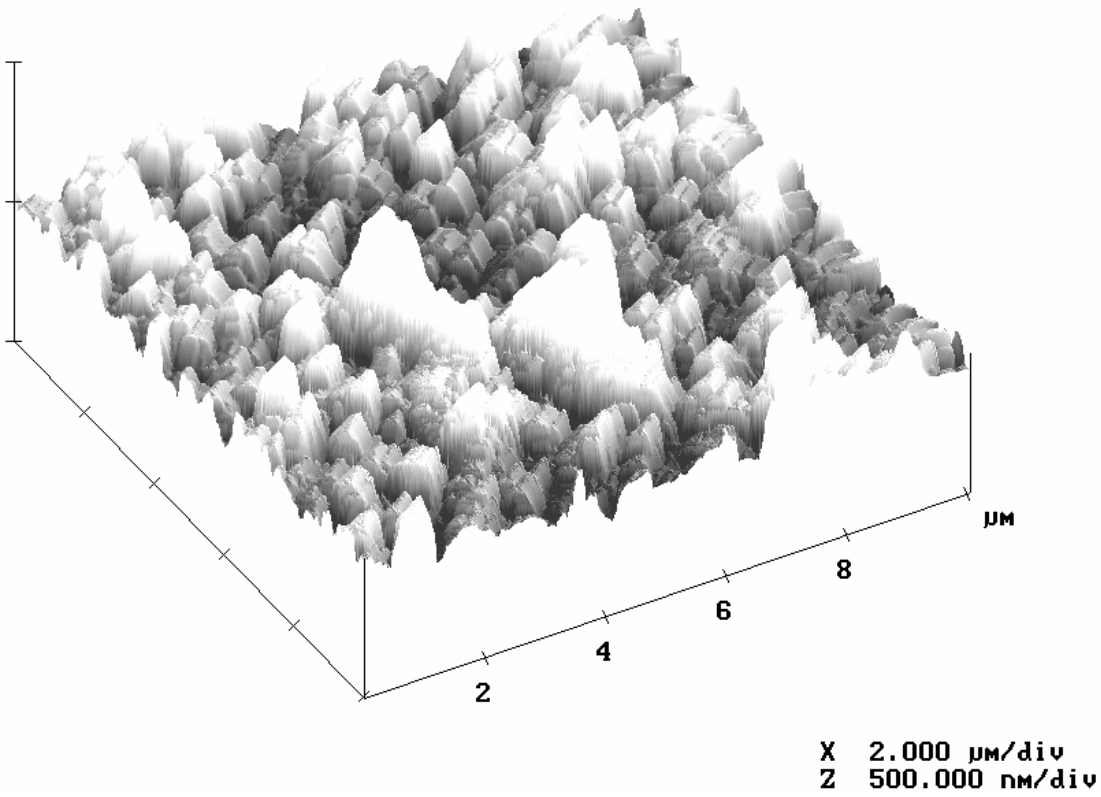

Table A.4: AFM Results for Saehan A

Parameter	Scan 1	Scan 2	Scan 3	Average
Z Range (nm)	468.11	566.67	549.98	528.25
Mean (nm)	0.039	0.052	0.063	0.051
RMS (nm)	67.514	78.281	85.748	77.181
R_a	52.548	59.012	70.835	60.798
Surface Area (μm^2)	113.51	113.44	111.68	112.88
Projected Surface Area (μm^2)	100.00	100.00	100.00	100.00
Surface Area Difference (%)	13.51	13.44	11.68	12.88
Peak Threshold (nm)	67.514	78.281	85.748	77.181
Peak Count	68	38	49	52

Figure A.5: 3-Dimensional AFM Image of Saehan B

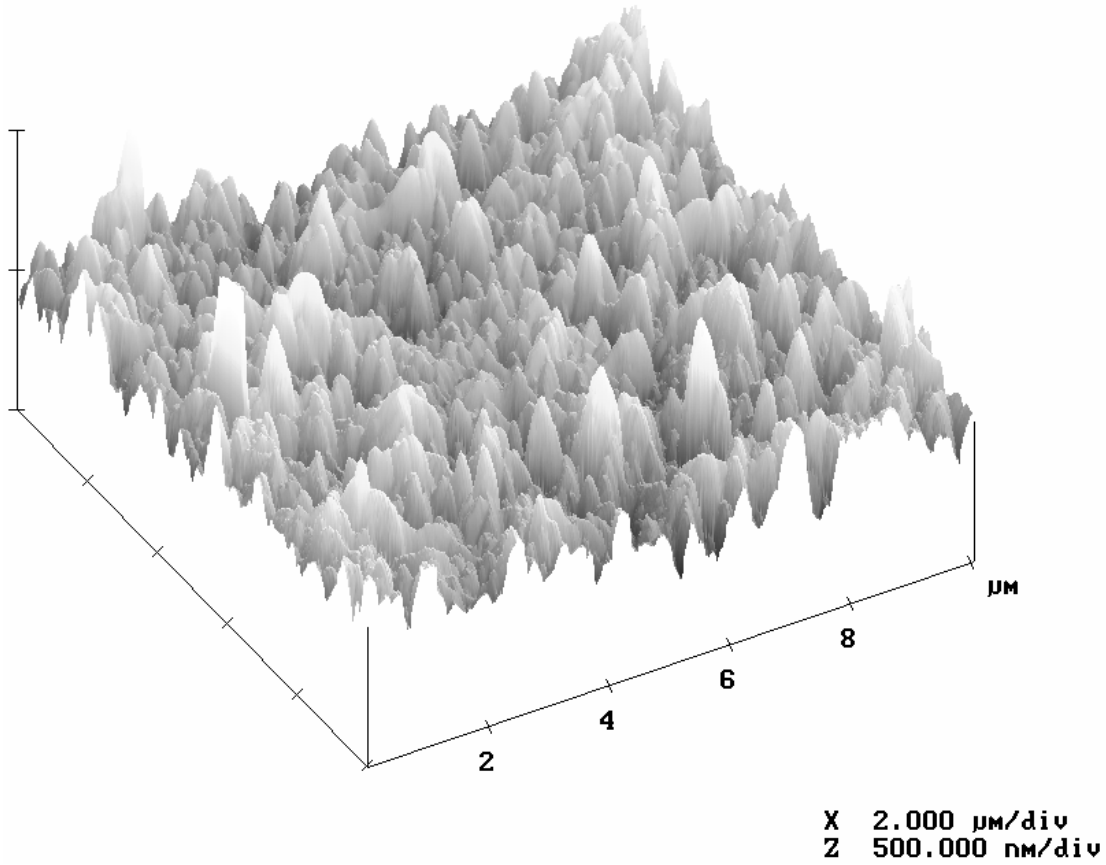

Table A.5: AFM Results for Saehan B

Parameter	Scan 1	Scan 2	Scan 3	Average
Z Range (nm)	537.80	901.67	1079.00	839.49
Mean (nm)	0.017	0.027	0.053	0.032
RMS (nm)	73.194	73.951	82.674	76.606
R_a	57.754	58.139	64.844	60.246
Surface Area (μm^2)	125.97	125.68	126.70	126.12
Projected Surface Area (μm^2)	100.00	100.00	100.00	100.00
Surface Area Difference (%)	25.97	25.68	26.70	26.12
Peak Threshold (nm)	73.194	73.951	82.674	76.606
Peak Count	194	190	141	175

Figure A.6: 3-Dimensional AFM Image of SN1CP

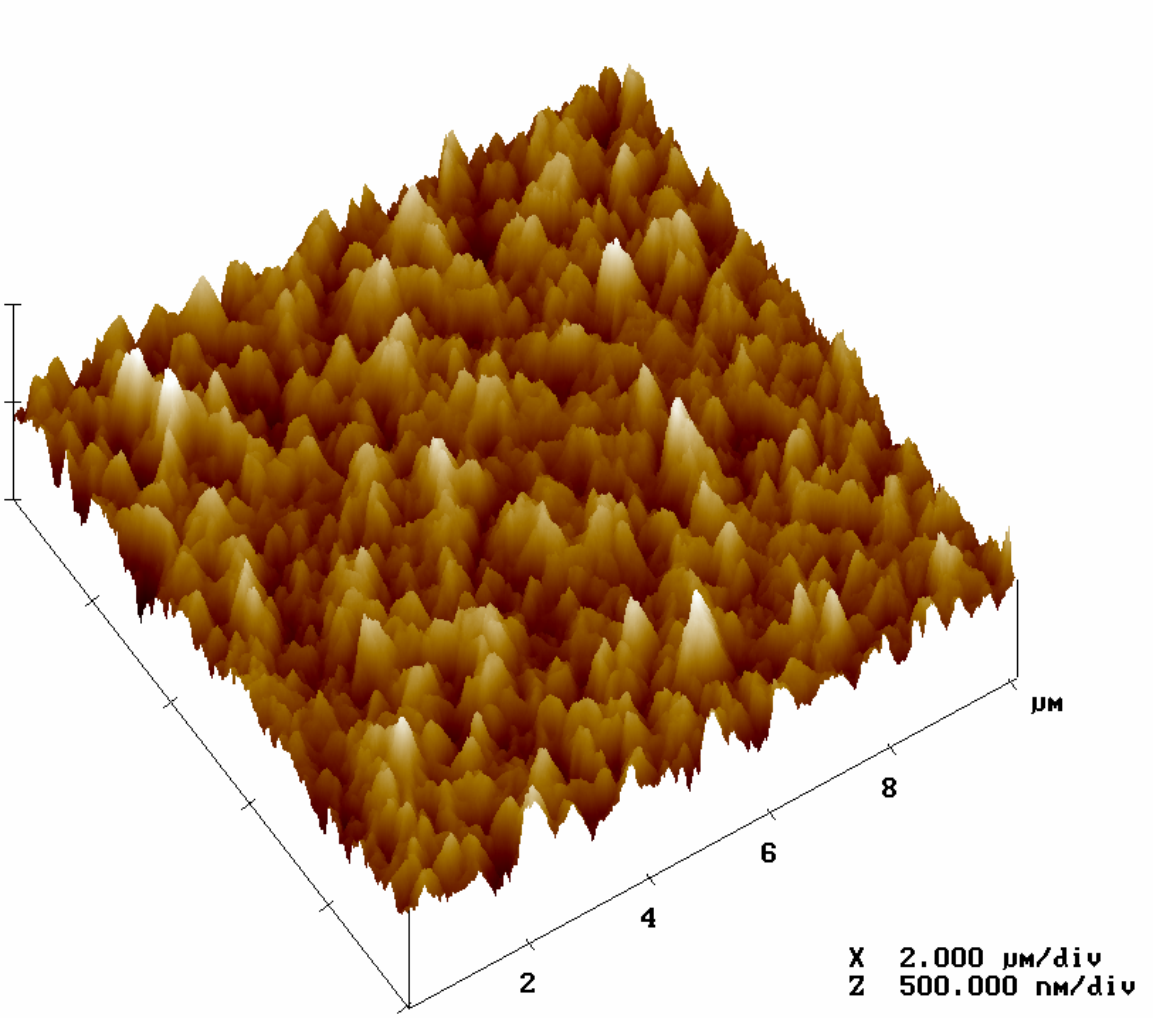

Table A.6: AFM Results for SN1CP

Parameter	Scan 1	Scan 2	Scan 3	Scan 4	Scan 5	Scan 6	Scan 7	Scan 8	Average
RMS (nm)	76.9	81.3	72.6	72.6	67.3	76.1	71.9	74.4	74.1
R_a (nm)	60.3	62.5	58.1	57.6	53.6	60.0	56.8	58.9	58.5
Surface Area Difference (%)	36.3	39.8	28.9	31.3	36.5	34.8	34.9	35.9	34.8
Peak Count	293	320	280	264	386	297	332	344	314.5

Figure B.7: 3-Dimensional AFM Image of SN2

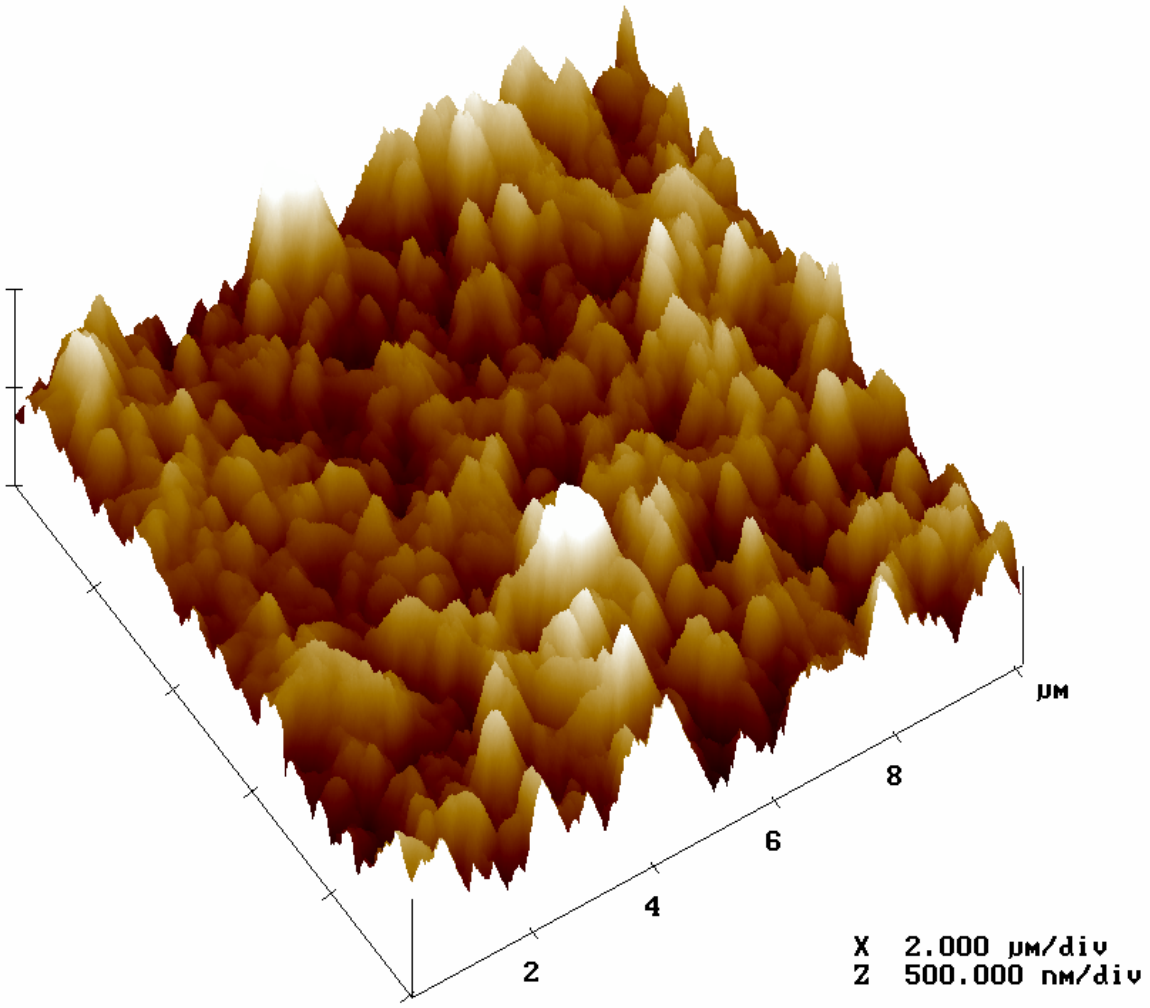

Table A.7: AFM Results for SN2

Parameter	Scan 1	Scan 2	Scan 3	Scan 4	Scan 5	Average
RMS (nm)	126.0	123.4	126.3	126.3	128.0	126.0
R_a (nm)	98.4	97.2	98.3	100.9	101.6	99.3
Surface Area Difference (%)	36.7	33.9	41.5	38.5	34.8	37.1
Peak Count	145	131	106	88	99	113.8

Figure A.8: 3-Dimensional AFM Image of SN2P

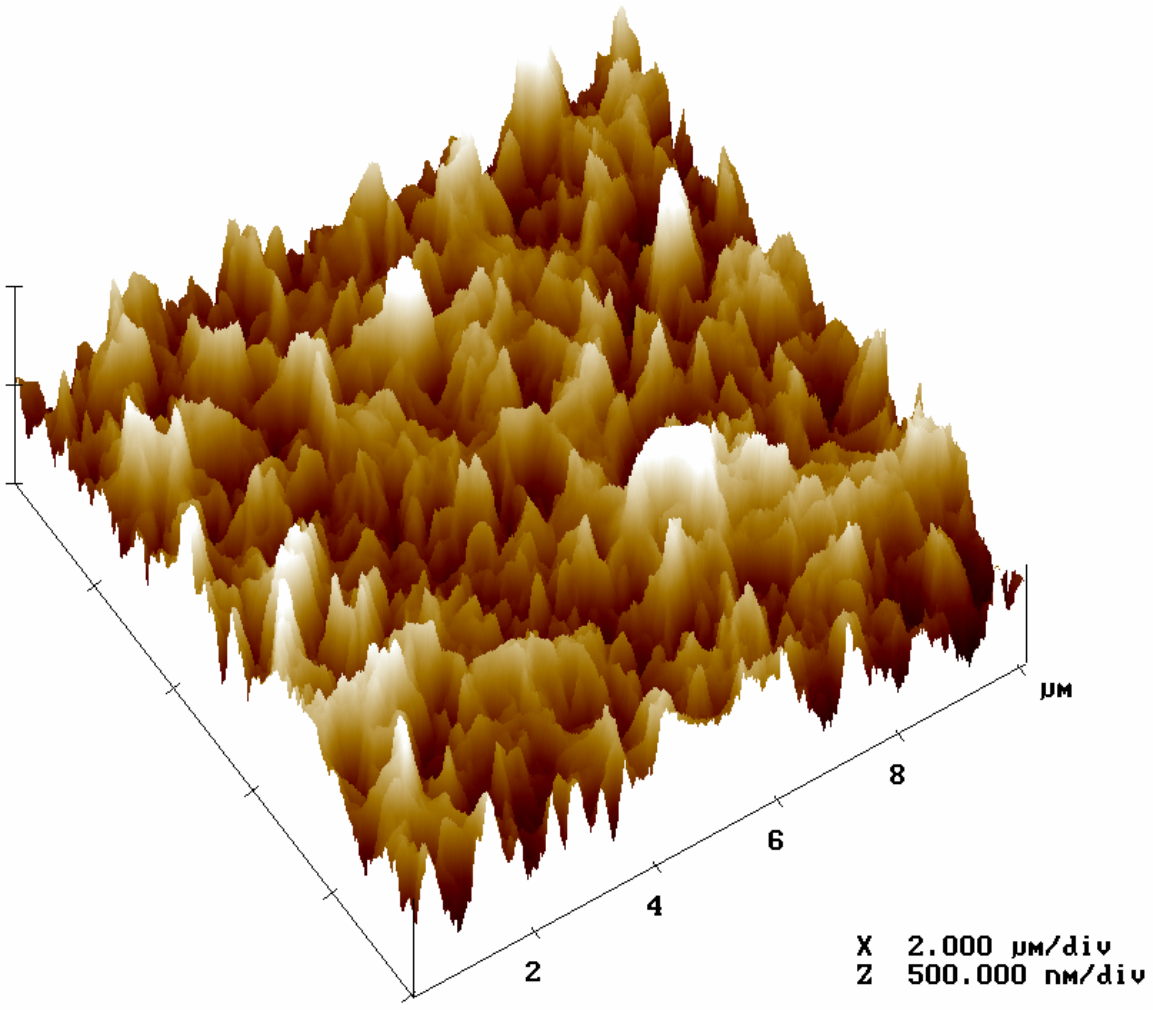

Table A.8: AFM Results for SN2P

Parameter	Scan 1	Scan 2	Scan 3	Scan 4	Scan 5	Scan 6	Scan 7	Scan 8	Average
RMS (nm)	127.1	124.9	124.5	126.6	133.3	135.0	137.3	132.4	130.1
R_a (nm)	101.7	99.0	98.1	101.7	106.3	108.6	108.3	106.8	103.8
Surface Area Difference (%)	72.7	68.1	62.0	66.6	66.2	64.8	63.6	67.7	66.5
Peak Count	246	237	188	182	195	172	155	198	196.6

Figure A.9: 3-Dimensional AFM Image of SN3

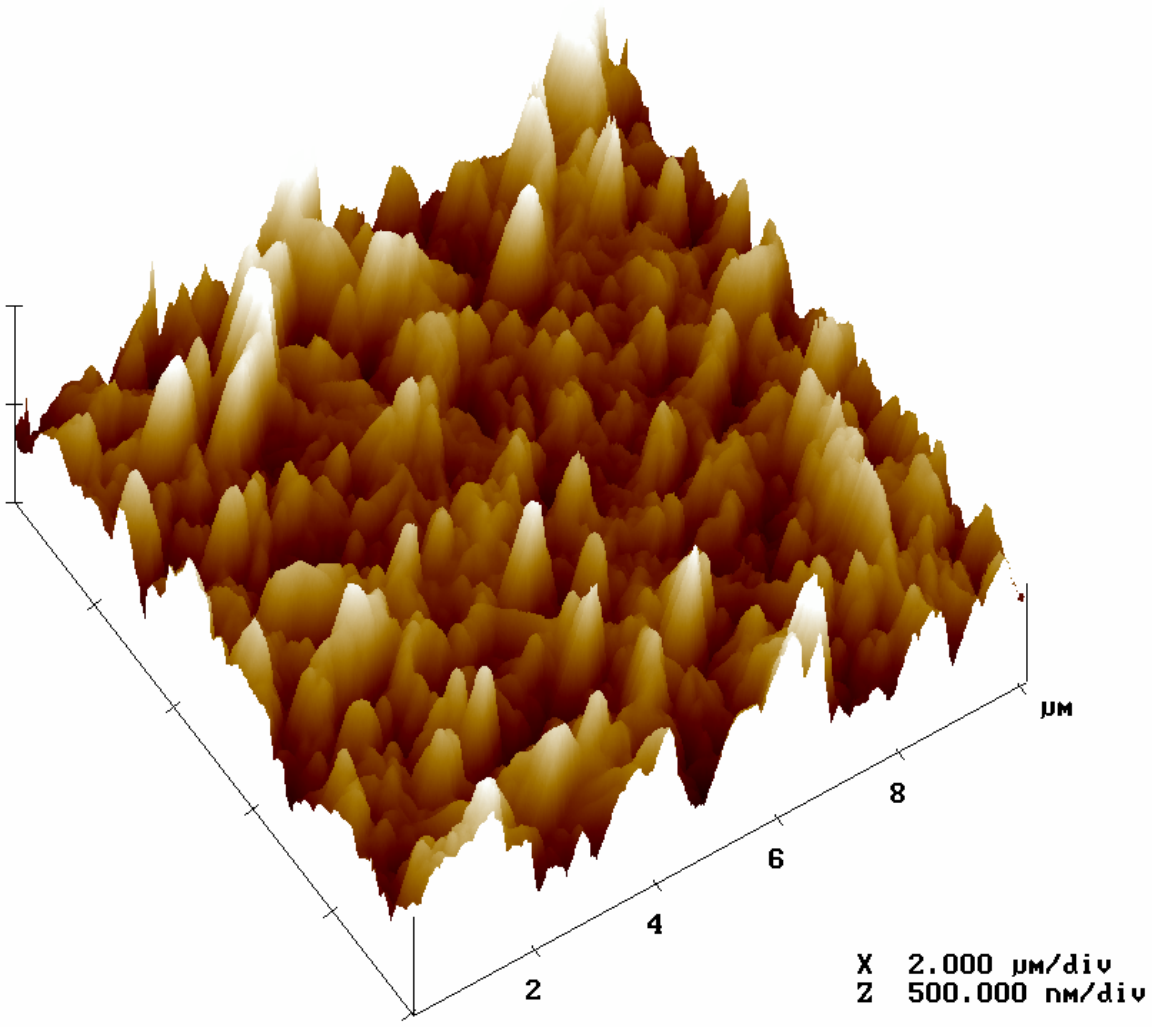

Table A.9: AFM Results for SN3

Parameter	Scan 1	Scan 2	Scan 3	Scan 4	Scan 5	Average
RMS (nm)	121.2	118.6	124.6	125.0	129.4	123.8
R_a (nm)	95.1	94.4	96.4	100.2	102.4	97.7
Surface Area Difference (%)	36.1	37.4	41.0	42.0	42.9	39.9
Peak Count	101	100	98	116	105	104.0

Figure A.10: 3-Dimensional AFM Image of SN3P

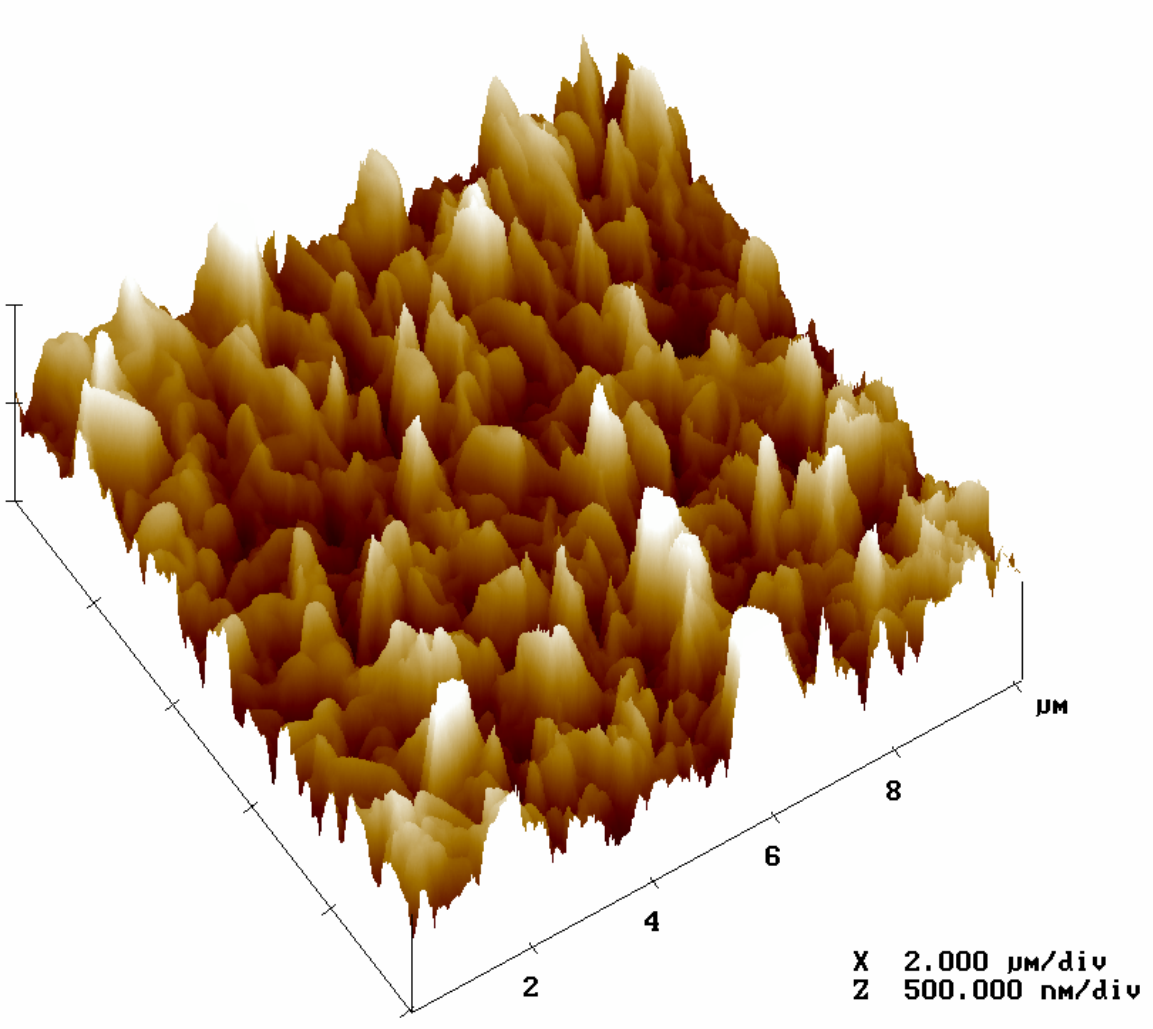

Table A.10: AFM Results for SN3P

Parameter	Scan 1	Scan 2	Scan 3	Scan 4	Scan 5	Scan 6	Scan 7	Scan 8	Average
RMS (nm)	138.7	140.9	133.0	149.5	137.5	134.9	144.3	134.5	139.2
R_a (nm)	112.1	111.0	108.2	118.8	109.8	107.9	114.4	109.8	111.5
Surface Area Difference (%)	57.9	59.8	55.7	59.6	60.5	64.6	63.9	57.4	59.9
Peak Count	140	125	130	106	135	164	120	129	131.1

Figure A.11: 3-Dimensional AFM Image of SN4

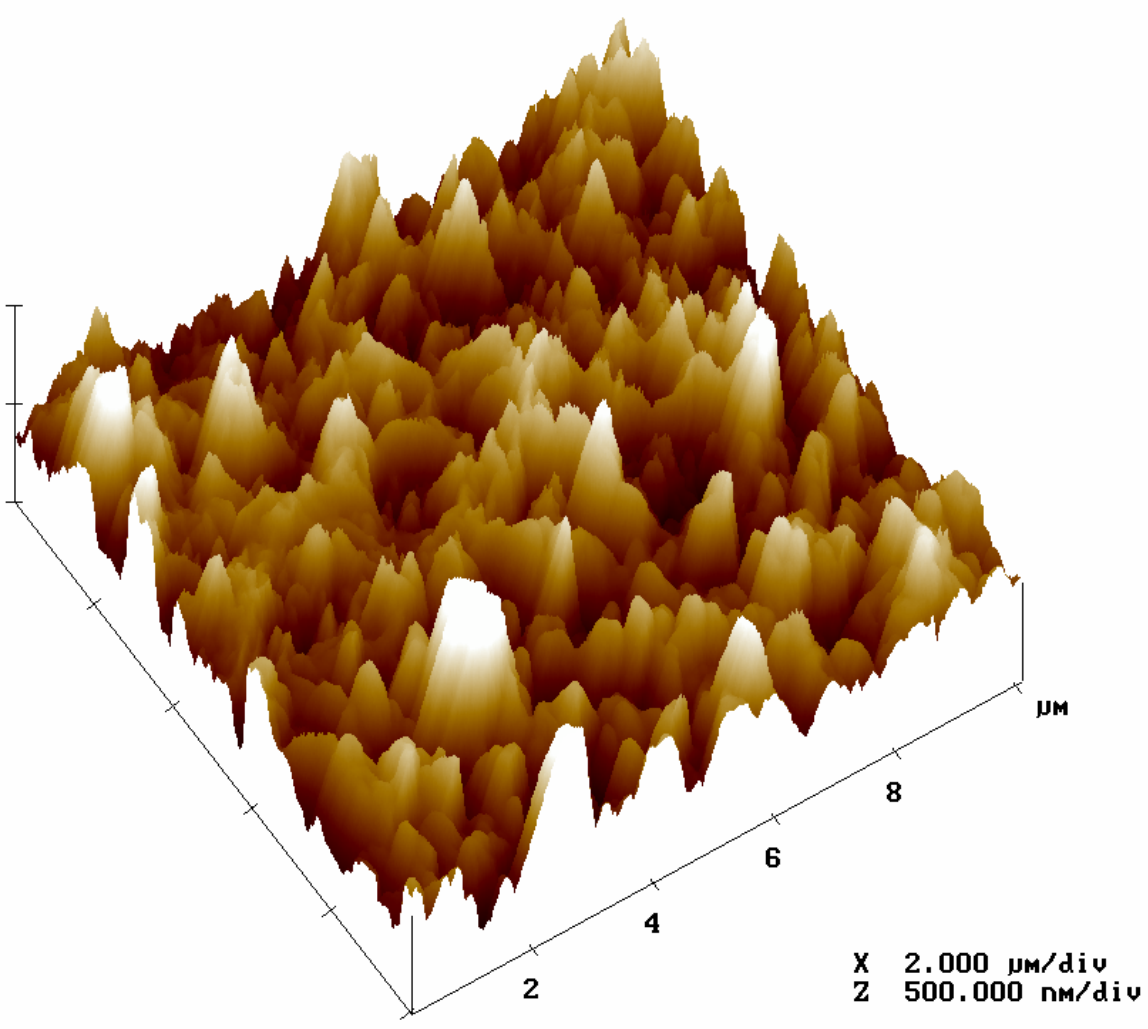

Table A.11: AFM Results for SN4

Parameter	Scan 1	Scan 2	Scan 3	Scan 4	Scan 5	Average
RMS (nm)	142.0	132.1	133.2	135.1	138.9	136.3
R_a (nm)	114.9	104.7	104.1	106.4	107.8	107.6
Surface Area Difference (%)	42.8	42.8	52.7	53.1	47.8	47.8
Peak Count	112	108	141	150	114	125.0

Figure A.12: 3-Dimensional AFM Image of SN4P

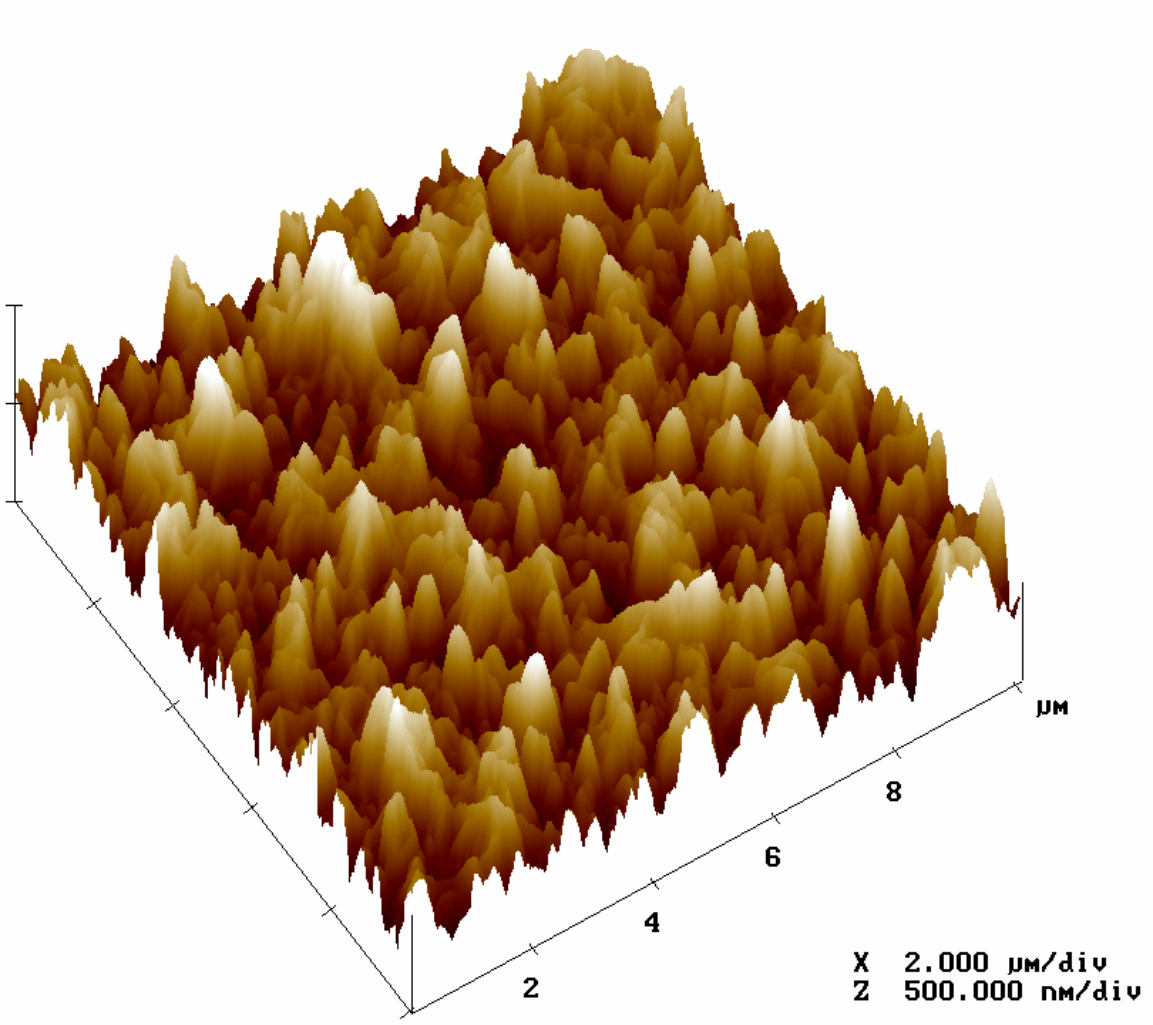

Table A.12: AFM Results for SN4P

Parameter	Scan 1	Scan 2	Scan 3	Scan 4	Scan 5	Scan 6	Scan 7	Scan 8	Average
RMS (nm)	122.6	127.9	124.2	130.5	123.9	140.6	141.8	123.3	129.4
R_a (nm)	99.3	102.9	100.4	105.3	99.8	111.3	113.0	98.9	103.9
Surface Area Difference (%)	64.5	64.7	61.5	69.6	65.7	70.9	68.4	63.8	66.1
Peak Count	187	157	177	159	155	151	152	148	160.8

Figure A.13: 3-Dimensional AFM Image of SN5

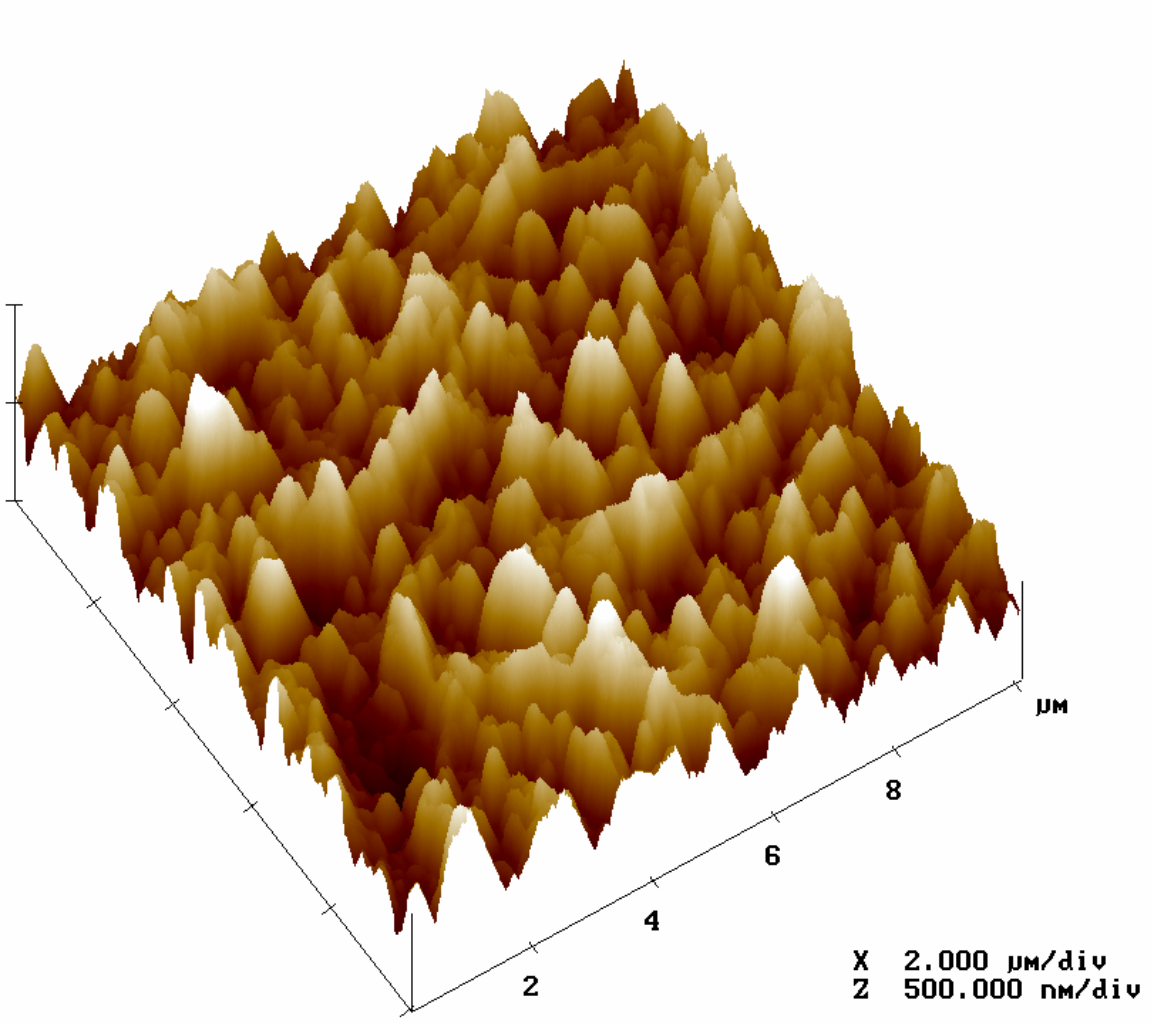

Table A.13: AFM Results for SN5

Parameter	Scan 1	Scan 2	Scan 3	Scan 4	Scan 5	Average
RMS (nm)	126.9	136.2	130.6	125.2	121.8	128.1
R_a (nm)	98.9	107.7	103.9	100.7	96.6	101.5
Surface Area Difference (%)	44.3	43.9	47.7	45.8	45.2	45.4
Peak Count	122	112	151	148	193	145.20

Figure A.14: 3-Dimensional AFM Image of SN5P

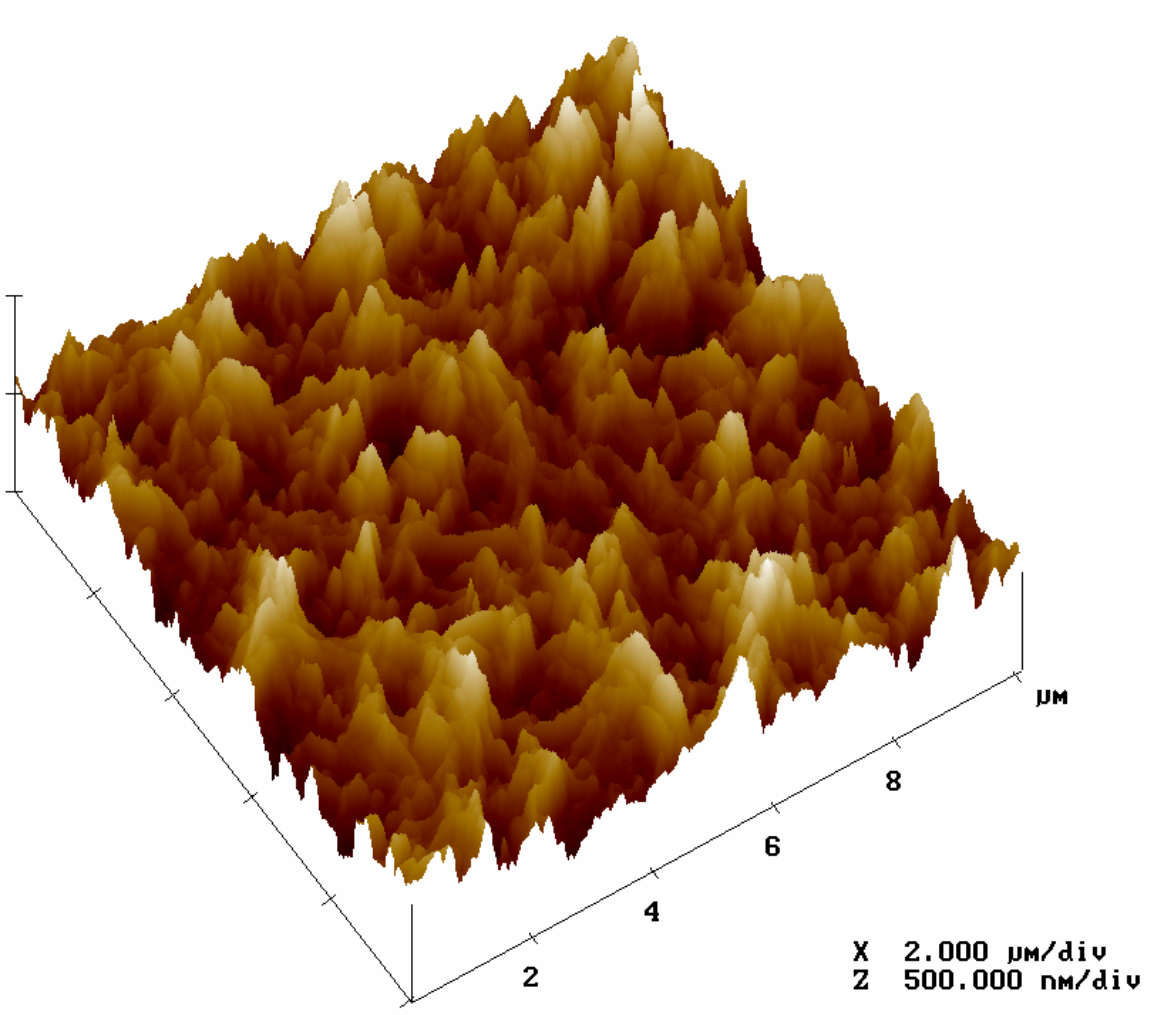

Table A.14: AFM Results for SN5P

Parameter	Scan 1	Scan 2	Scan 3	Scan 4	Scan 5	Scan 6	Scan 7	Scan 8	Average
RMS (nm)	98.1	100.6	96.8	91.4	91.5	106.2	103.8	99.0	98.4
R_a (nm)	77.9	79.9	75.5	71.4	72.5	82.0	83.9	79.1	77.8
Surface Area Difference (%)	38.3	40.4	38.7	41.5	41.1	40.3	39.9	42.2	40.3
Peak Count	180	178	200	229	216	168	159	206	192.0

Figure A.15: 3-Dimensional AFM Image of SN6

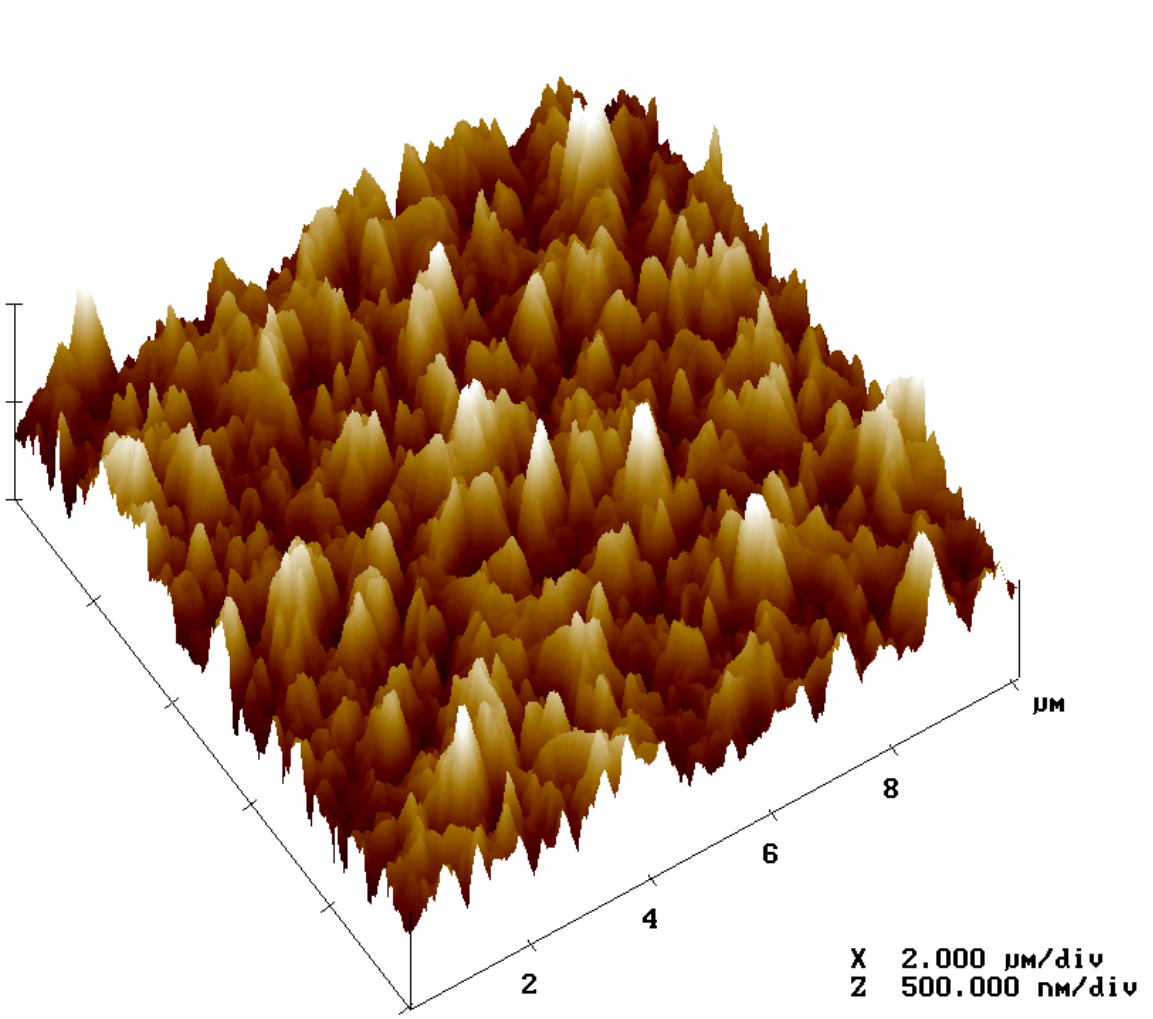

Table A.15: AFM Results for SN6

Parameter	Scan 1	Scan 2	Scan 3	Scan 4	Scan 5	Scan 6	Scan 7	Scan 8	Average
RMS (nm)	121.9	108.4	108.4	109.6	110.4	113.4	117.0	120.2	113.7
R_a (nm)	96.4	86.4	86.9	88.8	87.9	89.9	93.4	93.9	90.4
Surface Area Difference (%)	75.1	66.1	66.0	69.4	67.6	66.4	69.6	75.2	69.4
Peak Count	190	250	236	250	236	215	225	201	225.4

Figure A.16: 3-Dimensional AFM Image of SN6P

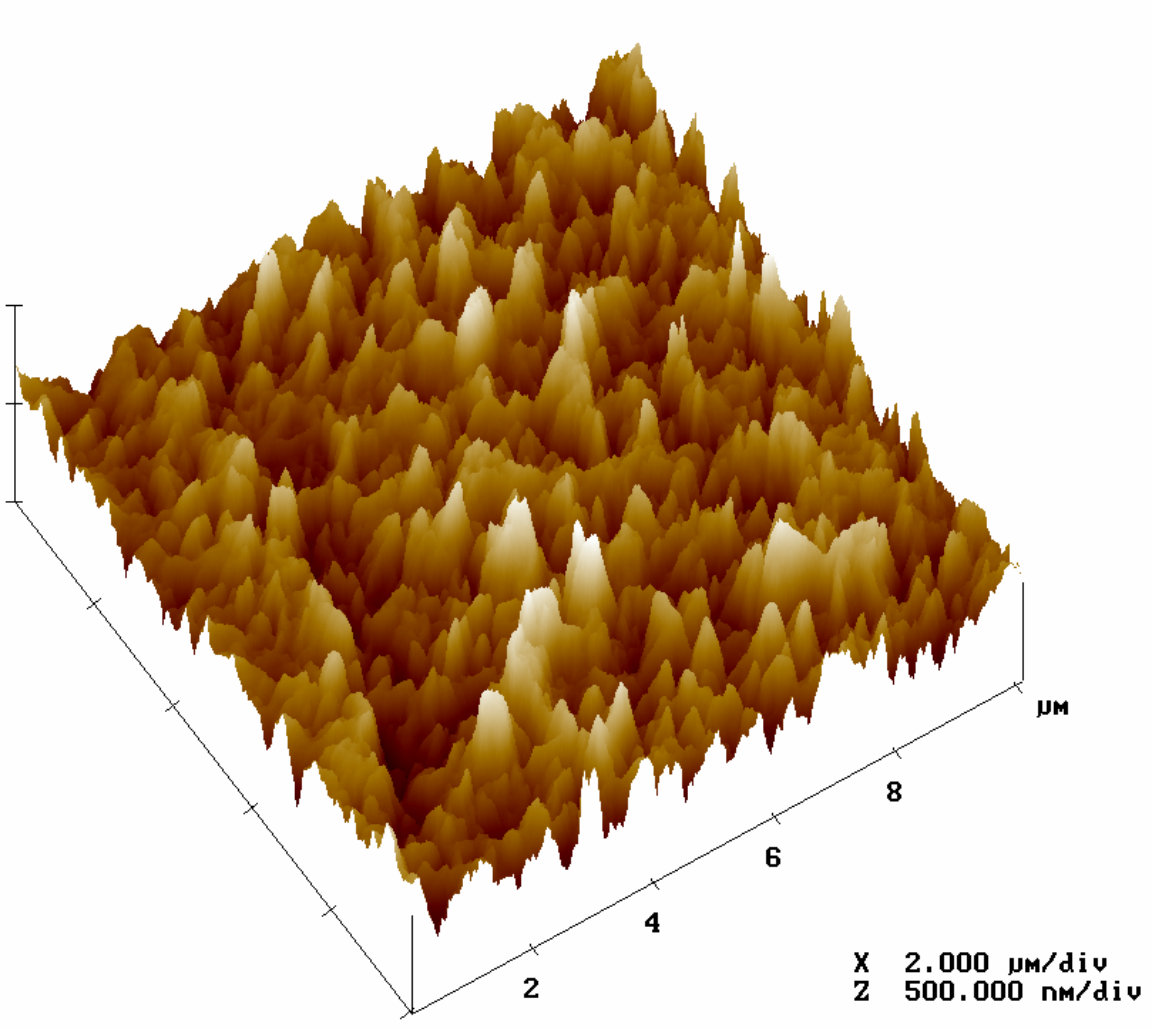

Table A.16: AFM Results for SN6P

Parameter	Scan 1	Scan 2	Scan 3	Scan 4	Scan 5	Scan 6	Scan 7	Scan 8	Average
RMS (nm)	91.2	87.3	112.8	89.8	99.7	107.1	100.6	96.5	98.1
R_a (nm)	72.8	69.5	88.7	71.5	78.4	84.9	79.0	74.9	77.5
Surface Area Difference (%)	48.7	49.6	53.3	53.1	46.7	56.3	57.4	44.1	51.1
Peak Count	228	418	301	346	196	219	254	258	277.5

Figure A.17: 3-Dimensional AFM Image of SN7

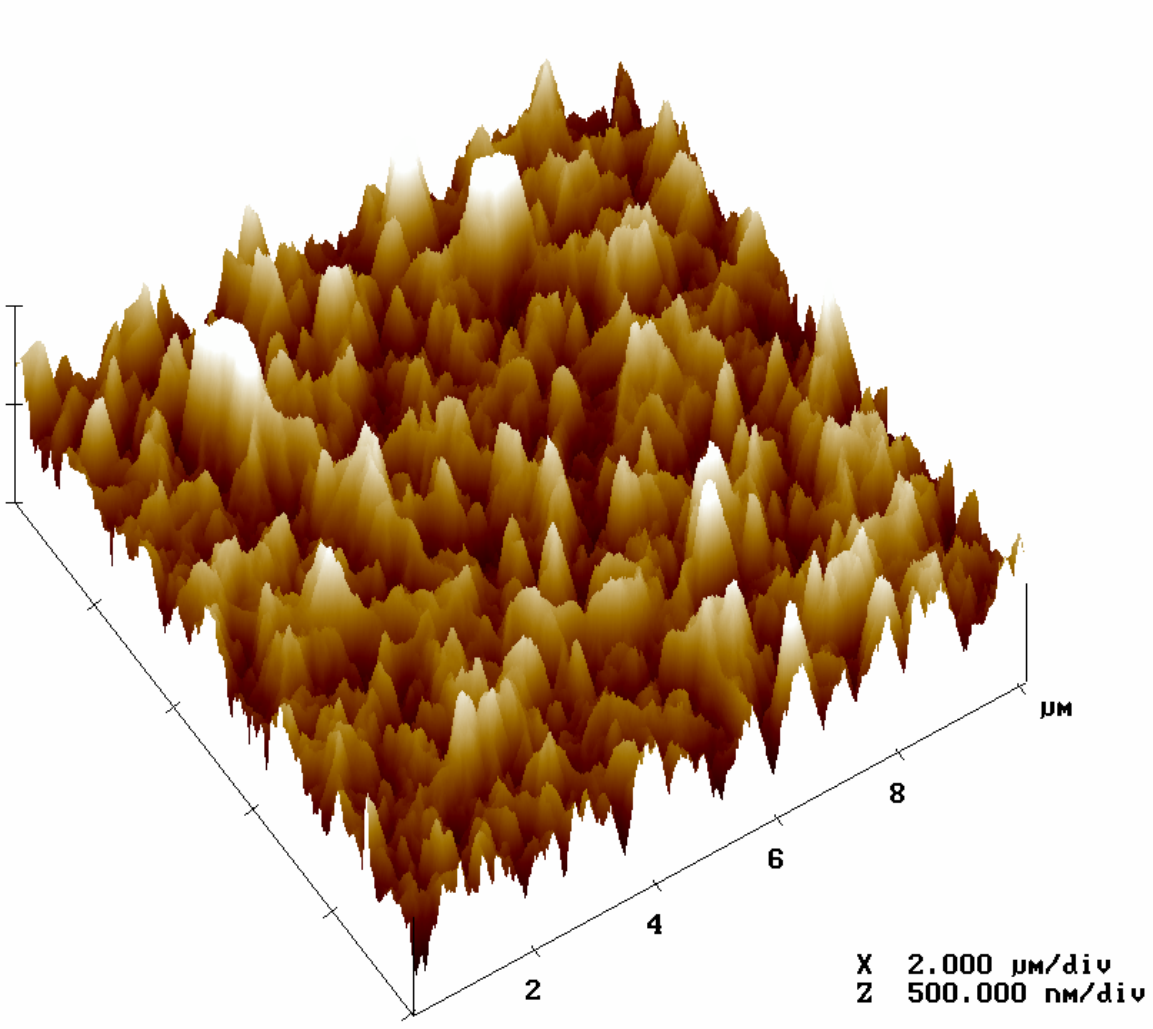

Table A.17: AFM Results for SN7

Parameter	Scan 1	Scan 2	Scan 3	Scan 4	Scan 5	Scan 6	Scan 7	Scan 8	Average
RMS (nm)	123.3	128.8	121.3	128.0	128.7	128.2	122.9	119.7	125.1
R_a (nm)	97.2	103.2	96.7	102.0	101.3	101.5	96.5	95.7	99.3
Surface Area Difference (%)	76.1	71.6	70.6	67.5	72.5	74.0	75.5	72.9	72.6
Peak Count	267	231	258	196	220	224	286	250	241.5

Figure A.18: 3-Dimensional AFM Image of SN7P

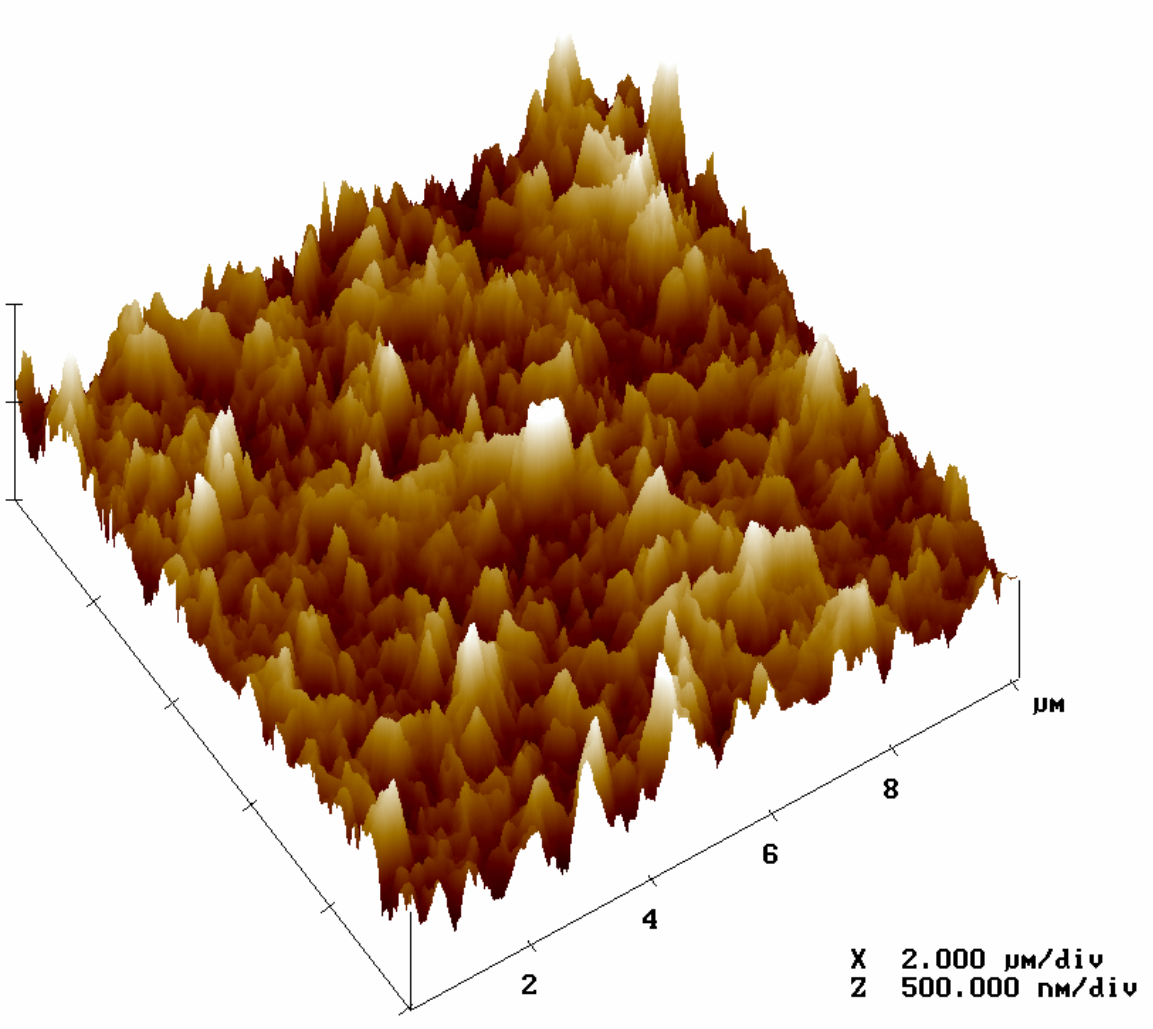

Table A.18: AFM Results for SN7P

Parameter	Scan 1	Scan 2	Scan 3	Scan 4	Scan 5	Scan 6	Scan 7	Scan 8	Average
RMS (nm)	103.7	120.1	104.8	106.6	119.6	120.1	111.8	114.7	112.7
R_a (nm)	81.7	94.7	84.7	83.6	92.2	94.7	89.9	91.8	89.1
Surface Area Difference (%)	65.0	67.2	66.2	58.4	64.8	67.2	67.5	68.8	65.6
Peak Count	249	197	227	246	226	197	275	286	237.9

Figure A.19: 3-Dimensional AFM Image of SN8

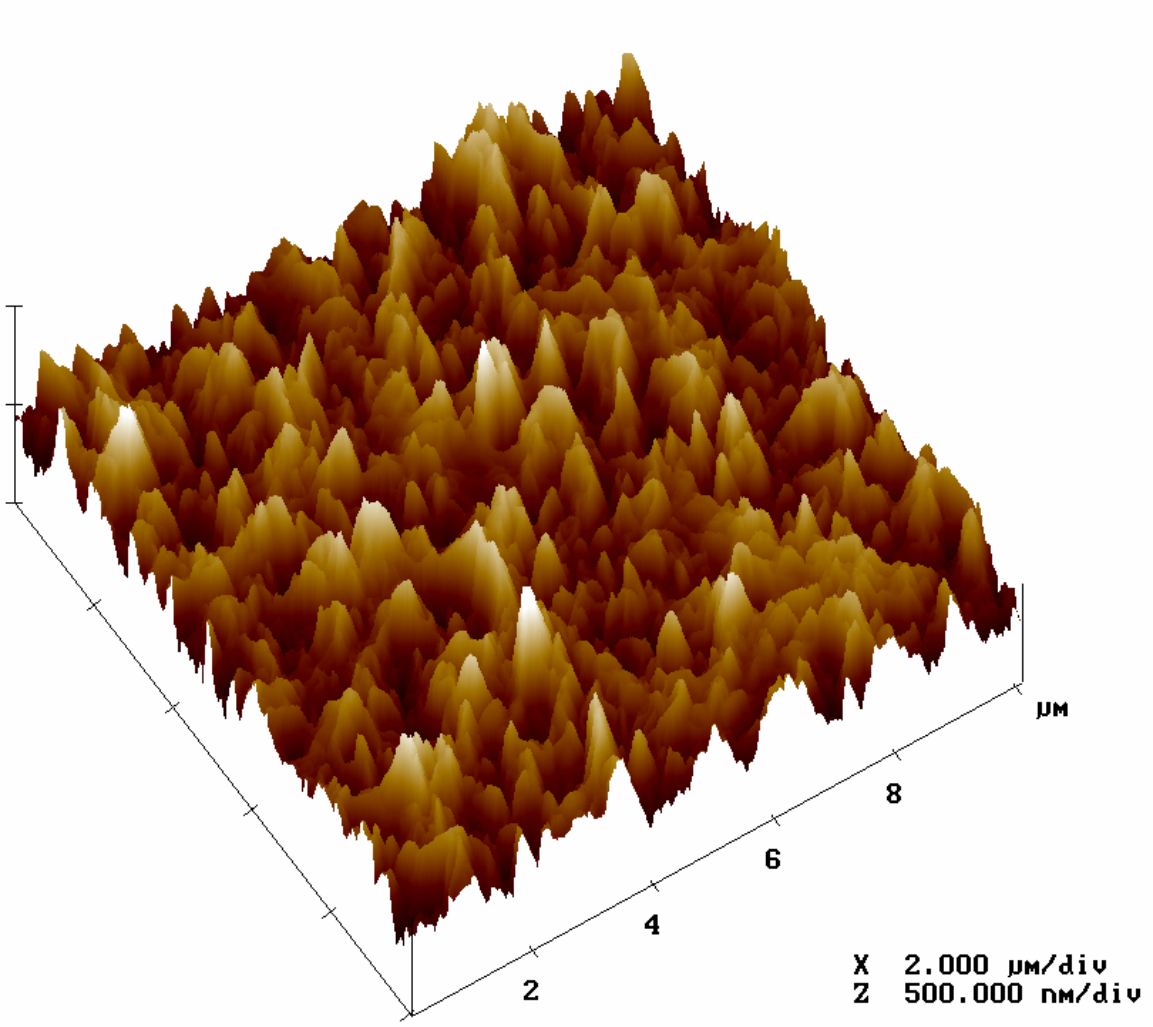

Table A.19 AFM Results for SN8

Parameter	Scan 1	Scan 2	Scan 3	Scan 4	Scan 5	Scan 6	Scan 7	Scan 8	Average
RMS (nm)	98.2	111.3	94.9	111.0	99.9	108.0	104.7	105.5	104.2
R_a (nm)	78.8	90.4	75.2	87.0	79.1	87.1	84.8	83.5	83.2
Surface Area Difference (%)	65.7	63.6	61.3	66.3	63.7	65.9	64.7	63.5	64.3
Peak Count	295	230	260	197	231	221	241	211	235.8

Figure A.20: 3-Dimensional AFM Image of SN8P

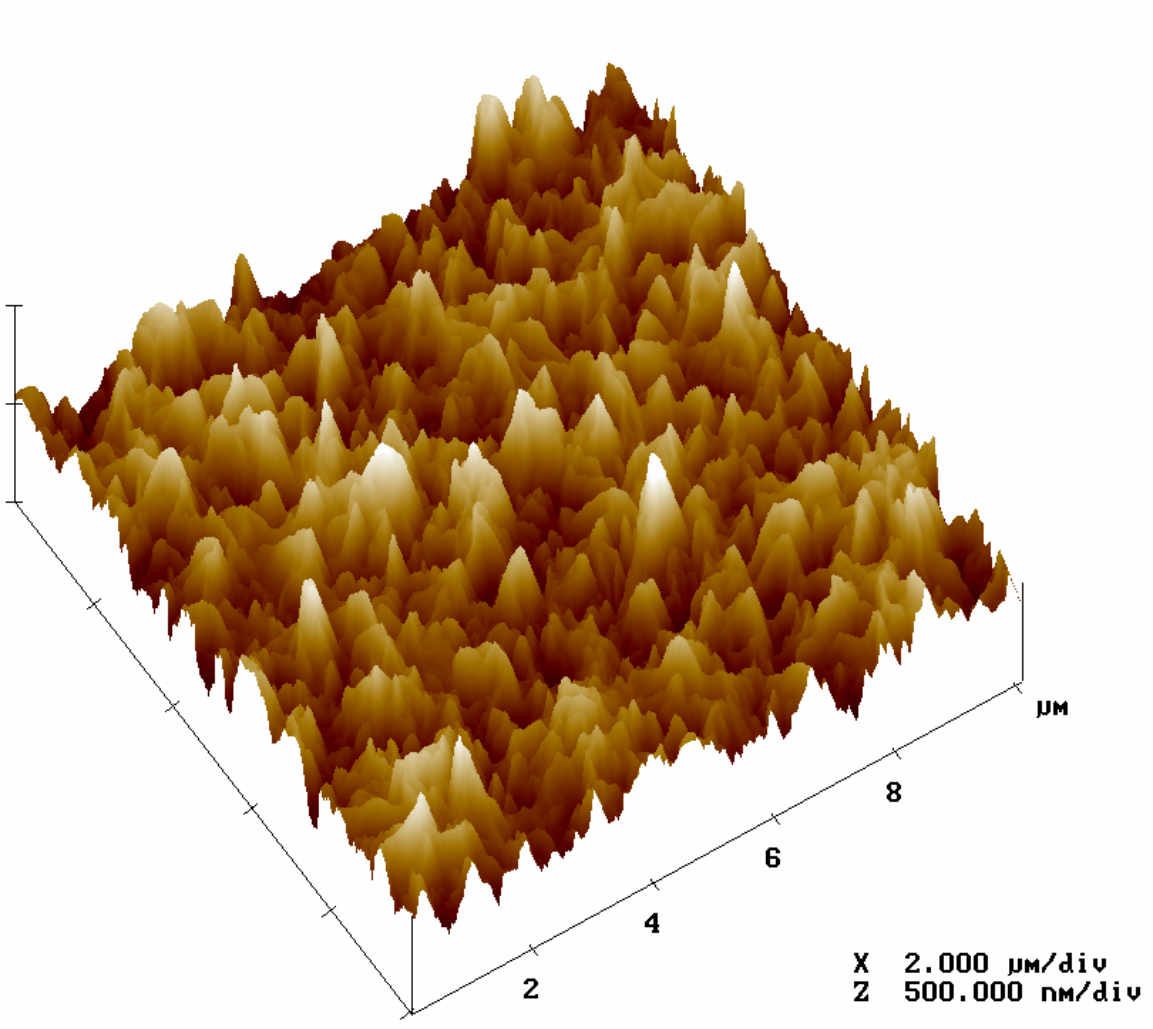

Table A.20: AFM Results for SN8P

Parameter	Scan 1	Scan 2	Scan 3	Scan 4	Scan 5	Scan 6	Scan 7	Scan 8	Average
RMS (nm)	102.8	101.1	101.1	106.3	103.2	102.8	102.4	109.9	103.7
R_a (nm)	82.3	80.1	80.1	83.3	80.6	81.4	81.2	86.6	81.9
Surface Area Difference (%)	59.8	55.4	55.4	54.3	52.9	62.5	60.9	63.1	58.0
Peak Count	199	201	201	196	188	228	231	214	207.3

APPENDIX B

PERMEATE FLUX FIGURES

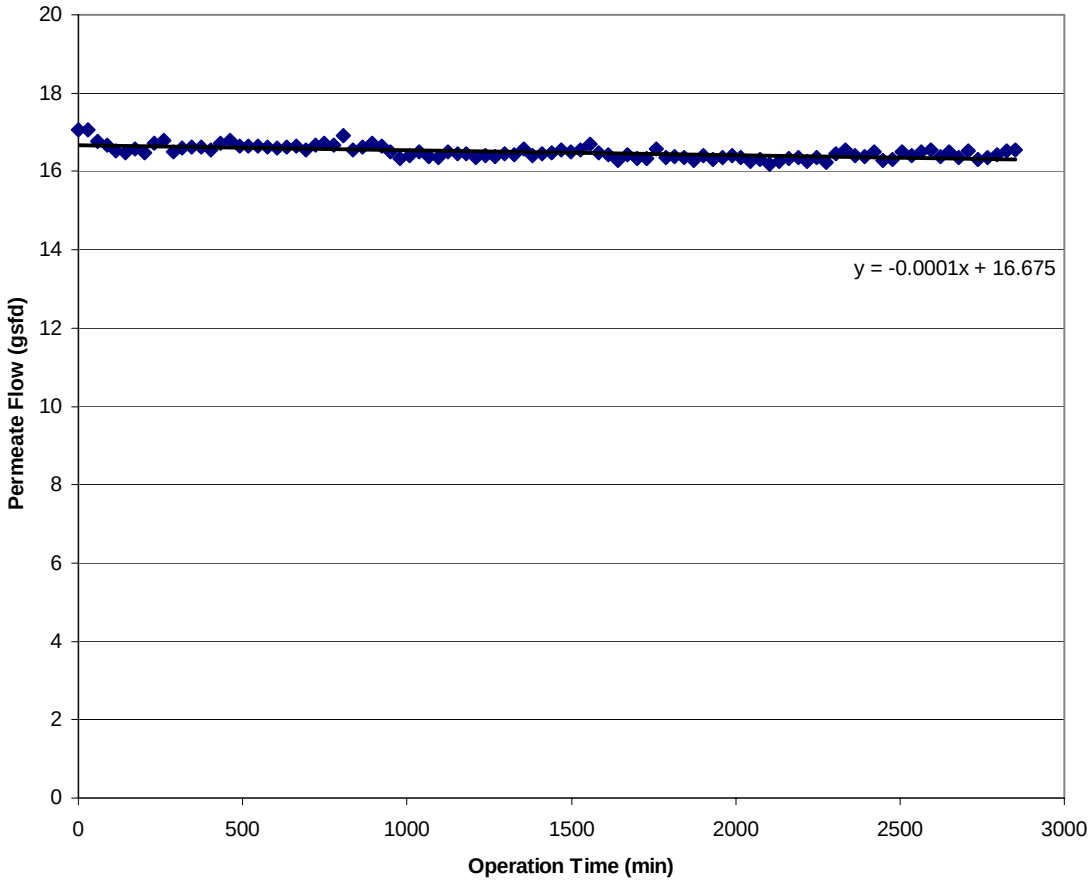

Figure B.1: SN1CP membrane run for 48 hour duration at initial flux of 17gsfd. Operational conditions consisted of a solution containing Cocoa Raw water. Rejection was 97.4% based on conductivity. Initial MTC was 0.1033 gsfd/psi.

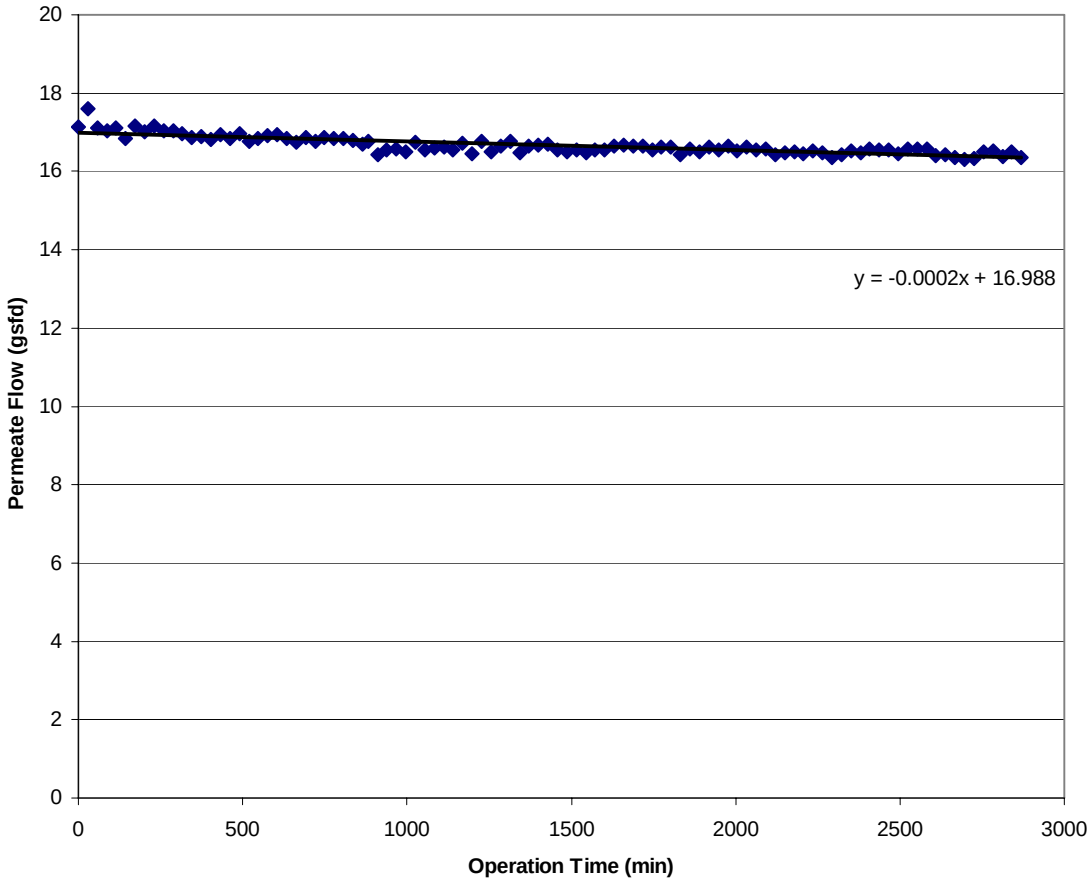

Figure B.2: SN2 membrane run for 48 hour duration at initial flux of 17gsfd. Operational conditions consisted of a solution containing Cocoa Raw water. Rejection was 96.5% based on conductivity. Initial MTC was 0.0562 gsfd/psi.

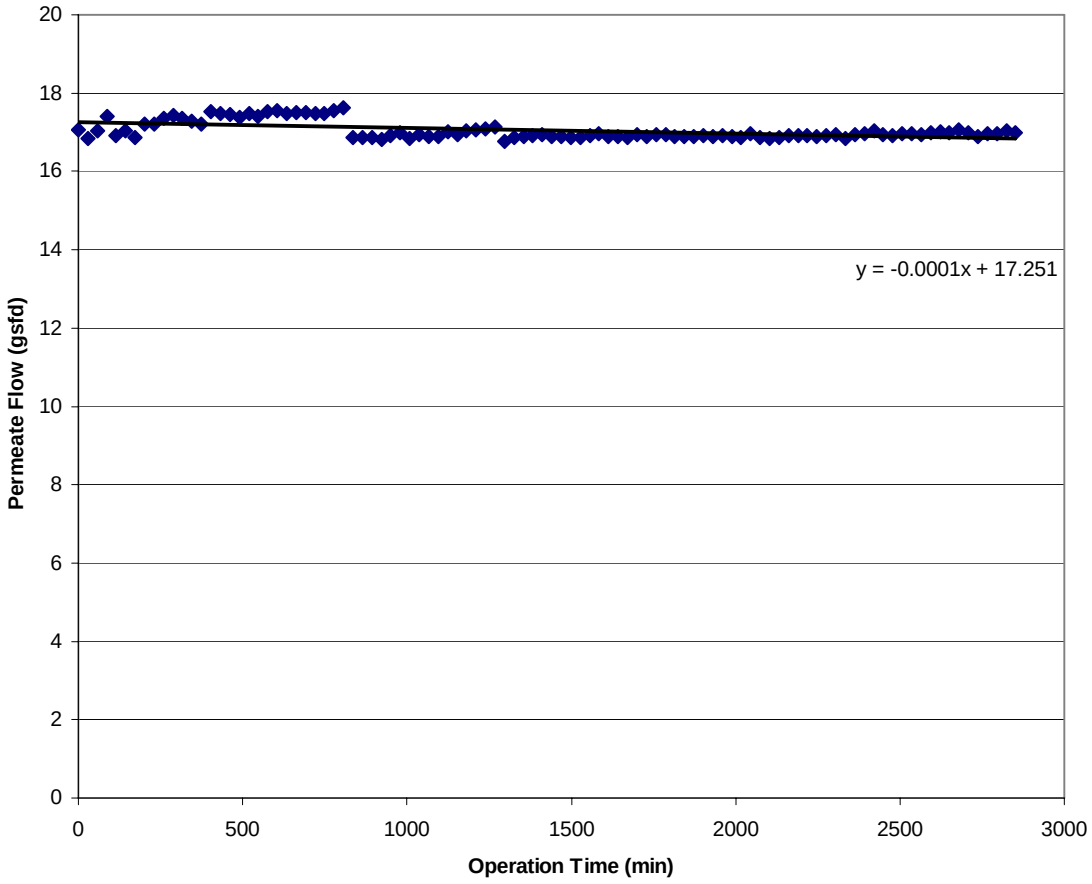

Figure B.3: SN2P membrane run for 48 hour duration at initial flux of 17gsfd. Operational conditions consisted of a solution containing Cocoa Raw water. Rejection was 97.6% based on conductivity. Initial MTC was 0.0741 gsfd/psi.

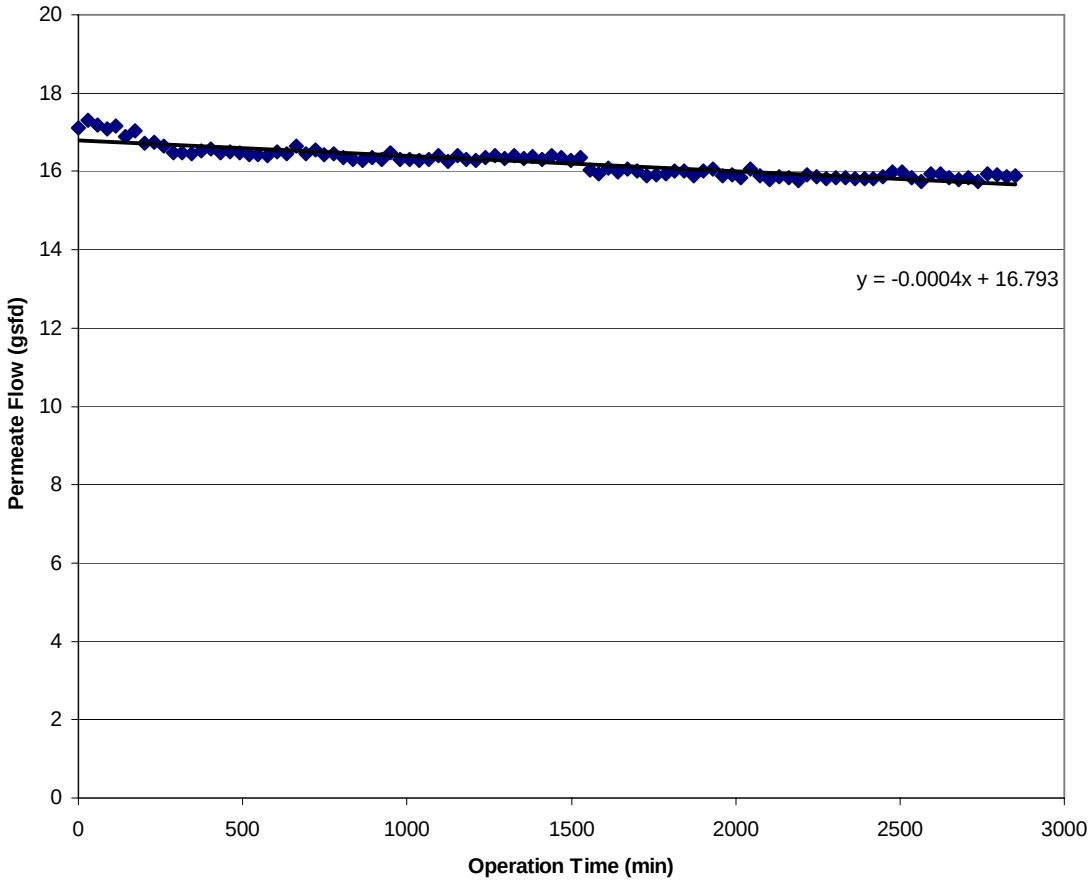

Figure B.4: SN3 membrane run for 48 hour duration at initial flux of 17gsfd. Operational conditions consisted of a solution containing Cocoa Raw water. Rejection was 96.4% based on conductivity. Initial MTC was 0.0632 gsfd/psi.

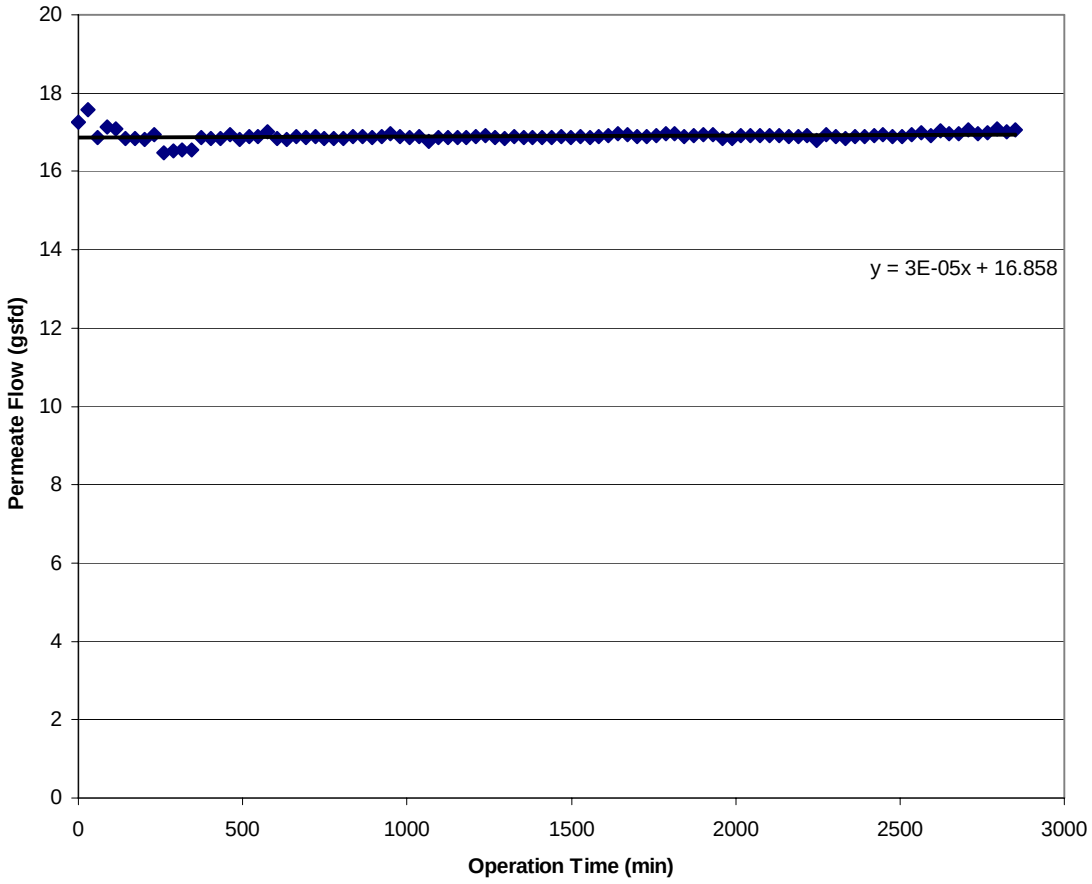

Figure B.5: SN3P membrane run for 48 hour duration at initial flux of 17gsfd. Operational conditions consisted of a solution containing Cocoa Raw water. Rejection was 97.3% based on conductivity. Initial MTC was 0.0719 gsfd/psi.

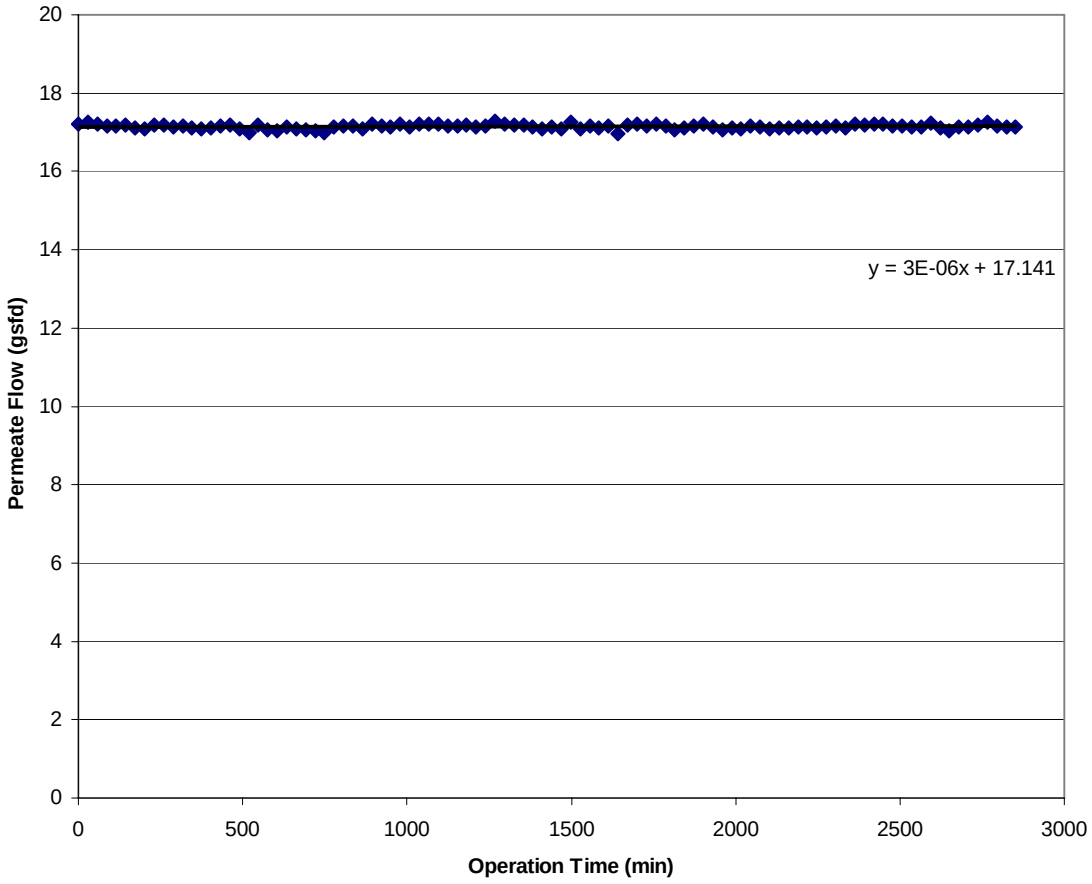

Figure B.6: SN4 membrane run for 48 hour duration at initial flux of 17gsfd. Operational conditions consisted of a solution containing Cocoa Raw water. Rejection was 98.0% based on conductivity. Initial MTC was 0.0637 gsfd/psi.

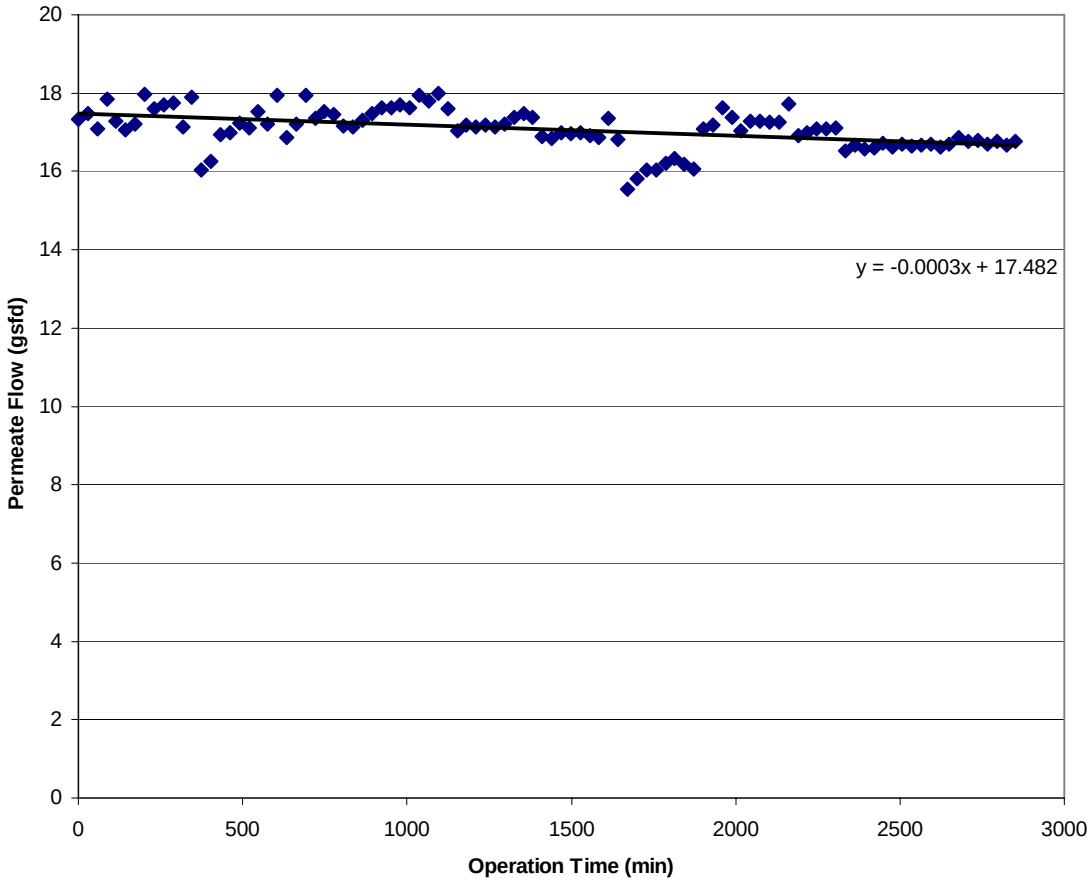

Figure B.7: SN4P membrane run for 48 hour duration at initial flux of 17gsfd. Operational conditions consisted of a solution containing Cocoa Raw water. Rejection was 98.1% based on conductivity. Initial MTC was 0.0867 gsfd/psi.

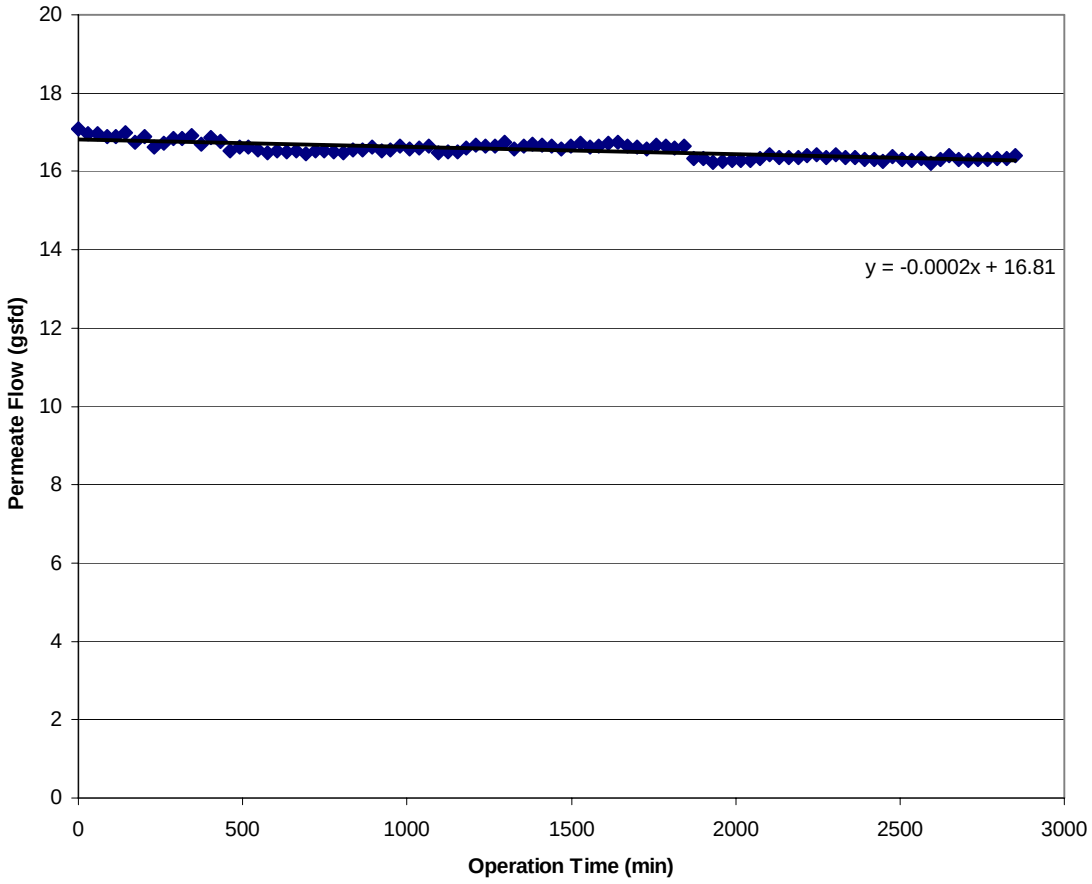

Figure B.8: SN4P2 membrane run for 48 hour duration at initial flux of 17gsfd. Operational conditions consisted of a solution containing Cocoa Raw water. Rejection was 96.3% based on conductivity. Initial MTC was 0.0813 gsfd/psi.

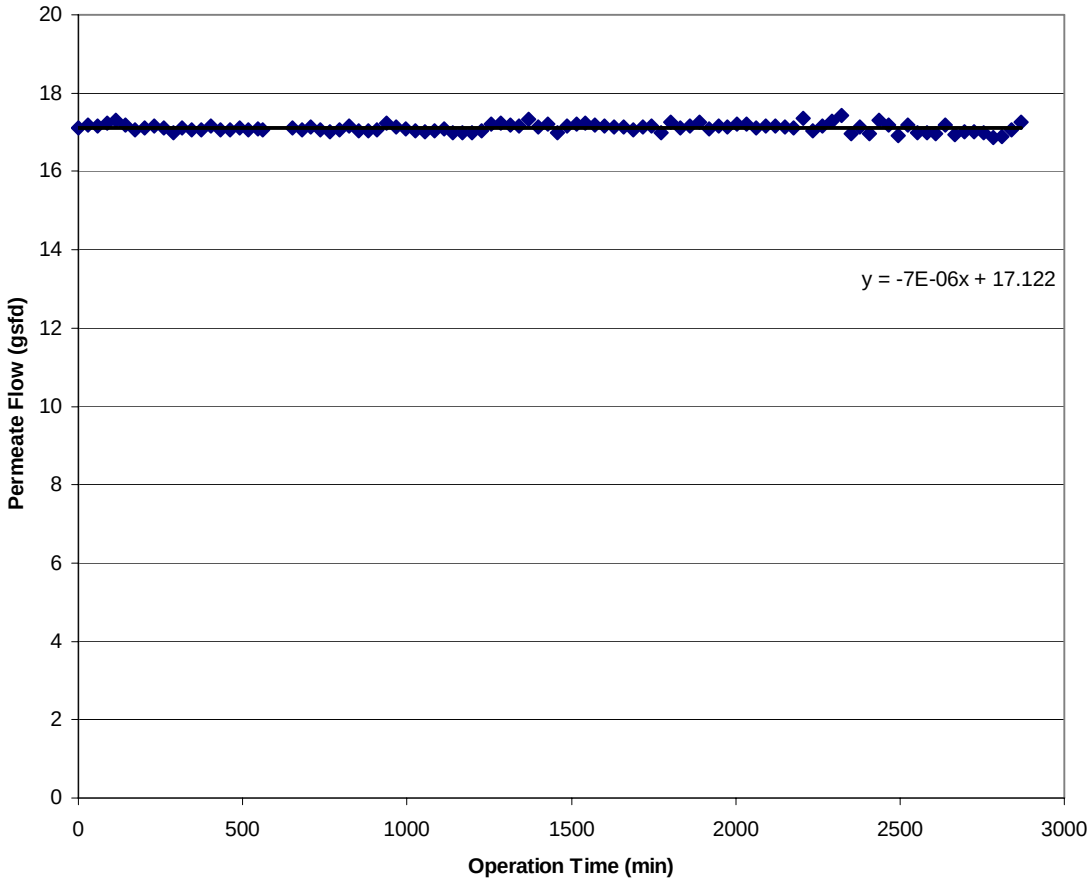

Figure B.9: SN5 membrane run for 48 hour duration at initial flux of 17gsfd. Operational conditions consisted of a solution containing Cocoa Raw water. Rejection was 96.5% based on conductivity. Initial MTC was 0.0704 gsfd/psi.

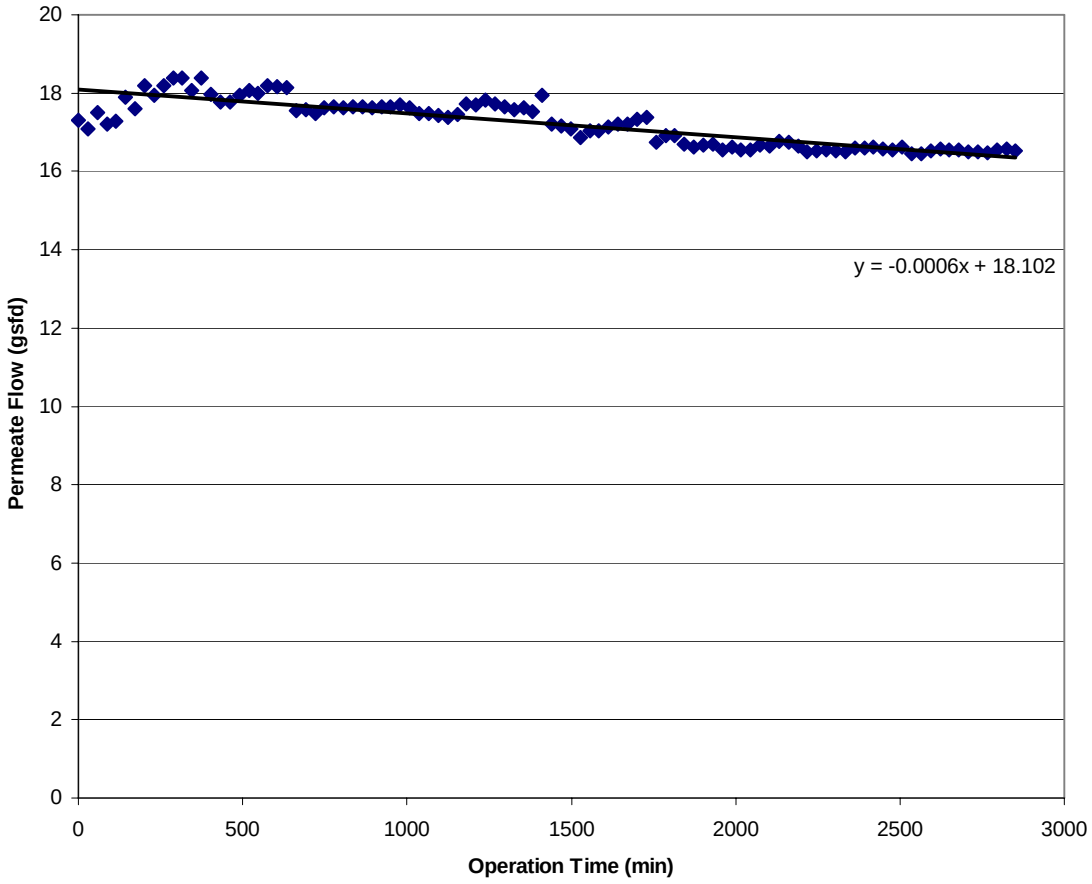

Figure B.10: SN5P membrane run for 48 hour duration at initial flux of 17gsfd. Operational conditions consisted of a solution containing Cocoa Raw water. Rejection was 97.8% based on conductivity. Initial MTC was 0.0911 gsfd/psi.

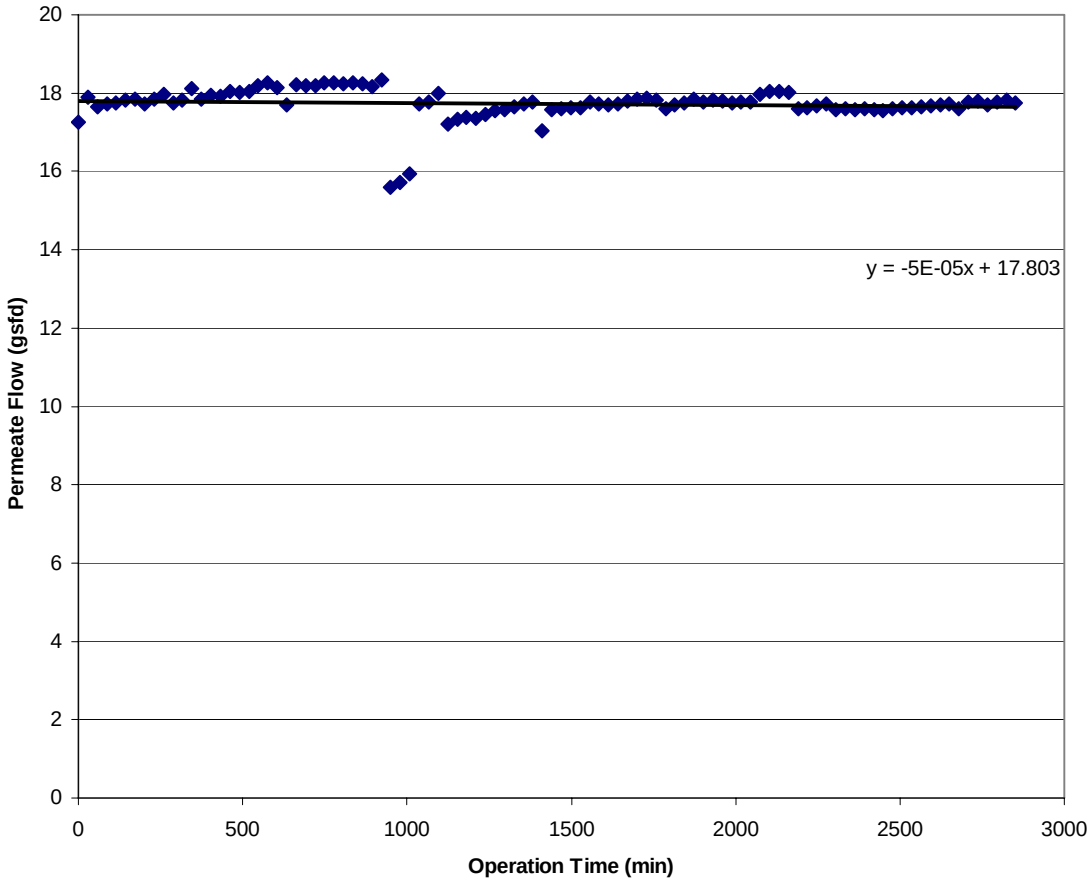

Figure B.11: SN6 membrane run for 48 hour duration at initial flux of 17gsfd. Operational conditions consisted of a solution containing Cocoa Raw water. Rejection was 98.0% based on conductivity. Initial MTC was 0.0702 gsfd/psi.

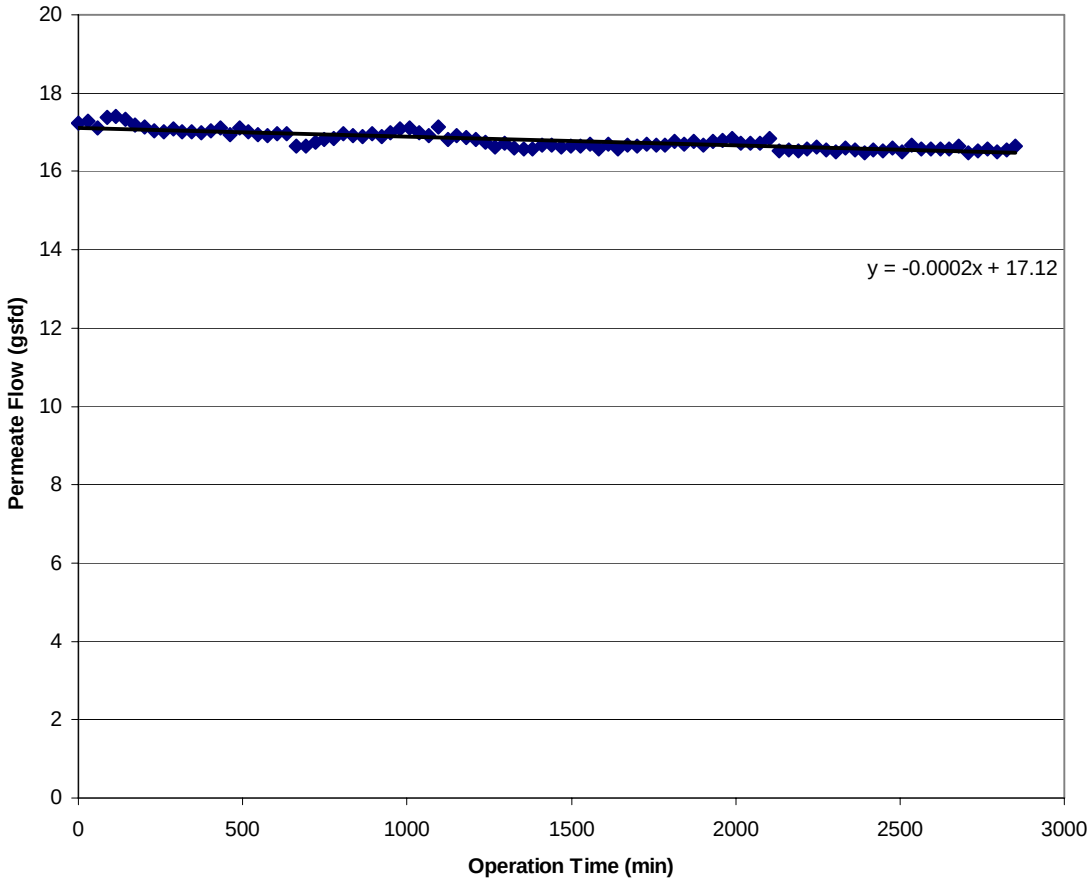

Figure B.12: SN6P membrane run for 48 hour duration at initial flux of 17gsfd. Operational conditions consisted of a solution containing Cocoa Raw water. Rejection was 95.9% based on conductivity. Initial MTC was 0.1014 gsfd/psi.

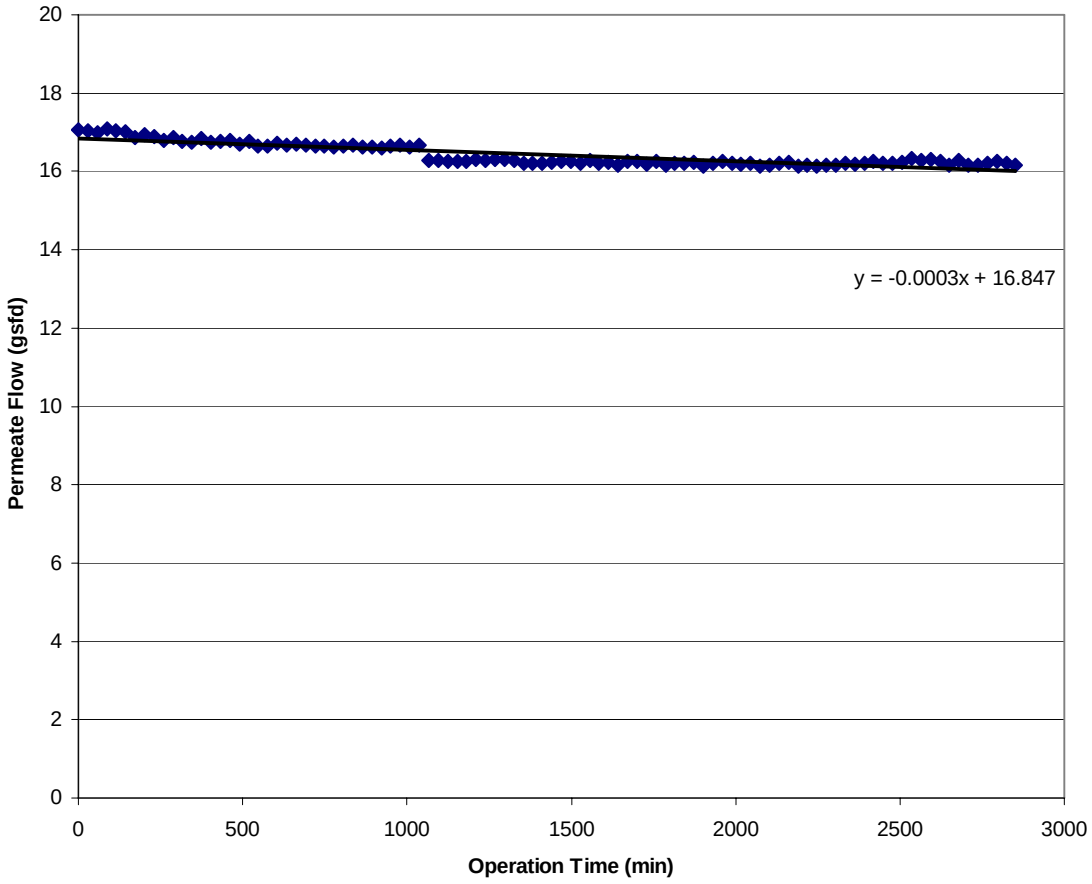

Figure B.13: SN6P2 membrane run for 48 hour duration at initial flux of 17gsfd. Operational conditions consisted of a solution containing Cocoa Raw water. Rejection was 96.2% based on conductivity. Initial MTC was 0.1004 gsfd/psi.

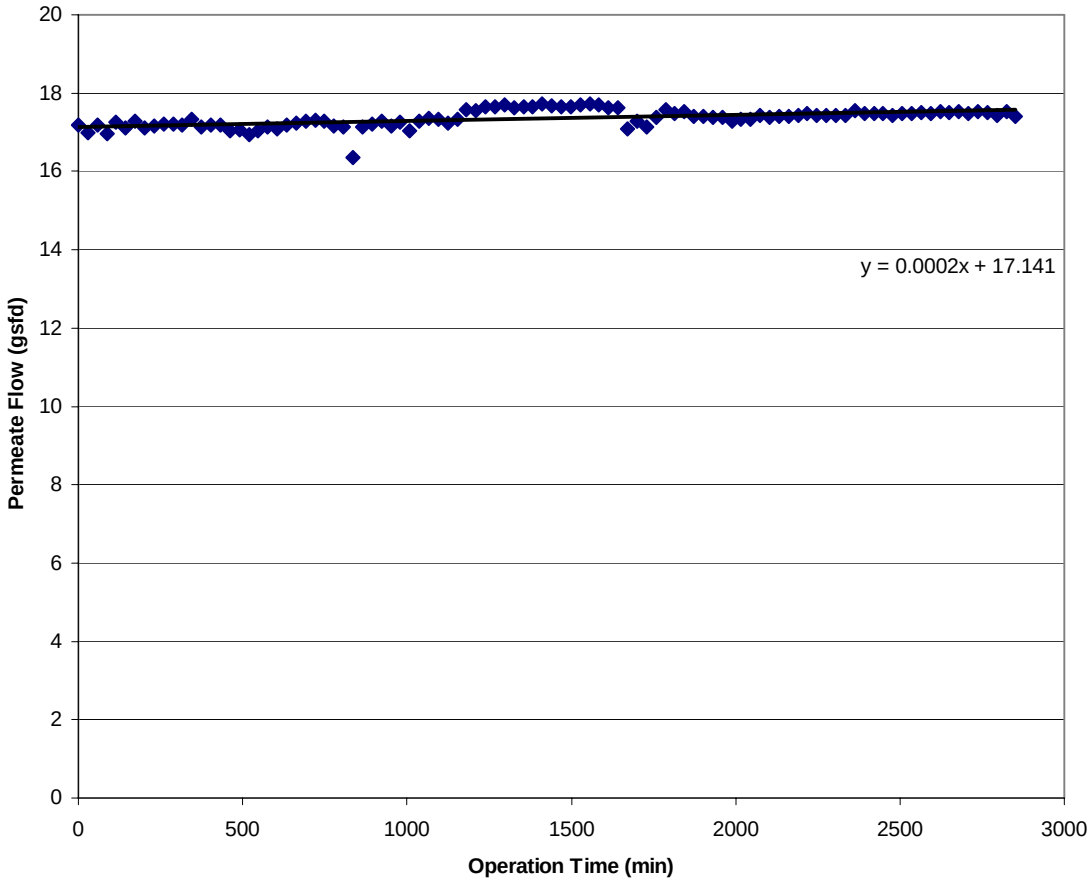

Figure B.14: SN7 membrane run for 48 hour duration at initial flux of 17gsfd. Operational conditions consisted of a solution containing Cocoa Raw water. Rejection was 96.9% based on conductivity. Initial MTC was 0.0748 gsfd/psi.

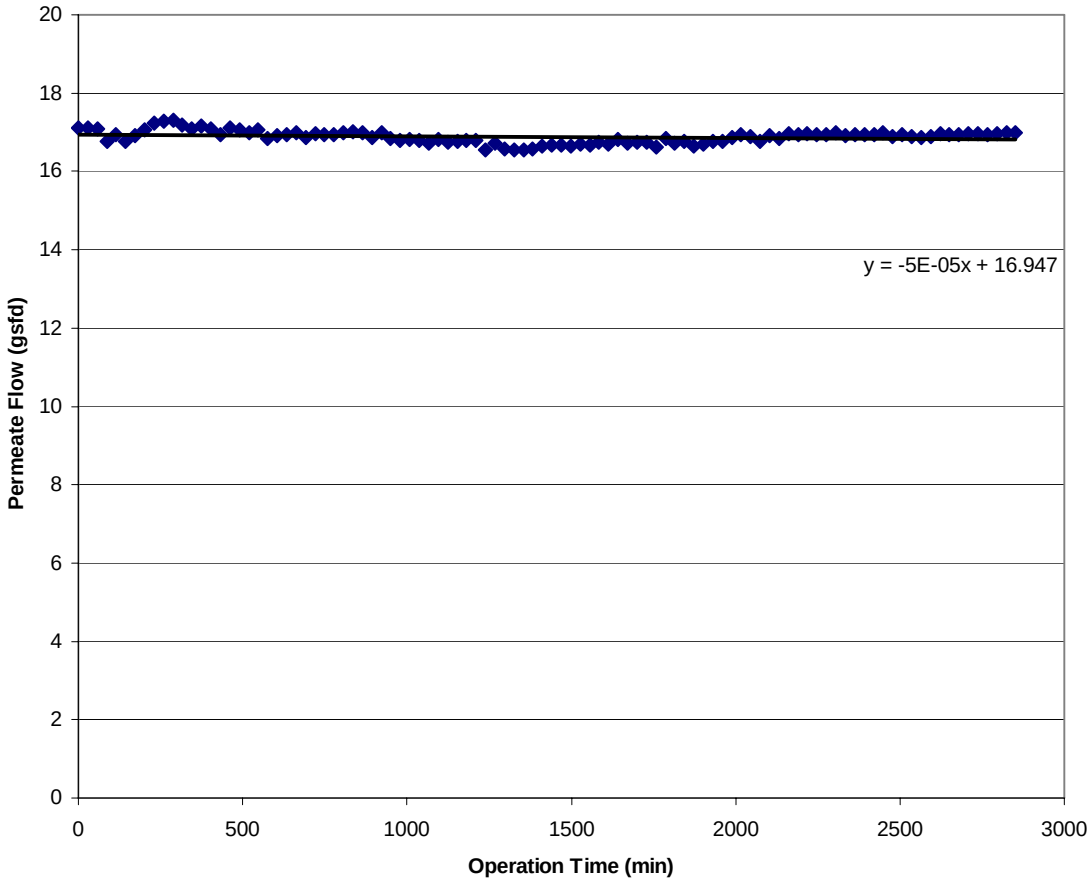

Figure B.15: SN7P2 membrane run for 48 hour duration at initial flux of 17gsfd. Operational conditions consisted of a solution containing Cocoa Raw water. Rejection was 96.7% based on conductivity. Initial MTC was 0.1141 gsfd/psi.

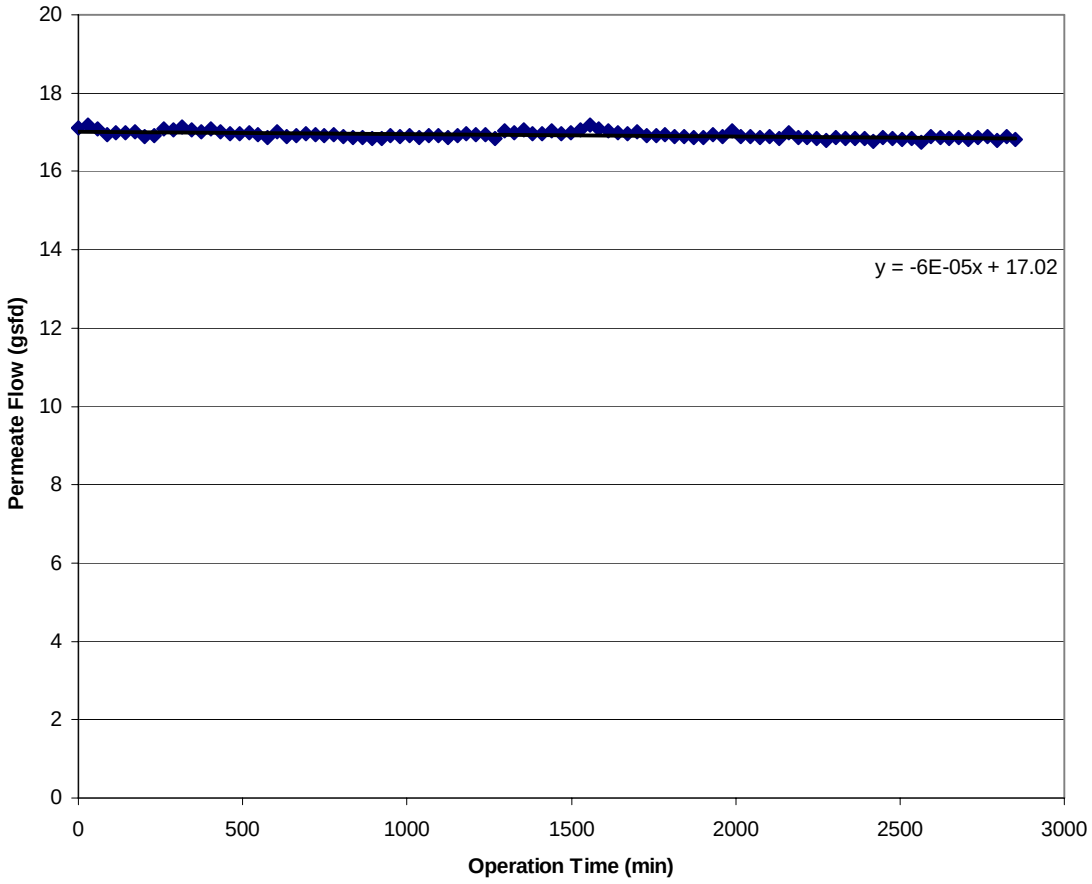

Figure B.16: SN7P3 membrane run for 48 hour duration at initial flux of 17gsfd. Operational conditions consisted of a solution containing Cocoa Raw water. Rejection was 96.8% based on conductivity. Initial MTC was 0.1134 gsfd/psi.

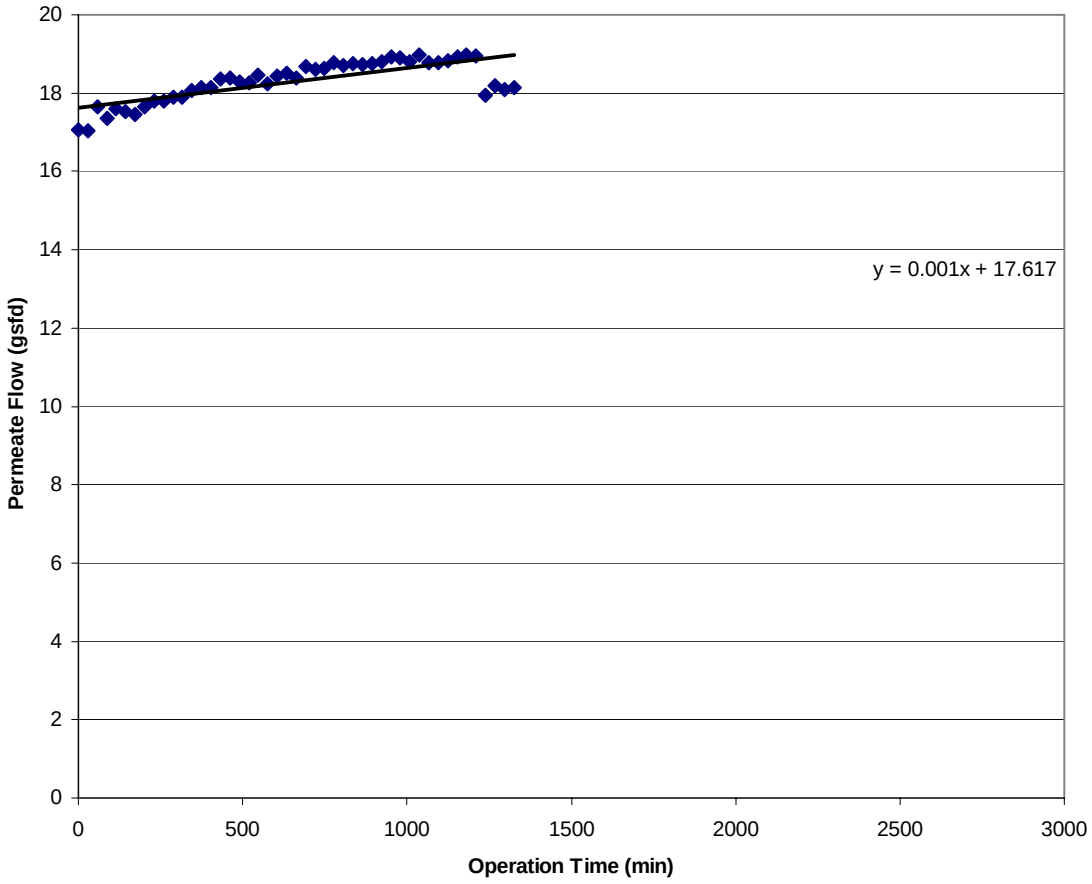

Figure B.17: SN8 membrane run for 48 hour duration at initial flux of 17gsfd. Operational conditions consisted of a solution containing Cocoa Raw water. Rejection was 98.0% based on conductivity. Initial MTC was 0.0741 gsfd/psi.

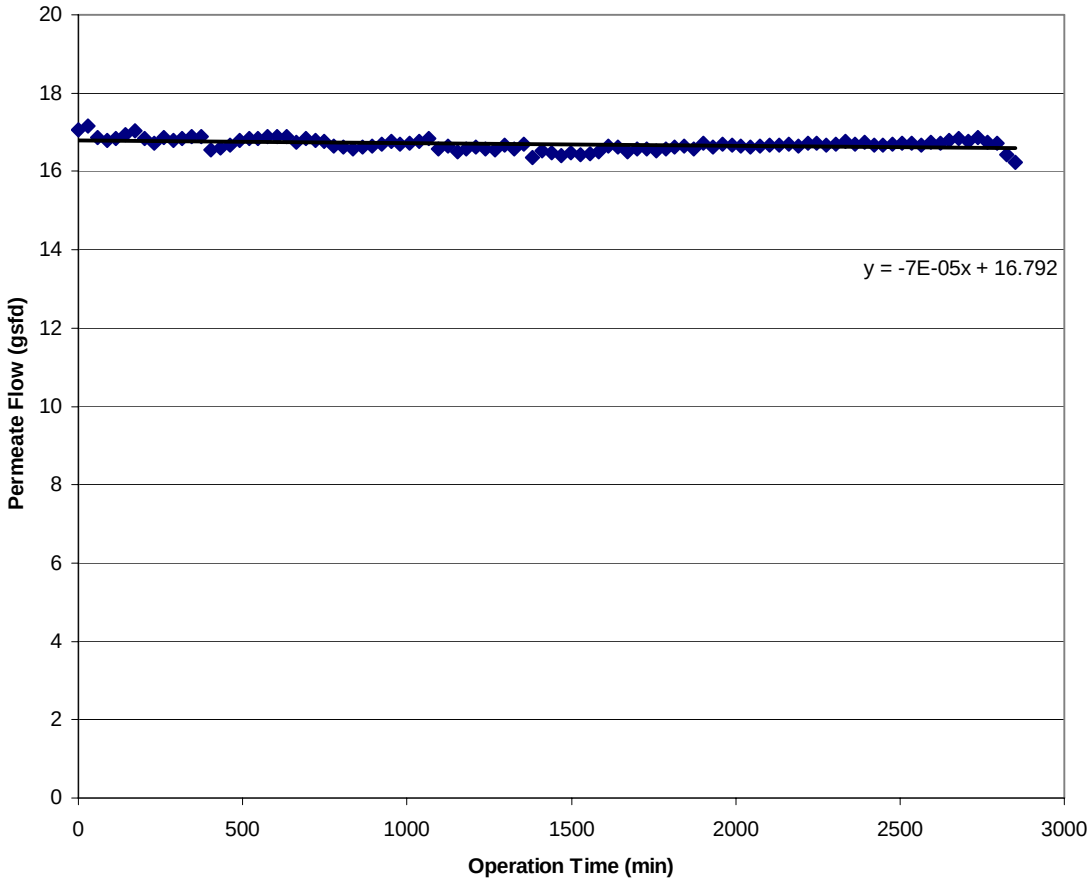

Figure B.18: SN8 2 membrane run for 48 hour duration at initial flux of 17gsfd. Operational conditions consisted of a solution containing Cocoa Raw water. Rejection was 97.1% based on conductivity. Initial MTC was 0.0853 gsfd/psi.

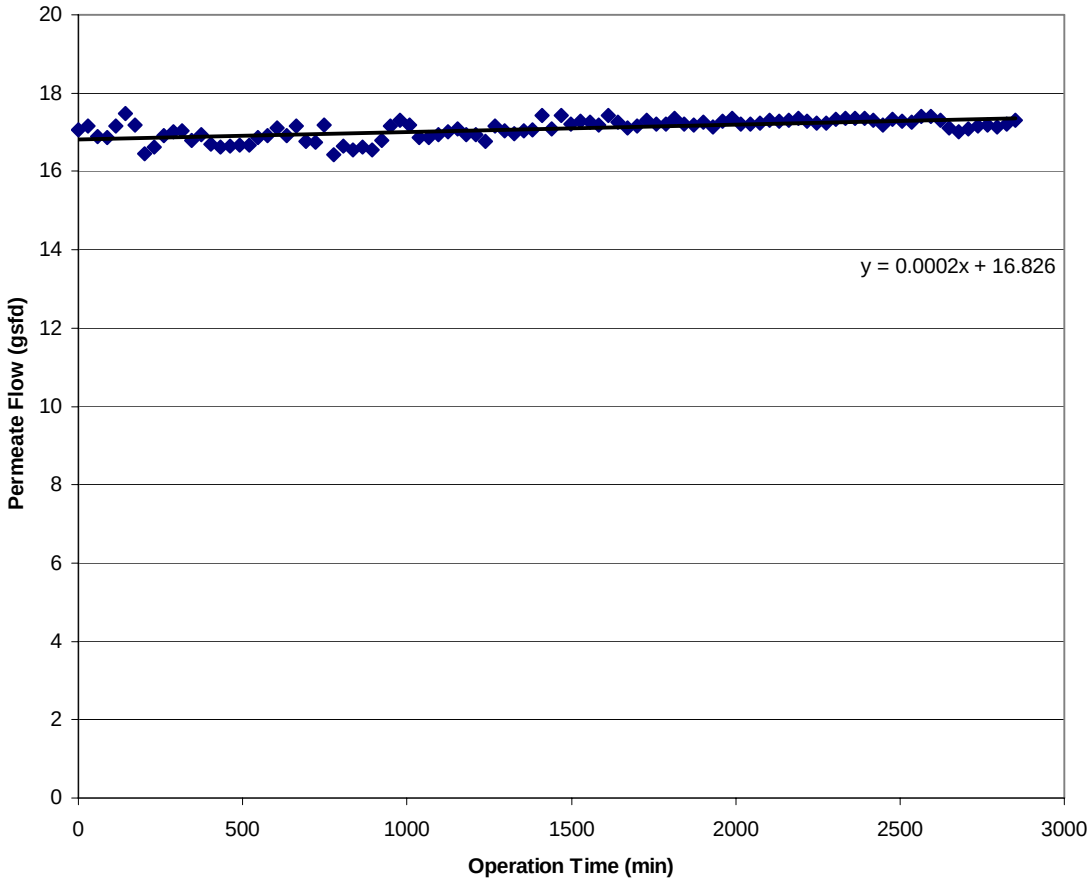

Figure B.19: SN8P2 membrane run for 48 hour duration at initial flux of 17gsfd. Operational conditions consisted of a solution containing Cocoa Raw water. Rejection was 97.6% based on conductivity. Initial MTC was 0.1093 gsfd/psi.

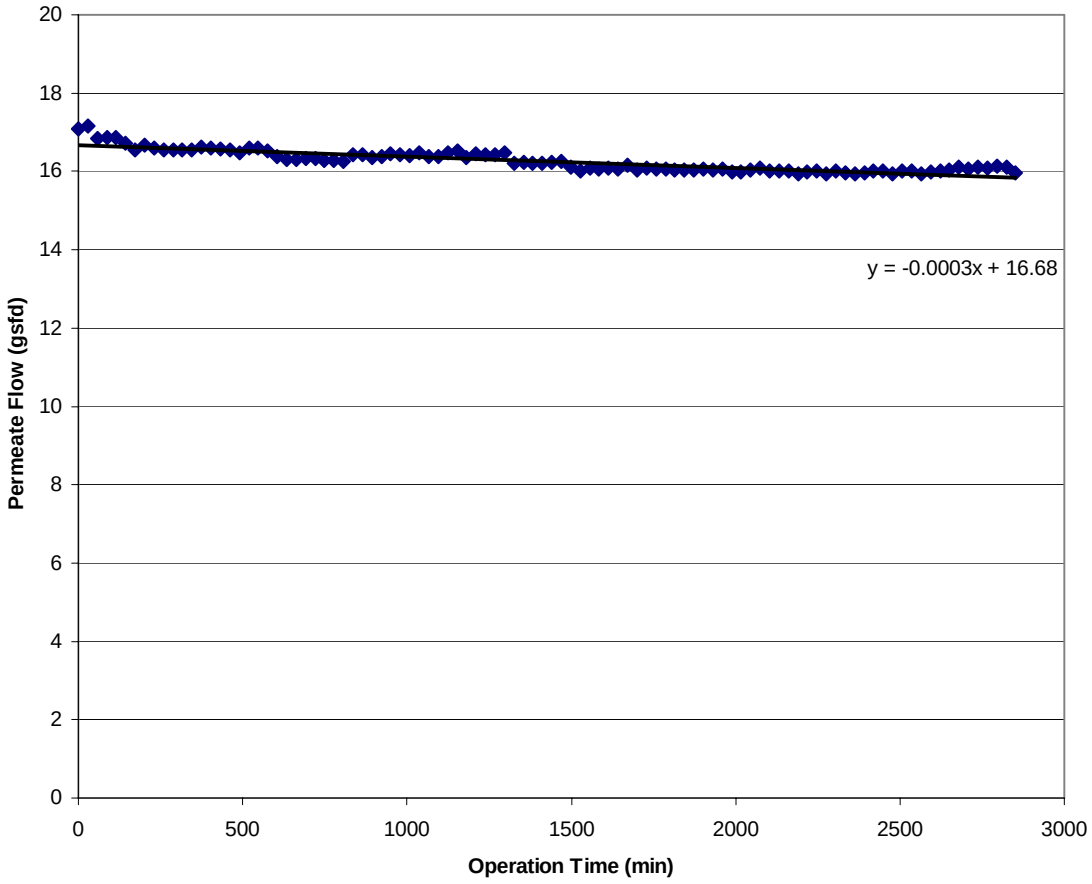

Figure B.20: SN8P3 membrane run for 48 hour duration at initial flux of 17gsfd. Operational conditions consisted of a solution containing Cocoa Raw water. Rejection was 96.9% based on conductivity. Initial MTC was 0.1132 gsfd/psi.

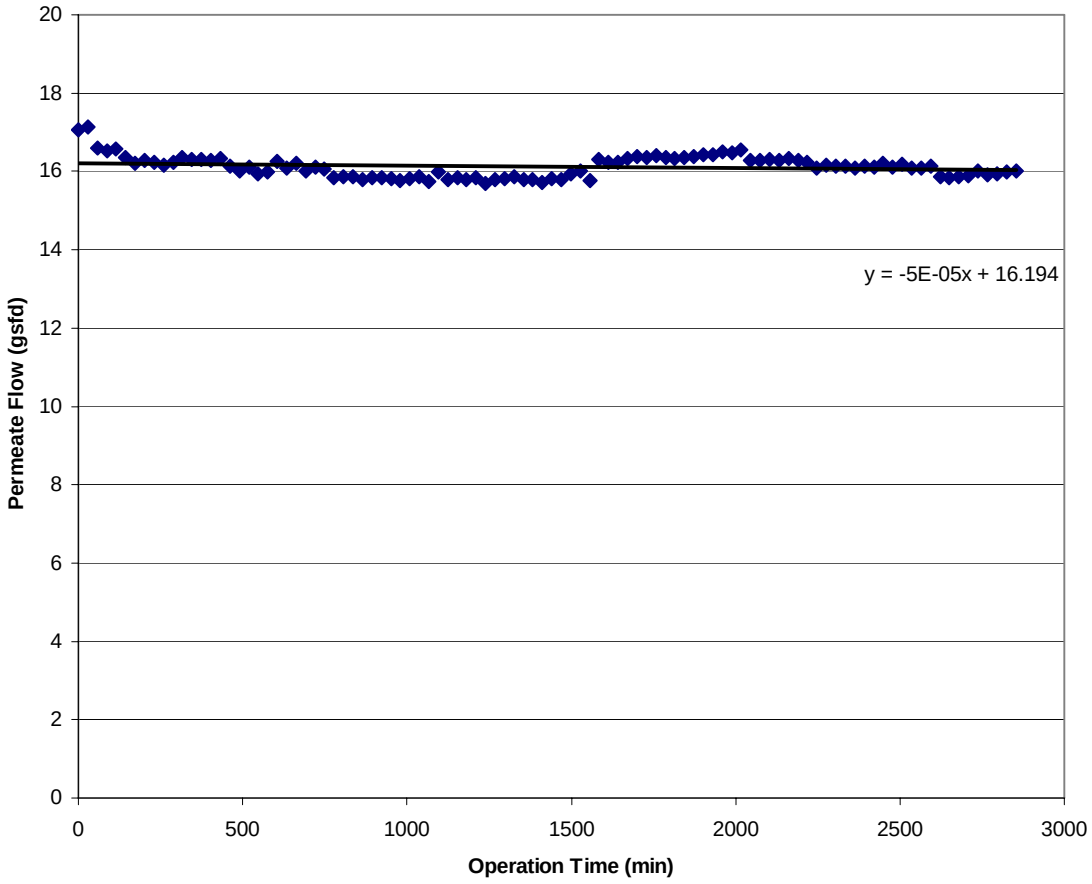

Figure B.21: SN8P4 membrane run for 48 hour duration at initial flux of 17gsfd. Operational conditions consisted of a solution containing Cocoa Raw water. Rejection was 97.6% based on conductivity. Initial MTC was 0.1202 gsfd/psi.

APPENDIX C

ZETA POTENTIAL FIGURES

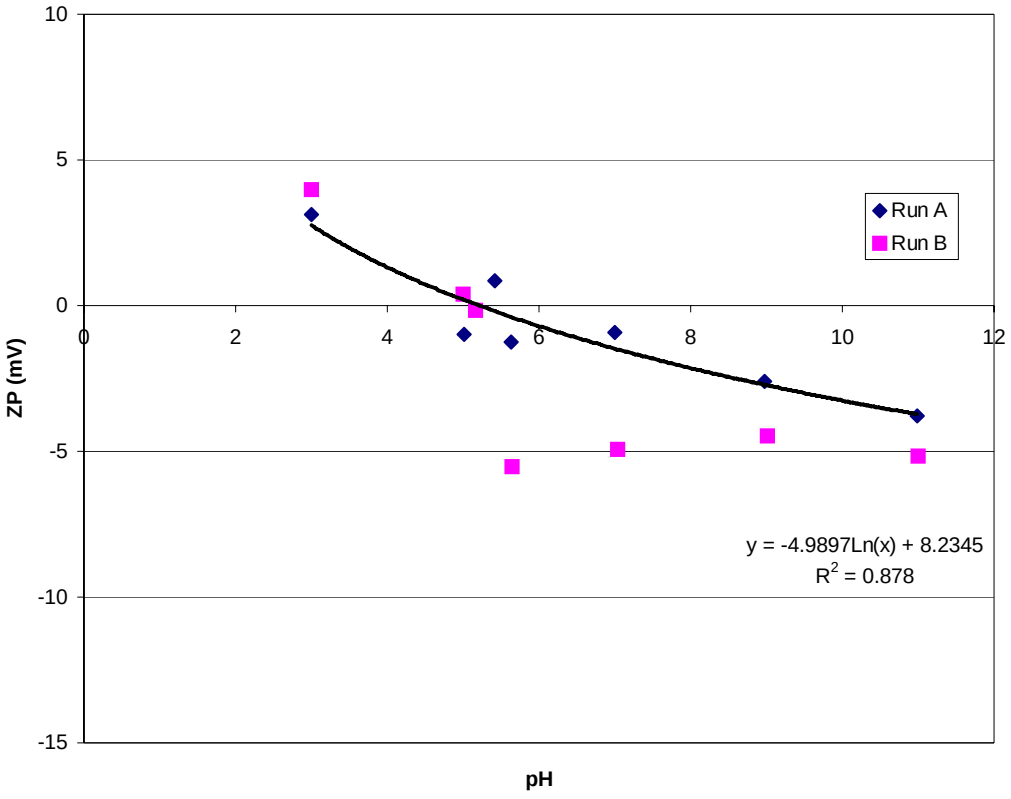

Figure C.1: Zeta Potential for SN1-CP.

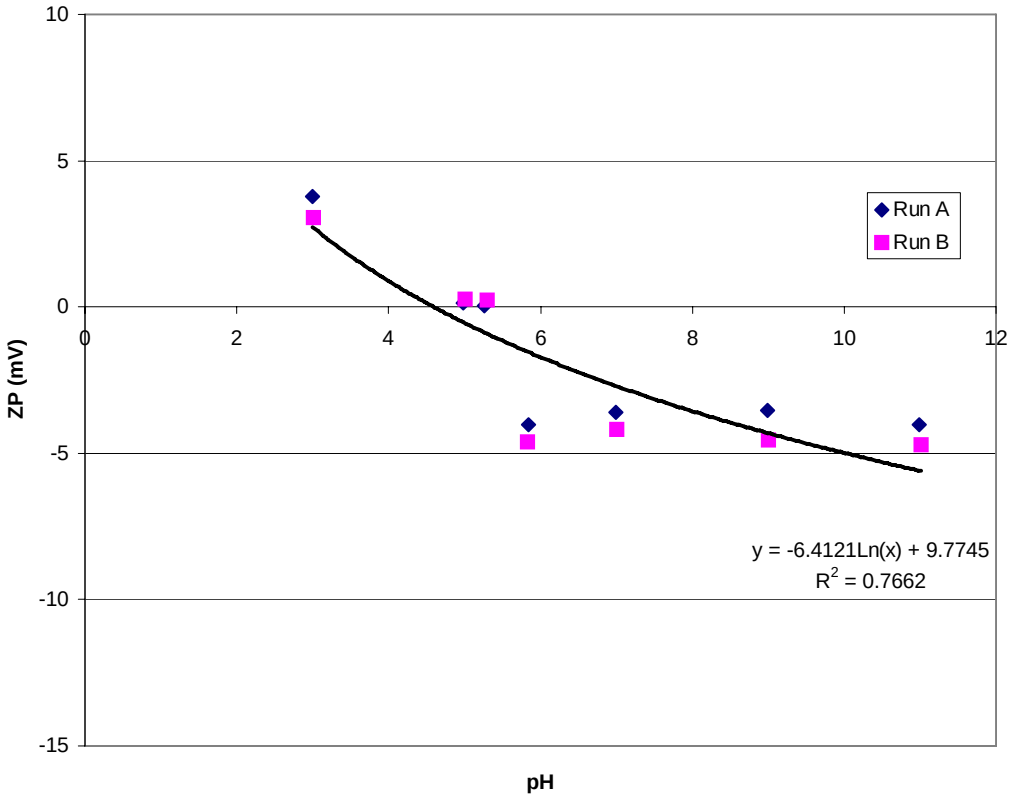

Figure C.2: Zeta Potential for SN2.

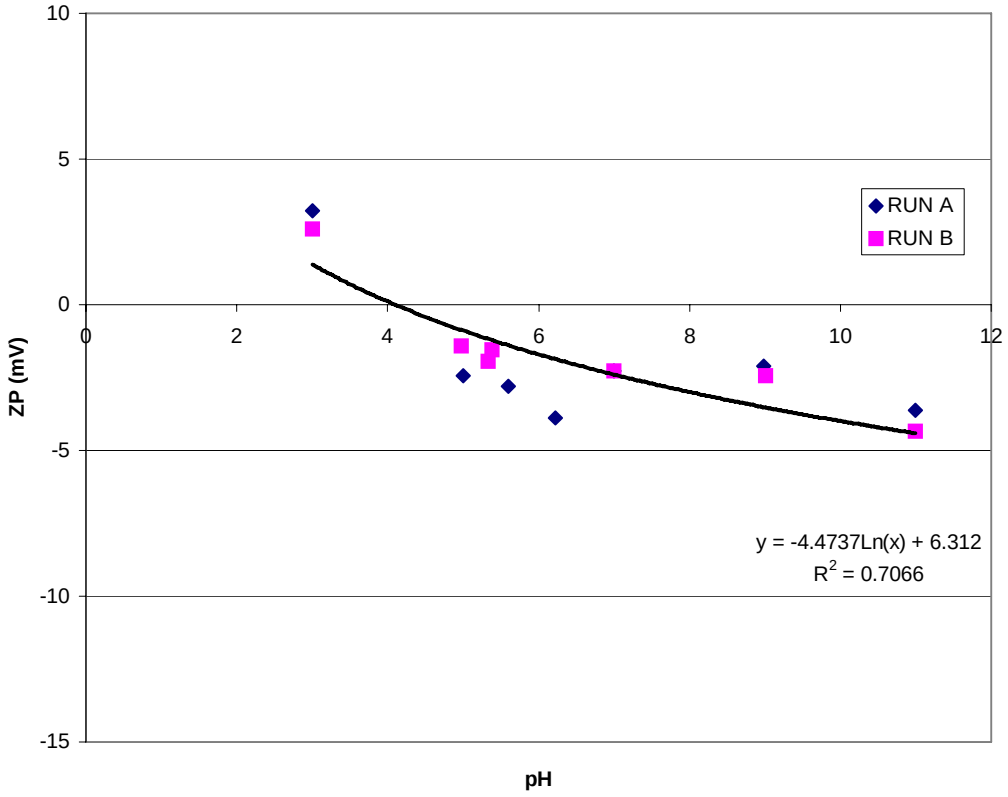

Figure C.3: Zeta Potential for SN2P.

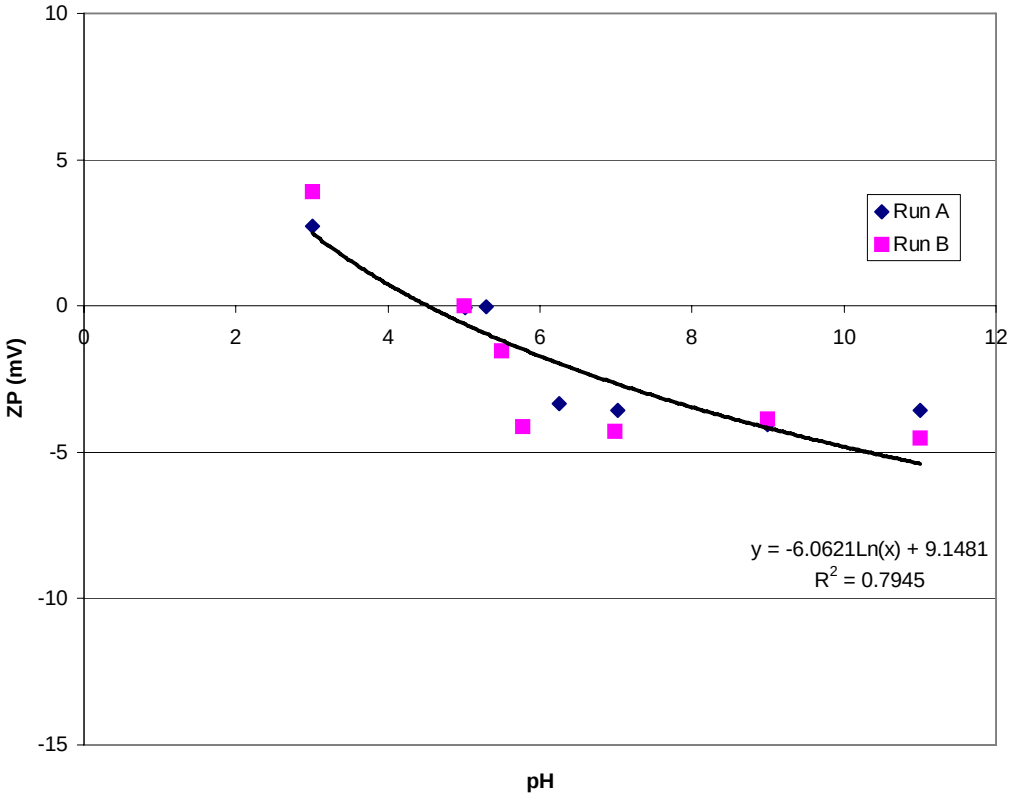

Figure C.4: Zeta Potential for SN3.

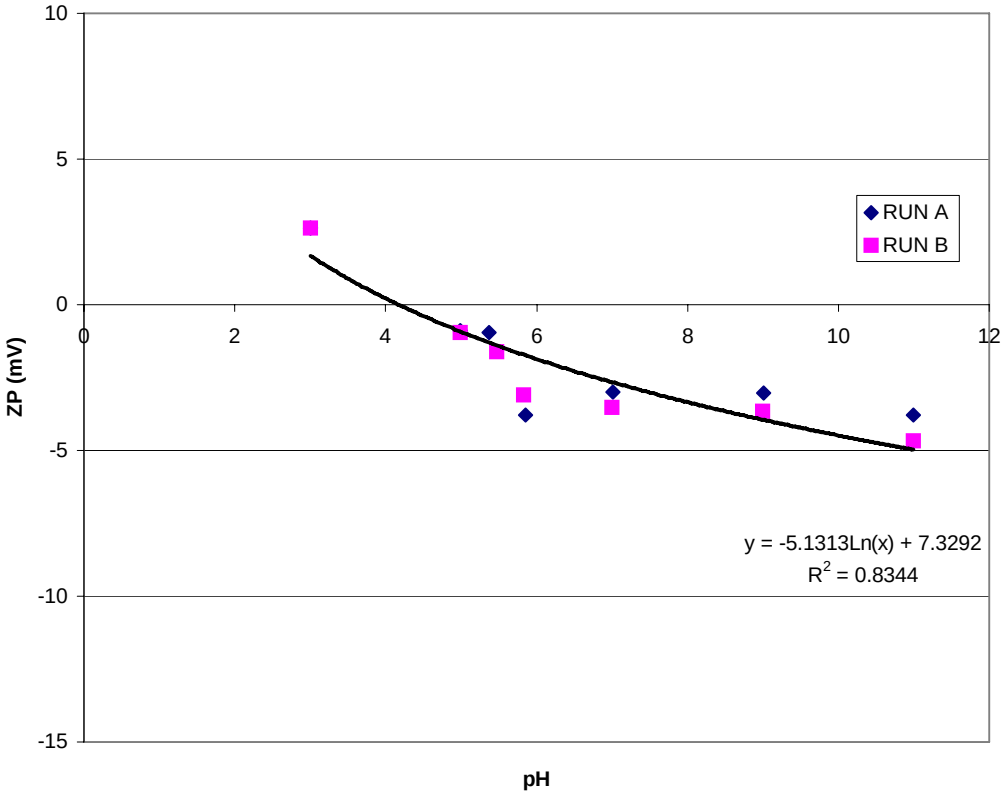

Figure C.5: Zeta Potential for SN3P.

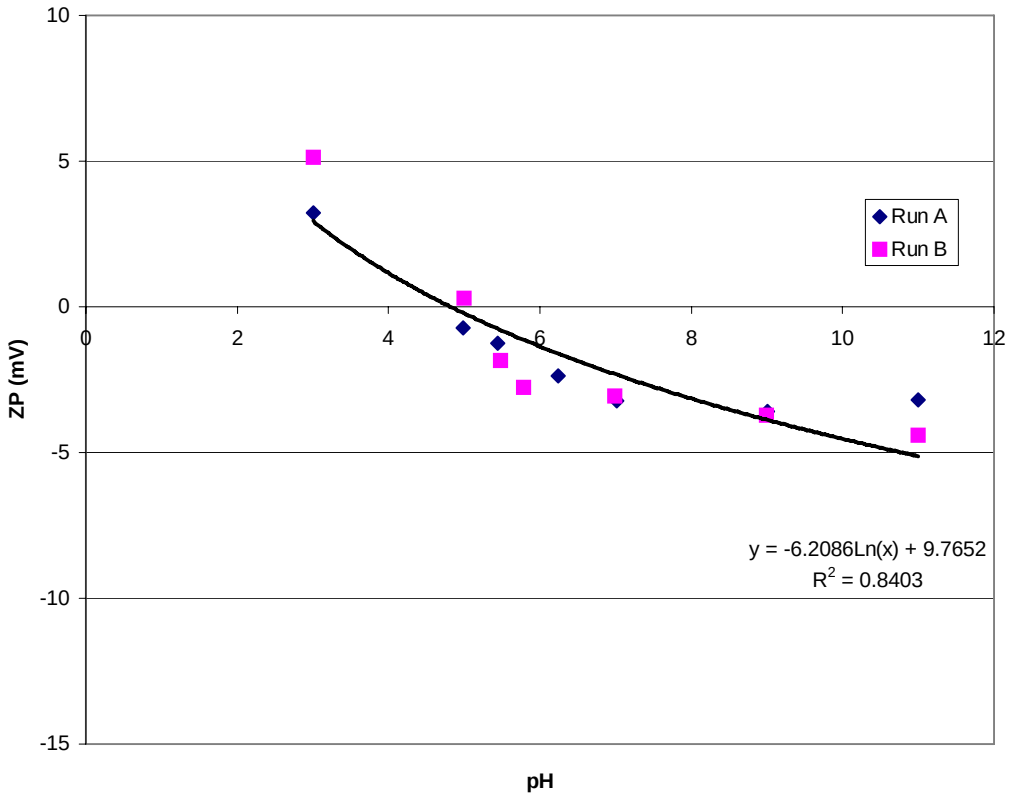

Figure C.6: Zeta Potential for SN4.

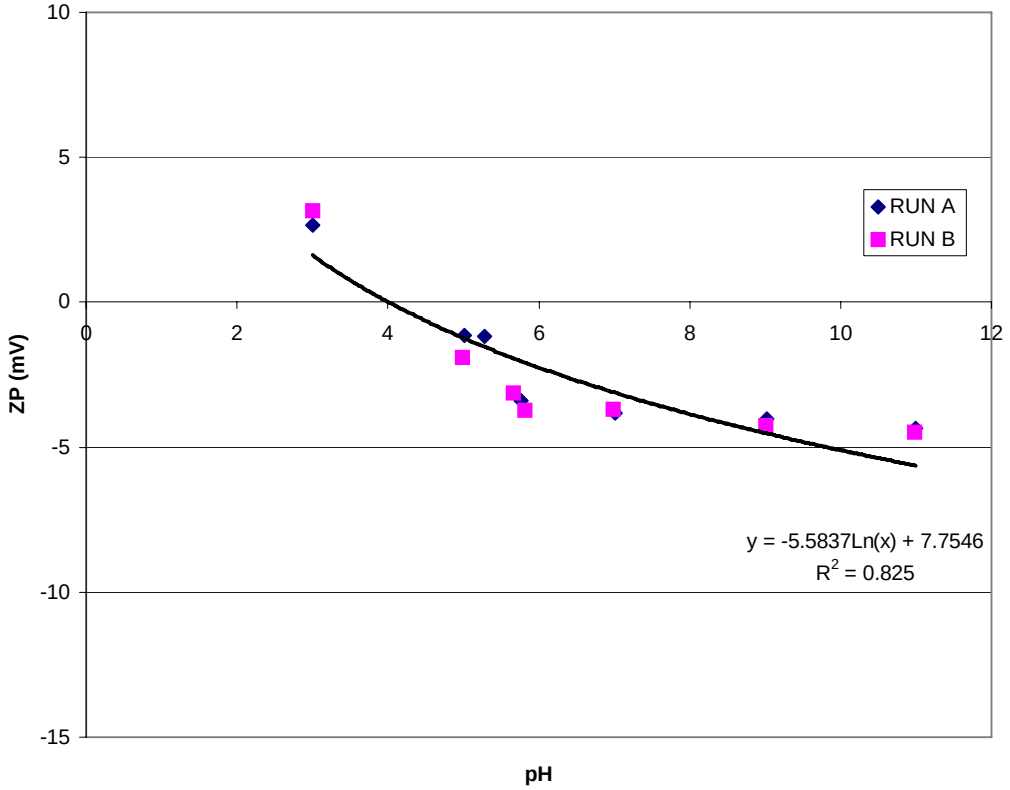

Figure C.7: Zeta Potential for SN4P.

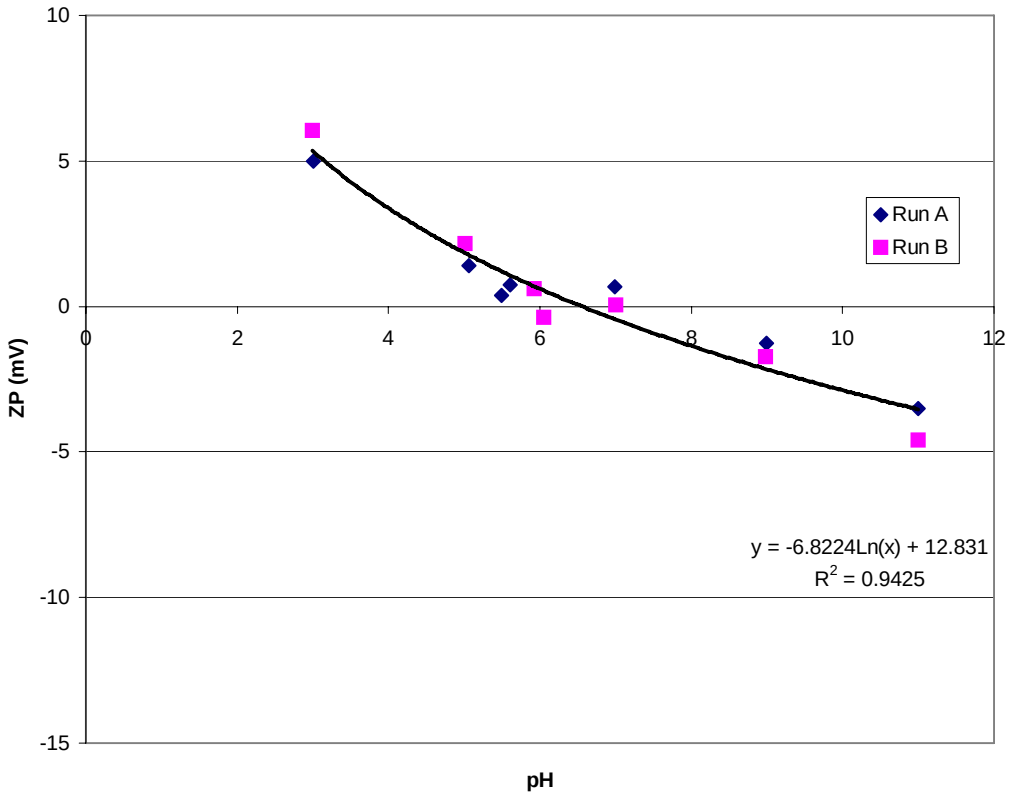

Figure C.8: Zeta Potential for SN5.

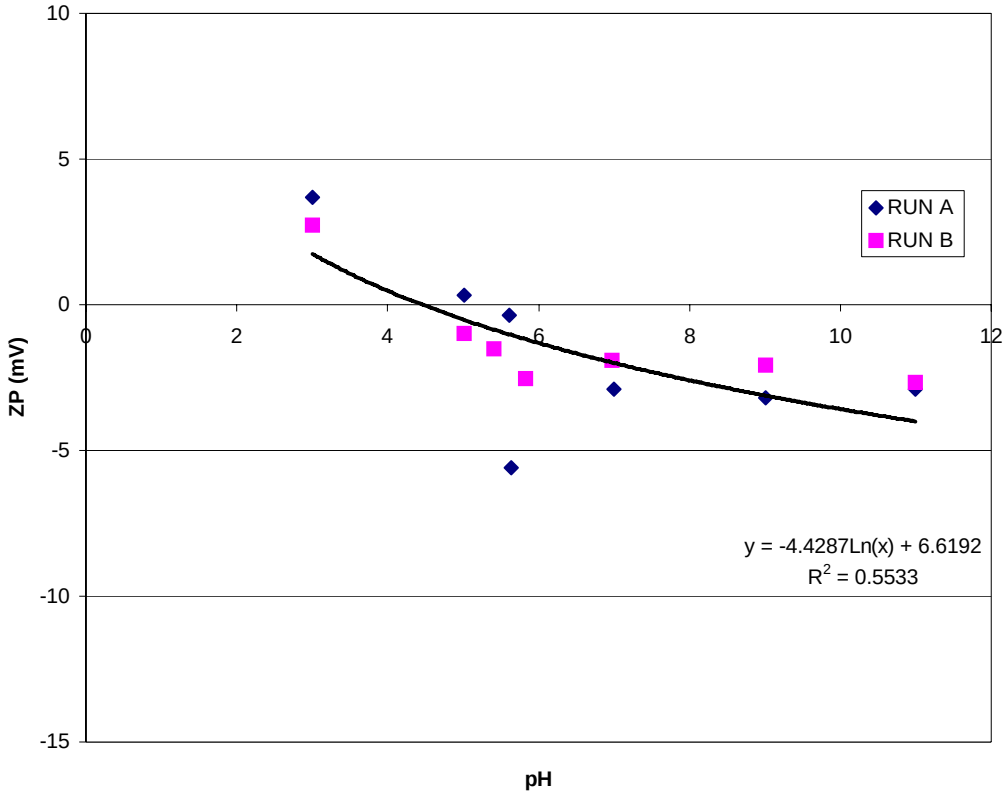

Figure C.9: Zeta Potential for SN5P.

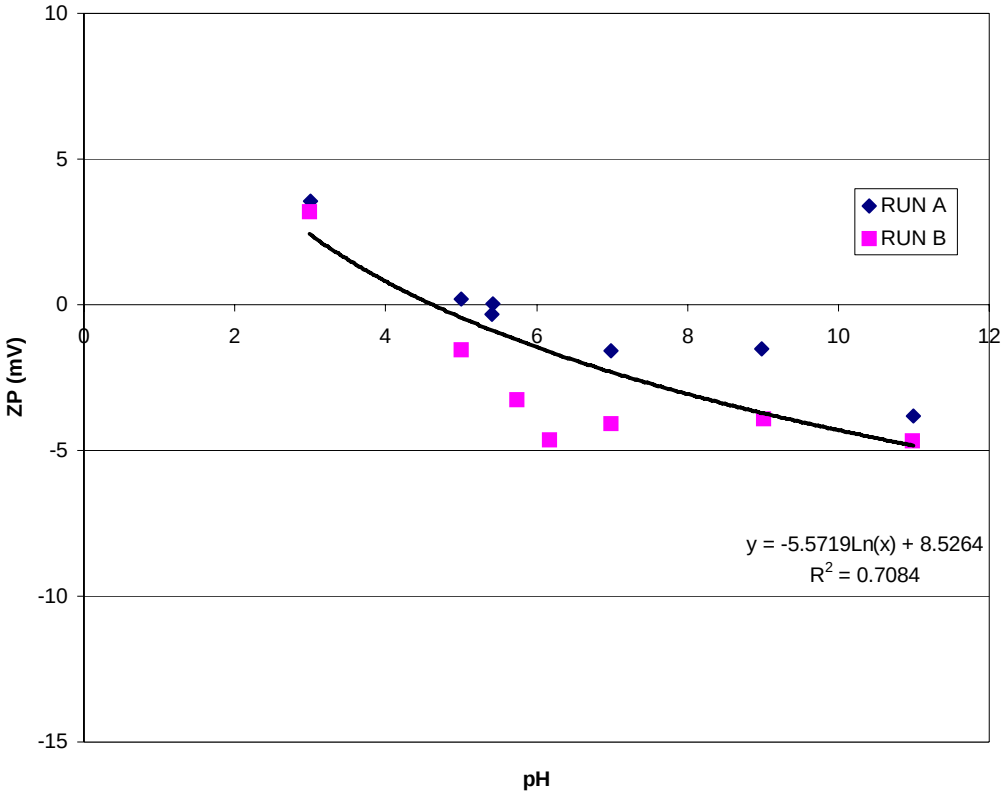

Figure C.10: Zeta Potential for SN6.

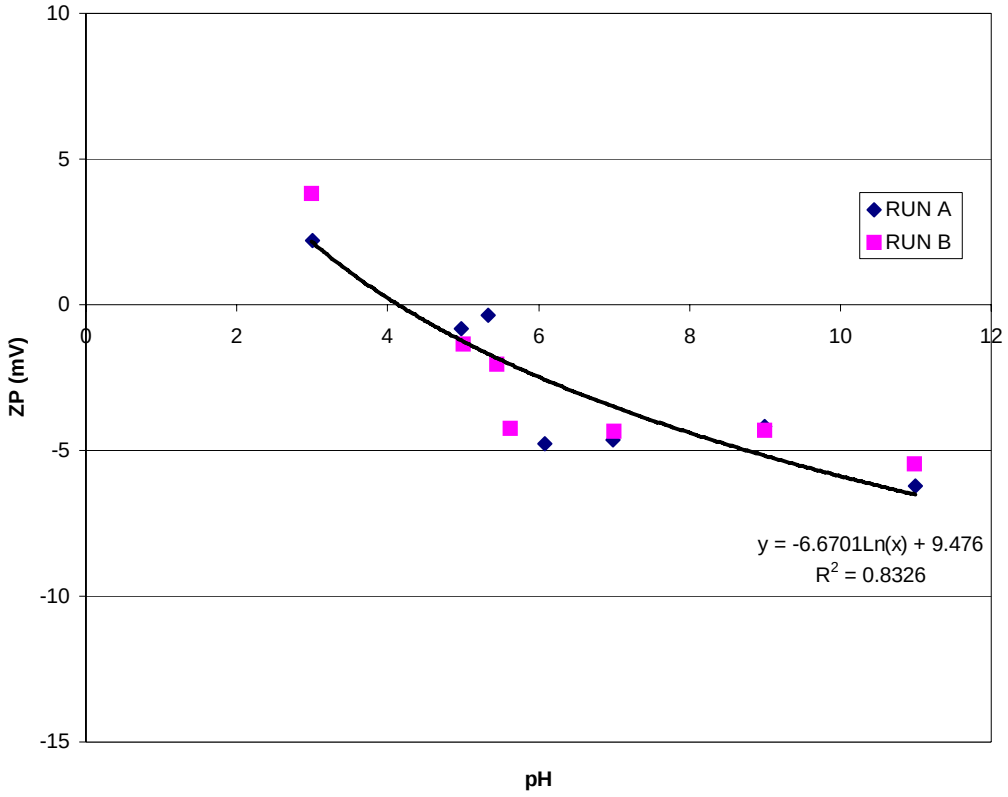

Figure C.11: Zeta Potential for SN6P.

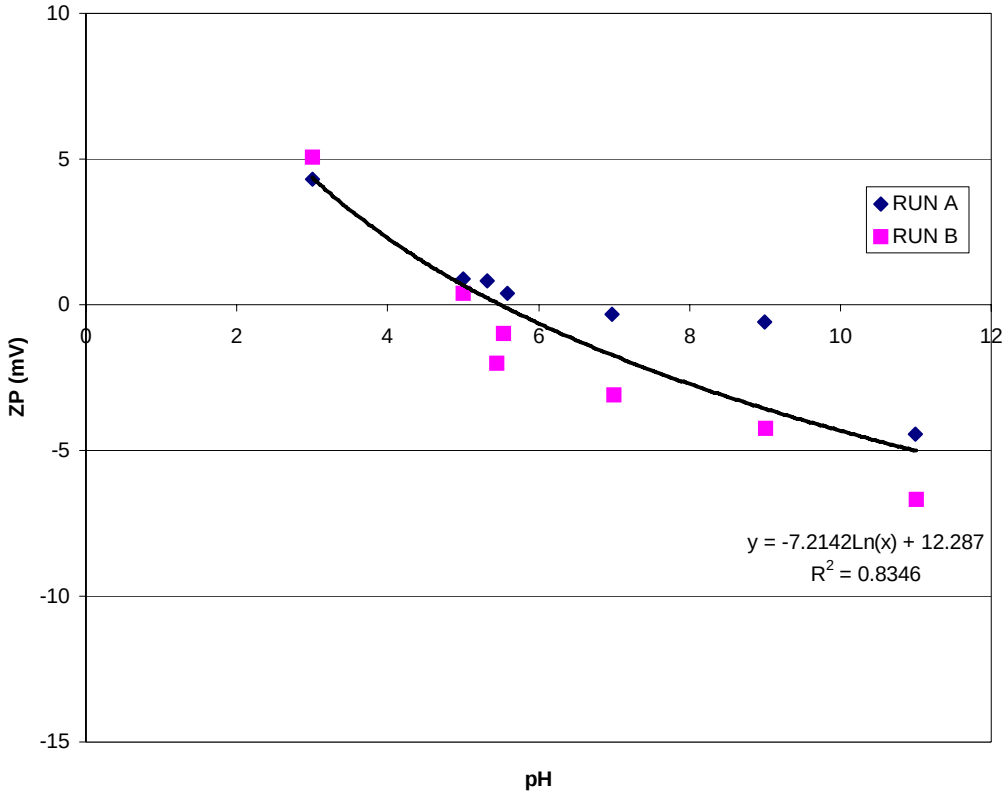

Figure C.12: Zeta Potential for SN7.

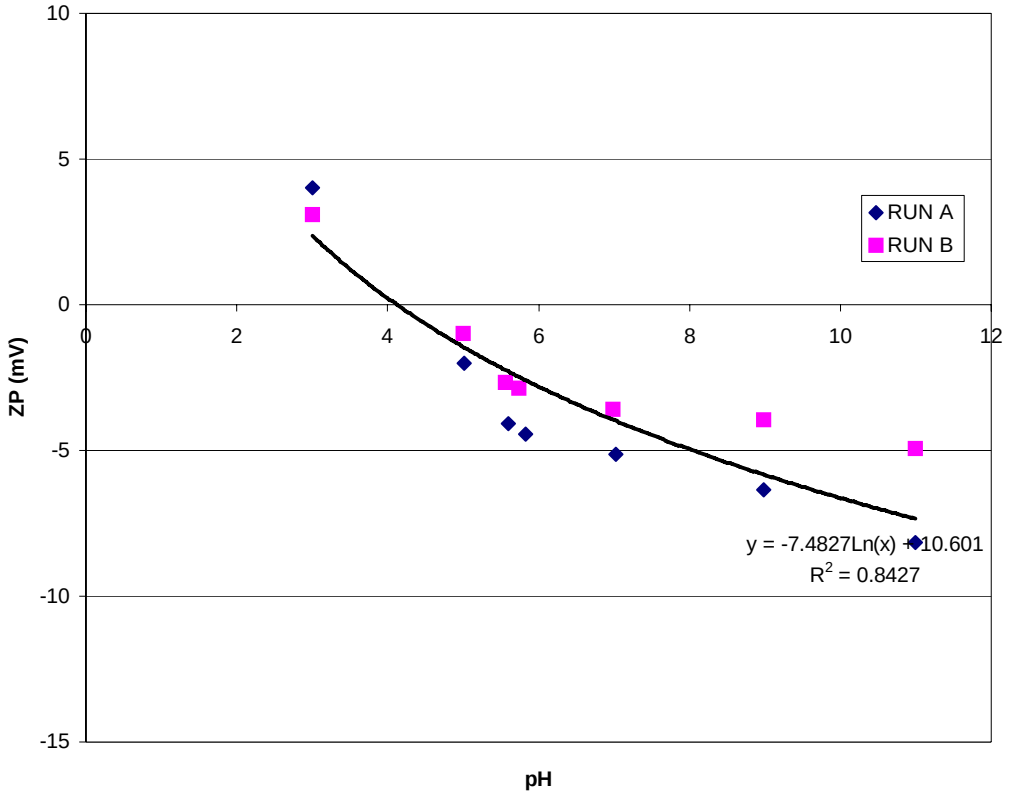

Figure C.13: Zeta Potential for SN7P.

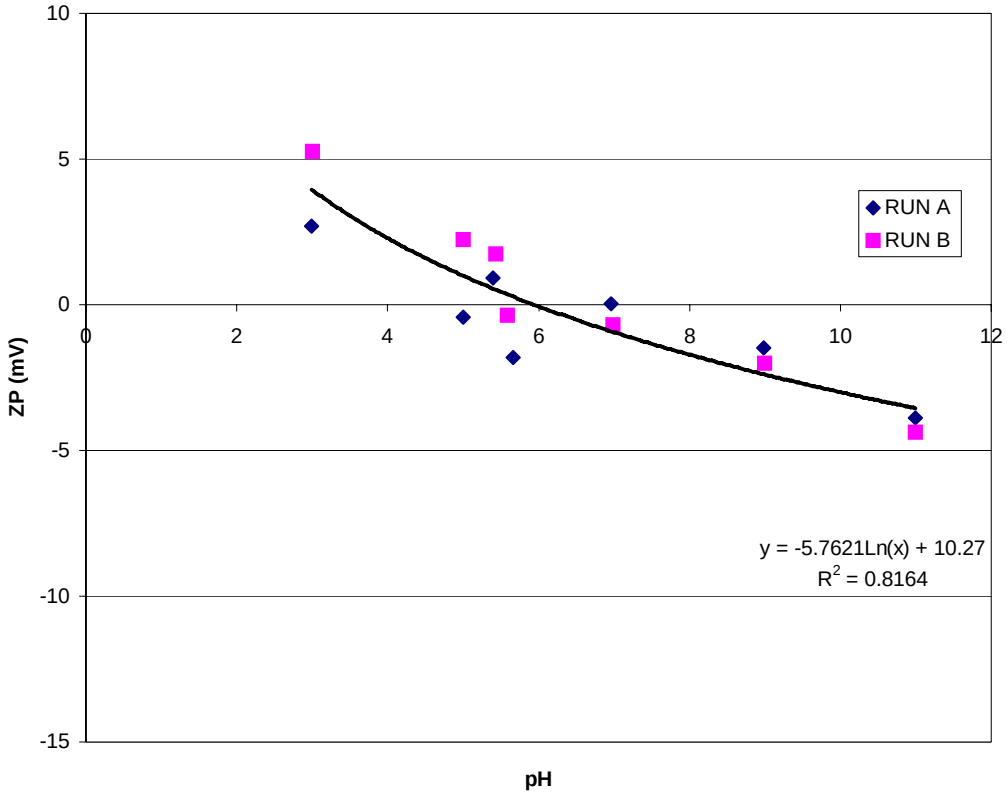

Figure C.14: Zeta Potential for SN8.

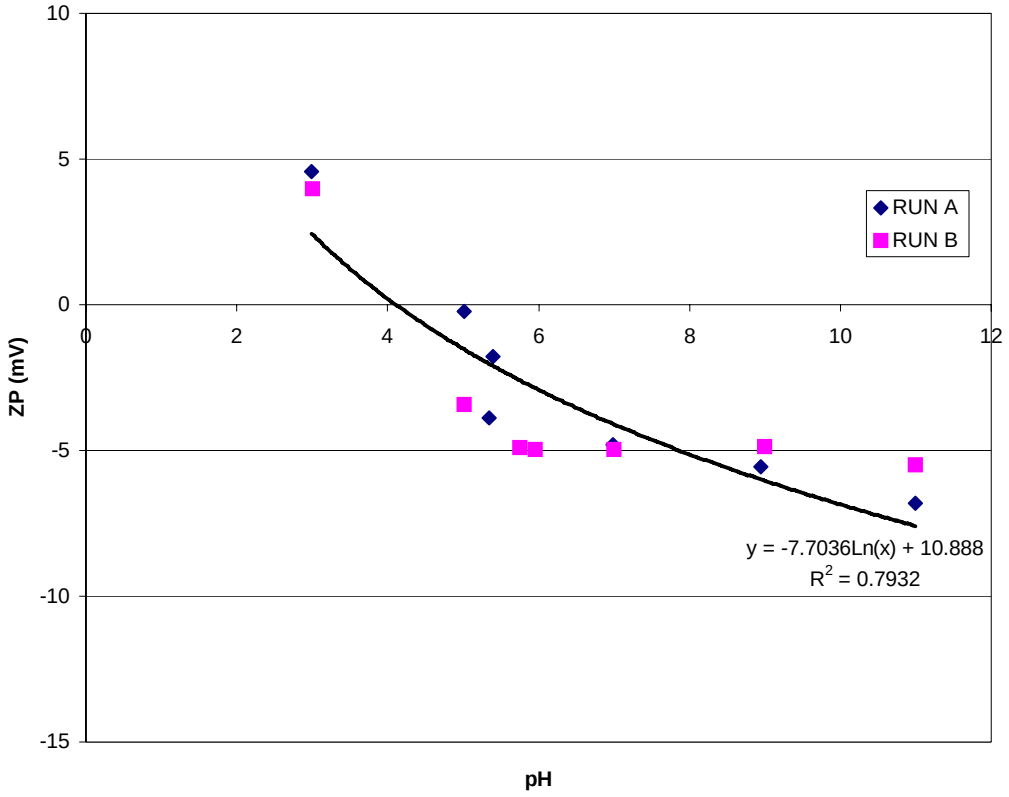

Figure C.15: Zeta Potential for SN8P.

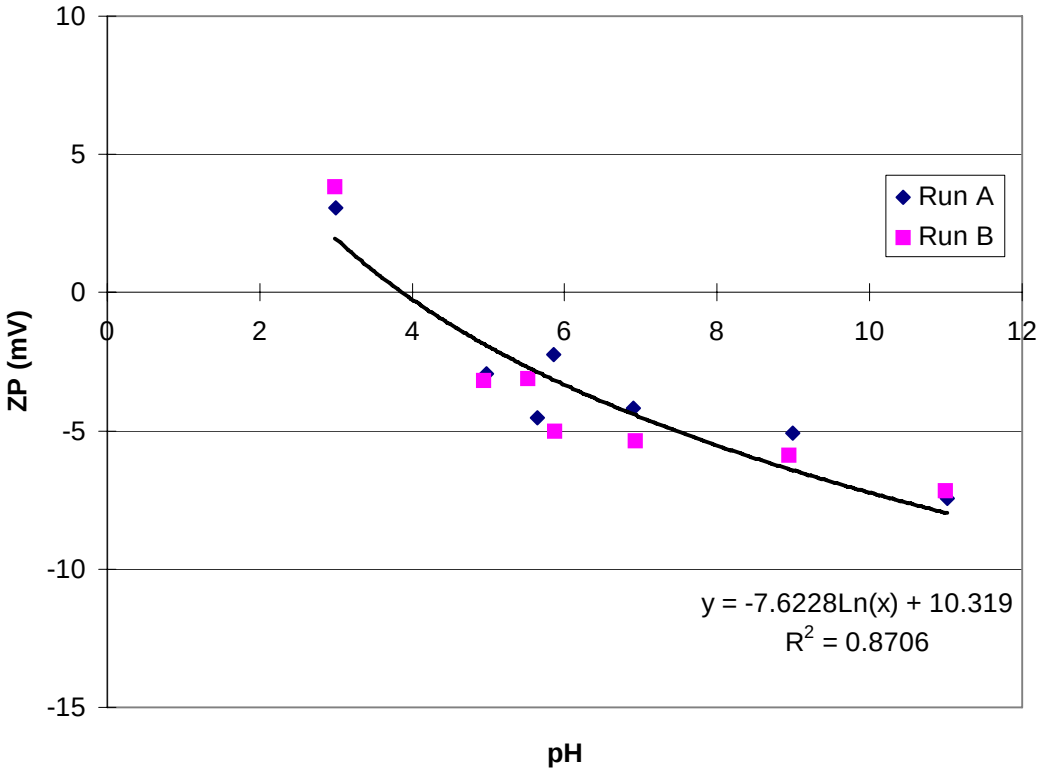

Figure C.16: Zeta Potential for LFC1.

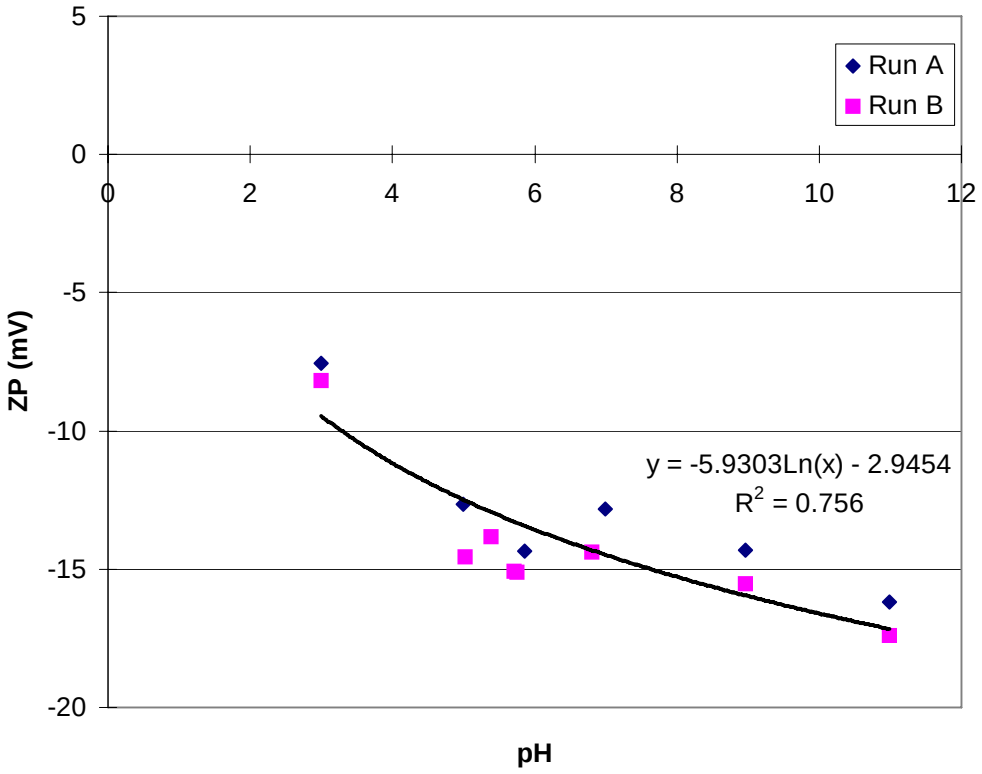

Figure C.17: Zeta Potential for X-20.

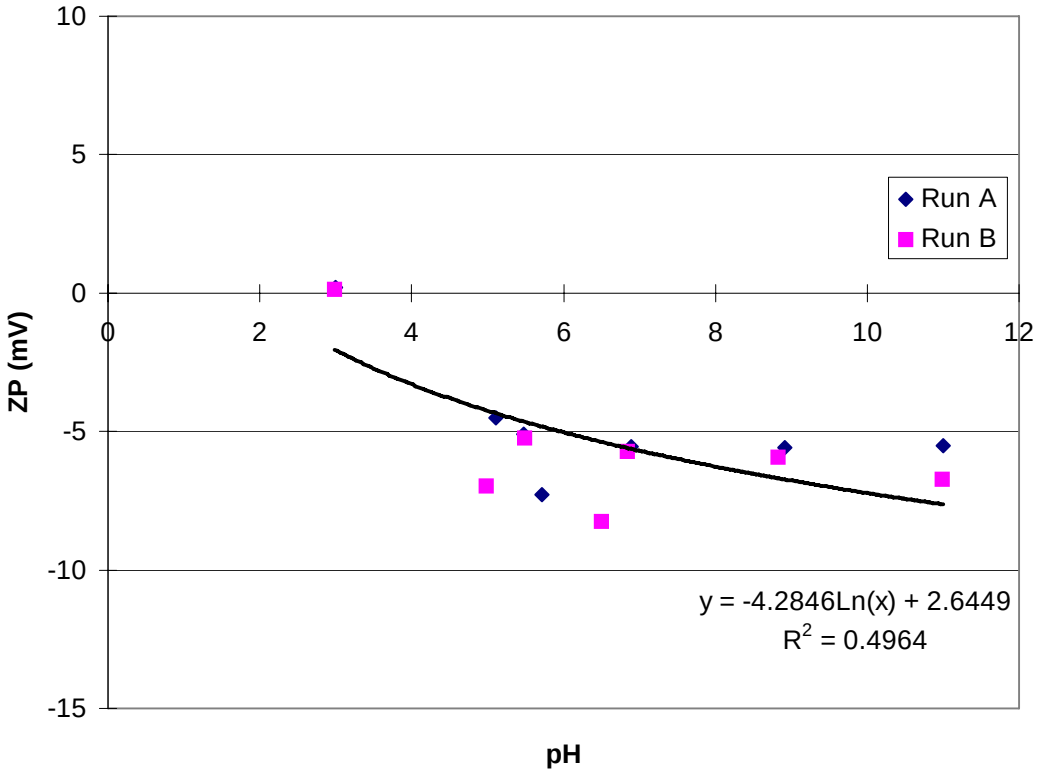

Figure C.18: Zeta Potential for BW30FR.

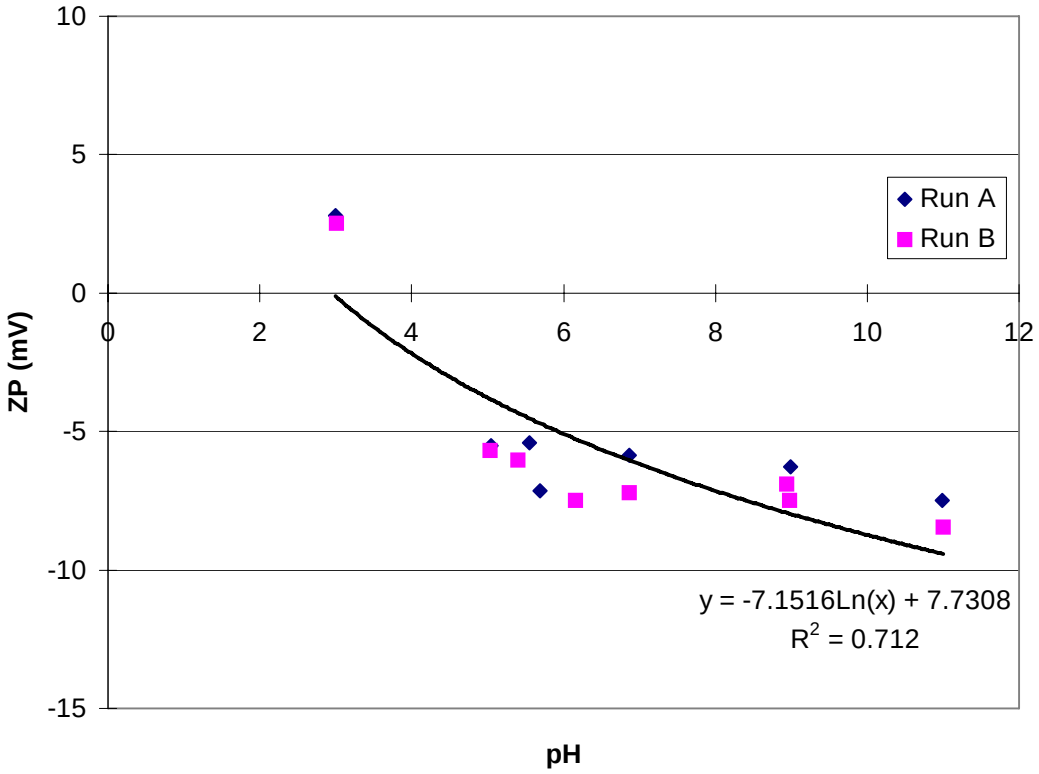

Figure C.19: Zeta Potential for Saehan A.

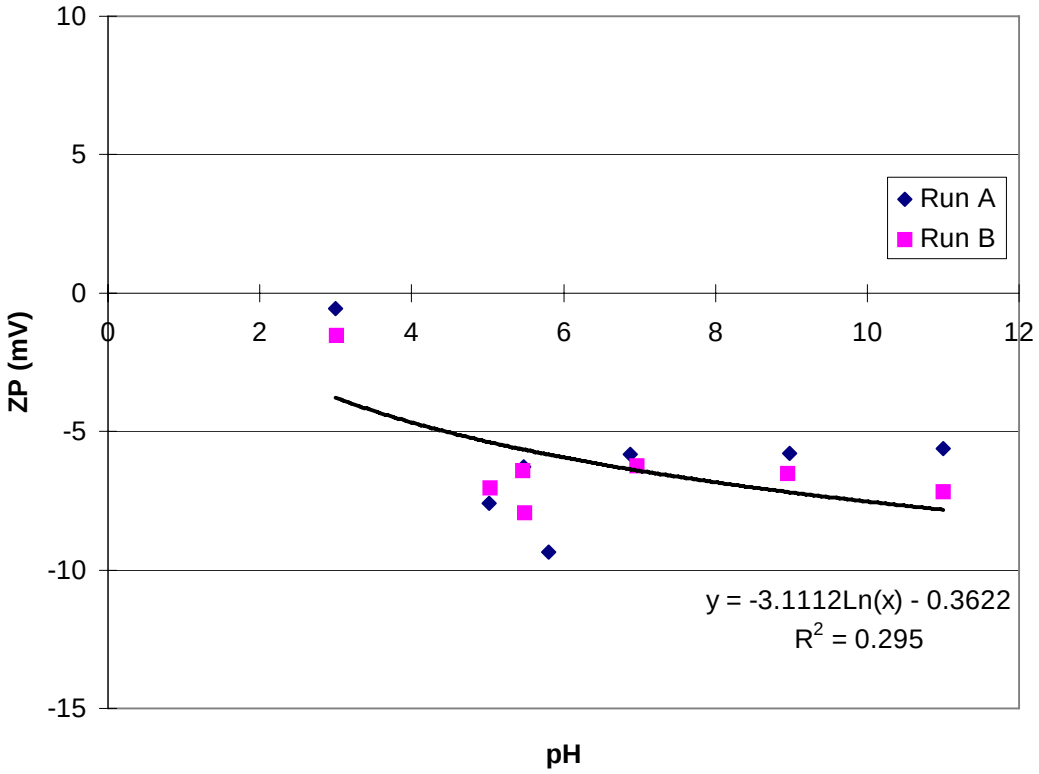

Figure C.20: Zeta Potential for Saehan B.

APPENDIX D

SAEHAN EXPERIMENTAL MEMBRANES SUMMARY FIGURES

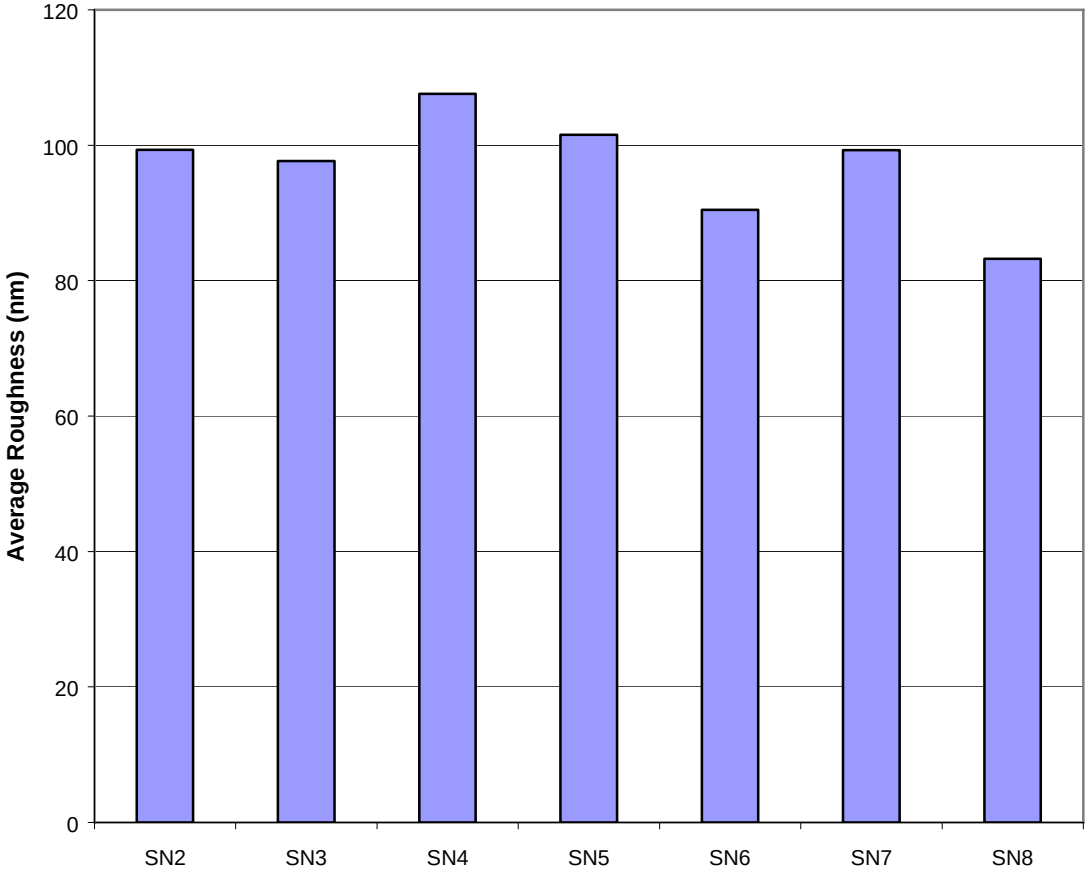

Figure D.1: Average Roughness for Saehan Developmental Membranes without Post-Treatment.

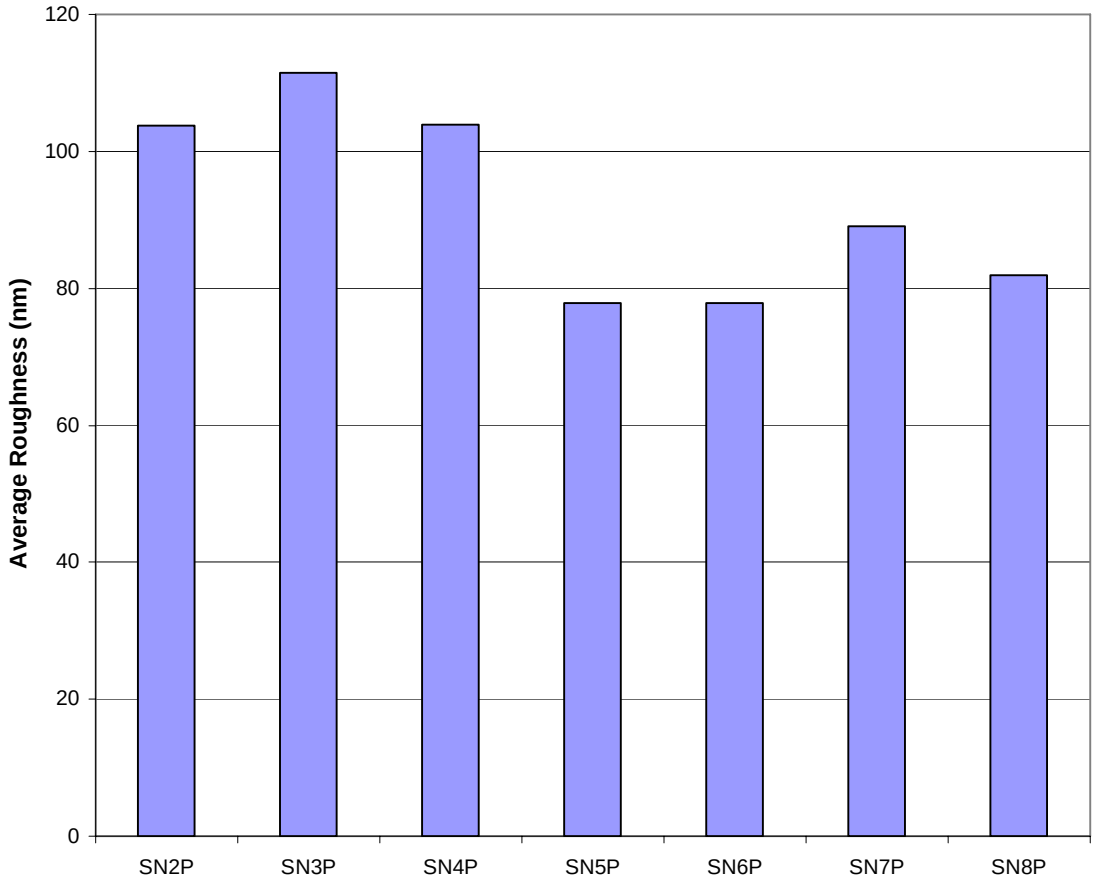

Figure D.2: Average Roughness for Saehan Developmental Membranes with Post-Treatment.

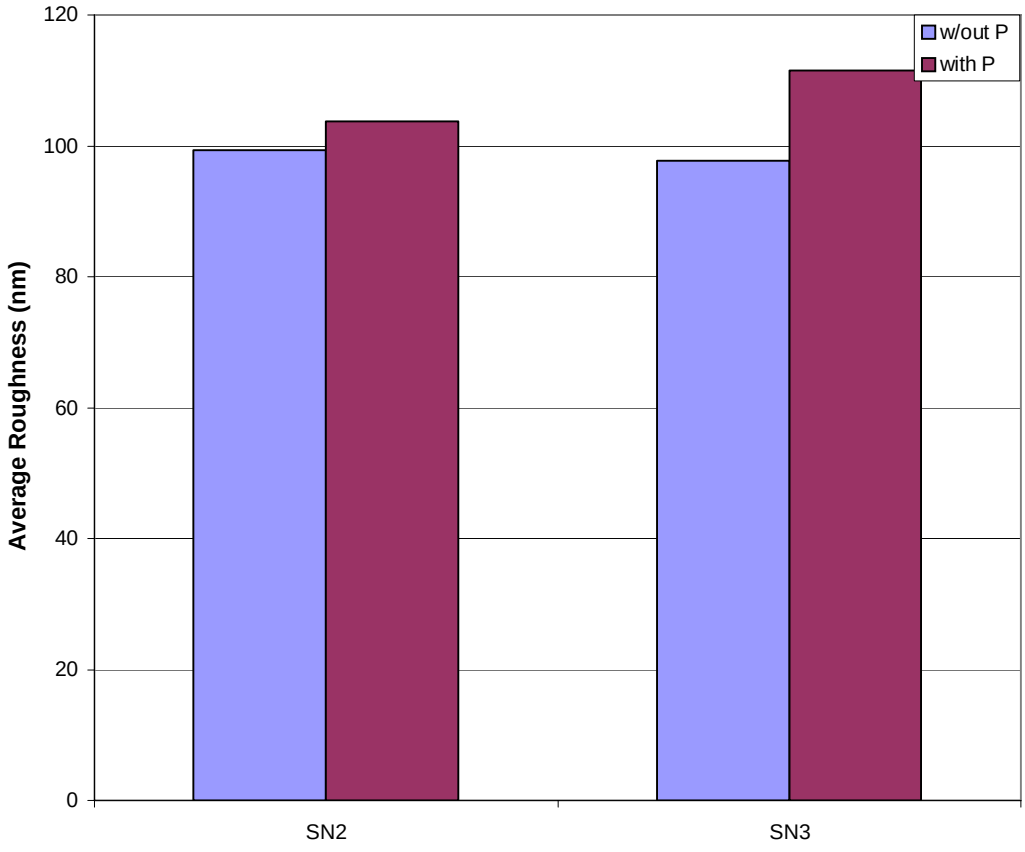

Figure D.3: Average Roughness for Saehan Developmental Membranes with Single Coating.

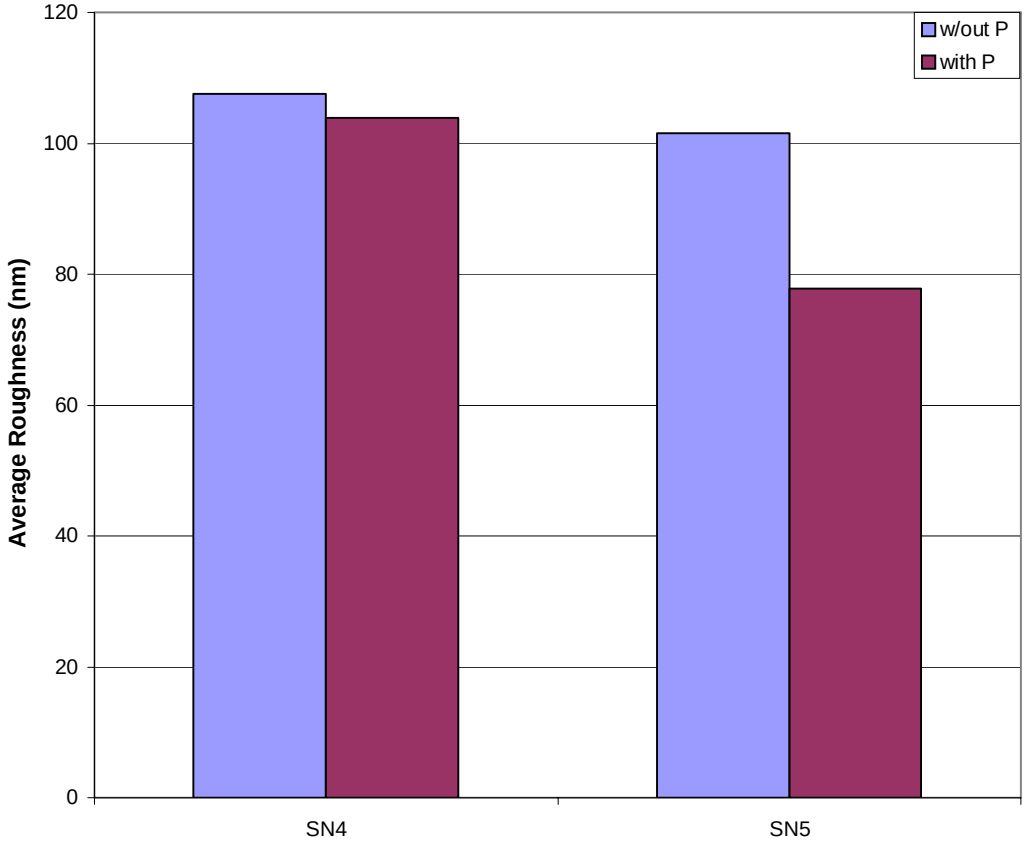

Figure D.4: Average Roughness for Saehan Developmental Membranes with Double Coating.

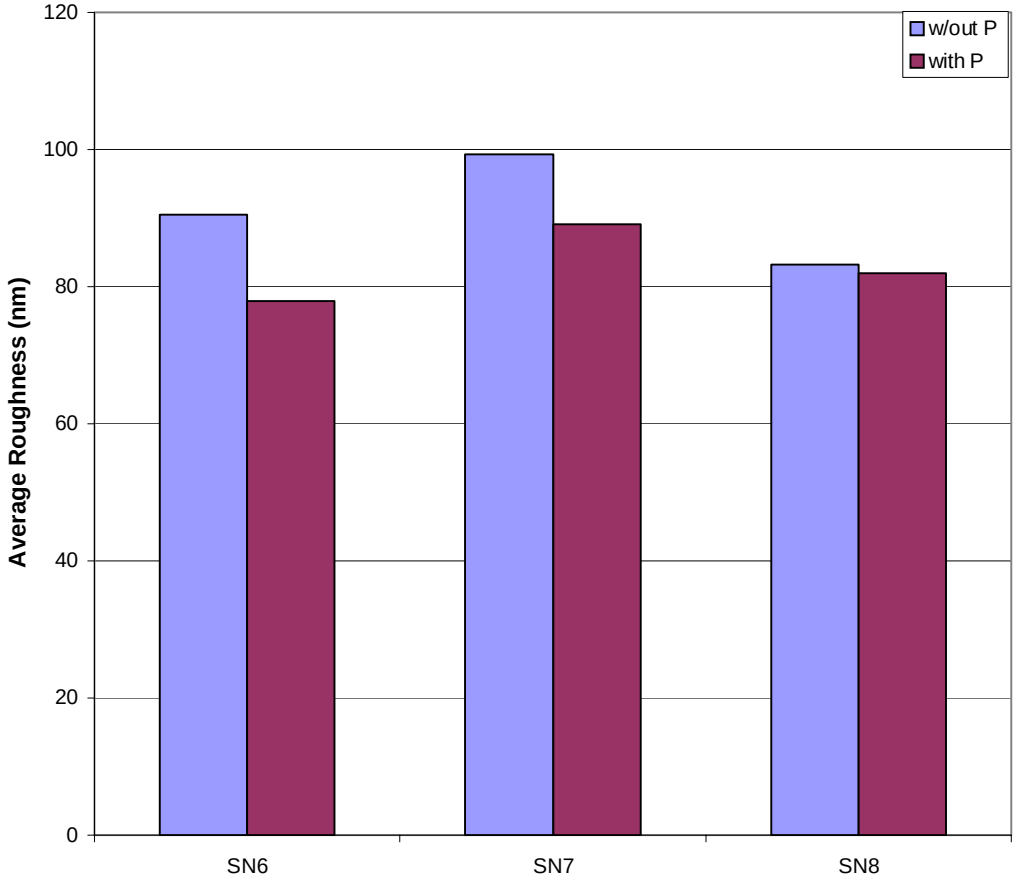

Figure D.5: Average Roughness for Saehan Developmental Membranes with Special Coating.

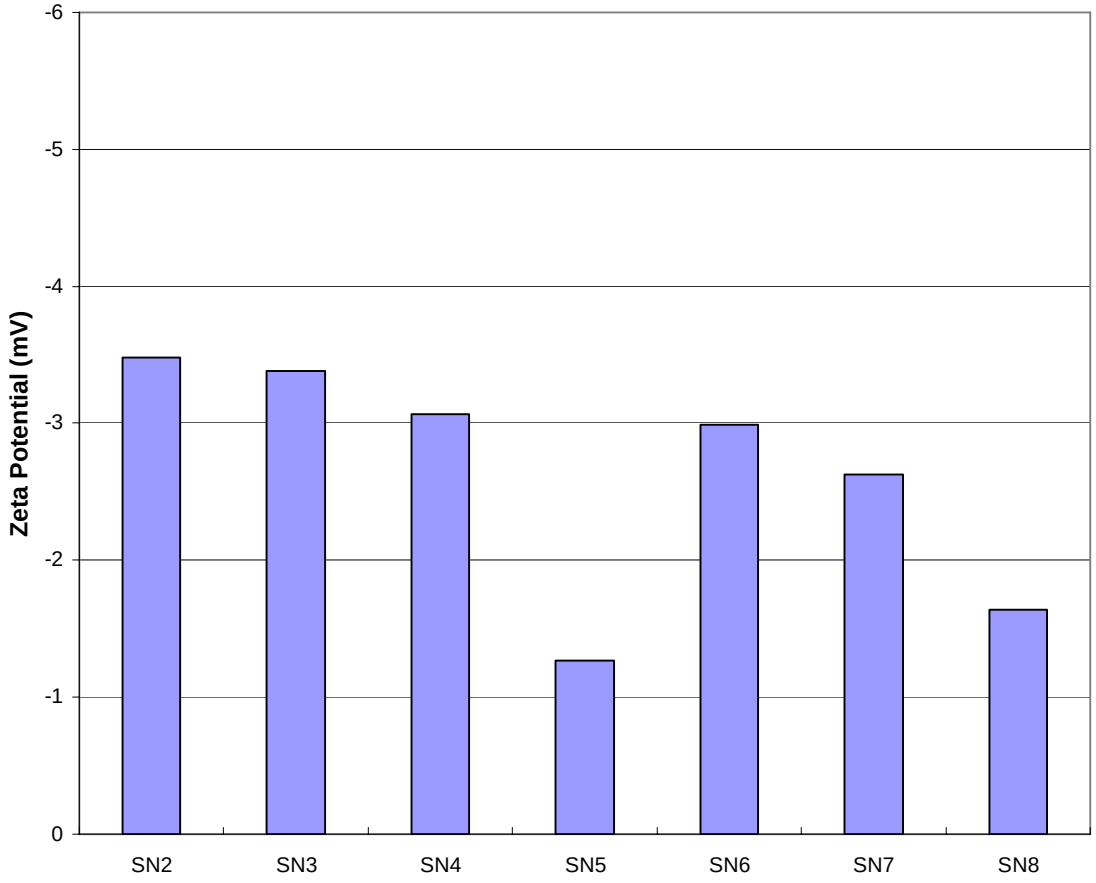

Figure D.6: Zeta Potential for Saehan Developmental Membranes without Post-Treatment.

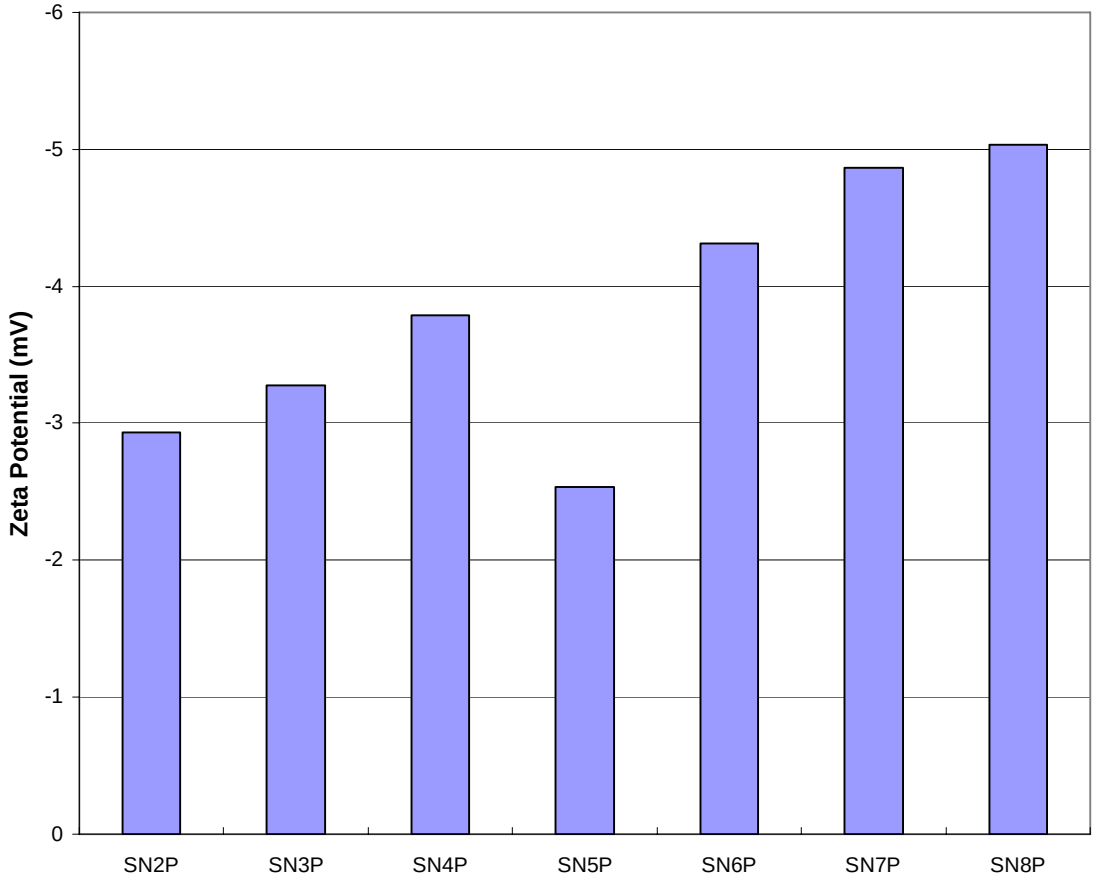

Figure D.7: Zeta Potential for Saehan Developmental Membranes with Post-Treatment.

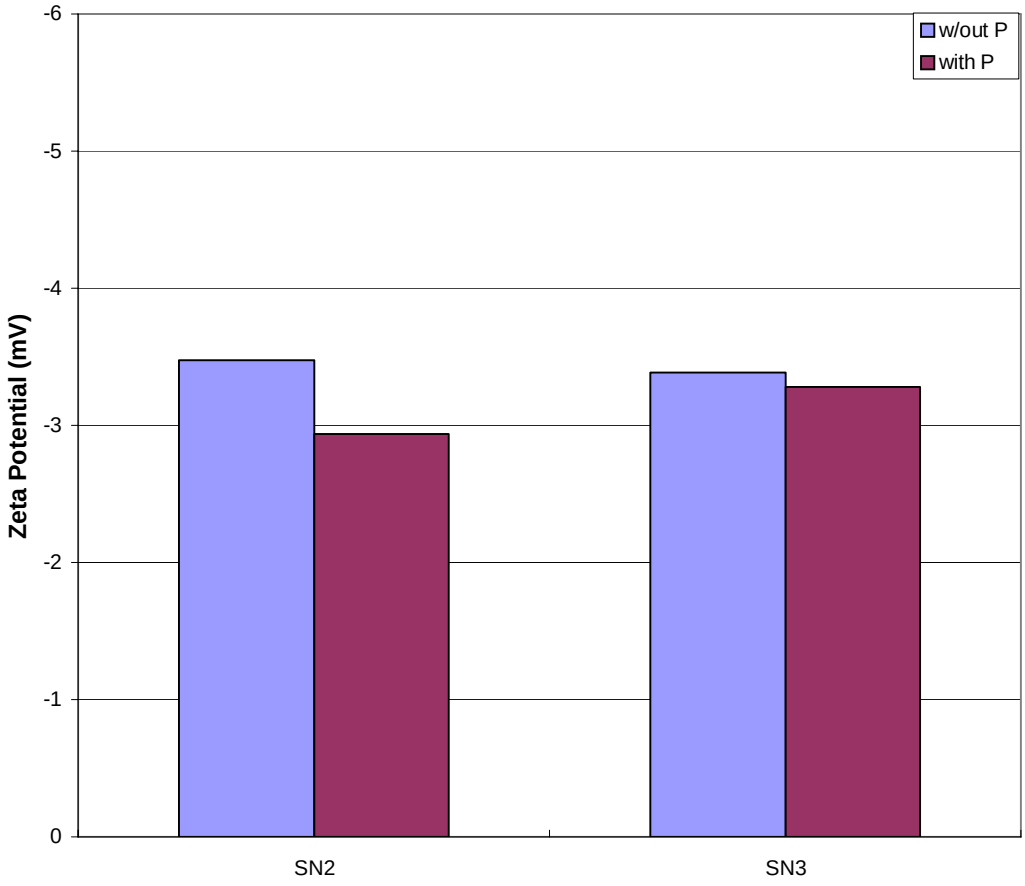

Figure D.8: Zeta Potential for Saehan Developmental Membranes with Single Coating.

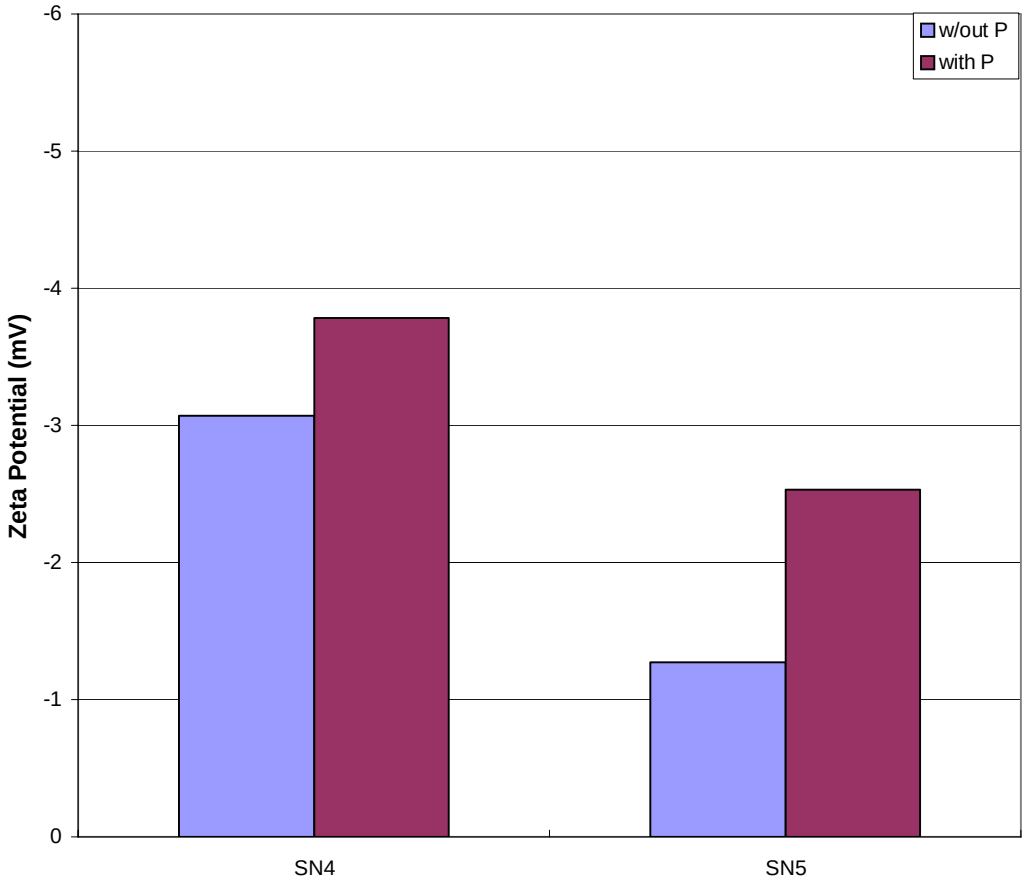

Figure D.9: Zeta Potential for Saehan Developmental Membranes with Double Coating.

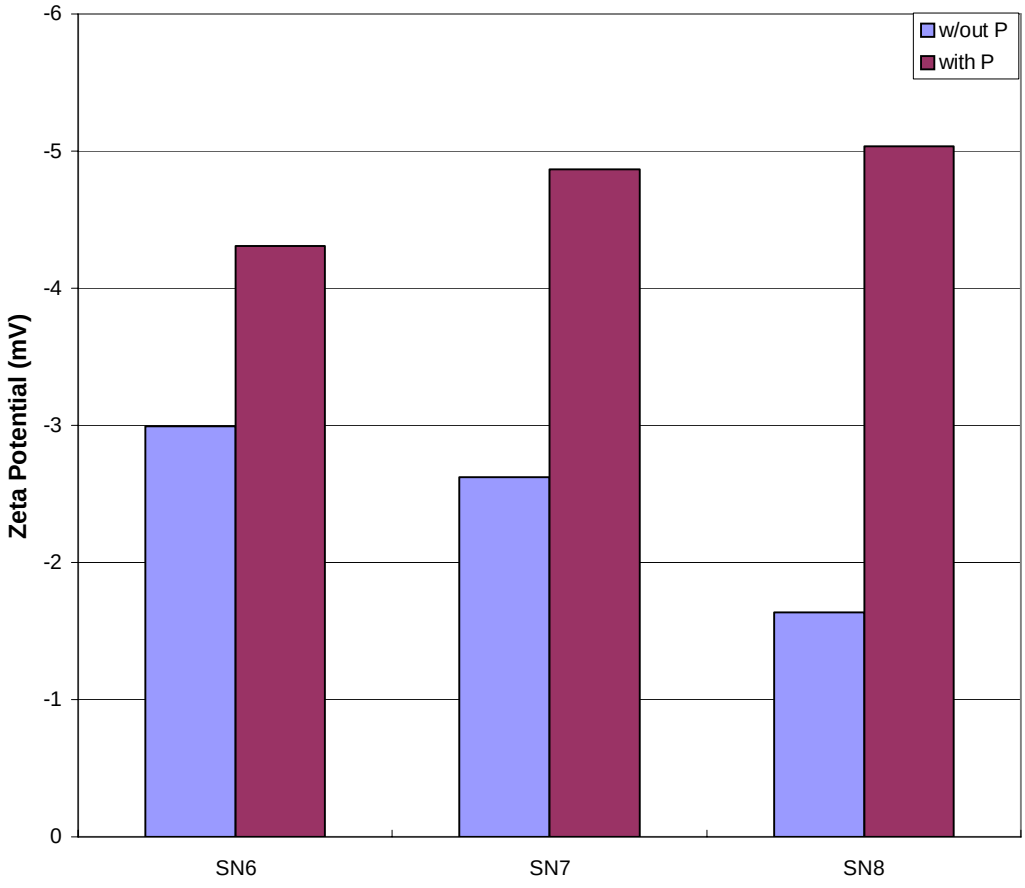

Figure D.10: Zeta Potential for Saehan Developmental Membranes with Special Coating.

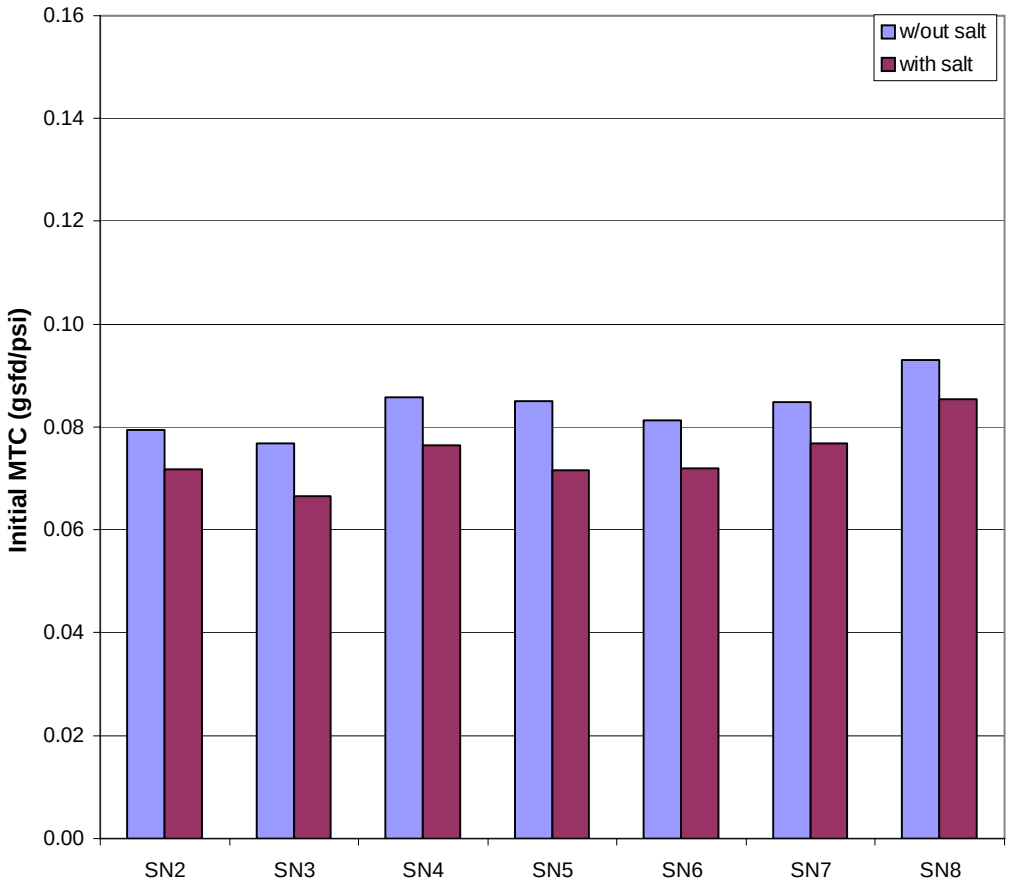

Figure D.11: Initial Mass Transfer Coefficient for Saehan Developmental Membranes without Post-Treatment.

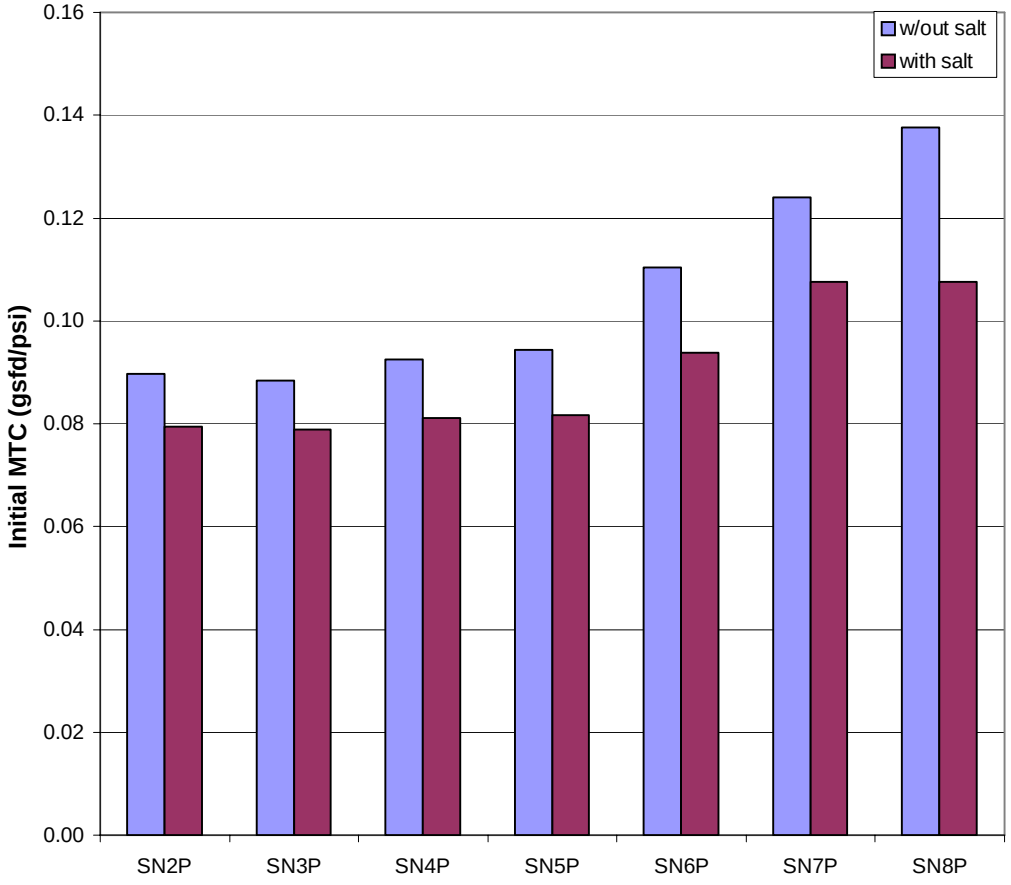

Figure D.12: Initial Mass Transfer Coefficient for Saehan Developmental Membranes with Post-Treatment for Clean Water Testing.

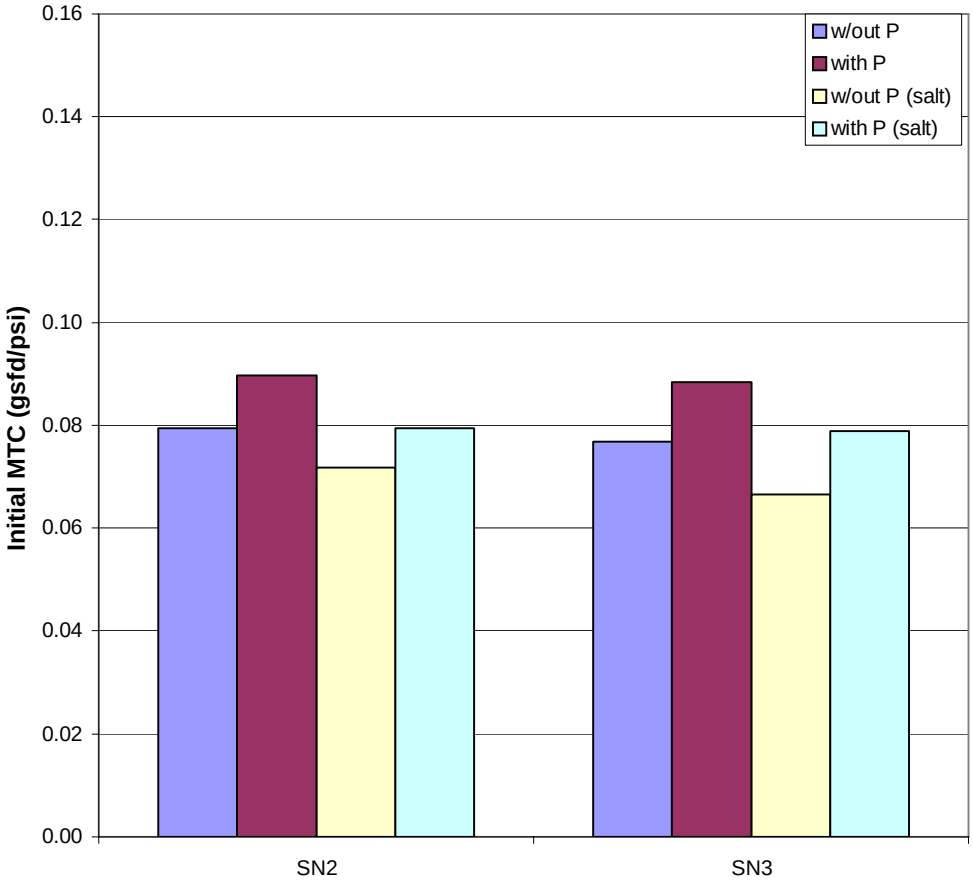

Figure D.13: Initial Mass Transfer Coefficient for Saehan Developmental Membranes with Single Coating for Clean Water Testing.

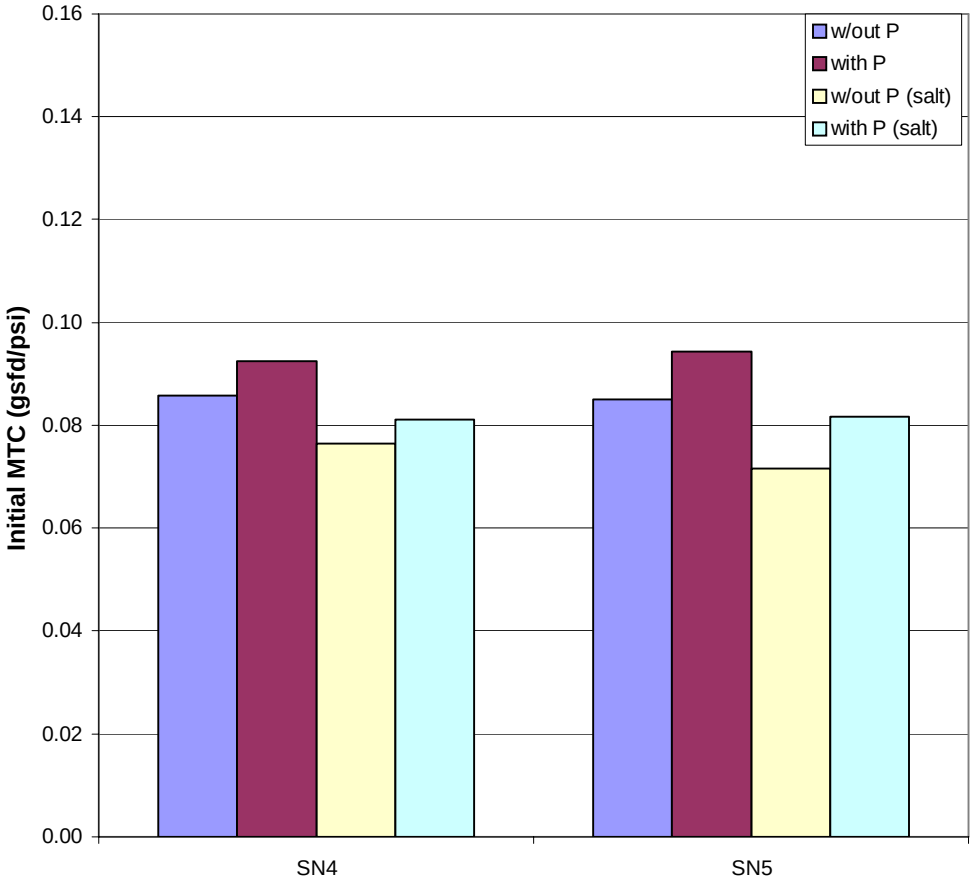

Figure D.14: Initial Mass Transfer Coefficient for Saehan Developmental Membranes with Double Coating for Clean Water Testing.

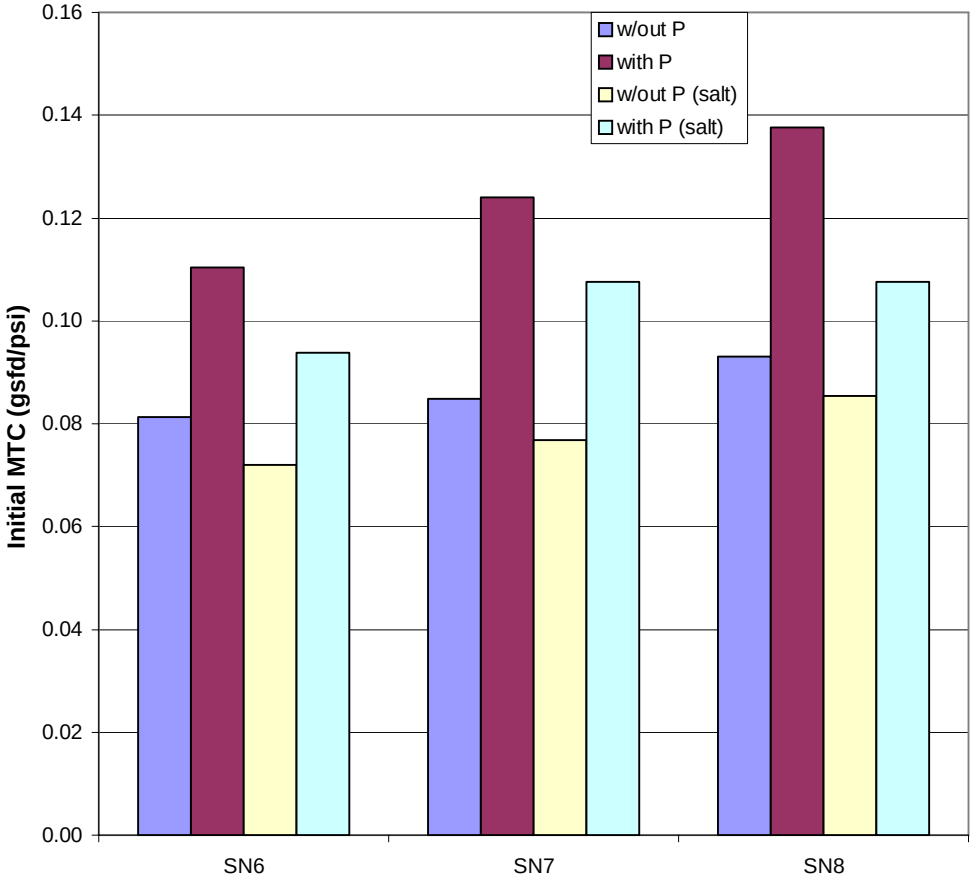

Figure D.15: Initial Mass Transfer Coefficient for Saehan Developmental Membranes with Special Coating for Clean Water Testing.

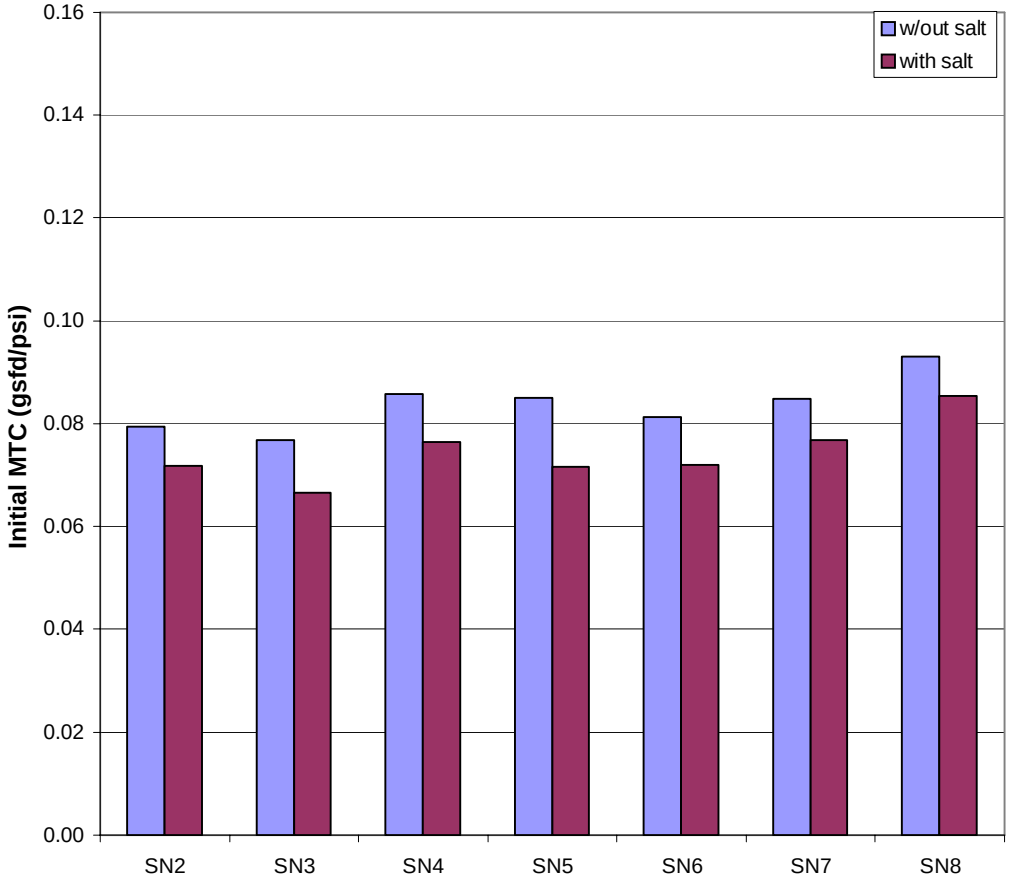

Figure D.16: Initial Mass Transfer Coefficient for Saehan Developmental Membranes without Post-Treatment for Clean Water Testing.

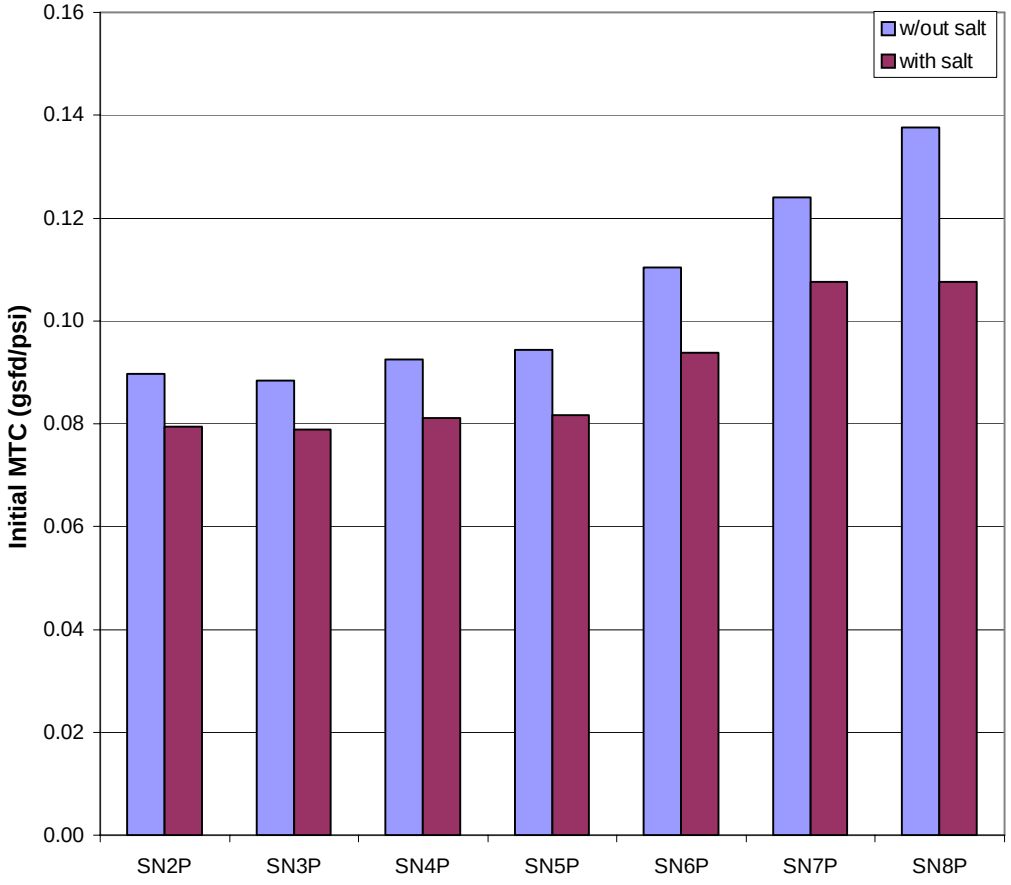

Figure D.17: Initial Mass Transfer Coefficient for Saehan Developmental Membranes with Post-Treatment for Clean Water Testing.

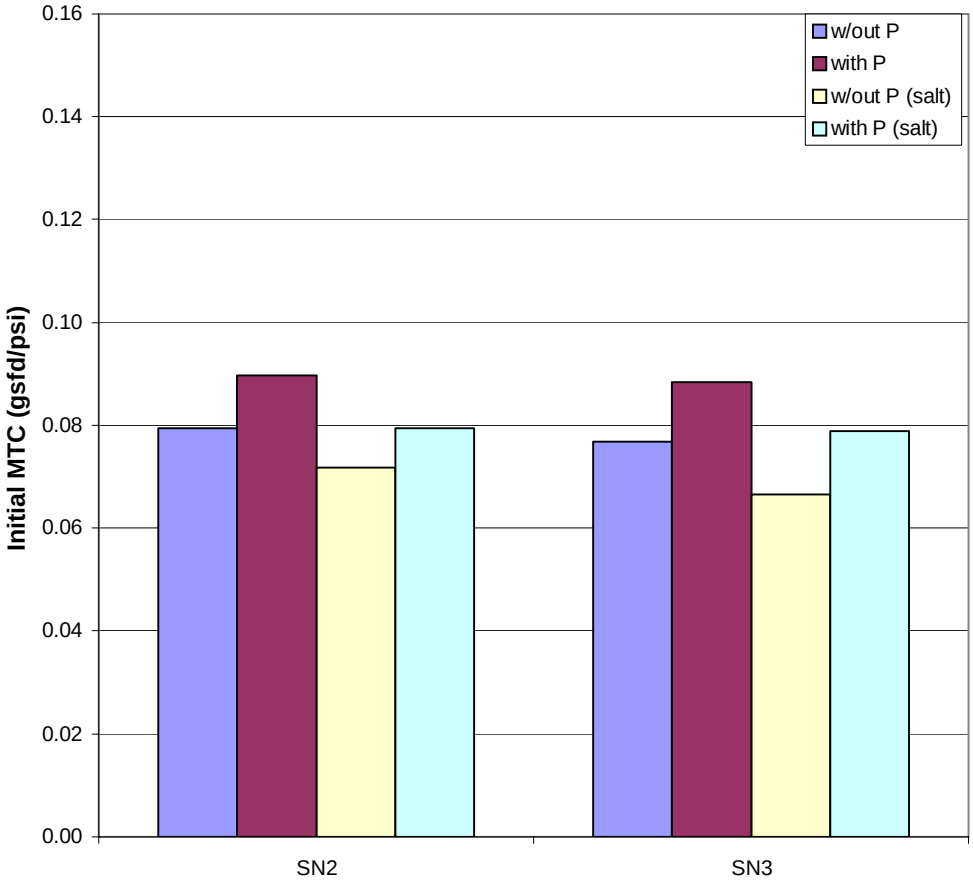

Figure D.18: Initial Mass Transfer Coefficient for Saehan Developmental Membranes with Single Coating for Clean Water Testing.

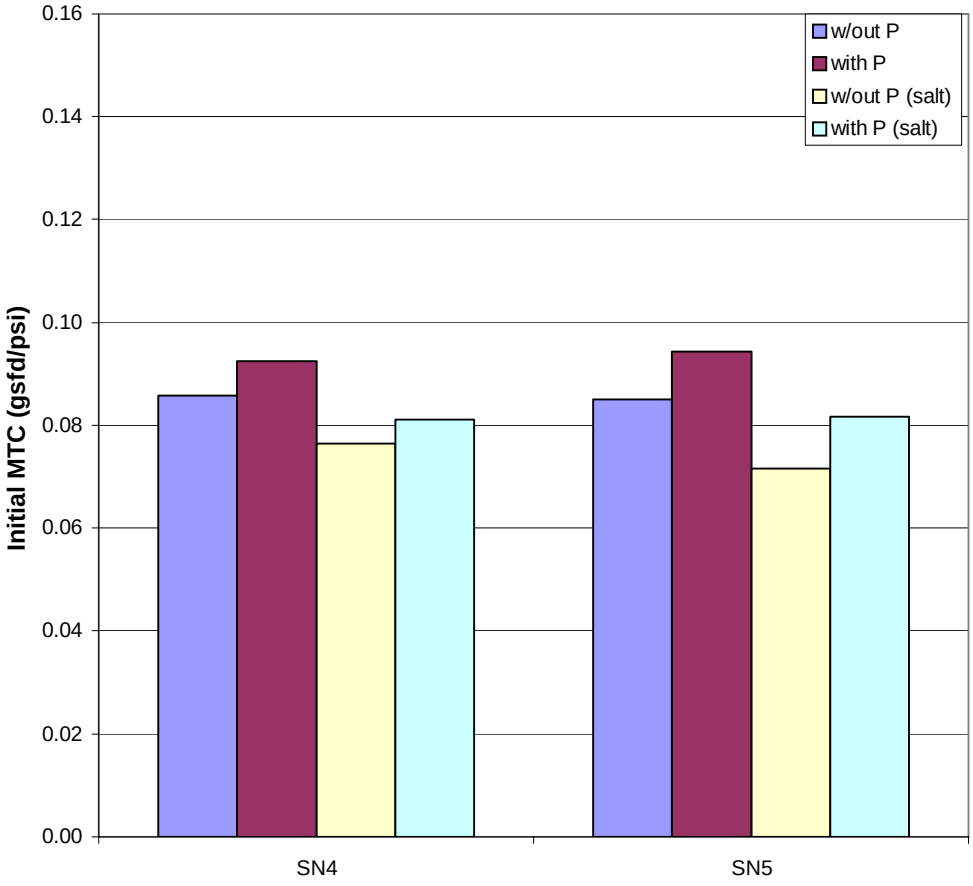

Figure D.19: Initial Mass Transfer Coefficient for Saehan Developmental Membranes with Double Coating for Clean Water Testing.

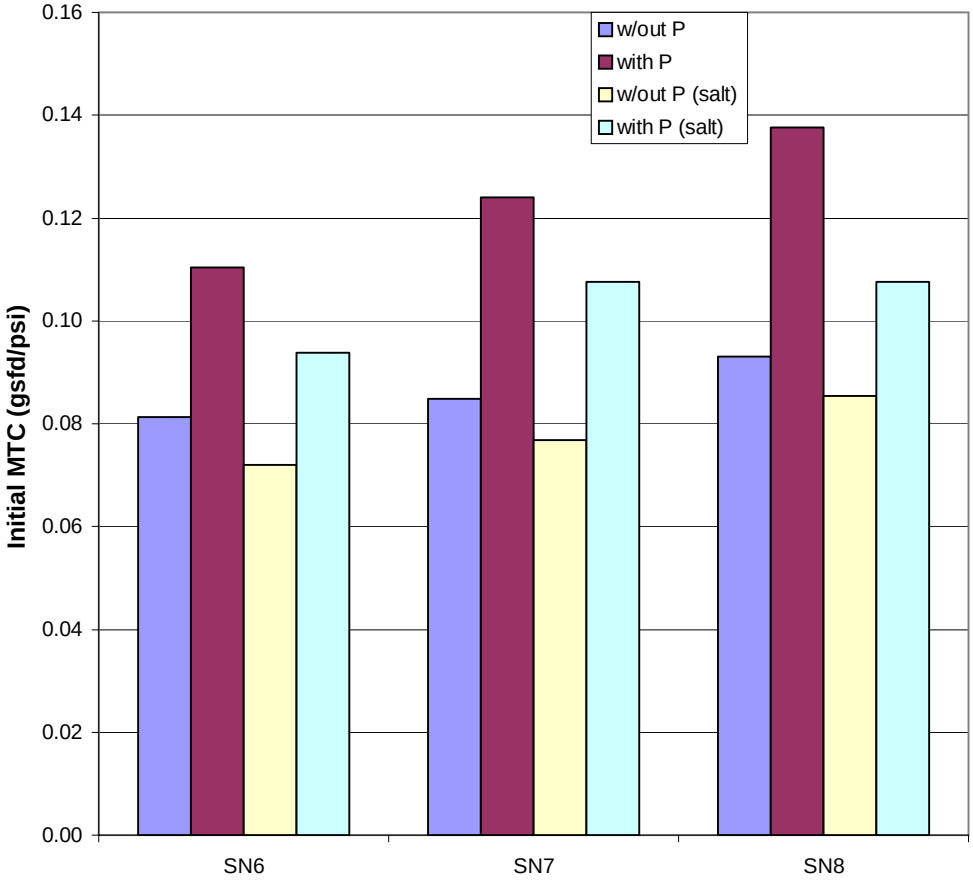

Figure D.20: Initial Mass Transfer Coefficient for Saehan Developmental Membranes with Special Coating for Clean Water Testing.

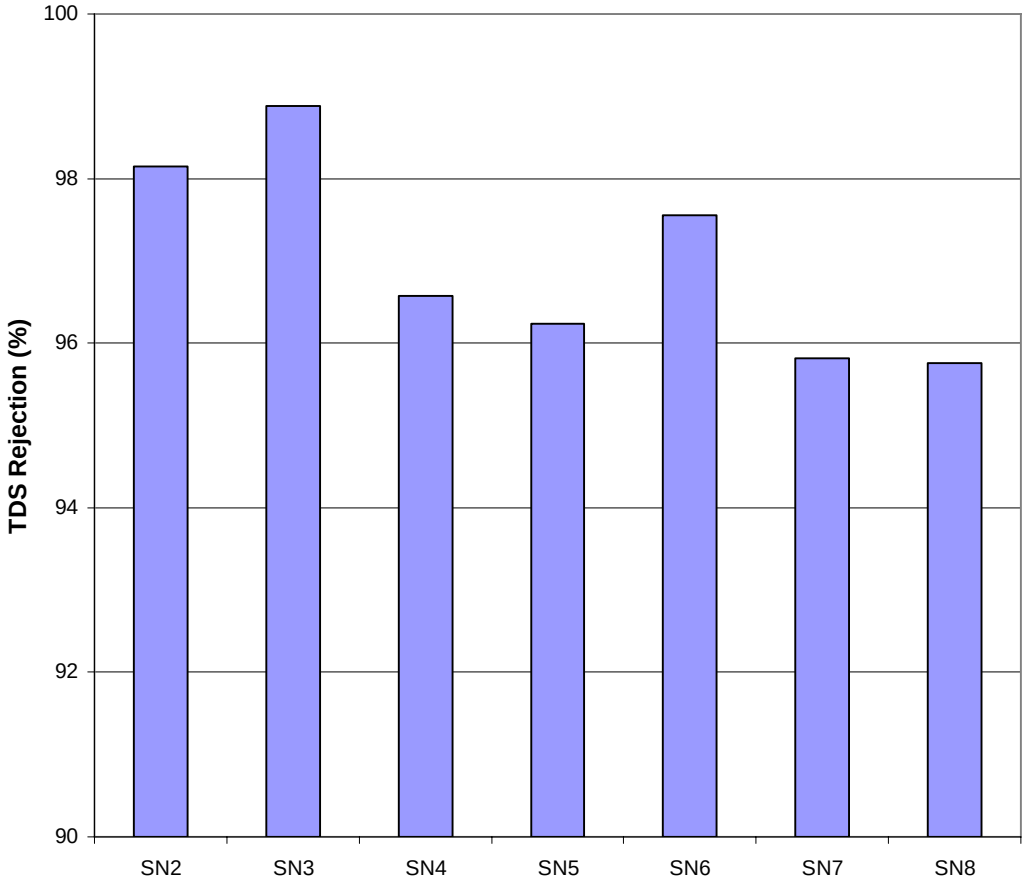

Figure D.21: Total Dissolved Solids Rejection for Saehan Developmental Membranes without Post-Treatment for Clean Water Testing.

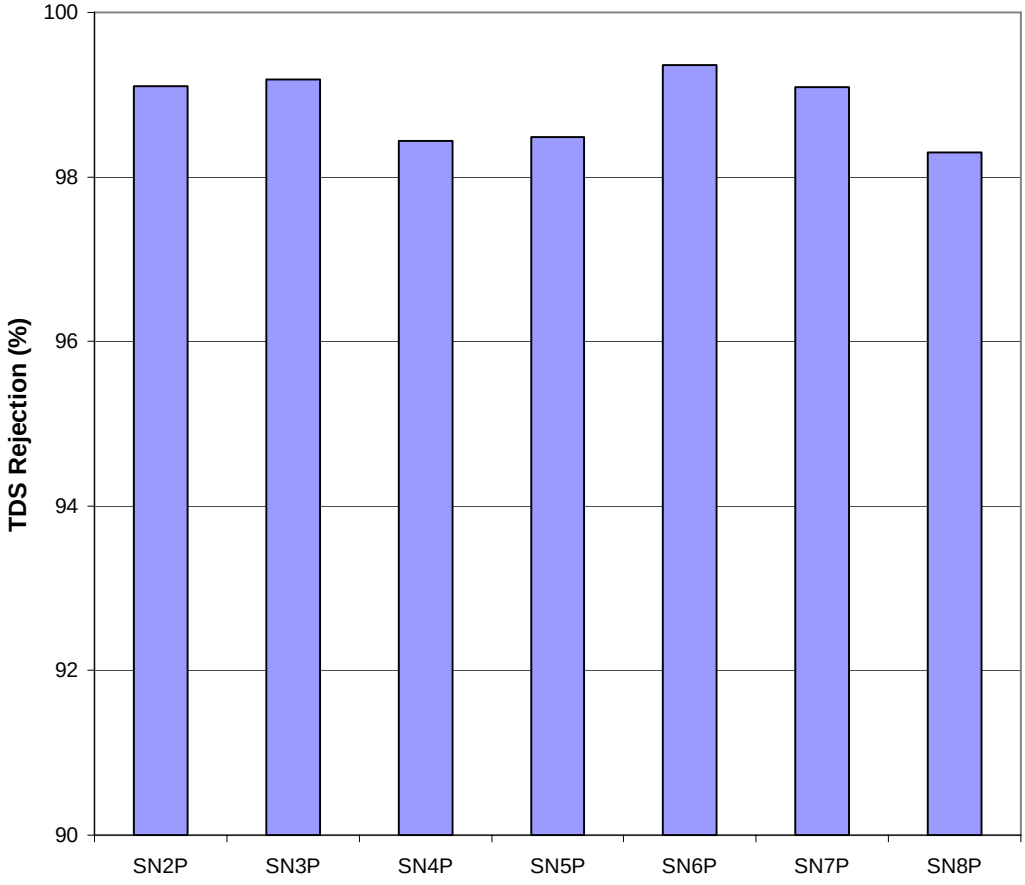

Figure D.22: Total Dissolved Solids Rejection for Saehan Developmental Membranes with Post-Treatment for Clean Water Testing.

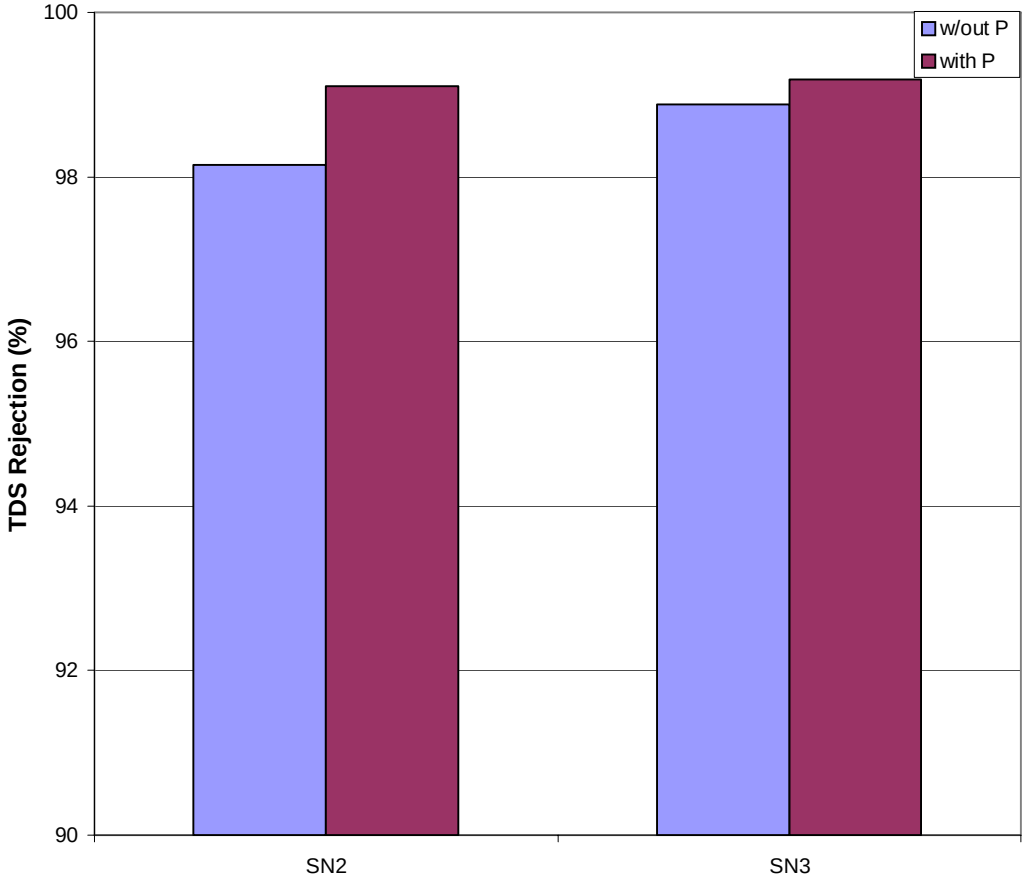

Figure D.23: Total Dissolved Solids Rejection for Saehan Developmental Membranes with Single Coating for Clean Water Testing.

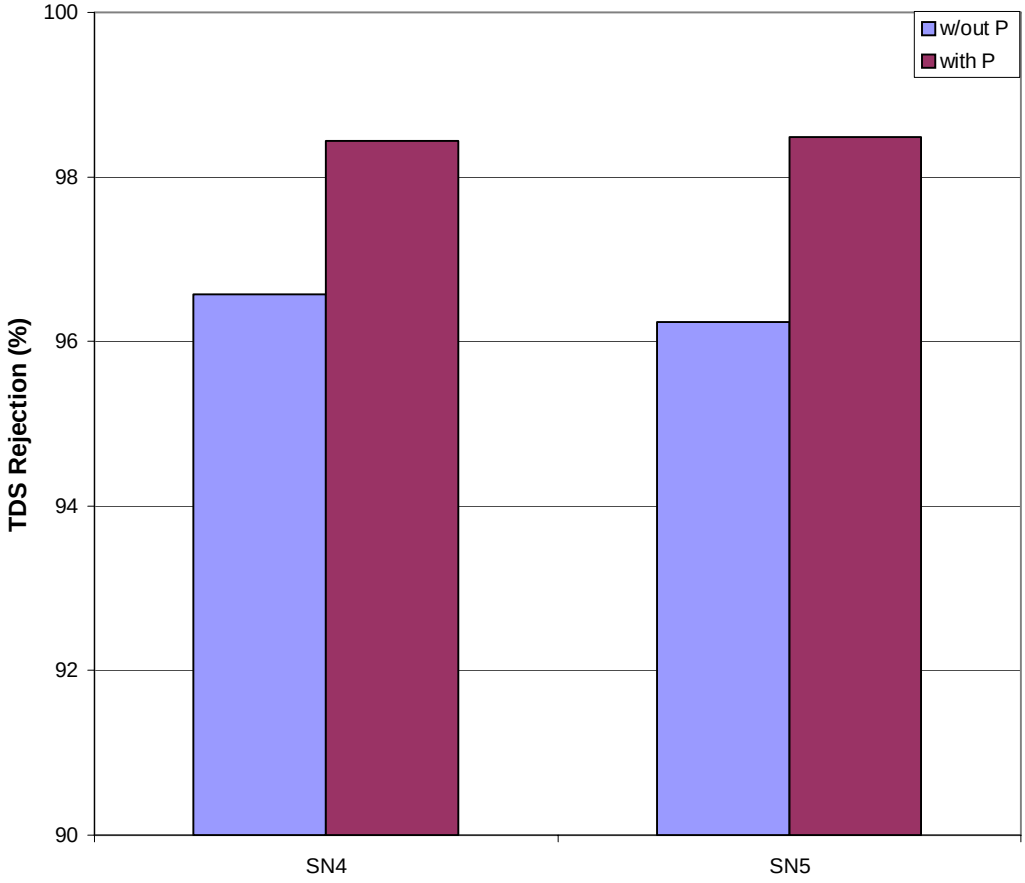

Figure D.24: Total Dissolved Solids Rejection for Saehan Developmental Membranes with Double Coating for Clean Water Testing.

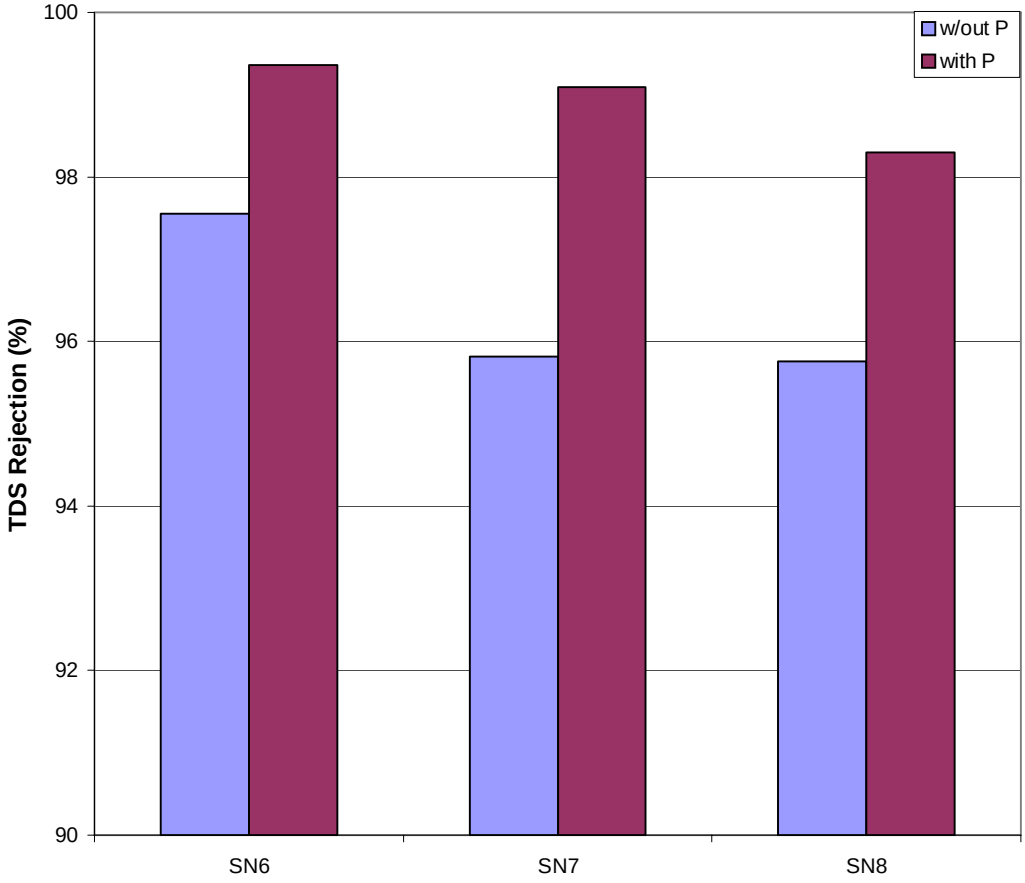

Figure D.25: Total Dissolved Solids Rejection for Saehan Developmental Membranes with Special Coating for Clean Water Testing.

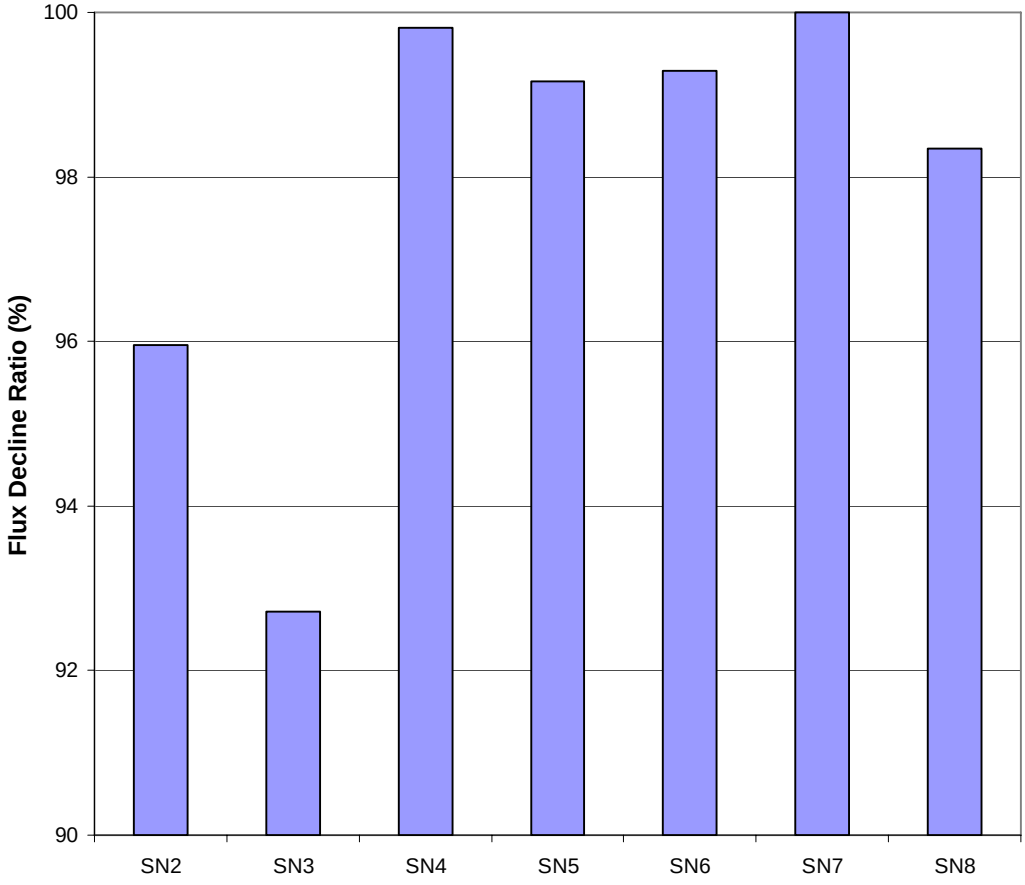

Figure D.26: Flux Decline Ratio for Saehan Developmental Membranes without Post-Treatment for Surface Water Testing.

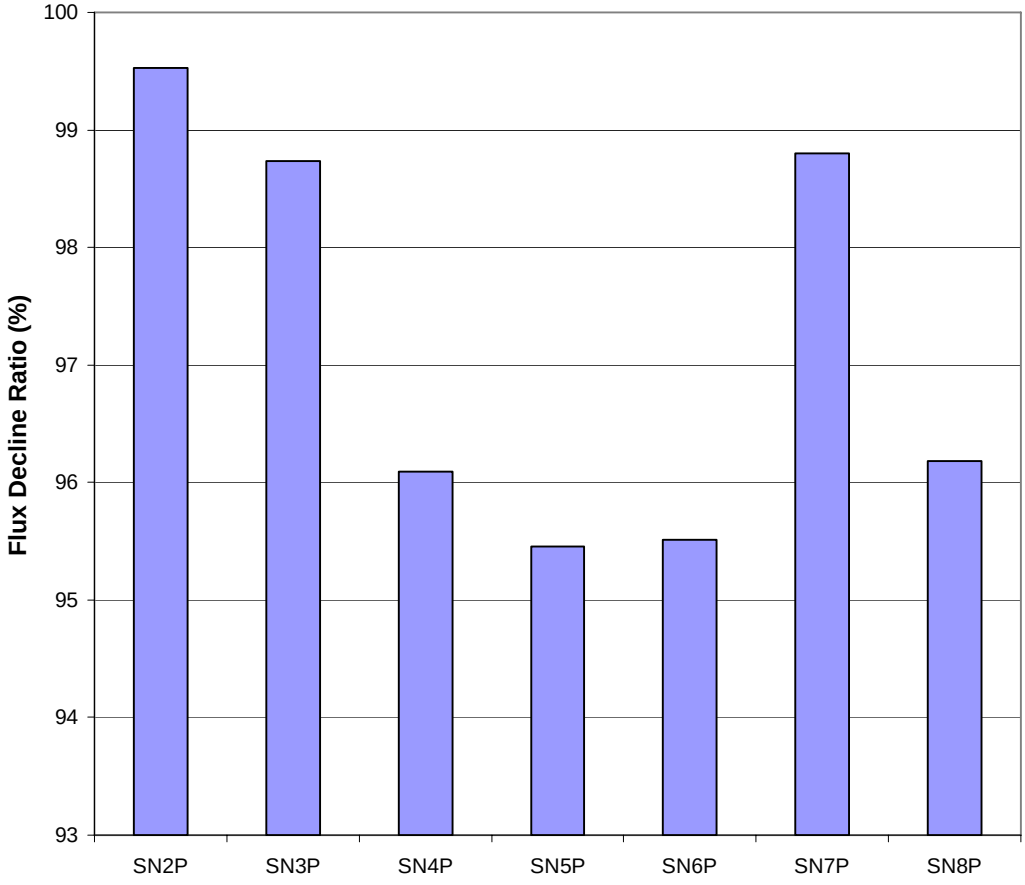

Figure D.27: Flux Decline Ratio for Saehan Developmental Membranes with Post-Treatment for Surface Water Testing.

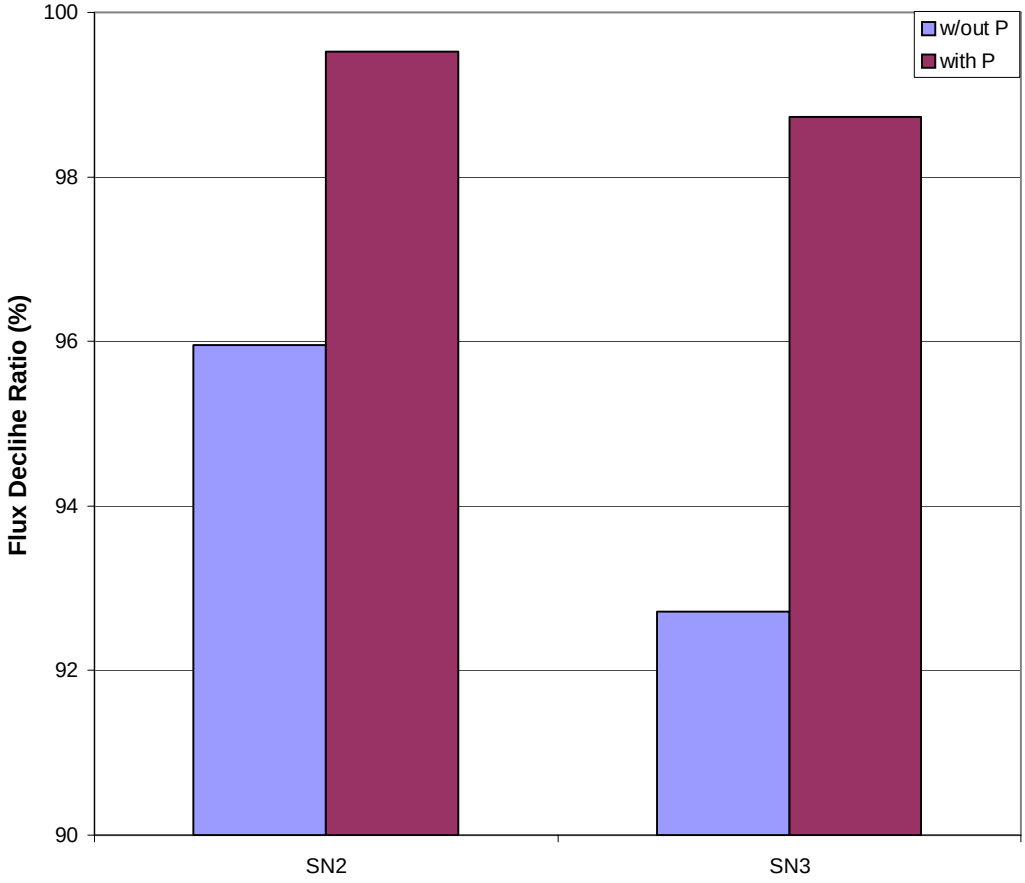

Figure D.28: Flux Decline Ratio for Saehan Developmental Membranes with Single Coating for Surface Water Testing.

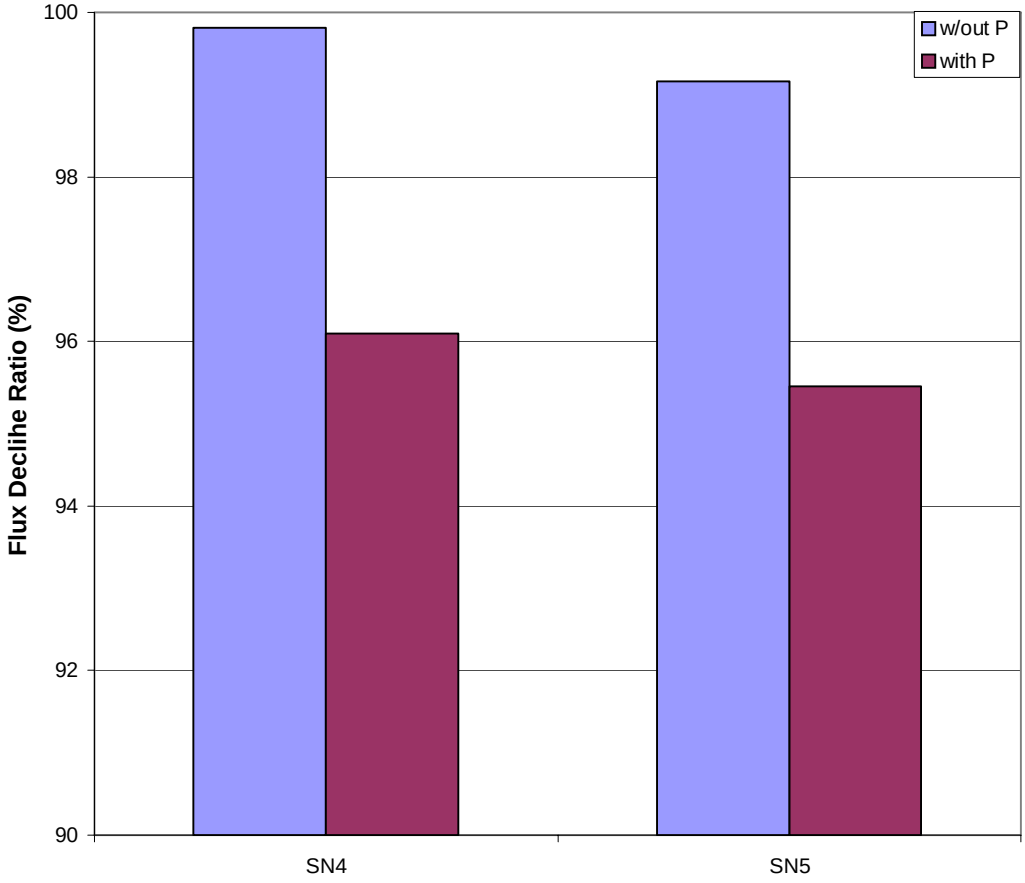

Figure D.29: Flux Decline Ratio for Saehan Developmental Membranes with Double Coating for Surface Water Testing.

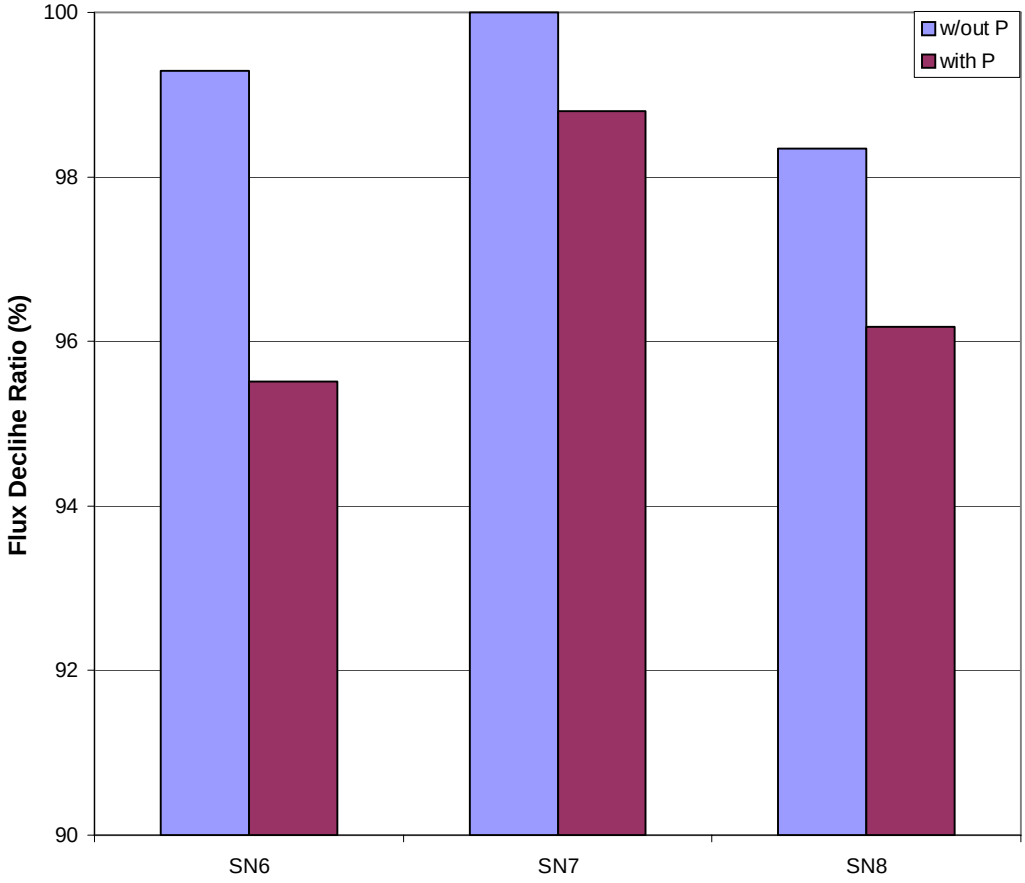

Figure D.30: Flux Decline Ratio for Saehan Developmental Membranes with Special Coating for Surface Water Testing.

APPENDIX E

STATISTICAL ANALYSIS

Saehan-Experimental (no post)	Clean Water							
MTC vs. SR and SC								
SUMMARY OUTPUT								
Regression Statistics								
Multiple R	0.595094487							
R Square	0.354137449							
Adjusted R Square	0.031206173							
Standard Error	0.005796							
Observations	7							
ANOVA								
	df	*SS*	*MS*	*F*	*Significance F*			
Regression	2	7.36798E-05	3.68399E-05	1.096634	0.417138			
Residual	4	0.000134374	3.35936E-05					
Total	6	0.000208054						
	Coefficients	*Standard Error*	*t Stat*	*P-value*	*Lower 95%*	*Upper 95%*	*Lower 75.0%*	*Upper 75.0%*
Intercept	0.106509051	0.029013838	3.670974196	0.021373	0.025954	0.187064	0.067503	0.145515
Roughness	-0.000258014	0.000311866	-0.82732265	0.454554	-0.001124	0.000608	-0.000677	0.000161
Charge	0.002674578	0.002881154	0.928300704	0.405797	-0.005325	0.010674	-0.001199	0.006548

Figure E.1: Statistical Analysis of Saehan Experimental Membranes without Post-Treatment with Clean Water. MTC vs. SR and SC.

Saehan-Experimental (no post)	Clean Water							
TDS vs. SR and SC								
SUMMARY OUTPUT								
Regression Statistics								
Multiple R	0.761771434							
R Square	0.580295718							
Adjusted R Square	0.370443577							
Standard Error	0.97653883							
Observations	7							
ANOVA								
	df	*SS*	*MS*	*F*	*Significance F*			
Regression	2	5.274059082	2.637029541	2.76526	0.176152			
Residual	4	3.814512346	0.953628087					
Total	6	9.088571429						
	Coefficients	*Standard Error*	*t Stat*	*P-value*	*Lower 95%*	*Upper 95%*	*Lower 75.0%*	*Upper 75.0%*
Intercept	96.01020158	4.888395215	19.64043359	3.96E-05	82.43784	109.5826	89.43825	102.5821
Roughness	-0.020383792	0.05254469	-0.38793248	0.717826	-0.166271	0.125504	-0.091025	0.050257
Charge	-1.13122346	0.485431173	-2.33034779	0.080222	-2.478996	0.21655	-1.783836	-0.478611

Figure E.2: Statistical Analysis of Saehan Experimental Membranes without Post-Treatment with Clean Water. TDS vs. SR and SC.

Saehan-Experimental (post)	Clean Water							
MTC vs. SR and SC								
SUMMARY OUTPUT								
Regression Statistics								
Multiple R	0.856296677							
R Square	0.733243999							
Adjusted R Square	0.626541599							
Standard Error	0.008662871							
Observations	8							
ANOVA								
	df	*SS*	*MS*	*F*	*Significance F*			
Regression	2	0.001031402	0.000515701	6.87186	0.036752			
Residual	5	0.000375227	7.50453E-05					
Total	7	0.001406629						
	Coefficients	*Standard Error*	*t Stat*	*P-value*	*Lower 95%*	*Upper 95%*	*Lower 75.0%*	*Upper 75.0%*
Intercept	0.125820313	0.018418863	6.831057338	0.001026	0.078473	0.173168	0.101858	0.149782
Roughness	-0.000643994	0.00018951	-3.3981959	0.019289	-0.001131	-0.000157	-0.000891	-0.000397
Charge	-0.006517807	0.003084936	-2.11278549	0.088309	-0.014448	0.001412	-0.010531	-0.002504

Figure E.3: Statistical Analysis of Saehan Experimental Membranes with Post-Treatment with Clean Water. MTC vs. SR and SC.

Saehan-Experimental (post)	Clean Water							
TDS vs. SR and SC								
SUMMARY OUTPUT								
Regression Statistics								
Multiple R	0.800545189							
R Square	0.640872599							
Adjusted R Square	0.497221639							
Standard Error	1.03376659							
Observations	8							
ANOVA								
	df	*SS*	*MS*	*F*	*Significance F*			
Regression	2	9.535383187	4.767691594	4.461318	0.07729			
Residual	5	5.343366813	1.068673363					
Total	7	14.87875						
	Coefficients	*Standard Error*	*t Stat*	*P-value*	*Lower 95%*	*Upper 95%*	*Lower 75.0%*	*Upper 75.0%*
Intercept	91.91703087	2.197978701	41.81889061	1.47E-07	86.26695	97.56711	89.05757	94.77649
Roughness	0.049978547	0.022614857	2.209987318	0.078106	-0.008155	0.108112	0.020558	0.079399
Charge	-0.567984977	0.368134712	-1.54287264	0.183507	-1.514305	0.378335	-1.046909	-0.08906

Figure E.4: Statistical Analysis of Saehan Experimental Membranes with Post-Treatment with Clean Water. TDS vs. SR and SC.

Saehan-Experimental (no post)	Surface Water - Cocoa							
J/J_0 vs. SR and SC								
SUMMARY OUTPUT								
Regression Statistics								
Multiple R	0.509603678							
R Square	0.259695908							
Adjusted R Square	-0.110456138							
Standard Error	2.803931072							
Observations	7							
ANOVA								
	df	*SS*	*MS*	*F*	*Significance F*			
Regression	2	11.03188218	5.515941089	0.701593	0.54805			
Residual	4	31.44811782	7.862029455					
Total	6	42.48						
	Coefficients	*Standard Error*	*t Stat*	*P-value*	*Lower 95%*	*Upper 95%*	*Lower 75.0%*	*Upper 75.0%*
Intercept	94.80747712	14.04611937	6.749727422	0.002512	55.8092	133.8058	75.92391	113.691
Roughness	0.06876452	0.149590654	0.459684598	0.669617	-0.346566	0.484095	-0.132345	0.269874
Charge	1.608904851	1.36924124	1.175033883	0.305153	-2.192718	5.410528	-0.2319	3.449709

Figure E.5: Statistical Analysis of Saehan Experimental Membranes without Post-Treatment with Cocoa Surface Water. J/J_0 vs. SR and SC.

Saehan-Experimental (no post)	Surface Water - Cocoa							
MTC vs. SR and SC								
SUMMARY OUTPUT								
Regression Statistics								
Multiple R	0.834469706							
R Square	0.69633969							
Adjusted R Square	0.544509535							
Standard Error	0.005327073							
Observations	7							
ANOVA								
	df	*SS*	*MS*	*F*	*Significance F*			
Regression	2	0.000260298	0.000130149	4.586307	0.09221			
Residual	4	0.000113511	2.83777E-05					
Total	6	0.000373809						
	Coefficients	*Standard Error*	*t Stat*	*P-value*	*Lower 95%*	*Upper 95%*	*Lower 75.0%*	*Upper 75.0%*
Intercept	0.122680734	0.026685643	4.597256076	0.010052	0.04859	0.196772	0.086805	0.158557
Roughness	-0.000434678	0.000284201	-1.52947316	0.200883	-0.001224	0.000354	-0.000817	-5.26E-05
Charge	0.005483393	0.002601365	2.107890584	0.102735	-0.001739	0.012706	0.001986	0.008981

Figure E.6: Statistical Analysis of Saehan Experimental Membranes without Post-Treatment with Cocoa Surface Water. MTC vs. SR and SC.

Saehan-Experimental (no post)	Surface Water - Cocoa							
TDS vs. SR and SC								
SUMMARY OUTPUT								
Regression Statistics								
Multiple R	0.261991741							
R Square	0.068639672							
Adjusted R Square	-0.397040492							
Standard Error	0.851545971							
Observations	7							
ANOVA								
	df	*SS*	*MS*	*F*	*Significance F*			
Regression	2	0.213763551	0.106881775	0.147397	0.867432			
Residual	4	2.900522164	0.725130541					
Total	6	3.114285714						
	Coefficients	*Standard Error*	*t Stat*	*P-value*	*Lower 95%*	*Upper 95%*	*Lower 75.0%*	*Upper 75.0%*
Intercept	99.3295982	4.265766902	23.28528503	2.02E-05	87.48593	111.1733	93.59471	105.0645
Roughness	-0.02455117	0.045430261	-0.54041446	0.617596	-0.150686	0.101583	-0.085628	0.036525
Charge	-0.081279912	0.415834709	-0.19546207	0.854559	-1.235822	1.073262	-0.640327	0.477767

Figure E.7: Statistical Analysis of Saehan Experimental Membranes without Post-Treatment with Cocoa Surface Water. TDS vs. SR and SC.

Saehan-Experimental (post)	Surface Water - Cocoa							
J/J_0 vs. SR and SC								
SUMMARY OUTPUT								
Regression Statistics								
Multiple R	0.617394176							
R Square	0.381175569							
Adjusted R Square	0.133645797							
Standard Error	1.524364044							
Observations	8							
ANOVA								
	df	*SS*	*MS*	*F*	*Significance F*			
Regression	2	7.156571307	3.578285654	1.539918	0.301244			
Residual	5	11.61842869	2.323685739					
Total	7	18.775						
	Coefficients	*Standard Error*	*t Stat*	*P-value*	*Lower 95%*	*Upper 95%*	*Lower 75.0%*	*Upper 75.0%*
Intercept	92.4357815	3.184318406	29.02843551	9.09E-07	84.25023	100.6213	88.29315	96.57842
Roughness	0.058745942	0.033538641	1.75158983	0.140235	-0.027468	0.14496	0.015114	0.102378
Charge	0.16504793	0.58907273	0.280182602	0.79056	-1.349212	1.679308	-0.601306	0.931402

Figure E.8: Statistical Analysis of Saehan Experimental Membranes with Post-Treatment with Cocoa Surface Water. J/J_0 vs. SR and SC.

Saehan-Experimental (post)	Surface Water - Cocoa							
MTC vs. SR and SC								
SUMMARY OUTPUT								
Regression Statistics								
Multiple R	0.963955806							
R Square	0.929210796							
Adjusted R Square	0.900895114							
Standard Error	0.005217646							
Observations	8							
ANOVA								
	df	*SS*	*MS*	*F*	*Significance F*			
Regression	2	0.001786761	0.00089338	32.81612	0.001333			
Residual	5	0.000136119	2.72238E-05					
Total	7	0.00192288						
	Coefficients	*Standard Error*	*t Stat*	*P-value*	*Lower 95%*	*Upper 95%*	*Lower 75.0%*	*Upper 75.0%*
Intercept	0.127240021	0.010899395	11.67404432	8.1E-05	0.099222	0.155258	0.11306	0.14142
Roughness	-0.000793023	0.000114797	-6.90803454	0.000974	-0.001088	-0.000498	-0.000942	-0.000644
Charge	-0.01139303	0.002016298	-5.6504679	0.002411	-0.016576	-0.00621	-0.014016	-0.00877

Figure E.9: Statistical Analysis of Saehan Experimental Membranes with Post-Treatment with Cocoa Surface Water. MTC vs. SR and SC.

Saehan-Experimental (post)	Surface Water - Cocoa							
TDS vs. SR and SC								
SUMMARY OUTPUT								
Regression Statistics								
Multiple R	0.585112781							
R Square	0.342356966							
Adjusted R Square	0.079299753							
Standard Error	0.53899333							
Observations	8							
ANOVA								
	df	*SS*	*MS*	*F*	*Significance F*			
Regression	2	0.756180949	0.378090475	1.301454	0.350732			
Residual	5	1.452569051	0.29051381					
Total	7	2.20875						
	Coefficients	*Standard Error*	*t Stat*	*P-value*	*Lower 95%*	*Upper 95%*	*Lower 75.0%*	*Upper 75.0%*
Intercept	97.59291565	1.125929458	86.67764656	3.87E-09	94.69862	100.4872	96.12814	99.05769
Roughness	0.00749726	0.011858784	0.632211504	0.555025	-0.022987	0.037981	-0.00793	0.022925
Charge	0.330584828	0.208287695	1.587154866	0.17334	-0.204836	0.866005	0.059613	0.601557

Figure E.10: Statistical Analysis of Saehan Experimental Membranes with Post-Treatment with Cocoa Surface Water. TDS vs. SR and SC.

LIST OF REFERENCES

Adams, C., et al, 2002. Removal of Antibiotics from Surface and Distilled Water in Conventional Water Treatment Processes. Journal of Environmental Engineering, 128, 253-260.

Bellona, C., et al, 2003. Factors Driving the Rejection of Emerging Micropollutants in Indirect Potable Reuse – A Literature Review. WaterReuse Association Symposium 2003.

Christopher, J., et al, 2002. Reducing Acid Demand and Enhancing Membrane Treatment Operations by Optimizing Acid Feed Point Locations. FWRC Proceedings 2002.

Drewes, J., et al, 2004. Rejection of Emerging Organic Micropollutants in Nanofiltration/Reverse Osmosis Membrane Applications. WEFTEC Proceedings 2004.

Duranceau, S. and Henthorne, L., 2004. Membrane Pretreatment for Seawater Reverse-Osmosis Desalination. Florida Water Resources Journal, 56:11, 33-37.

Elimelech, M., and Childress, A. E., 1996. Zeta Potential of Reverse Osmosis Membranes: Implications for Membrane Performance. Water Treatment Technology Program Report, 10.

Elimelech, M., et al, 1997. Role of Membrane Surface Morphology in Colloidal Fouling of Cellulose Acetate and Composite Aromatic Polyamide Reverse Osmosis Membranes. Journal of Membrane Science, 127, 101-109.

Faibish, R., et al, 1998. Effect of Interparticle Electrostatic Double Layer Interactions on Permeate Flux Decline in Crossflow Membrane Filtration of Colloidal Suspensions: An Experimental Investigation. Journal of Colloid and Interface Science, 204, 77-86.

Farahbakhsh, K., et al, 2003. Monitoring the Integrity of Low-Pressure Membranes. Journal AWWA, 95:6, 95-107.

Fonseca, A., et al, 2003. Biofouling of Nanofiltration Membranes – Detection Using Ultrasonic Frequency – Domain Reflectometry. AWWW Annual Conference

Her, N., et al, 2000. Seasonal Variations of Nanofiltration (NF foulants: Identification and Control. Desalination, 132, 143-160.

Hobbs, C., 2000. Effect of Membrane Properties on Fouling in RO/NF Membrane Filtation of High Organic Groundwater. Thesis, 28.

Hong, S., et al, 1997. Kinetics of Permeate Flux Decline in Crossflow Membrane Filtration of Colloidal Suspensions. Journal of Colloid and Interface Science, 196, 267-277.

Hong, S. and Elimelech, M., 1997. Chemical and Physical Aspects of Natural Organic Matter (NOM) Fouling of Nanofiltration Membranes. Journal of Membrane Science, 132, 159-181.

Hong, S., 1999. Particle Processes in Aquatic Systems. Course Handout.

Kavanaugh, M. 2003. Unregulated and Emerging Chemical Contaminants: Technical and Institutional Challenges. WEFTEC Proceedings 2003.

Kimura, K., et al, 2003. Rejection of Organic Micropollutants (DBPs, EDCs, PACs) by NF/RO Membranes. Journal of Membrane Science, 227, 113-121.

Kinslow, J. and Hudkins J., 2004. The Evolution of Pretreatment Chemicals in Membrane Processes an Analysis of Innovations in Chemical Pretreatment Practices. Florida Water Resources Journal, 56:11, 21-28.

Kitis, M., et al, 2003. Microbial Removal and Integrtity Monitoring of RO and NF Membranes. Journal AWWA, 95:12, 105-119.

Letterman, R., et al, 1999. Chapter 6: Coagulation and Flocculation. Water Quality and Treatment: A Handbook of Community Water Supplies (5th Edition). New York: McGraw-Hill. American Water Works Association.

Li, S., et al, 2004. Application of Ultrafiltration to Improve the Extraction of Antibiotics. Separation and Purification Technology. 34, 115-123.

Manning Hudkins, J. and Schmidt, H. 2003. Membrane Treatment Processes ant Their Ability to Address Emergent Pollutants of Concern. SFWMD Advanced Water Treatment Technologies and Emergent Pollutants of Concern Workshop, October 2003.

Nemeth, J., 1997. Scale Inhibitors: Application, Developments and Trends. Proceedings of IDA World Congress on Desalination and Water Reuse. Madrid, Spain: IDA, 1997.

Schmidt, H. and Manning Hudkins J., 2004. Addressing Emerging Pollutants of Concern: Reverse Osmosis for the Advanced Treatment of Wastewater Effluent. Florida Section AWWA Proceedings.

Vrijenhoek, E., et al, 2001. Influence of Membrane Surface Properties on Initial Rate of Colloidal Fouling of Reverse Osmosis and Nanofiltration Membranes. Journal of Membrane Science, 188, 115-128.